

**SCHOOL OF
CIVIL ENGINEERING**

INDIANA

DEPARTMENT OF HIGHWAYS

JOINT HIGHWAY
RESEARCH PROJECT
JHRP-82-10

EVALUATION OF METHODS FOR
PREDICTING DURABILITY
CHARACTERISTICS OF
ARGILLACEOUS CARBONATE
ROCK

Abdul Shakoor



PURDUE UNIVERSITY

Final Report

EVALUATION OF METHODS FOR PREDICTING DURABILITY
CHARACTERISTICS OF ARGILLACEOUS CARBONATE ROCK

TO: H. L. Michael, Director
Joint Highway Research Project

April 6, 1982

FROM: C. F. Scholer
Research Associate

File: 5-9-12

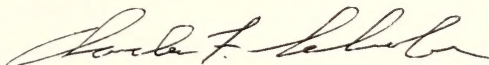
Project: C-36-42M

The attached Final Report "Evaluation of Methods for Predicting Durability Characteristics of Argillaceous Carbonate Rock" is by Mr. Abdul Shakoor, Graduate Instructor in Research on the staff of the School of Civil Engineering, and also, Graduate Instructor in the Department of Geoscience. This report is his Ph.D. thesis and, as such, represents his work and conclusions.

The study was initiated as a JHRP project in July 1981. This report is submitted as a final report for the project which has the same title as this report.

The implications of the study findings warrant discussion with personnel of the Division of Materials and Research, IDOH after they have read the report. Further research would be desirable, however, some changes in current specifications should be considered.

Respectfully submitted,



Charles F. Scholer
Research Associate

CFS:ms

cc: A. G. Altschaeffl
J. M. Bell
W. L. Dolch
R. L. Eskew
G. D. Gibson
W. H. Goetz

M. J. Gutzwiller
G. K. Hallock
J. F. McLaughlin
R. D. Miles
P. L. Owens
G. T. Satterly

C. F. Scholer
K. C. Sinha
C. A. Venable
L. E. Wood
E. J. Yoder
S. R. Yoder

Digitized by the Internet Archive
in 2011 with funding from
LYRISIS members and Sloan Foundation; Indiana Department of Transportation

Final Report

EVALUATION OF METHODS FOR PREDICTING DURABILITY
CHARACTERISTICS OF ARGILLACEOUS CARBONATE ROCK

by

Abdul Shakoor
Graduate Instructor in Research

Joint Highway Research Project

Project No.: C-36-42M

File No.: 5-9-12

Prepared as Part of an Investigation

Conducted by

Joint Highway Research Project
Engineering Experiment Station
Purdue University

In Cooperation With

Indiana Department of Highways

Purdue University
West Lafayette, Indiana
April 6, 1982

ACKNOWLEDGEMENTS

The author would like to express his appreciation and gratitude to his major professor, Dr. T.R. West, for his guidance, help, and encouragement throughout this research work. The author also wishes to express his sincere appreciation to Dr. C.F. Scholer for his readily available help and valuable suggestions.

Special thanks are extended to Dr. A.G. Altschaeffl and professor G.W. Prescott for their comments, counselling, and encouragement.

The financial support for this research was provided by the Indiana Department of Highways and the Federal Highway Administration. This support is gratefully acknowledged. Sincere thanks are extended to Mr. Larry John and the staff of the Division of Materials and Tests, Indiana Department of Highways, for their support and help in the sampling and the experimental work.

Mrs. Janet Lovell assisted in the x-ray diffraction analysis and other laboratory tests. Mr. Matthew R. Fein assembled the apparatus for the Iowa pore index test. Mr. Earl Geist prepared the thin sections and the polished slabs. Mr. Shaheen Ariaey-Nejad and Ms. Michele Ratcliff helped with the drafting work. Ms. Virginia Ewing typed the final manuscript. Thanks are extended to all of them.

Finally, the author wants to thank his wife, Roohi, for her understanding and encouragement during the course of this research work.

TABLE OF CONTENTS

	Page
LIST OF TABLES.	vii
LIST OF FIGURES	viii
LIST OF ABBREVIATIONS AND SYMBOLS	xv
ABSTRACT.	xvi
CHAPTER 1 - INTRODUCTION.	1
1.1 Statement of Problem.	1
1.2 Significance of Problem	2
1.3 Statement of Objectives	4
CHAPTER 2 - LITERATURE REVIEW	5
2.1 Aggregate Properties that Control Freeze-Thaw Failures.	5
2.2 Identification of Frost Susceptible Aggregate . . .	9
2.3 Mechanisms Involved in Freeze-Thaw Failures	11
CHAPTER 3 - GEOLOGY OF QUARRY SITES AND DESCRIPTION OF PAVEMENT DETERIORATION.	13
3.1 Quarry T	14
3.1.1 North Vernon Limestone.	14
3.1.2 Jeffersonville Limestone.	14
3.1.3 Wabash Formation.	17
Liston Creek Limestone Member.	17
Mississinewa Shale Member.	17
Huntington Lithofacies	18
Ledge 801.	19
Ledge 802.	19
Ledge 803A	21
Ledge 803B	21
3.2 Quarry K.	22
3.2.1 Ledge 1	23
3.2.2 Ledge 2	23
3.2.3 Ledge 3	26
3.2.4 Ledge 4	27
3.2.5 Ledge 5	27

	Page
3.3 Quarry L.	29
3.3.1 Huntington Lithofacies.	31
3.3.2 Louisville Limestone.	33
3.3.3 Waldron Formation	34
3.3.4 Salamonie Dolomite.	34
3.4 Mode of Pavement Failure.	34
3.4.1 Bituminous Pavements.	35
State Road 160E.	35
State Road 213	38
3.4.2 Concrete Pavements.	38
I-265.	38
US24	40
CHAPTER 4 - LABORATORY INVESTIGATIONS	44
4.1 Sampling Procedure.	44
4.2 Petrographic Analysis	47
4.2.1 Petrographic Analysis of Ledge Samples.	47
Acid Etching	48
4.2.2 Petrographic Analysis of Core Samples	49
4.2.3 Petrographic Analysis of Insoluble Residue.	49
4.3 Laboratory Testing.	49
4.3.1 Specific Gravity and Absorption	50
4.3.2 Insoluble Residue Test.	51
4.3.3 Atterberg Limits of Insoluble Residue	52
4.3.4 Hydrometer Analysis of Insoluble Residue.	53
4.3.5 X-ray Diffraction Analysis of Insoluble Residue	53
4.3.6 Absorption-Adsorption Test.	55
Procedure.	55
Absorption	55
Adsorption	56
4.3.7 Pore-Size Distribution.	56
Apparatus.	58
Corrections Applied to Intrusion Data.	58
Procedure.	60
4.3.8 Iowa Pore Index Test.	61
Apparatus.	61
Procedure.	63
4.3.9 Sodium Sulphate Soundness Test.	63
4.3.10 Unconfined Freeze-Thaw Test	65
4.3.11 Modified Freeze-Thaw Test	65
CHAPTER 5 - RESULTS AND DISCUSSION.	67
5.1 Petrographic Analysis	67
5.1.1 Thin Section Study.	67
5.1.2 Acid Etching.	68
5.2 Specific Gravity, Absorption, and Degree of Saturation.	73
5.3 Amount and Nature of Insoluble Residue.	75
5.3.1 Plasticity Characteristics.	78

	Page
5.3.2 Amount of Clay	78
5.3.3 Type of Clay Minerals by X-ray Diffraction	87
5.4 Absorption-Adsorption Characteristics	87
5.5 Pore Characteristics	99
5.5.1 Pore Size Distribution	99
5.5.2 Iowa Pore Index Test	108
5.6 Sulphate Soundness and Freeze-Thaw Tests	108
5.7 Correlations	110
5.7.1 Percent Residue vs EDF	113
5.7.2 Percent Residue vs Pore Index	115
5.7.3 Percent Residue vs Sulphate Soundness	115
5.7.4 Percent Residue vs Freeze-Thaw Loss	118
5.7.5 EDF vs Pore Index	118
5.7.6 EDF and Pore Index vs Freeze-Thaw Loss	121
5.7.7 Texture vs Physical Properties	127
5.8 D-Cracking vs Pitting and Popouts	127
CHAPTER 6 - MECHANISMS OF FREEZE-THAW DETERIORATION	130
6.1 Critical Saturation	130
6.2 Influence of Pore Characteristics	131
6.3 Failure Mechanisms	132
6.3.1 Elastic Accommodation	132
6.3.2 Critical Size of the Aggregate	133
6.3.3 Expulsion of Water from Aggregate into Paste	134
6.3.4 Dunn and Hudec's Hypothesis of Sorbed Water	134
6.4 Role of De-icing Salts	135
6.5 Application of Failure Mechanisms to Aggregates Studied	137
CHAPTER 7 - SUMMARY, CONCLUSIONS, AND RECOMMENDATIONS	143
7.1 Summary	143
7.2 Conclusions	145
7.3 Recommendations	145
BIBLIOGRAPHY	147
APPENDICES	
Appendix A: Petrographic Analysis	157
Appendix B: Acid Etching of Ledge Samples	195
Appendix C: Insoluble Residue and Atterberg Limits	200
Appendix D: Pore Size Distributions	212
Appendix E: Results of Sodium Sulphate Soundness and Freeze-Thaw Tests	240
Appendix F: Degree of Saturation	245
Appendix G: Deterioration of Ledge Samples on Wetting and Drying	249
VITA	252

LIST OF TABLES

Table	Page
4.1 Location of Samples Studied.	45
4.2 Location of Pavement Cores Studied	46
4.3 Correction Factors in Mercury Porosimetry.	60
5.1 Specific Gravity, Absorption, and Degree of Saturation .	74
5.2 Amount of Silt and Clay Size Residue	77
5.3 Chemical Analyses of Ledge Samples from the Three Quarries	86
5.4 Results of Absorption-Adsorption Test.	95
5.5 Expected Durability Factors for Ledge Samples.	105
5.6 Results of Iowa Pore Index Test.	109
5.7 Results of Sodium Sulphate Soundness Test.	111
5.8 Results of Freeze-Thaw Test.	112
Appendix Table	
E-1 Itemized Listing of Soundness Losses on Individual Portions of the Test Samples and Calculated Weighted Loss	240
F-1 Determination of Degree of Saturation from Specific Gravity and Absorption Data.	246
F-2 Determination of Degree of Saturation from Vacuum Absorption Values and Mercury Porosimeter Data	248
G-1 Loss in Weight of Ledge Samples on Wetting and Drying. .	250

LIST OF FIGURES

Figure	Page
3.1 Stratigraphic Section of Quarry T.	15
3.2 Rock Formations Exposed in Quarry T.	16
3.3 Different Ledges of the Mississinewa Shale Member, Quarry T	20
3.4 Foliated Structure of Ledge 803B	20
3.5 Stratigraphic Section at Quarry K.	24
3.6 Different Ledges of Quarry K	25
3.7 Close-up View of Ledge 5, the Main Source of Nondurable Aggregate from Quarry K.	28
3.8 Stratigraphic Section at Quarry L.	30
3.9 Panoramic View of Quarry L and the Portals for the Mine.	32
3.10 Rock Formations Exposed in Quarry L.	32
3.11 General View of Bituminous Pavement Deterioration.	36
3.12 Close-up View of the Bituminous Pavement Deterioration	36
3.13 Fracturing and Removal of the Aggregate from the Bitum- inous Overlay of SR 160E	37
3.14 Aggregate Deterioration in Concrete Pavement of I-265.	39
3.15 Size Variation of Nondurable Aggregate in Case of I-265.	39
3.16 Concrete Pavement Deterioration at the Intersection of US24 and Albert Street	41
3.17 Concrete Pavement Deterioration at the Intersection of US24 and SR15.	41
3.18 Extent of Pavement Deterioration at the Intersection of US24 and SR15.	42
3.19 Pitting of US24 near Wabash Down Town Exit	42

Figure	Page
3.20 Extent of Deterioration of US24 Near Wabash Down Town Exit	43
4.1 Mercury Intrusion Porosimeter	59
4.2 Apparatus for Iowa Pore Index Test.	62
5.1 Breakage of the Aggregate Along Microfractures.	69
5.2 Comparison of the Etched Samples from the Three Quarries (a) Unetched, (b) Etched.	70
5.3 Concrete Cores Showing that Only the Aggregate is Involved in Concrete Pavement Damage.	72
5.4 Cassagrande's Plasticity Chart Showing Type of Insoluble Residue (-200 sieve) from Quarry T.	79
5.5 Cassagrande's Plasticity Chart Showing Type of Insoluble Residue (-200 sieve) from Quarry K.	80
5.6 Cassagrande's Plasticity Chart Showing Type of Insoluble Residue (-200 sieve) from Quarry L.	81
5.7 Cassagrande's Plasticity Chart Showing Type of Insoluble Residue (-200 sieve) from the Three Quarries.	82
5.8 Grain Size Distribution of Insoluble Residue (passing 200 sieve), Ledge 801, Quarry T	83
5.9 Grain Size Distribution of Insoluble Residue (passing 200 sieve), Ledge 5, Quarry K	84
5.10 Grain Size Distribution of Insoluble Residue (passing 200 sieve), Ledge 6 (1' from roof), Quarry L.	85
5.11 X-ray Diffractograms of Insoluble Residue for Different Ledges of Quarry T.	88
5.12 X-ray Diffractograms of Insoluble Residue for Different Ledges of Quarry K.	89
5.13 X-ray Diffractograms of Insoluble Residue for Ledge 6 (different sites) of Quarry L	90
5.14 X-ray Diffractograms of Insoluble Residue for Quarries T, K, and L	91
5.15 X-ray Diffractograms of Oriented Mounts of Differently Treated Clay from Quarry T.	92
5.16 X-ray Diffractograms of Oriented Mounts of Differently Treated Clay from Quarry K.	93

Figure		Page
5.17	X-ray Diffractograms of Oriented Mounts of Differently Treated Clay from Quarry L.	94
5.18	Absorption-Adsorption Test Results for Quarry T	96
5.19	Absorption-Adsorption Test Results for Quarry K	97
5.20	Absorption-Adsorption Test Results for Quarry L	98
5.21	Absorption-Adsorption Test Results for the Three Quarries.	100
5.22	Pore-Size Distributions for Different Ledges of Quarry T	101
5.23	Pore-Size Distributions for Different Ledges of Quarry K	102
5.24	Pore-Size Distributions for Different Ledges of Quarry L	103
5.25	Comparison of Pore-Size Distributions for Ledges 801 and 803A of Quarry T and Unsound Aggregate from I-265 Cores	106
5.26	Comparison of Pore-Size Distributions for Ledge 5 of Quarry K and Unsound Aggregate from US24 Cores. . . .	107
5.27	Relationship Between Insoluble Residue Content (passing 200 sieve) and Expected Durability Factor	114
5.28	Relationship Between Insoluble Residue Content (passing 200 sieve) and Pore Index	116
5.29	Relationship Between Insoluble Residue Content (passing 200 sieve) and Sodium Sulphate Soundness Loss	117
5.30	Relationship Between Insoluble Residue Content (passing 200 sieve) and Freeze-Thaw Loss in Water.	119
5.31	Relationship Between Insoluble Residue Content (passing 200 sieve) and Freeze-Thaw Loss in 5% Salt Solution . .	120
5.32	Relationship Between Pore Index and Expected Durability Factor.	122
5.33	Relationship Between Expected Durability Factor and Freeze-Thaw Loss in Water	123
5.34	Relationship Between Expected Durability Factor and Freeze-Thaw Loss in 5% Salt Solution.	124
5.35	Relationship Between Pore Index and Freeze-Thaw Loss in Water.	125

Figure	Page
5.36 Relationship Between Pore Index and Freeze-Thaw Loss in 5% Salt Solution	126
5.37 Relationship Between Texture and Physical Properties of Argillaceous Carbonates Regarding Freeze-Thaw Durability	128
Appendix A	
Figure	
A-1: Photomicrograph of Sample T1 (magnification: 250x). . .	158
A-2: Photomicrograph of Sample T2 (magnification: 125x). . .	159
A-3: Photomicrograph of Sample T3 (magnification: 250x). . .	160
A-4: Photomicrograph of Sample T4 (magnification: 250x). . .	161
A-5: Photomicrograph of Sample T5 (magnification: 250x). . .	162
A-6: Photomicrograph of Sample T6 (magnification: 125x). . .	163
A-7: Photomicrograph of Sample T7 (magnification: 62.5x) . .	164
A-8: Photomicrograph of Sample T8 (magnification: 62.5x) . .	165
A-9: Photomicrograph of Sample T9 (magnification: 62.5x) . .	166
A-10: Photomicrograph of Sample T10 (magnification: 62.5x). .	167
A-11: Photomicrograph of Sample K1 (magnification: 125x). . .	168
A-12: Photomicrograph of Sample K2 (magnification: 125x). . .	169
A-13: Photomicrograph of Sample K3 (magnification: 125x). . .	170
A-14: Photomicrograph of Sample K4 (magnification: 125x). . .	171
A-15: Photomicrograph of Sample K5 (magnification: 125x). . .	172
A-16: Photomicrograph of Sample K6 (magnification: 125x). . .	173
A-17: Photomicrograph of Sample K7 (magnification: 125x). . .	174
A-18: Photomicrograph of Sample K8 (magnification: 125x). . .	175
A-19: Photomicrograph of Sample K9 (magnification: 125x). . .	176
A-20: Photomicrograph of Sample K10 (magnification: 125x) . .	177
A-21: Photomicrograph of Sample K11 (magnification: 125x) . .	178
A-22: Photomicrograph of Sample K12 (magnification: 125x) . .	179

Figure	Page
A-23: Photomicrograph of Sample K13 (magnification: 125x) . .	180
A-24: Photomicrograph of Sample K14 (magnification: 125x) . .	181
A-25: Photomicrograph of Sample K15 (magnification: 125x) . .	182
A-26: Photomicrograph of Sample K16 (magnification: 125x) . .	183
A-27: Photomicrograph of Sample K17 (magnification: 125x) . .	184
A-28: Photomicrograph of Sample K18 (magnification: 125x) . .	185
A-29: Photomicrograph of Sample K19 (magnification: 125x) . .	186
A-30: Photomicrograph of Sample L1 (magnification: 62.5x) . .	187
A-31: Photomicrograph of Sample L2 (magnification: 62.5x) . .	188
A-32: Photomicrograph of Sample L3 (magnification: 62.5x) . .	189
A-33: Photomicrograph of Sample L4 (magnification: 62.5x) . .	190
A-34: Photomicrograph of Sample L5 (magnification: 62.5x) . .	191
A-35: Photomicrograph of Sample L6 (magnification: 62.5x) . .	192
A-36: Photomicrograph of Sample L7 (magnification: 62.5x) . .	193
A-37: Photomicrograph of Sample L8 (magnification: 62.5x) . .	194

Appendix B

Figure

B-1: Results of Etching Test on Samples T1, T2, and T6: Unetched (top); Etched (bottom)	196
B-2: Results of Etching Test on Samples T3, T4, T7, and T9: Unetched (top); Etched (bottom)	197
B-3: Results of Etching Test on Samples K1, K2, and K4: Unetched (top); Etched (bottom)	198
B-4: Results of Etching Test on Samples K13, K14, K16, and K17: Unetched (top); Etched (bottom)	199

Appendix D

Figure

D-1: Pore-Size Distributions for Samples T1 (top) and T2 (bottom).	213
D-2: Pore-Size Distributions for Samples T3 (top) and T4 (bottom).	214

Figure	Page
D-3: Pore-Size Distributions for Samples T5 (top) and T6 (bottom).	215
D-4: Pore-Size Distributions for Samples T7 (top) and T8 (bottom).	216
D-5: Pore-Size Distributions for Samples T9 (top) and T10 (bottom).	217
D-6: Pore-Size Distributions for Samples K1 (top) and K2 (bottom).	218
D-7: Pore-Size Distributions for Samples K3 (top) and K4 (bottom).	219
D-8: Pore-Size Distributions for Samples K5 (top) and K6 (bottom).	220
D-9: Pore-Size Distributions for Samples K7 (top) and K8 (bottom).	221
D-10: Pore-Size Distributions for Samples K9 (top) and K10 (bottom).	222
D-11: Pore-Size Distributions for Samples K11 (top) and K12 (bottom).	223
D-12: Pore-Size Distributions for Samples K13 (top) and K14 (bottom).	224
D-13: Pore-Size Distributions for Samples K15 (top) and K16 (bottom).	225
D-14: Pore-Size Distributions for Samples K17 (top) and K18 (bottom).	226
D-15: Pore-Size Distributions for Samples K19 (top) and K20 (bottom).	227
D-16: Pore-Size Distributions for Samples L1 (top) and L2 (bottom).	228
D-17: Pore-Size Distributions for Samples L3 (top) and L4 (bottom).	229
D-18: Pore-Size Distributions for Samples L5 (top) and L6 (bottom).	230
D-19: Pore-Size Distributions for Samples L7 (top) and L8 (bottom).	231
D-20: Pore-Size Distributions for Samples L1' (top) and L2' (bottom).	232

Figure	Page
D-21: Pore-Size Distributions for Samples L3' (top) and K18-b (bottom).	233
D-22: Pore-Size Distributions for Damaged Aggregate from Cores 1 (top) and 2 (bottom) taken from I-265	234
D-23: Pore-Size Distributions for Damaged Aggregate from Cores 3 (top) and 5 (bottom) taken from I-265	235
D-24: Pore-Size Distributions for Damaged Aggregate from Cores 2 (top) and 3 (bottom) taken from US24.	236
D-25: Pore-Size Distributions for Damaged Aggregate from Cores 4 (top) and 6(bottom) taken from US24	237
D-26: Pore-Size Distributions for Damaged Aggregate from Cores 7 (top) and 8 (bottom) taken from US24.	238
D-27: Pore-Size Distributions for Damaged Aggregate from Cores 9 (top) and 15 (bottom) taken from US24	239
Appendix G	
Figure	
G-1: Wetting and Drying of Ledge Samples: (a) Original Samples; (b) After 10 Cycles of Wetting and Drying. . .	251

LIST OF ABBREVIATIONS AND SYMBOLS

Å	Angstroms (10^{-7} mm)		
AASHTO	American Association of State Highway and Transportation Officials		
argil.	argillaceous		
ASTM	American Society for Testing and Materials		
cc	cubic centimeter		
cm	centimeter		
E	modulus of elasticity		
ft	feet		
g	gram		
in	inch		
IDOH	Indiana Department of Highways		
K	permeability		
lb	pound		
L_{\max}	maximum permissible size - "critical size"		
L.S.	Limestone		
m	meter	**	
med.	medium	sec	second
min	minute	T	tensile strength
ml	milliliters	u	micron (10^{-3} mm)
mm	millimeters	u	poisson's ratio
psi	pounds per square inch	Wt.	weight
**			

ABSTRACT

Shakoor, Abdul, Ph.D., Purdue University, May 1982. Evaluation of Methods for Predicting Durability Characteristics of Argillaceous Carbonate Aggregates for Highway Pavements. Major Professor: Terry R. West.

Argillaceous carbonate aggregates are particularly prone to freeze-thaw failures, yet standard acceptance tests commonly do not prevent their use. Recently several Indiana highways have experienced such extensive pitting and popouts of highly argillaceous carbonates that resurfacing was required within one year. Coarse aggregate from three quarries and from pavement cores were studied to determine petrography, insoluble residue and clay contents, and pore size distribution.

Results indicate the poorly performing ledges are highly argillaceous, fine grained, dolomites and dolomitic limestones with insoluble residues ranging from 20-50% consisting of low plasticity silts to medium plasticity silty clays. Illite is the predominant clay mineral (by x-ray diffraction).

Aggregates with poorest performance are not necessarily those with the greatest insoluble residue percentage; the nature and mode of insolubles control extremes of deterioration. Rocks with more clay as insolubles, evenly distributed throughout the rock, are less durable than those with greater total insolubles consisting of silty concentrations of streaks and laminations.

Insoluble residue content of silt and clay size and pore characteristics, as measured by the mercury intrusion or the Iowa pore index test, are the most reliable indicators of freeze-thaw durability. Nondurable aggregates have a residue content in excess of 20%, a large pore volume with small pore diameters, most being less than 0.1 microns, and an Iowa pore index value more than 50 ml.

Additional tests including sulphate soundness, unconfined freeze-thaw, and absorption-adsorption tests were conducted and their results compared with percent residue, mercury porosimeter data, and pore index values. Sulphate soundness and freeze-thaw tests are found to pass some unsound aggregates and reject some sound ones. Also, the criteria based on D-cracking are found to be more stringent than those required to prevent pitting and popouts. Use of D-cracking criteria will exclude many aggregates which can be safely used in bituminous pavements. The purpose of this research is to develop a simpler, more economical test to exclude nondurable argillaceous carbonate aggregates.

CHAPTER 1

INTRODUCTION

1.1 Statement of Problem

Durability of concrete frequently implies resistance to climatic conditions such as heating and cooling, wetting and drying, and freezing and thawing (1, 2, 3, 4). To ensure this durability concrete aggregates must be both physically and chemically sound. This requires an accurate identification of the aggregate inadequacies as well as reliable acceptance tests to determine whether the aggregate involved is sound or unsound. Standard tests for predicting durability of concrete aggregates include the following: the sulphate soundness test, absorption test, unconfined freeze-thaw tests, confined freeze-thaw tests (concrete beam tests), and the insoluble residue test (5, 6, 7).

Argillaceous carbonate aggregates are particularly prone to freeze-thaw failures (5, 7, 8, 9, 10), yet the standard acceptance tests commonly do not identify all poor performances nor is the mechanism involved in their failure clearly understood. This has recently been verified through experience in Indiana where several pavements constructed during 1977 and 1978 developed extensive pitting and popouts by as early as the beginning of 1979 (11). The coarse aggregate used in these pavements contained large proportions of highly argillaceous dolomite and dolomitic limestone which had passed the acceptance tests and had hence complied with state specifications. The coarse aggregate

was supplied by three quarries. In two of them the argillaceous portion was obtained from the Mississinewa Shale Member of the Wabash Formation and in the third from the Louisville Limestone.

Realizing a need for isolating poor quality aggregate, the Division of Materials and Tests of the Indiana Department of Highways (IDOH) has considered a new method which involves total immersion of the aggregate in a 5 percent aqueous solution of sodium chloride for 24 hours before placing it in the freezing chamber. This is much more stringent than the previous freeze-thaw test (AASHTO T103, procedure C) and has resulted in losses as high as 100 percent. The main concern about this test is that it may also reject some acceptable aggregate material from sources in the State while it also eliminates marginal and poor aggregates. As an intermediate step a freeze-thaw test of aggregate using total immersion in water has been instigated by the IDOH.

The present state of affairs clearly indicates the need to determine the physical and chemical properties of argillaceous carbonate aggregates as related to their freeze-thaw durability, to develop a rapid and reliable test to detect unsound aggregates, and to better understand the mechanism involved in their deterioration. Petrographic methods are commonly used to evaluate these properties and to explain unexpected failures (6-9, 12-21).

1.2 Significance of Problem

For long life and high quality of pavements, high quality materials are required. A serious problem facing highway engineers is that of providing sound materials which are durable under the extremes of climatic conditions experienced in Indiana. The quality of coarse

aggregate is of primary concern in this respect. Coarse aggregate is a major constituent of both concrete and bituminous pavements, and its reaction to climatic effects has much to do with the degree of durability that can be achieved (6, 22, 25).

Carbonate rocks constitute the most extensively used coarse aggregate material in United States (23, 24). A large proportion of these can be argillaceous in composition. Frequently in a quarry, relatively pure limestone and dolomite beds alternate with argillaceous limestones and dolomites. These argillaceous seams may appear massive and acceptable in quality but frequently they cause concrete deterioration in freezing and thawing when the silt and clay content is high. It is necessary to distinguish these poor quality materials from the rest of the geologic units. On the other hand, with increasing costs of transportation and rapid depletion of sources of good quality aggregate, it is becoming increasingly necessary that readily available stone be used for construction purposes if at all possible. Blending of good and poor quality stone, in suitable proportions to be both economical and safe, is also a need of the day. How much of the poor quality material should be used will depend on how bad it is.

The problem becomes particularly important when one realizes that current tests cannot distinguish between rock materials which are marginally adequate from those which fail long before the end of the designed life of the structure. It is relatively easy to distinguish those which are excellent from those which are quite poor but it is the intermediate quality aggregate which must be categorized and identified if economics and conservation of natural resources are to be served while ensuring the required durability.

There are numerous cases in the United States as a whole in which rock of poor durability was used on the one hand and marginally satisfactory rock was rejected on the other because of the inexact methods of predicting their performance.

1.3 Statement of Objectives

The main objectives of this study are as follows:

1. To evaluate methods for predicting durability characteristics of argillaceous carbonate rocks, with special emphasis on the usefulness of petrographic techniques.
2. To investigate the relationship between physical properties and freeze-thaw durability of argillaceous carbonates.
3. To establish a reliable but simple procedure which will enable the materials engineer to predict the performance of argillaceous carbonate aggregates from other sources.

CHAPTER 2

LITERATURE REVIEW

Literature covering freeze-thaw durability of concrete has expanded rapidly during the past 40 years. Only the literature that deals with the influence of coarse aggregate, especially of carbonate composition, is reviewed here. A survey of the literature reveals that three aspects of durability problem have been of particular interest to the investigators. These are:

1. Aggregate properties that control freeze-thaw failures.
2. Identification of frost-susceptible aggregate.
3. Mechanisms involved in freeze-thaw failures.

2.1 Aggregate Properties that Control Freeze-Thaw Failures

In Indiana, the earliest studies on the properties of nondurable aggregates as related to frost resistance were conducted by Sweet (25), and Woods, Sweet, and Shelburne (26). These and other similar studies (27-29) showed that unsound aggregates are characterized by a low specific gravity, a high absorption, and a high degree of saturation which gave rise to the "degree of saturation" hypothesis. Rhoades and Mielenz (30) pointed out that these three properties are related to the pore characteristics of aggregates, namely absolute-pore volume, size of the pores, and their continuity. Since then many studies have confirmed the importance of pore size distribution. Sweet (25) concluded

that "no other property is of greater importance than porosity characteristics (amount, size, and continuity)", the size and continuity being of primary importance. He found that the volume of voids smaller in diameter than 0.005 mm, expressed as a ratio to the volume of solids, was less than 0.06 for aggregates with good field performance and greater than 0.10 for the aggregates with bad service record.

Dolch (31-35) has pointed out that most of the important properties of concrete aggregates, such as density, strength, absorption, and freeze-thaw resistance, are influenced strongly by the volume and dimensions of the internal pore system of the material. He discussed in detail the parameters related to the pore system of an aggregate, the methods for their measurement, and the properties of the aggregate and concrete influenced by them. In his earlier work Dolch studied the permeability and absorptivity characteristics of limestone aggregates from Indiana (31-33) and showed that nondurable aggregates had higher absorptivities and larger rates of saturation increase when imbibing water by capillarity. He suggested the ratio of absorptivity to permeability as a measure of frost susceptibility.

Lemish, Rush, and Hiltrop (9) and Hiltrop and Lemish (36) studied the physical properties and pore-size distributions respectively of carbonate aggregate from Iowa to determine the factors in aggregate that cause distress in concrete. They concluded that carbonate rocks with high insoluble residue content had poor freeze-thaw resistance while pure rock types of high carbonate content, low residue, and little if any clay had a good service record. However, they did not fix any upper limit of the insoluble residue content to accept or reject an aggregate. Their porosity data were not conclusive but they

did find a relationship between the pore size distribution curves and the lithology and potential freeze-thaw performance. Rocks with high insoluble residue contents were also found to contain large volumes of uniformly small sized pores, one micron or less in diameter, giving rise to a stronger tendency to absorb and retain water. Bisque and Lemish (10) investigated chemical characteristics of the same rocks and found that those carbonate rocks which contained clay, a high percentage of insoluble residue, and high magnesium content were characterized by marked reaction rims. They postulated that effective porosity and pore-size distribution were also related to chemical reactivity.

Another study on the quality of limestone aggregates from Iowa was conducted by Roy, Thomas, Weissmann, and Schneider (37). Their analysis included insoluble residue, calcite-dolomite ratios, and identification of clay minerals. They found no direct correlation between the amount and type of residues and the service record of the containing stone. However, a combination of swelling type clay mineral and absorption capacities in excess of 20 percent was found to seriously affect concrete durability.

Several other investigators measured the pore-size distribution of aggregates using the mercury porosimeter technique (38-40). In all cases, nondurable aggregates had pores in the range of 0.01 to 0.15 microns. On the basis of the above mentioned studies of physical properties it can be qualitatively concluded that nondurable aggregates have a large volume of small pores, a low bulk specific gravity, a high insoluble residue content, a high degree of saturation and a high absorptivity. However, no quantitative measure, based on the physical properties, was suggested by these investigators to predict aggregate performance in freezing and thawing.

Two recent studies at Purdue University have attempted to fill this gap. Kaneuji (41) found a good correlation between pore size distribution of an aggregate and its normalized durability factor based on the rapid freeze-thaw test. He developed the following correlation equation between the pore-size distribution of the aggregates and frost durability of concrete using multiple regression:

$$EDF = \frac{0.579}{PV} + 6.12 (MD) + 3.04$$

where: EDF = expected durability factor

PV = intruded volume of pores larger than 45 Å in diameter, cc/g

MD = median diameter of pores larger than 45 Å in diameter, u,
as measured by mercury porosimeter.

This equation can be used to predict the frost durability of an aggregate. Aggregates from pavement concrete with varying degrees of D-cracking were tested and, on the basis of the results, he proposed the following limits to distinguish between potentially good and potentially poor aggregates:

<u>EDF</u>	<u>Predicted Durability</u>
up to 40	non-durable
40 to 50	marginal
over 50	durable

The second study conducted by Lindgren (42) was designed to refine the validity of Kaneuji's correlation. Aggregates from 52 Indiana highway cores were tested. The EDF values were determined from the pore-size distributions, and an "average" value was assigned to each pavement associated with the cores. These values were then compared with the field performance of the pavement (in terms of D-cracking) to ascertain the borderline between EDF values for durable and for

nondurable aggregates. A good correlation between the field performance and the "average" EDF values was found. A pavement will be durable if its coarse aggregate has an EDF value greater than 50 for 90% or more of the aggregate. This criterion applies to stone and gravel aggregate with maximum size of 1.5" to 2.5".

2.2 Identification of Frost-Susceptible Aggregate

Development of suitable test methods for predicting freeze-thaw durability has been a subject of major concern in the field of concrete technology. Many researchers (5-13, 25, 30, 31, 38-79) have tried to develop and improve these methods. A comprehensive review of the literature treating these test methods was accomplished by Larson, Cady, Franzen and Reed (7). They classified the available methods into seven types:

1. Sulphate Soundness Tests
2. Petrographic Analysis
3. Pore System Studies
4. Physio-chemical Properties Studies
5. Unconfined Freezing-and-Thawing Tests
6. Freezing-and-Thawing Tests of Concrete Beams
7. Powers Modified Freezing-and-Thawing Test

Sulphate soundness tests have been widely used for many years and have been investigated in detail by Bloem (43), Woolf (44, 45), and others (46-50). Many of these authors have emphasized that the sulphate test does not simulate exposure to freezing and thawing in concrete, does not correlate with field performance, and is not reproducible.

Significant contributions have been made in the use of petrographic techniques by Rhoades and Mielenz (13, 30, 54, 56), B. and K. Mather

(12, 57, 58), Dolar-Mantuani (8, 51-53), and West (14-19). Their work shows that petrographic methods serve as a powerful tool in aggregate evaluation and help to better understand the results of other tests.

The important influence of pore characteristics on freeze-thaw durability and other engineering properties of aggregates, and the methods of measuring porosity and pore size distribution have been discussed by Dolch (31-35), Sweet (25), Hiltrop and Lemish (36), Kaneuji (41), and several others (38-40, 42, 59-61). Mercury intrusion porosimetry is considered by these investigators to be the most accurate and efficient method of measuring pore characteristics.

Bisque and Lemish (10) have outlined the procedure to determine the type and quantity of potentially deleterious constituents (including clay) in carbonate aggregates. Insoluble residue test and x-ray diffraction analysis are important parts of this procedure.

Sweet (25) was also one of the earliest investigators to conclude that freezing and thawing tests on concrete beams containing the aggregates under study can be used to differentiate those materials which yield good field performance from those causing poor performance. This now forms the basis of the commonly used freezing and thawing test - the ASTM method C 666. Many other researchers (62-76) have investigated freeze-thaw tests (unconfined as well as confined beam tests) but space does not permit a review of their work. Larson's report (7) provides a good summary of these investigations.

In 1955, Powers (77) criticized the rapid freezing and thawing method and proposed instead a new test method. He pointed out that the laboratory conditions in rapid freezing and thawing test were too severe compared with the natural field conditions and did not take into

consideration the effects of seasonal drying. He claimed that this might reject aggregates that may not be frost susceptible under natural weathering conditions. He proposed a new procedure which better simulates the field conditions and uses the length of drying period as a primary measure of frost resistance. This forms the basis of "critical dilation test", C 671 and C 682.

One recent test which has been successfully used in Iowa and Illinois is the "Iowa Pore Index Test" described by Myers and Dubberke (78). The test is designed to readily identify the potential of an aggregate to cause D-cracking because of its susceptibility to critical saturation. Water is forced into the sample under a pressure of 35 psi. The amount of water that enters the sample under this pressure during the first minute measures the macropores and is termed primary load while the amount injected during the next 14 minutes is taken to represent the micropores and is termed secondary load. The secondary load is considered to be a measure of frost susceptibility.

Etching and staining techniques are not routine procedures but have been used and recommended by Dolar-Mantuani (52), Lamar (79) Friedman (80) and others (81, 82) for analysis of carbonate rocks, especially those of argillaceous composition.

2.3 Mechanisms Involved in Freeze-Thaw Failures

Powers (83-85) has made significant contributions to explain the failure mechanism of concrete subjected to freezing and thawing. He proposed the "hydraulic pressure hypothesis" and explained in detail the role of air entrainment. Later on, Powers and Helmuth (86) proposed another hypothesis called "the gel water diffusion mechanism".

A more recent and a very important study which added substantially to our present understanding of the role of coarse aggregate in failure process was made by Verbeck and Landgren (22). They proposed three classes of aggregate behaviour in response to freezing conditions: (1) elastic accommodation, (2) failure due to hydraulic pressure and critical size concept, and (3) expulsion of water from the aggregate into the paste. Their analysis will be discussed in greater detail in chapter 6.

In 1966, Dunn and Hudec (87, 88) advanced a different type of hypothesis to explain the failure of argillaceous carbonate aggregates. They postulated that the disruptive force in these rocks is not due to the expansion of freezing water but results from the expansion of sorbed, ordered water on clay surfaces. They suggested that the relationship between the unfilled rock pores after 24 hour water saturation and the water sorbed at 85 percent humidity at 30°C be used to delineate the sound and unsound carbonate rocks.

The effect of maximum aggregate size on frost resistance of concrete has been studied by several investigators (89, 92). Reducing the maximum size of the coarse aggregate reduces the likelihood of freeze-thaw failure owing to a reduction in the hydraulic pressure. This is in keeping with the concept of critical size.

CHAPTER 3

GEOLOGY OF QUARRY SITES AND DESCRIPTION OF PAVEMENT DETERIORATION

Aggregate samples from three different quarries were evaluated in this study. These quarries are referred to as quarry T, quarry K, and quarry L respectively in the description given below and in the chapters to follow.

The texture, mineral composition, and mode of origin of rocks have long been recognized as important properties which determine their suitability as a source of concrete aggregate. Proper importance is generally not given to the mode of origin, but as stated by Fulton (93), "A knowledge of the ways in which rocks are formed and of the various natural processes whereby their original characteristics are altered may lead to a better understanding of those intrinsic properties which determine the suitability of a rock also as a source of concrete aggregate". Stratigraphic position of an aggregate source is also important because certain stratigraphic horizons may consistently be associated with poor quality material extending over large areas (covering an entire state or several states). Therefore, a brief geologic and petrographic description of the various rock units exposed in the three quarries is considered necessary and is provided below. Thin sections were studied for all the poor quality ledges and also for some of the good quality ones so that a comparison between them could be made. Thin section descriptions for individual samples are supplied in Appendix A.

3.1 Quarry T

Figure 3.1(a) shows the stratigraphic section of the rock formations through which this quarry has been cut whereas Figure 3.1(b) shows details of various ledges within the Wabash Formation - the main source of nondurable aggregates. Figure 3.2 presents a pictorial view of the rock formations as seen in the quarry.

3.1.1 North Vernon Limestone

The North Vernon Limestone consists of a grey phosphatic limestone (Beechwood Member), an argillaceous limestone (Silver Creek Member), and a thin argillaceous skeletal limestone (Speed Member). In the evaluation of the crushed stone aggregate resources of Indiana, Carr et al. (94) point out that only the limestones of Beechwood and Speed members of this formation are sound enough to be used as aggregate.

3.1.2 Jeffersonville Limestone

The Jeffersonville consists mainly of greyish brown carbonaceous limestones or dolomitic limestones which are about 42 feet thick at this quarry. Three zones are present in the formation; the middle and the upper zones contain very thin argillaceous and pyritic laminations. The lower zone contains a profuse coral fauna and generally lacks these argillaceous and pyritic laminations. On the whole the formation is medium bedded and very dense.

Under the microscope the limestone consists of coarse to medium grained (0.2 mm - 4.0 mm) crystalline calcite cemented together by a fine grained matrix of calcite and dolomite. The calcite crystals are well interlocked giving rise to a dense and hard rock. Replacement of calcite by chalcedony is a common feature. Approximately 85% of the

TIME UNIT		Thickness (Feet)	Lithology	ROCK UNIT	DESCRIPTION
Period	Epoch				
Quaternary	Illinoian & Wisconsinan	17		Soil & Glacial Drift	Gravel, sand and silt; valley train deposits.
DEVONIAN		25		North Vernon Limestone	Dolomitic limestone; blue grey, fine grained, argillaceous.
		42		Jeffersonville Limestone	Limestone; grey to brown, fine to medium grained, carbonaceous; massive, medium bedded.
SILURIAN	NIAGARAN	17		(Mississinewa Shale Member) Wabash Formation	Dolomite and dolomitic limestone; grey to tan grey, fine grained, argillaceous; shale laminations.

(a)

SILURIAN	NIAGARAN	6		Wabash Formation (Mississinewa Shale Member)	Ledge 801	Dolomite; greenish grey, fine grained, argillaceous; massive; conchoidal fractures.
		2.5			Ledge 802	Dolomitic limestone; tan grey med. grained; thinly bedded; shale partings.
		3.5			Ledge 803A	Dolomite; greenish grey, fine grained, argillaceous.
		5'			Ledge 803B	Dolomitic limestone; tan grey med. grained, argillaceous; shale partings and cherty lenses.

(b)

FIGURE 3.1: STRATIGRAPHIC SECTION AT QUARRY T

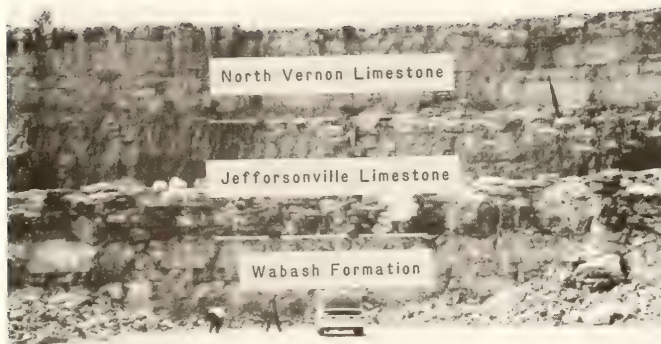


FIGURE 3.2 : ROCK FORMATIONS EXPOSED IN QUARRY T

rock consists of crystalline and fibrous calcite; euhedral to subhedral dolomite (0.3 mm and smaller) constitutes 10%, finely distributed clay 2.0%, chalcedony 1.5%, and carbonaceous matter 1.5%.

According to Carr et al. (94), the Jeffersonville generally provides good aggregate where ever it is quarried. Patton (95) considers that when Jeffersonville Limestone performs poorly in soundness and absorption tests it may be because of the presence of argillaceous and pyritic laminations which may act as planes of higher porosity.

3.1.3 Wabash Formation

This formation deserves a detailed discussion because it is exposed at all the three quarries under study and, except for the Huntington Lithofacies Member, it is consistently a source of bad aggregate.

Pinsak and Shaver (96, 97) in 1964 defined the Wabash Formation as all the strata lying above the Louisville Limestone and below the Salina Formation. It consists of three major lithofacies which are exposed at many locations in Indiana:

1. Liston Creek Limestone Member
2. Mississinewa Shale Member
3. Huntington Lithofacies

Liston Creek Limestone Member:

This represents the uppermost part of the Wabash Formation and consists of grey to tan limestone which is very cherty, fine grained, slightly fossiliferous, and thin bedded.

Mississinewa Shale Member:

This underlies the Liston Creek Limestone Member and consists of grey to green or buff silty dolomite that is argillaceous and fine

grained and grades to dolomitic siltstone. It is massive, thick bedded, and characteristically weathers into irregular blocks with conchoidal fracture. In the type area (Wabash & Grant counties), non-carbonate clastic materials may exceed 50 percent of the volume. Along the north bank of the Wabash River at Wabash, Indiana, 75 feet of the Mississinewa is exposed but its maximum thickness in the subsurface of the type area is about 110 feet. In the Western Clark county it is approximately 70 feet thick (98).

Huntington Lithofacies:

The Huntington Lithofacies consist of reef, bank, and biohermal deposits of light-grey to cream dolomite that are fine to coarse grained, porous, and fossiliferous. The dolomite laterally replaces both the Mississinewa Shale Member and the Liston Creek Limestone Member. The strata are generally inclined and are well defined except in the reef-core areas which tend to be more massive. According to Cummings and Shrock (99), and Pinsak and Shaver (96, 97), these biohermal, reef detrital rocks can be found at any stratigraphic level in the Wabash Formation and thus they are lateral equivalents of interreef rocks of the Wabash (either Mississinewa or Liston Creek).

During the time the Wabash Formation was being deposited, the Silurian sea that covered Indiana was dotted by reefs which consisted almost wholly of organisms with CaCO_3 skeletons. In the interreef areas both carbonate and non-carbonate materials were deposited. During Wabash time, however, the amount of clastic materials, especially silt and clay, was considerably larger than earlier times. This resulted in the deposition of Mississinewa Shale Member of the Wabash Formation. The reef rock converted to nearly pure dolomite over geological time and today is referred to as the Huntington Lithofacies.

At the site of quarry T, the Liston Creek Limestone Member of the Wabash Formation is absent. Here, Jeffersonville Limestone unconformably overlies the Mississinewa Shale Member and this unit extends to the base of the quarry. Aggregate from the Mississinewa Shale, when used in concrete and bituminous pavements proved nondurable in freeze-thaw. It is this lower part of the quarry which is the subject of investigations in this study.

On the basis of lithological differences the Mississinewa Shale has been further separated into three distinct ledges as shown in Figure 3.3.

Ledge 801: This ledge is 6 feet thick and consists of light greenish grey, very fine grained, argillaceous dolomite. The rock is thick bedded, massive, irregularly jointed, and breaks yielding conchoidal fracture.

Under the microscope euhedral to subhedral dolomite rhombs are seen to surround the interstitial calcite and quartz. Grain size varies from 0.01 mm to 0.05 mm. Macropores (0.05 mm - 0.1 mm) are present throughout the rock. The major constituents include dolomite 60%, calcite 15%, silt and clay 15%, quartz 8%; pyrite is the important accessory mineral and constitutes 2%.

Silt and clay occur mostly as finely distributed material throughout the rock and occasionally as concentrations around grain boundaries. Thin long flakes aligned parallel to each other are not uncommon. The clay mineral is illitic in composition.

Ledge 802: This 2.5 foot thick ledge consists of dolomitic limestone which is light grey, medium grained, clastic, argillaceous, and well bedded. Thin layers of highly shaly limestone

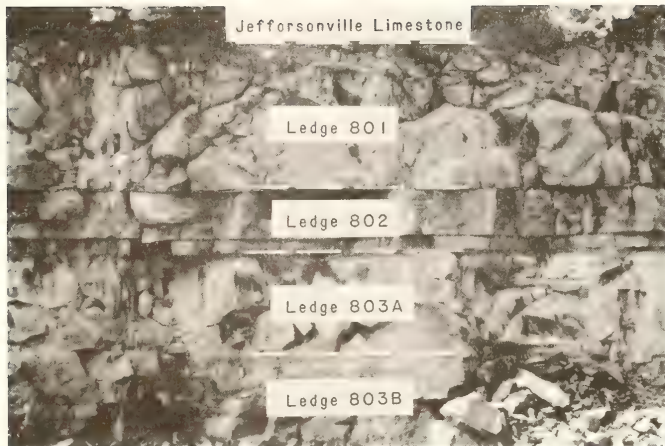


FIGURE 3.3 : DIFFERENT LEDGES OF THE MISSISSINEWA SHALE MEMBER, QUARRY T

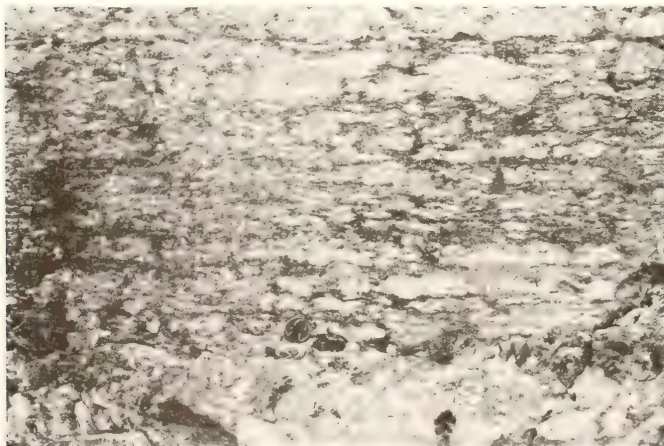


FIGURE 3.4 : FOLIATED STRUCTURE OF LEDGE 803B

are found along the bedding planes as can be seen in Figure 3.3.

Under the microscope, larger calcite grains (0.5 mm - 1.5 mm) can be seen which are surrounded by a fine grained, granular matrix of dolomite, calcite, and clay. Dolomite (0.01 mm - 0.05 mm) is euhedral and calcite and clay are intimately associated. The composition of the rock is: calcite 65%, dolomite 25%, clay 6%, quartz 3%, and pyrite 1%. Clay mostly occurs as finely distributed material throughout the rock but a few elongated flakes can also be seen.

The thin layers of shaly material along the bedding planes also consist of dolomitic limestone but here it is much more argillaceous with the argillaceous material concentrated along streaks and bands. Silt and clay amount to as much as 20% or more in these highly argillaceous layers.

Ledge 803A: This ledge consists of argillaceous dolomite very similar to ledge 801. The dolomite is light grey, fine grained, and massive. Small cavities (upto 0.2 mm) are common. Euhedral, equidimensional rhombs (0.02 mm - 0.05 mm) of dolomite form a loose but continuous mosaic disturbed only by occasional cavity fillings and irregular streaks of pyrite. Dolomite constitutes 65% of the rock, calcite 10%, silt and clay 22%, quartz 2.5%, and pyrite 0.5%. Proportions of calcite and dolomite vary laterally. Except a few scattered flakes, clay is finely divided and uniformly disseminated throughout the rock.

Ledge 803B: This ledge, which is about 5 feet thick and extends to the bottom of the quarry, shows a foliated structure due to the parallel arrangement of more calcareous lenses with argillaceous

material curving around them (Figure 3.4). Both dolomite and limestone are present in this ledge with the latter being more cherty and argillaceous.

The dolomite is light grey to tan grey, clastic, medium grained, and argillaceous. Larger calcite fragments (0.5 mm - 1.0 mm) are embedded in a fine grained granular matrix of euhedral to subhedral dolomite (0.01 mm - 0.05 mm), anhedral calcite, and finely divided, intimately associated, silt and clay. Clay is also present in the form of thin streaks and as occasional, elongated flakes. Replacement of calcite by dolomite is very common. The rock is composed of calcite 50%, dolomite 28%, silt and clay 10%, quartz 1.5%, and pyrite and chalcedony together 0.5%.

The argillaceous limestone part of the ledge consists of medium to coarse grained cherty rock with irregular fractures. Calcite fragments (0.25 mm - 2.0 mm) of organic origin are embedded in a fine grained matrix of dolomite, calcite, and silt and clay. Replacement of calcite by euhedral dolomite, chalcedony, and microcrystalline quartz is very common. Irregular fractures are filled with calcite and silica. Clay streaks are frequent. The rock contains calcite 65%, dolomite 15%, silt and clay 15%, chalcedony 4.5%, and pyrite 0.5%.

Most of the bad aggregate comes from ledges 801 and 803A both of which consist of argillaceous, silty dolomite.

3.2 Quarry K

Quarry K is located in the Mississinewa Shale Member of the Wabash Formation. The exposed stratigraphic section which is about 100 feet

thick has been divided into five ledges. Figure 3.5 shows the relative thickness and lithological composition of various ledges while Figure 3.6 presents an overall pictorial view. A brief petrographic description for each ledge is given below.

3.2.1 Ledge 1

This ledge is 19 feet thick and consists of argillaceous limestone or calcareous shale. The rock is grey, fine grained, laminated, and very argillaceous. Beds are medium thick. The ledge is no longer used as an aggregate source and, therefore, was not studied in detail.

3.2.2 Ledge 2

This ledge consists of dolomitic limestone which is fine to medium grained and thin to medium bedded. Light grey bands of relatively less argillaceous dolomite alternate with yellow brown bands of more highly argillaceous material.

Under the microscope the rock is seen to be biofragmental with medium size (0.2 mm - 1.0 mm) calcareous fragments embedded in a fine grained matrix. The argillaceous material is concentrated in the form of parallel streaks. The calcite fragments are frequently distorted, stretched out, and clearly aligned parallel to the clay streaks. This imparts a semi-gneissic structure to the rock. The matrix is composed of finely crystalline (less than 0.01 mm to 0.08 mm), euhedral dolomite, microcrystalline calcite, quartz, and finely distributed clay. Alteration of calcite to dolomite and chalcedony is common. Some argillaceous streaks show microfolding. Pyrite is a conspicuous accessory. Mineral composition includes calcite 20-30%, dolomite 50%, silt and clay 15-25%, quartz 3%, chalcedony 1%, and pyrite 2%. Silt and clay occur as fine,







TIME UNIT		Thickness (Feet)	LITHOLOGY	ROCK UNIT	LEDGE NO.	DESCRIPTION
PERIOD	EPOCH					
S I L U R I A N	Quater- nary	3		Till	0	Mainly ground moraine
	N I A G A R A N	19		Wabash Formation (Mississinewa Shale Member)	1	Argillaceous limestone or calcareous shale; grey, laminated; finely crystalline; med. bedded.
		12			2	Dolomitic L.St.; light grey to yellow brown, fine to med. grained, argillaceous; thin to med. bedded.
		30			3	Dolomitic limestone; light grey to tan brown, fine to med. grained; argillaceous, cherty, pyritic stylolitic, laminated; med. bedded.
		21			4	Dolomite; light olive grey, fine to med. grained, argillaceous; med. bedded.
		6			5	Silty dolomite to dolomitic siltstone; greenish grey, fine grained; thick bedded; conchoidal fracture.

FIGURE 3.5: STRATIGRAPHIC SECTION AT QUARRY K

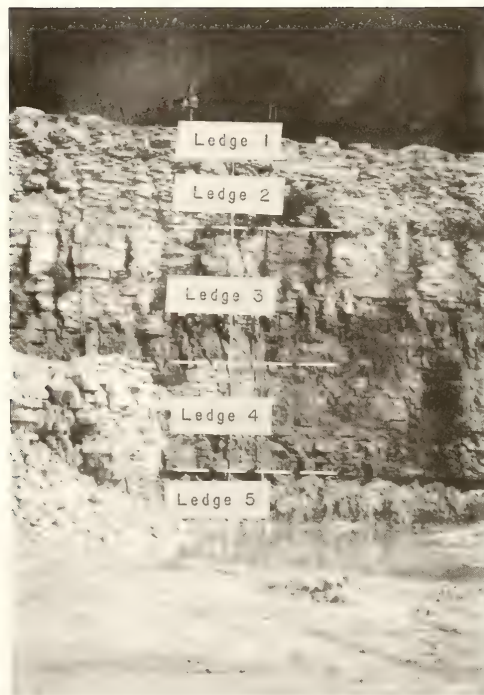


FIGURE 3.6 : DIFFERENT LEDGES OF QUARRY K

evenly distributed material, as irregular streaks, as impurities within carbonate grains, and as thin elongated flakes.

3.2.3 Ledge 3

This is the thickest (30 ft) of the five ledges and consists of dolomitic limestone. The rock is light grey to tan brown, fine to coarse grained, argillaceous, cherty, pyritic, and stylonitic. It is medium bedded with argillaceous laminations.

Texturally this limestone is very heterogeneous; more argillaceous parts of the rock alternate with the less argillaceous ones in a very irregular fashion. Micro-cavities of irregular shape and microfractures, filled with secondary calcite, are common.

Under the microscope, biofragments of coarse, crystalline calcite which are highly variable in size (0.2 mm - 4.0 mm) and shape are seen embedded in a fine grained matrix of euhedral dolomite (0.07 mm and less), microcrystalline calcite, and finely divided silt and clay. Argillaceous material is also present as streaks which cut across both the matrix and larger fragments, as thin flakes, and as inclusions in carbonate minerals. Chert is chalcedonic and occurs as a replacement product of calcite in the microcrystalline form. However, spherulitic growths of chalcedony are quite common. The average mineralogic composition of the rock includes calcite 45-55%, dolomite 25-30%, silt and clay 15%, chert 3-10%, pyrite 0.5%.

The bottom part of the ledge is more cherty than the rest and the amount of argillaceous material increases towards top marking a gradational contact with the overlying ledge 2. Also, the proportion of calcite vs. dolomite is quite variable from one part of the ledge to the other.

3.2.4 Ledge 4

This ledge is composed of light tan-grey dolomite which is fine to medium grained, biofragmental, argillaceous, and medium bedded.

Fossil fragments of crystalline calcite ranging in size from 0.25 mm to 2.0 mm are cemented together by a dense matrix of euhedral crystalline dolomite, microcrystalline calcite, quartz, and clay. Mineral composition includes dolomite 67%, calcite 20%, silt and clay 10%; chert, pyrite, and quartz together make up 3.0%. Chert is more conspicuous towards the top.

Very small cavities and micro-cracks are frequently present.

3.2.5 Ledge 5

This lower most ledge is the most problematic in the entire quarry as it contains highly nondurable aggregate. It consists of very argillaceous (silty) dolomite at the top which quickly grades downward into a dolomitic siltstone. The rock is greenish grey, fine grained, thick bedded, streaky, and poorly laminated. The most striking feature of the rock is its lower resistance to erosion because of which it weathers differentially and stands out distinctly with respect to the overlying ledges as seen in Figure 3.7. Joint pattern is rather irregular. However, two directions are fairly consistent, one perpendicular to the bedding and the other at 45° to it. Joint spacing ranges from 1' to 3'. At some places the siltstone is very intensely jointed with joint spacing being as small as 2". Along some horizontal joints shearing even has occurred where the rock takes on an appearance like shale. Towards the top of the ledge, the rock shows banding due to concentrations of parallel laminations of argillaceous material. Also, in the upper part, small, calcite filled pockets are quite common.



**FIGURE 3.7 : CLOSEUP VIEW OF LEDGE 5 - THE
MAIN SOURCE OF NONDURABLE
AGGREGATE FROM QUARRY K**

Small cavities (0.2 mm - 2.0 mm) are common and have likely resulted from a volume decrease that accompanies the alteration of calcite into dolomite. The rock breaks with conchoidal fracture; near the quarry floor it breaks into slabs.

Under the microscope euhedral to subhedral grains of dolomite and anhedral grains of quartz are seen cemented together by an even finer grained matrix of calcite, dolomite, and silt and clay. Quartz forms the largest grains but are highly variable in size, the range being 0.02 mm - 0.15 mm. Dolomite rhombs (0.02 mm - 0.1 mm) are fairly well interlocked in the upper part of the ledge where silt and clay content is 20% or less. With an increase in the amount of silt and clay toward the bottom, the interlocking of dolomite grains is disrupted.

The mineral composition of the ledge varies from top to bottom. Both clay and quartz increase toward the bottom; argillaceous material increases from 15% at the top to 35% near the bottom while quartz increases from 5% to 15%. The upper 3 feet of the ledge can be considered as argillaceous dolomite and the lower 4 feet as dolomitic siltstone. The average mineral composition near the middle of the ledge is as follows: calcite 5%, dolomite 45%, silt and clay 35%, quartz 15%. Pyrite is the only accessory mineral present.

3.3 Quarry L

Figure 3.8 shows the stratigraphic succession of the rock units exposed at the quarry site. The quarry has been excavated down 210 feet through steeply dipping reef flank beds of Wabash Formation, through the Louisville limestone, and into the Salamonie Dolomite. The quarry operator, prevented from further open pit expansion by






TIME UNIT		Thickness (Feet)	LITHOLOGY	ROCK UNIT	DESCRIPTION
PERIOD	EPOCH				
S I L U R I A N	Quaternary	9		Soil & Glacial Drift	Mostly ground moraine
	N I A G A R A N	99		Huntington Lithofacies (Wabash Formation)	Dolomite; light grey to cream, fine to coarse grained; fossiliferous; well bedded.
		79		Louisville Limestone	Dolomitic limestone; light grey to light tan brown, fine to med. grained, hard; argillaceous, pyritic; slightly cherty; med. bedded.
		5		Waldron Em.	Dolomite; light grey, argillaceous; fine to med. grained.
		30		Salamonie Dolomite	Dolomite; light grey to white; hard, porous, sugary; med. bedded.

FIGURE 3.8: STRATIGRAPHIC SECTION AT QUARRY L

adjacent land use began in 1972 to extend the operation by going to underground mining. Figure 3.9 shows a panoramic view of the quarry and the portals for the underground mine while Figure 3.10 shows the various rock formations.

3.3.1 Huntington Lithofacies (Wabash Formation)

As mentioned previously, the Wabash Formation consists of three major lithologies, the Liston Creek Limestone, the Mississinewa Shale, and the Huntington Lithofacies. Underlying the glacial cover, the top 99 feet of the section at quarry L extends through the Huntington Lithofacies. The Huntington Lithofacies here consist of light grey to cream dolomite that is fine to coarse grained, porous, and fossiliferous. The strata are medium to thick bedded and show variable dips and local faulting.

The Huntington Lithofacies represent a part of an ancient organic reef. The reef rock is massive and resistant to erosion; therefore, many reefs formed the interstream divides for the pre-glacial land surface. Now following glacial deposition and subsequent erosion, they protrude through the glacial drift cover. The reefs in Indiana have been studied in detail by Pinsak and Shaver (96), Cummings and Shrock (99), and Cummings (100). According to Wayne (101) the reef dissected by quarry L is one of the best exposures of reef structure in the midwest. Well preserved fossils and crystals of calcite, pyrite, and sphalerite are clearly seen. The quarry shows clearly the relationships between the rocks of the reef and the interreef areas of the Silurian Sea.



**FIGURE 3.9 : PANORAMIC VIEW OF QUARRY L AND
THE PORTALS FOR THE MINE**

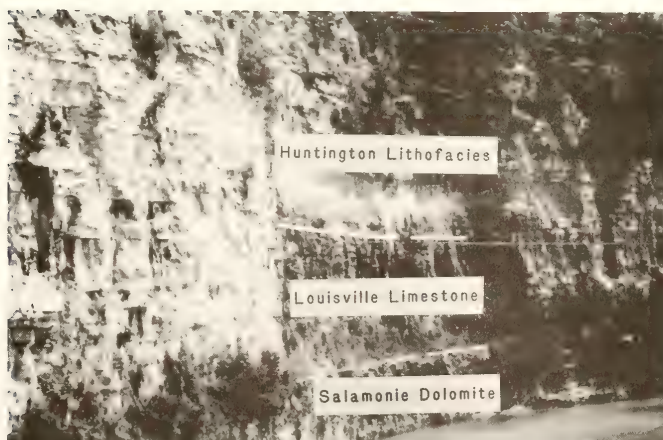


**FIGURE 3.10 : ROCK FORMATIONS EXPOSED IN
QUARRY L.**

3.3.2 Louisville Limestone

Louisville Limestone, as exposed in this quarry, is a light grey to light tan brown, dolomitic limestone. It is fine to medium grained, biofragmental, argillaceous, silty, and contains pyrite and chert nodules. The strata are medium bedded, hard, and massive. The formation is designated as ledge 6 and it is in this unit that the underground mine is located. The upper part of the ledge is more argillaceous than the rest with the argillaceous material sometimes arranged as bands and streaks. Only the top few feet below the roof, which mark a transition zone with the overlying Huntington Lithofacies, were reported to cause durability problems. In the transition zone thin beds (6"-1') of highly argillaceous and dolomitic limestone occur in a discontinuous fashion horizontally. Specimens from the upper part of the ledge were studied in detail microscopically.

Under the microscope, the rock is fine to medium grained, biofragmental. Biofragments of crystalline calcite, ranging in size from 0.2 mm to 2.0 mm, are embedded in a fine grained matrix of euhedral, crystalline dolomite (0.01 mm - 0.1 mm), microcrystalline calcite, and finely divided silt and clay. The calcite and the clay in the matrix are intimately associated and difficult to distinguish from each other. Replacement of calcite by fine grained dolomite and chalcedony is a common feature. Pyrite is the most common accessory mineral. Silt and clay occur in the following three forms:

- 1) as finely divided material evenly distributed throughout the rock (the most common mode of occurrence).
- 2) as inclusions in calcite and dolomite grains, especially concentrated along cleavage traces.

3) as a few irregular streaks.

On the average, the rock contains 50-55% calcite, 30-35% dolomite, 10-12% argillaceous material (except in one case where it amounts to more than 20%), 1% chalcedony and 0.5% each of pyrite and quartz.

3.3.3 Waldron Formation

The Waldron Shale Formation of Pinsak and Shaver is a richly fossiliferous, grey to green calcareous shale. However, in this quarry it again is represented by light grey dolomite with a massive sugary texture. It does not appear in the underground mine.

3.3.4 Salamonie Dolomite

Salamonie Dolomite consists of two units: an upper cherty limestone and dolomite unit (Laural Member), and a lower argillaceous dolomitic limestone unit (Osgood Member), with the contact between the two being gradational in nature. Here, the Salamonie Dolomite is light grey to white, fine to medium grained, hard, sugary, and porous. Beds are medium thick and dip very gently. Salamonie dolomite does not occur in the mine and it was not studied microscopically.

Salamonie dolomite has been rated as an acceptable source of crushed stone except where the Osgood Member is too argillaceous.

3.4 Mode of Pavement Failure

Coarse aggregate from the three sources of crushed stone described above was used in several concrete and bituminous pavements. Both types showed extensive aggregate deterioration after one severe winter but the damage to bituminous pavements was most acute. In bituminous pavements it occurred as a severe break up of individual aggregate

particles accompanied by a "drying" of the paving material to form a "prematurely aged" pavement. In concrete pavements the immediate result was a partial or total loss of such aggregate due to aggregate disintegration leaving behind an extensively pitted surface. Some of the damaged pavements were examined in the field to collect further information concerning the form and extent of deterioration.

3.4.1 Bituminous Pavements

The damage to bituminous pavements was so extensive that they had to be resurfaced quickly and therefore the original surface could not generally be seen. Figures 3.11 and 3.12 (obtained from Indiana Department of Highways) typify the nature and the extent of damage to the bituminous pavements before they were resurfaced. State Road 160E and State Road 213 were examined.

State Road 160E

This pavement was constructed in the fall of 1978 using coarse aggregate from quarry T which included the lower part of the Jeffersonville Limestone and ledges 801 through 803 of the Mississinewa Shale Member. The pavement deteriorated quickly in the winter of 1978-79 and was subsequently resurfaced. Only patches of original surface could be seen at a few locations. Figure 3.13 indicates how the surface appears at the present. The coarse aggregate in the bituminous overlay ranges in size from $3/4"$ - $1/2"$. The more argillaceous particles have been removed entirely from the overlay while many others have fractured in place as can be seen from Figure 3.13. Most likely the aggregate particles were first fractured and then were popped out.



**FIGURE 3.11 : GENERAL VIEW OF THE BITUMINOUS
PAVEMENT DETERIORATION**



**FIGURE 3.12 : CLOSEUP VIEW OF THE BITUMINOUS
PAVEMENT DETERIORATION**



**FIGURE 3.13 : FRACTURING AND REMOVAL OF THE
AGGREGATE FROM THE BITUMINOUS
OVERLAY OF SR 160E**

State Road 213

Aggregate from Ledge 6 of quarry L, the upper few feet of which are quite argillaceous, was used on this road. Again there was a rapid break up of this aggregate and the broken particles continued to come loose. Pitting of the pavement surface was the dominant mode of failure. The pavement was overlaid with a bituminous sand mix and today only isolated portions of the original surface are seen.

3.4.2 Concrete Pavements

I-265 near Jeffersonville and US 24 near Wabash are good illustrations of aggregate failure in concrete pavements.

I-265

Figures 3.14 and 3.15 show the form and severity of deterioration of this pavement. The following features were observed during the on-site examination:

1. Coarse aggregate ranged in size from 1/2" to 2".
2. Coarse aggregate showed 3 forms or stages of deterioration:
 - i) complete disintegration and removal of aggregate resulting in pitting.
 - ii) partial disintegration and removal of the particles resulting in depressions of various depth depending on the stage of disintegration.
 - iii) popouts where part of the aggregate had broken out at one time instead of continuous deterioration. The broken surface showed a sort of spalling effect and was probably controlled by an inherent surface of weakness such as a micro-fracture or a clay streak.
3. Coarse aggregate associated with damage was identified to come from ledges 801 and 803A - the highly argillaceous dolomite.

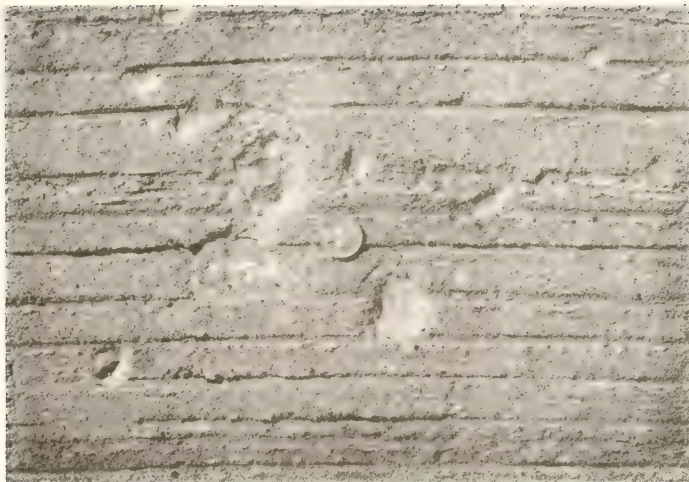


**FIGURE 3.14 : AGGREGATE DETERIORATION IN CONCRETE
PAVEMENT OF I - 265**



**FIGURE 3.15 : SIZE VARIATION OF NONDURABLE
AGGREGATE IN CASE OF I - 265**

4. Although pitting occurred in all areas, it was more prominent near the wheel paths.
5. Aggregate pieces as large as 2" and as small as 1/2", or even less, were seen to have disintegrated and were as closely spaced as 1/2" apart in some places (Figure 3.15).
6. No damage was seen to have occurred in the cement paste surrounding the aggregate.

US24

Coarse aggregate from quarry K was used to construct this pavement. The following features were observed as being associated with aggregate failure in this case:

1. As before, the pitting was the chief form of damage.
 2. In nearly every case the failed aggregate was identified to come from Ledges 2 and 5.
 3. The intensity of aggregate deterioration was found to be directly proportional to the amount of de-icing salts used.
 4. The crossovers for SR 115 and SR 15 at their intersections with US24 showed greater deterioration, resulting in complete loss of the aggregate, than did the rest of the highway.
- These crossovers were used before the main highway (US24) was opened and more salt had been placed on them during the early period following construction than was the case elsewhere.

Figures 3.16-3.18 show the extent of damage on the crossovers whereas Figures 3.19 and 3.20 present an overall picture of the pavement damage near Wabash down town exit. Here too, as elsewhere, only the aggregate was involved in failure and no damage occurred in the surrounding paste.



**FIGURE 3.16 : CONCRETE PAVEMENT DETERIORATION AT
THE INTERSECTION OF US 24 AND
ALBERT STREET**

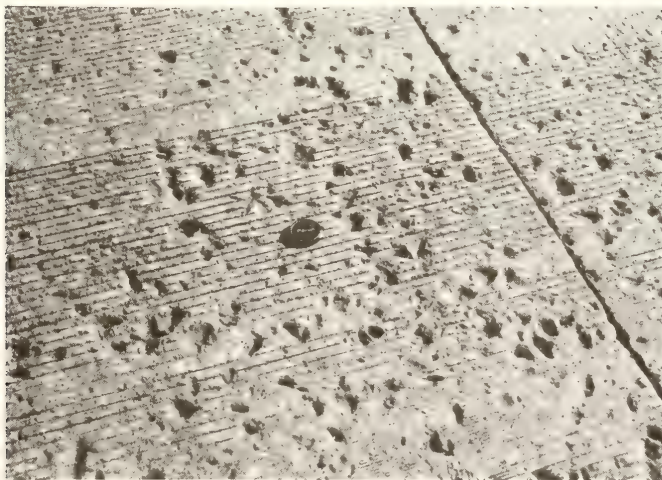


**FIGURE 3.17 : CONCRETE PAVEMENT DETERIORATION AT
THE INTERSECTION OF US 24 AND SR 15**



**FIGURE 3.18 : EXTENT OF PAVEMENT DETERIORATION AT
THE INTERSECTION OF US 24 AND SR 15**



**FIGURE 3.19 : PITTING OF US 24 NEAR WABASH DOWN
TOWN EXIT**



**FIGURE 3.20 : EXTENT OF DETERIORATION OF
US 24 NEAR WABASH DOWN
TOWN EXIT**

CHAPTER 4

LABORATORY INVESTIGATIONS

Laboratory studies conducted on the aggregate samples are reported in this section. Results obtained from these studies are presented in the next chapter. Laboratory work was accomplished in two phases. In phase 1 petrographic analysis was conducted whereas in phase 2 standard laboratory tests for aggregate evaluation were performed.

4.1 Sampling Procedure

Rock samples from the three quarries under study were obtained for laboratory testing on a ledge by ledge basis. For each ledge, samples were taken from different elevations and, in some cases, from different locations in the quarry to account for any vertical or lateral variation in lithology and texture. Ledges of good as well as poor quality were included for purposes of comparison. With a few exceptions, about 200 pounds of rock was collected from each sampling location. A total of 38 ledge samples were taken from the three quarries. Table 4.1 shows the numbers and locations of these samples.

In addition to ledge samples, random cores were taken from both concrete and bituminous pavements which had shown distress and which contained the aggregate from the three quarries. Table 4.2 shows the location of these cores.

Table 4.1 Location of Samples Studied

Sample #	Quarry	Ledge		Position Within Ledge
		Ledge #	Thickness	
T1	T	801	6.0(ft)	Site 1*, middle
T2	"	801	6.0	Site 2, middle
T3	"	802	2.5	Site 1, argil. part
T4	"	802	2.5	Site 1, less argil. part
T5	"	803A	3.5	Site 1, middle
T6	"	803A	3.5	Site 2, middle
T7	"	803B	5.0	Site 1, middle
T8	"	803B	5.0	Site 1, more argil. part
T9	"	803B	5.0	Site 1, cherty part
T10	"	Jeff.LS	5.0	Site 1, middle
K1	K	5	6.0	Site 1**, top
K2	"	5	6.0	Site 2, top
K3	"	5	6.0	Site 1, 9" from top
K4	"	5	6.0	Site 2, 9" from top
K5	"	5	6.0	Site 1, 2' from top
K6	"	5	6.0	Site 2, 2' from top
K7	"	5	6.0	Site 1, 4' from top
K8	"	5	6.0	Site 2, 4' from top
K9	"	5	6.0	Site 1, bottom
K10	"	5	6.0	Site 1, bottom
K11	"	4	21.0	Site 1, 2' from bottom
K12	"	4	21.0	Site 1, 5' from bottom
K13	"	4	21.0	Site 1, middle
K14	"	4	21.0	Site 1, top
K15	"	3	30.0	Site 1, bottom
K16	"	3	30.0	Site 1, 6' from bottom
K17	"	3	30.0	Site 1, 8' from top
K18	"	3	30.0	Site 1, top
K18(b)	"	3	30.0	Site 1, top transition zone
K19	"	2	12.0	Site 1, grey part
K20	"	2	12.0	Site 1, yel. brown part
L1	L	6	22.0	Site 1,*** 3' from roof
L2	"	6	22.0	Site 1, 2' from roof
L3	"	6	22.0	Site 1, 1' from roof
L4	"	6	22.0	Site 2, 2' from roof
L5	"	6	22.0	Site 2, 2.5' from roof
L6	"	6	22.0	Site 3, close to roof
L7	"	6	22.0	Site 3, 2' from roof
L8	"	6	22.0	Site 3, 8' from roof

* Sites 1 and 2 in quarry T are 350' apart.

** Sites 1 and 2 in quarry K are 150' apart.

*** Site 1 in quarry L is near NE end, Site 2 in the middle, and Site 3 near SW end of the mine.

Table 4.2 Location of Pavement Cores Studied

Core No.	Highway	Pavement Type	Location
1	I-265	Concrete	1 mile from SR 311, SBL, Shoulder
2	I-265	"	1 mile from SR 311, SBL, Shoulder
3	I-265	"	1 mile from SR 311, SBL, LWP
4	I-265	"	1 mile from SR 311, SBL, LWP
5	I-265	"	1 mile from SR 311, SBL, Center
6	I-265	"	1 mile from SR 311, SBL, Center
7	SR 160E	Bituminous	1 mile from intersection of SR 31 & SR 161
8	SR 160E	"	" " " "
9	SR 160E	"	" " " "
10	SR 160E	"	" " " "
11	US 24	Concrete	Station 894 + 96', near intersection SR 115, EBL
12	US 24	"	Station 895 + 18', near intersection SR 115, EBL
13	US 24	"	Station 908 + 6', east of SR 115, EBL
14	US 24	"	Station 908 + 52', east of SR 115, EBL
15	US 24	"	Station 152 + 27', intersection Wabash St., WBL
16	US 24	"	Station 152 + 30', intersection Wabash St., WBL
17	US 24	"	Station 119 + 67', intersection Albert St., WBL
18	US 24	"	Station 119 + 62', intersection Albert St., WBL
19	US 24	"	Station 91 + 49', intersection SR 15, WBL
20	US 24	"	Station 204 + 13', Wabash Downtown Exit, EBL
21	US 24	"	Station 204 + 17', Wabash Downtown Exit, EBL
22	SR 213	Bituminous	1.8 miles east of SR 19, EBL
23	SR 213	"	0.15 miles east of SR 19, EBL
24	SR 213	"	0.5 miles east of Co. Rd 100 East, WBL
25	SR 213	"	0.1 miles east of Co. Rd Meridian, EBL

Cores 1 to 6 were taken from a stretch of 300' on I-265.

EBL = East Bound Lane; WBL = West Bound Lane; SBL = South Bound Lane; LWP = Left Wheel Path

4.2 Petrographic Analysis

A detailed petrographic analysis was performed on the ledge samples, pavement cores, and insoluble residue because of the considerable utility of such an analysis in aggregate evaluation (8, 12, 13, 14-21, 51-58). Both megascopic and microscopic features were examined.

4.2.1 Petrographic Analysis of Ledge Samples

This included the following:

1. Megascopic examination of hand specimens and polished slabs.
2. Microscopic examination of polished slabs.
3. Microscopic examination of thin sections.
4. Acid etching of smooth surfaced slabs.
5. Acid etching of uncovered thin sections.

During the megascopic examination of hand specimen and polished slab of each sample the following features were observed and recorded:

1. Structural features such as laminations and banding due to the concentration of argillaceous material, fractures, and vein fillings.
2. Textural features such as grain size, crystallinity, macroporosity, and surface characteristics.
3. Mineral composition.

Microscopic examination included thin section and polished section analysis. During this analysis the following features were observed and described:

1. Quantitative description of texture such as grain size and shape, percentage of the grains comprising various sizes and shapes, amount and thickness of laminations, degree of recrystallization, etc.

2. Mineral composition in percent.
3. Alteration products.
4. Microfractures - their intensity and continuity.
5. Size, shape, and distribution of pores when observed microscopically.
6. Mode of distribution of argillaceous material - whether uniformly distributed throughout the rock mass or concentrated in the form of streaks, bands, lenses or pockets.

The thin section description for individual samples is given in Appendix A.

Acid Etching

The manner in which the argillaceous material is distributed in carbonate rocks was assumed at the outset to provide a significant influence on their physical properties and frost susceptibility. It was, therefore, considered necessary to verify the importance of the thin section study using etching techniques. Studies by Lamar (79), Willman (82), and others (80, 81) have shown that information from etched specimens, particularly that relating to the nature and distribution of noncarbonate materials, has important practical significance in connection with studies of abrasiveness, structural soundness, and weathering resistance. Etching tests were performed on slabs and on thin sections which lacked cover slips obtained from the ledge samples.

Slabs with two parallel, flat surfaces were prepared for each specimen. Each slab was placed in a flat bottomed glass container in such a way that the top surface was parallel to the surface of the acid to be added. Acid was added until the specimen was submerged to a depth of 1/2 inch or more. The acid solution consisted of 8-10 parts by volume of commercial grade concentrated hydrochloric acid diluted with water to 100 parts. The reaction was allowed to proceed for a

few minutes depending on the fabric and mineralogy. Next, slab was removed from the acid, washed thoroughly but gently, allowed to dry, and examined under binocular microscope. Photographs were taken of each slab before and after etching. Thin sections were etched similarly but for a shorter duration and examined under the petrographic microscope. Appendix B shows the results of acid etching.

4.2.2 Petrographic Analysis of Core Samples

Core samples taken from distressed pavements were examined visually, with hand lens, and under binocular microscope to evaluate the following features:

1. Percentage of poor quality aggregate present.
2. Identification of physical changes that occurred due to freeze-thaw failure.
3. Identification of any chemical reaction between coarse aggregate and concrete paste.
4. Evaluation of failure mechanism based on the above mentioned observations.

4.2.3 Petrographic Analysis of Insoluble Residue

Various size fractions of insoluble residue, obtained from the insoluble residue test, were examined under the binocular microscope to determine the nature of the insoluble particles.

4.3 Laboratory Testing

In the second phase of laboratory investigations, the following tests were performed to evaluate aggregate quality:

1. Specific gravity and absorption
2. Insoluble residue test

3. Atterberg limits of insoluble residue (passing 200 sieve)
4. Hydrometer analysis of insoluble residue (passing 200 sieve)
5. X-ray diffraction analysis of insoluble residue (passing 200 sieve)
6. Absorption-adsorption test
7. Pore-size distribution
8. Iowa pore index test
9. Sulphate soundness test
10. Unconfined freeze-thaw test in water, total immersion
11. Modified freeze-thaw test, as proposed by the Division of Materials and tests, total immersion in 5% solution of sodium chloride.

4.3.1 Specific Gravity and Absorption

Nondurable aggregates are characterized by low bulk specific gravity and high absorption values. ASTM method C 127 was used to obtain specific gravity and absorption values for each sample. A small representative piece from each sample was oven dried for 24 hours at 105°C, cooled to room temperature and then immersed in distilled water for 48 hours. At the end of this period, pieces were removed from the water bath one at a time, surface dried with a damp cloth, and weighed. Immediately following this, each piece was also weighed in the submerged condition using a wire basket. The bulk specific gravity on dry and saturated surface dry bases and absorption were calculated as follows:

$$\text{Bulk specific gravity} = A/(B-C)$$

$$\text{Bulk specific gravity (SSD)} = B/(B-C)$$

$$\text{Percent absorption} = (B-A)/A \times 100$$

where: A = weight of oven dried specimen

B = weight of soaked and surface dried specimen in air

C = weight of the soaked specimen in water.

4.3.2 Insoluble Residue Test

This test was performed to determine the amount and nature of argillaceous material in the ledge samples. ASTM procedure D 3042 was used. Each sample was tested in triplicate. The crushed sample, weighing 500 g, was dissolved in 6N hydrochloric acid (HCl), adding more acid until no further reaction occurred, even on heating. When the reaction was complete, water was added to fill the container. The dilute solution and the residue were then washed thoroughly over nested sieves consisting of the following series placed in a receiving tank:

No. 4
No. 8
No. 16
No. 30
No. 50
No. 100
No. 200

After this, both the sieves and the residues were oven dried, cooled to room temperature, and the weight of the insoluble material retained on each sieve was determined. The solution that passed the No. 200 sieve was filtered and the filtrate oven dried and weighed to determine the amount of insoluble residue of silt and clay size. The cumulative percent of the insoluble residue retained on each of the sieves, expressed as a percentage of the total sample weight, was then determined. The results, based on an average of three tests for each sample, are provided in Appendix C.

The residue was later examined petrographically for rock and mineral identification. It has been established (102) that the mineral composition of the residue also influences the skid resistance qualities of the aggregate.

4.3.3 Atterberg Limits of Insoluble Residue

This test was conducted to determine the plasticity characteristics of insoluble residue passing 200 sieve so that it could be classified as silt, silty clay or clay. Liquid limit, plastic limit, and plasticity index were determined and the values for each sample were plotted on Cassagrande's plasticity chart.

The liquid limit of a soil is the water content, expressed as a percentage of the oven-dried weight of the soil, at which two halves of a soil pat separated by a groove of standard dimensions will close at the bottom of the groove along a distance of 1/2 inch under the impact of 25 blows in a standard liquid limit device. The plastic limit of a soil is the water content, expressed as a percentage of the oven-dried weight of the soil, at which the soil begins to crumble when rolled into a thread 1/8 inch in diameter. The plasticity index is the difference between the two limits and is an important parameter in determining the engineering behaviour of soils. The ASTM Test for the Liquid Limit of Soils (D-423), and the Test for Plastic Limit and Plasticity Index of Soils (D-424) were followed for these determinations. The results for individual samples are supplied in Appendix C along with those of insoluble residue.

4.3.4 Hydrometer Analysis of Insoluble Residue

This test was performed to determine the amount of clay particles present in the minus 200 fraction of insoluble residue which consists of both silt and clay. The hydrometer method of analysis is based on Stokes' Law, which relates the terminal velocity of a sphere falling freely through a fluid to its diameter. The relation is expressed according to the equation:

$$V = \frac{\gamma_s - \gamma_f}{180\eta} D^2$$

where: V = terminal velocity of sphere, cm per sec

γ_s = density of sphere, g per cm³

γ_f = density of fluid, g per cm³

η = viscosity of fluid, g-sec per cm²

D = diameter of sphere, mm.

It is assumed that Stokes' Law can be applied to a mass of dispersed soil particles of various shapes and sizes. The hydrometer is used to determine the percentage of dispersed soil particles remaining in suspension at a given time. The maximum grain size equivalent to a spherical particle is computed for each hydrometer reading using Stokes' Law.

A hydrometer graduated in specific gravity and designated as type 152H was used. The ASTM procedure, Particle-Size Analysis of Soils (D 422), was followed. Only the residue from poor quality stone from each quarry was included in this analysis.

4.3.5 X-ray Diffraction Analysis of Insoluble Residue

The objective of this test was to determine the type of clay minerals which comprised the insoluble residue. A Siemens D500

diffractometer was used to obtain the diffraction patterns. The analysis was first accomplished on the powdered specimens and then on oriented mounts. Powdered specimens were used to provide coverage on diffraction patterns for all the ledges so that any differences in the clay and non-clay minerals from ledge to ledge and from one quarry to another quarry could be detected. Subsequently, oriented mounts were used for clay mineral analysis only in order to confirm the presence or absence of a particular clay mineral by enhancing basal reflections.

Oriented specimens are prepared on a glass slide in which a suspension of clay is allowed to evaporate while free from disturbance. Alternative techniques intended to improve the perfection of the orientation of the clay platelets by the application of pressure have been recommended by Mitchell (103). Brown (104) and Kinter and Diamond (105) have proposed the use of centrifuge. A paste technique in which the sample is smeared on the slide has been described by Thiesen and Harward (106).

For the present study a method similar to that of Mitchell was used. The insoluble residue was dispersed in demineralized water, allowed to stand overnight, and then the clay suspension from it was decanted off and filtered through a flat-bottomed funnel while applying an aspirator. The layer of sedimented clay was then transferred gently from the filter paper to a glass slide. Three oriented mounts were prepared from each specimen, one air dried, the second treated with glycerol, and the third heated to 550°C for 1 hour. X-ray diffraction patterns were recorded for these differently treated specimens from 3° to 14° 2 θ since most of the first order peaks appear in this range.

4.3.6 Absorption-Adsorption Test

This test was proposed and described by Klieger et al. (91) to identify nondurable aggregates and is based on the absorption and adsorption values. The absorption value roughly indicates pore volume whereas the adsorption value at 92 percent humidity is a rough indicator of surface area. Both pore volume and surface area are closely related to frost susceptibility of an aggregate. Klieger and his coworkers established a pass-fail criterion based on the service record of the aggregates studied. The test was included in the current study to determine how well it correlates with the results of other tests and to check its usefulness in identifying nondurable argillaceous carbonate aggregates.

Procedure

The same procedure was used in the current study as described by Klieger et al. One inch diameter cores were drilled from the aggregate samples. These cores were cut into 1/16 to 1/8 inch thick slices using a low speed saw (Isomet 11-1180, Buehler Ltd.). Alternate slices were used for absorption and for adsorption measurements.

Absorption

In the absorption study, slices were vacuum oven dried for 48 hours, then transferred to a desicator and cooled to room temperature. Slices were weighed in a weighing bottle on an analytical balance. Next, slices were vacuum saturated in a desicator using boiled demineralized water and applying an aspirator. On alternate days, the slices were removed from water, towel dried to the saturated surface dry condition, and placed in the weighing bottle for reweighing. This

weighing procedure was repeated until weight gains were no longer recorded. The absorption was determined as follows:

$$\text{Absorption(\%)} = \frac{\text{Final Weight} - \text{Oven dry weight}}{\text{Oven dry weight}} \times 100$$

Adsorption

The adsorption measurements were made on the alternate set of slices. These were first crushed to the 8 to 16 sieve size, then vacuum oven dried and placed in a weighing bottle of known tare weight. The material was subsequently cooled to room temperature in a desiccator containing calcium chloride. The bottle was stoppered and weighed on the analytical balance to obtain the oven dried weight. After this the bottle was opened and placed, together with the stopper, in a desiccator containing a saturated solution of KNO_3 which maintains a relative humidity of 92 percent. After one day of storage, and on alternate days, the sample was weighed in the stoppered weighing bottle until a weight increase was no longer recorded. The adsorption was determined as follows:

$$\text{Adsorption(\%)} = \frac{\text{Final weight} - \text{Oven dry weight}}{\text{Oven dry weight}} \times 100$$

4.3.7 Pore-Size Distribution

Pore-size distribution of ledge samples and the unsound aggregate pieces from pavement cores was measured because of its strong influence on freeze-thaw durability. The mercury intrusion method was used to measure the pore-size distribution. The equipment used was capable of intruding pores from approximately 500 microns to .0027 microns (27 \AA) in size. Pores smaller than 27 \AA are unimportant because the water in

them does not freeze at ordinary freezing temperatures while pores larger than 500 microns are also harmless as water can be easily expelled from them as the water expands on freezing.

The mercury intrusion technique employs the principle that the surface tension of a non-wetting liquid (a liquid that forms a contact angle of at least 90° with a solid) will oppose the entry of the liquid into a small pore of a solid. Washburn (107) determined that the non-wetting liquid (in this case mercury) can be forced into the pores using external pressure, and this pressure was found to be inversely proportional to the pore diameter. Assuming a cylindrical pore Washburn calculated the relation to be:

$$p = \frac{-4T_d \cos \theta}{d}$$

where: p = external pressure required for intrusion

T_s = surface tension of the intruding liquid

θ = contact angle between the liquid and the solid

d = limiting pore diameter

The most commonly used liquid is mercury because of its low vapor pressure, its nonreactivity, and non-wetting characteristics. By assuming that the quantity $(-4\gamma \cos\theta)$ is constant for a given solid, the relation between the pressure and the pore diameter becomes a linear inverse. The pore size distribution is then obtained by measuring the volume of intruded mercury at various pressure intervals that correspond to diameters of interest. Based on the previous studies by Winslow and Diamond (108), and Kaneuji (41), values of 484 erg/cm^2 and 125° were assumed for γ and θ respectively.

Apparatus

The mercury porosimeter used in this study was manufactured by American Instrument Company, Maryland, and has a maximum capacity of 60,000 psi. Figure 4.1 shows the complete assembly of the instrument. Basically, the porosimeter consists of a pressure vessel, pressure generating pump, and electronic attachments for measuring pressure and intrusion. A fan was added to the side wall of the lower cabinet of the porosimeter to keep the pressure vessel cool. The commercial unit is equipped with the two pressure gauges, 0-5,000 psi and 0-60,000 psi. To increase the accuracy of measurement in the range of pore diameters from 15 microns to 0.5 microns, a third gauge of 0-500 psi was added. A horizontal filling device was used for measuring the intrusion below one atmosphere of pressure, which corresponds to pore diameters of about 500 microns to 10 microns. The hydraulic fluid used was a mixture of two parts transformer 10C oil and one part kerosene.

Corrections Applied to Intrusion Data

Two kinds of corrections are applied:

1. Below atmospheric pressure, continued compression of the air left in the penetrometer after evacuation has to be subtracted from intrusion reading. This value can be calculated using Boyle's Law.
2. At higher pressures, the mercury is compressed and its volume decreases on the one hand while the heat generated by the pressure causes the mercury to expand on the other hand. Blank tests (tests with a non-porous sample) were made to determine the high pressure corrections.

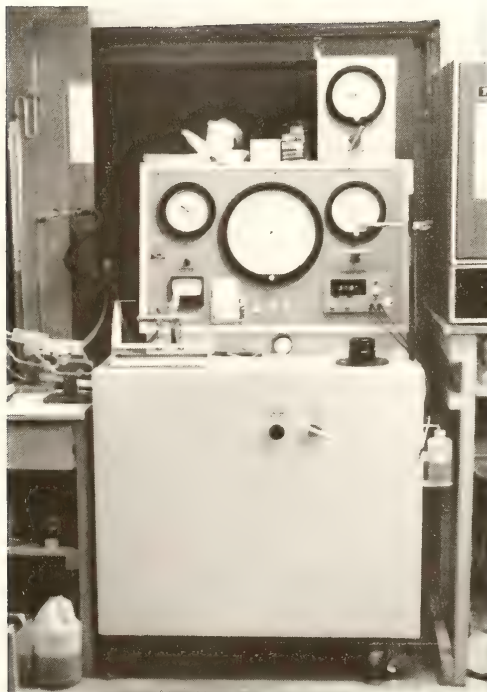


FIGURE 4.1 : MERCURY INTRUSION POROSIMETER

The correction factors for 15 pressure intervals above the atmospheric pressure are shown in Table 4.3. These intervals were chosen because they give approximately equal spacing of data points on a logarithmic scale.

Table 4.3 Correction Factors in Mercury Porosimetry

Pressure (psi)	Correction (ml/ml of Hg in Penetrometer)
30	0.00000
50	0.00000
90	0.00002
150	0.00003
250	0.00005
450	0.00008
800	0.00011
1300	0.00015
2300	0.00020
4000	0.00026
7000	0.00034
12000	0.00042
20000	0.00051
35000	0.00063
60000	0.00076

Procedure

Pore-size distributions were determined for 38 ledge samples and the failed aggregate pieces from 11 pavement cores. At least two pieces of each sample were tested and when the intruded volume was quite different for the first two pieces, the distribution of a third piece was also measured to account for the variation within the same sample. Depending on the porosity of the rock, about 2 to 5 grams of specimen was used. The oven dried sample was initially evacuated and surrounded by mercury inside a penetrometer. The pressure was raised in small increments and the volume of the mercury entering the sample in 1 minute after each pressure increment was recorded. With each pressure

increment, the mercury was forced into the accessible pores in the sample, of a diameter larger than or equal to that calculated by the Washburn equation. For the cumulative intrusion values at different pressures, the corresponding pore diameters were computed using a computer program. The pore-size distribution curves, based on cumulative intrusion for individual samples are supplied in Appendix D.

4.3.8 Iowa Pore Index Test

The ASTM procedure C-666, Method B, used for freeze-thaw testing of aggregate in concrete is not completely satisfactory because of the wide variation in the properties of carbonate aggregate associated with D-cracking. Also a very long time, 5 to 6 months, is required to complete the test. Because of these shortcomings, Wendell Dubberke (78) a geologist with the Office of Materials, Iowa Department of Transportation, developed a shorter and more efficient test called the "Iowa Pore Index Test". The objective of the test was to readily identify the potential of an aggregate for causing D-cracking because of its susceptibility to critical saturation. Because of the promising results of this test in Iowa and Illinois, it was decided to include this test method in the present study.

Apparatus

The apparatus used is shown in Figure 4.2. It is a modified form of a pressuremeter in which the air chamber was replaced with a 1 inch diameter plastic tube graduated to read in milliliters. A 60 psi pressure gauge was added to the lid. A hole was drilled through the side of the pot at the bottom and is used for loading and unloading the pot with cold tap water. Two valves were located at the top of the plastic

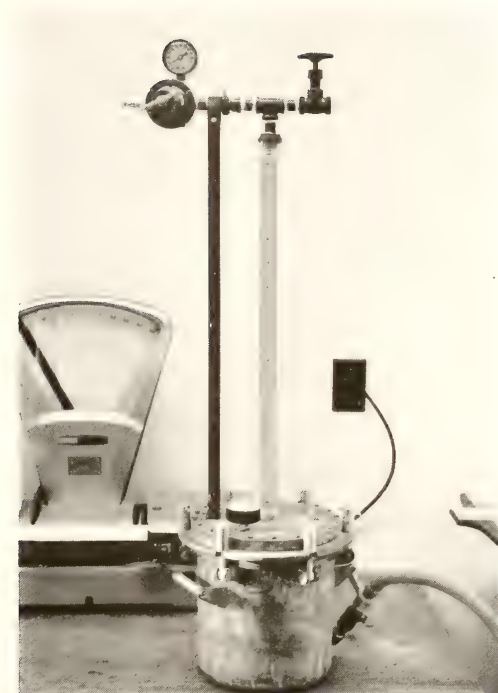


**FIGURE 4.2 : APPARATUS FOR IOWA PORE
INDEX TEST**

tube. One valve was connected to a line supplying air at a constant 35 psi. The other valve was opened while charging the unit with water.

Procedure

9000 grams of oven dried aggregate, ranging from 1/2" - 1 1/2" in size and cooled to room temperature, was placed in the container and covered with tap water to the zero mark in the plastic tube. Air pressure at 35 psi was introduced through the top of the plastic tube. The air valve was kept open throughout the test and a pressure regulator was used to maintain constant pressure. The amount of water injected during the first minute filled the aggregate macropores and was referred to as the primary load. The second reading was taken after a total elapsed time of 15 minutes. The volume of water injected between one minute and 15 minutes was the secondary load and represented the aggregate's micropore system. A secondary load of 50 milliliters was taken to indicate a poor quality aggregate based on the service records of the aggregates tested. The secondary load in milliliters was reported as the final "pore index" value.

4.3.9 Sodium Sulphate Soundness Test

The sulphate soundness test was included in the present study because of its frequent use by the highway agencies. The method is believed to furnish information in judging the soundness of aggregates subject to weathering action. The accumulation and growth of Na_2SO_4 crystals in the pores of the particles is thought to produce disruptive internal forces similar to the action of freezing water. Loss is measured after a specified number of cycles, usually five, in terms of the amount of sample that will pass a sieve smaller than the size upon which it was originally retained.

The test was performed as set out in AASHTO T104. Each portion was placed in an individual pan covered with the solution, and maintained in a temperature controlled water bath for 16 hours, then removed, oven dried for 6 hours, and allowed to cool. Five cycles were performed to complete the test.

Details of the mechanism by which the sulphate test disrupts rock particles have been discussed by several authors (43, 46, 49, 50). It is probable that a combination of actions is involved, including not only the pressure of crystal growth but also the effects of heating and cooling, wetting and drying, and pressure developed by migration of solution through pores (43).

The sulphate test has been much criticized by many investigators (22, 28, 45, 46) who believe that it does not simulate exposure to freezing and thawing in concrete nor does it provide a reliable indication of field performance. According to Verbeck and Landgren (22), the mechanism of disruption in the sulphate soundness test is different from the development of pressure by an advancing front of freezing water. It has been suggested that the sulphate soundness test loss depends more upon the quantity of pores than upon their more critical characteristics of size and distribution (44, 109). However, it is generally agreed that a low soundness test loss is usually, but not always, evidence of good durability, whereas a high loss places the aggregate in a questionable category until performance data become available.

The results of sodium sulphate soundness and Freeze-Thaw tests are presented in Appendix E. These tests were performed by the personnel of the Division of Materials and Tests, IDOH, on the samples provided by the writer.

4.3.10 Unconfined Freeze-Thaw Test

Freezing and thawing tests of unconfined aggregate have been the most frequently suggested alternative to sulphate soundness (67, 68, 110, 111). The method appears to be more directly comparable to that of severe exposure of concrete. Over the years many attempts have been made to improve the correlation between the laboratory freeze-thaw test and the performance of aggregates in concrete. Variables investigated include sample type and size, pretest treatment, rate and conditions of freezing and thawing and addition of small volume of alcohol (67), usually 5%, to water. A general correlation has been found and confidence has been expressed. However, Verbeck (22) has pointed out that the destructive effects of particles freezing in concrete are not simulated by freezing them in an unconfined state.

Freezing and thawing of unconfined aggregate in a dilute solution of alcohol is increasingly being used for evaluating soundness (67). The use of alcohol accelerates the destructiveness.

The unconfined freeze and thaw test in water was performed as set out in AASHTO T103, procedure A. The samples were tested in a Conrad automatic freezing unit. The freeze time was approximately 3 hours and the thaw time was approximately 2 hours per cycle. Each portion of the sample was placed in plastic bags and totally covered with water. The samples were tested for 50 cycles.

4.3.11 Modified Freeze-Thaw Test

In an effort to develop a better test method for determining the soundness of aggregates, the Division of Materials and Tests, Indiana Department of Highways, has proposed a new method (11). It is pointed

out that the present method (AASHTO T103, procedure C) of determining the freeze and thaw losses of aggregates does not duplicate the actual in-place conditions to which the material gets subjected. The present method specifies freezing the specimens in 1/4 inch of water. Because of the salt solutions used for ice and snow removal the actual in-place conditions commonly result in the materials being frozen in a totally immersed salt solution. With this criteria in mind, the following test method was established:

1. The individual, oven dried samples, after cooling to room temperature, are placed in plastic bags, completely covered with a 5% (by mass) aqueous solution of sodium chloride (NaCl), allowed to soak for 24 hours, and then placed in the freezing chamber.
2. The samples are subjected to 25 cycles of alternate freezing and thawing.
3. The freezing time is kept at 3 hours or more at -15° to 5°F and the thawing time is 55 minutes or more at $75^{\circ}\text{F} \pm 5^{\circ}$.

Studies by the Division of Materials and Tests have shown that the results from the proposed test method appear more realistic than those obtained from the current test method. Those materials which have a good service record show very low losses and those which have a poor service record show very high losses (close to 100%) when subjected to the proposed test method.

The modified method, however, appears to be too stringent. In order to check its validity, tests on all the ledge samples included the proposed, modified freeze-thaw test (NaCl test).

CHAPTER 5

RESULTS AND DISCUSSION

This chapter is concerned with the results of laboratory investigations and the implications and significance of these results. Data from different tests were correlated with field performance of the aggregates involved to establish a relationship between physical characteristics and their frost resistance. Results from different tests were also correlated with the percent insoluble residue and measures of pore characteristics, these being the two most reliable indicators of freeze-thaw durability.

5.1 Petrographic Analysis

5.1.1 Thin Section Study

Petrographic description of individual ledge samples is supplied in Appendix A and a brief description on ledge by ledge basis is given in Chapter 3. One of the main objectives of the petrographic analysis was to determine the amount, type, and manner of distribution of argillaceous material. The term argillaceous material is used here to include both silt and clay. The analysis shows that nondurable argillaceous carbonates are characterized by a large amount and a uniform distribution of argillaceous material and generally by a fine grained texture. A comparison with field performance also shows that some highly argillaceous rocks, if laminated, can be frost resistant.

Argillaceous material is found to exhibit three modes of distribution:

1. As finely divided material uniformly distributed throughout the rock.
2. As thin, irregular streaks.
3. As small, elongated flakes.

The high relief and high birefringence of the flakes suggest that the clay is illite in composition. Because of a very fine grained, dust-like nature of the argillaceous material an accurate value for its content cannot be determined with certainty under the microscope. Also, the relative proportions of silt and clay cannot be estimated from thin section study. Other tests are needed in this regard to supplement petrographic information.

Fine, hair-like cracks were found to be a common feature in some samples, especially those from Quarry L. Figure 5.1 shows the presence of such cracks and the ease with which the rock breaks along them. The presence of such cracks would aid in aggregate disintegration once high hydraulic pressure develops.

5.1.2 Acid Etching

Acid etching techniques were used to supplement petrographic information concerning the distribution of argillaceous material. Etching the smooth rock surfaces with hydrochloric acid brings out structural features such as laminations etc., which are not evident on fresh surfaces. The results of etching tests on some specimens are shown in Figure 5.2 and in Appendix B. Where the rock is laminated, the shaly partings clearly stand above the etched surface. By contrast, when the argillaceous material is evenly distributed throughout the rock, the

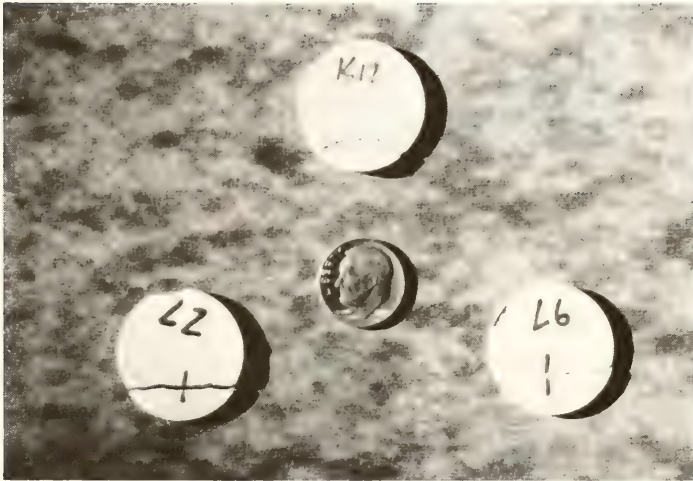


**FIGURE 5.1 : BREAKAGE OF THE AGGREGATE ALONG
MICROFRACTURES**

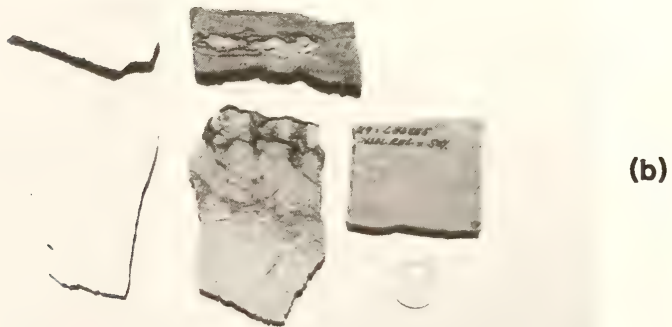
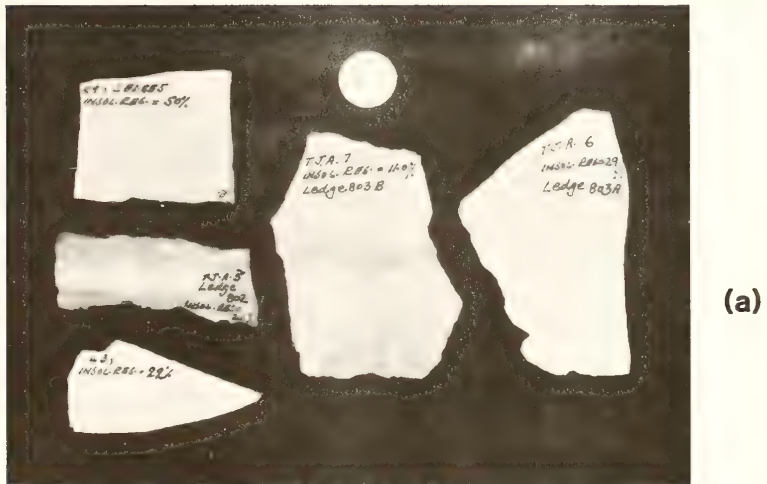


**FIGURE 5.2 : COMPARISON OF THE ETCHED SAMPLES
FROM THE THREE QUARRIES :
(a) UNETCHED, (b) ETCHED**

etched surface stays more or less smooth or finely pitted with a few pyrite grains sticking out. The silt and clay particles are removed as the surrounding carbonate material is dissolved away giving rise to a false impression that the rock is either non-argillaceous or less argillaceous than the laminated one. In case of ledge 5 from quarry K, which contains upto 50% argillaceous material, the etched surface is again smooth but the concentration of silt and clay in short lenticular areas can be clearly seen. These lenticules are evenly distributed throughout.

The results of the acid etching test confirm the findings of the thin section analysis in that the unsound rocks under consideration in this study are those with argillaceous materials uniformly distributed throughout and are not necessarily the laminated samples as concluded by Patton (95) or Willman (82).

Petrographic examination of pavement cores showed that:

1. Aggregate damage is purely of physical nature and is confined only to the pavement surface.
2. Only the aggregate is involved in pavement damage; the surrounding concrete remains intact as shown in Figure 5.3.
3. The aggregate damage generally is not controlled by any plane of weakness such as laminations. However, in some cases presence of microfractures or an argillaceous streak might have aided aggregate breakage.
4. Low strength, weak matrix, and hydraulic pressures appear to be the chief factors in failure mechanism.

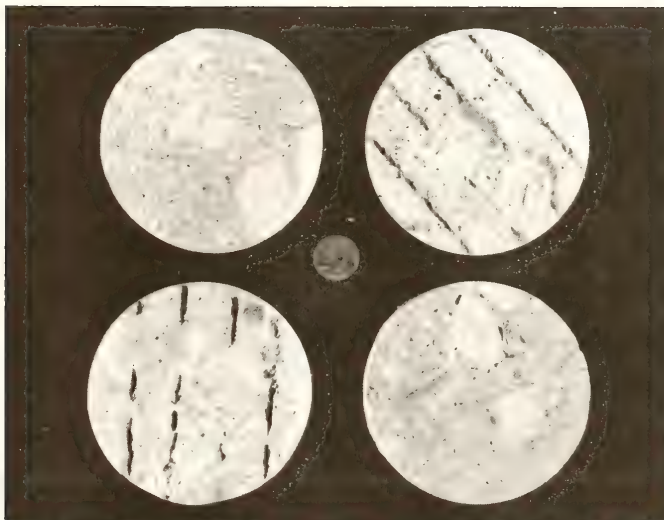


**FIGURE 5.3 : CONCRETE CORES SHOWING THAT ONLY
THE AGGREGATE IS INVOLVED IN
CONCRETE PAVEMENT DAMAGE**

Petrographic examination of insoluble residue shows that chert, quartz, and pyrite are the chief minerals in the material coarser than the 200 sieve whereas quartz, pyrite, and illite constitute the materials that pass the 200 sieve.

5.2 Specific Gravity, Absorption, and Degree of Saturation

Specific gravity and absorption values are shown in Table 5.1. Ledges 801 and 803A from quarry T and 2 and 5 from quarry K have a bulk specific gravity of less than 2.5 and an absorption of 4% or more. It is these ledges that yield the nondurable aggregate. On the other hand those ledges which yield acceptable aggregate have relatively higher specific gravities and low absorption values. Sample L3 from quarry L is an exception. Although it performed poorly in the field, yet its specific gravity is more than 2.5 and its absorption less than 4%. However, the damage caused by this aggregate, which comes from the upper transition zone of Louisville Limestone, was not as severe as that shown by the Mississinewa Shale Member. Other tests show that Louisville Limestone is a good quality aggregate except in the transition zone where it degrades into a marginal aggregate.

Sample T3 is highly laminated but its absorption is quite low. This is contrary to the earlier work by Patton (95) who concluded that laminated rocks are nondurable because of their higher absorption.

Table 5.1 also shows the degree of saturation values. Degree of saturation was calculated in two ways:

1. From the specific gravity and absorption data. Based on the mineral composition of the rock, a weighed average value of the specific gravity of solids was assigned to each sample.

Table 5.1 Specific Gravity, Absorption, and Degree of Saturation

Sample No.	Quarry	Ledge No.	Specific Gravity		Percent Absorption	Degree of Saturation (%)
			Bulk	SSD		
T1	T	801*	2.36	2.48	5.13	91.73
T2	T	801*	2.33	2.46	5.23	86.00
T3	T	802	2.47	2.51	1.38	44.21
T4	T	802	2.64	2.66	0.70	37.36
T5	T	803A*	2.44	2.55	4.86	110.71**
T6	T	803A*	2.35	2.69	5.33	92.83
T7	T	803B	2.66	2.67	0.48	39.75
T8	T	803B	2.61	2.66	2.00	94.71
T9	T	803B	2.59	2.62	0.94	52.27
T10	T	7	2.68	2.69	0.32	60.97
K1	K	5*	2.43	2.55	4.39	98.96
K3	K	5*	2.48	2.58	4.00	99.06
K5	K	5*	2.41	2.52	4.64	93.69
K7	K	5*	2.39	2.51	4.86	96.15
K9	K	5*	2.40	2.52	2.86	94.25
K11	K	4	2.51	2.58	2.70	78.70
K12	K	4	2.57	2.64	2.45	90.00
K13	K	4	2.62	2.67	2.00	99.17
K14	K	4	2.62	2.67	2.00	91.60
K15	K	4	2.54	2.60	2.50	85.71
K16	K	3	2.60	2.63	1.77	88.75
K17	K	3	2.62	2.65	1.47	92.59
K18	K	3	2.62	2.67	1.79	96.38
K19	K	2*	2.41	2.54	5.50	99.12
K20	K	2*	2.33	2.49	6.75	97.59
L1	L	6	2.59	2.65	0.86	45.87
L2	L	6	2.65	2.67	0.80	72.54
L3	L	6*	2.55	2.61	2.50	97.11
L4	L	6	2.56	2.61	1.96	63.69
L5	L	6	2.60	2.64	1.83	93.68
L6	L	6	2.57	2.62	2.25	91.60
L7	L	6	2.60	2.62	0.79	75.22
L8	L	6	2.69	2.71	0.50	80.00

* Unsound on the basis of field performance.

** Data may be erroneous.

The following specific gravity values were assigned to each mineral: calcite 2.72; dolomite 2.86; illite 2.6; quartz 2.65; and pyrite 5.0 (112).

2. From the mercury porosimeter and the absorption-adsorption test data.

Both calculation methods are illustrated in Appendix F. The unsound aggregates from this study exhibit degree of saturation values greater than 90% except for sample T2. However, several sound aggregates, with low absorption values, also show saturation values in excess of 90%. Thus both a high absorption and a high degree of saturation are required for an aggregate to fail in freeze-thaw. Based on these findings an absorption of 4% or greater and a degree of saturation of 90% or greater indicate those aggregates studied which fail by the pitting and popout mechanism.

The specific gravity, absorption, and degree of saturation values confirm the studies conducted by others (25-29) that unsound coarse aggregates can be characterized by a low bulk specific gravity, a high absorption, and a high degree of saturation. The test, however, is not fool proof and can pass certain poor quality aggregates.

5.3 Amount and Nature of Insoluble Residue

Lemish, Rush, and Hiltrop (9), Bisque and Lemish (10), and Willman (82) found that the amount and type of insoluble residue play an important role in determining the frost susceptibility of argillaceous carbonates from Iowa and Illinois. The insoluble residue test was performed to determine the total amount of residue in Indiana aggregates under study. Details of residue including the amount of residue

retained on each sieve, mineral composition, and Atterberg Limits of the silt and clay size material are given in Appendix C. The amount of silt and clay size residue for each sample is shown in Table 5.2.

Residues coarser than the 200 sieve consist chiefly of quartz, pyrite, and chert. Quartz is the major constituent and its amount increases rapidly with decreasing grain size. It constitutes 70-90% of the fractions retained on 100 and 200 sieves, the rest being mostly pyrite. Except for a few highly cherty samples, the silt and clay size fractions make up the major part of the residue.

Table 5.2 shows that those ledges which yield unsound aggregate are characterized by high silt and clay content ranging from 20 to 45%. In the case of samples K5, K7, K9, K19, and K20, even the material coarser than 200 sieve consists of lumps of fine sand, silt, and clay. If this is included, the upper limit of silt and clay size material will be close to 50%. Other ledges which yield acceptable aggregate have silt and clay contents of approximately 10% except near their contacts with the more argillaceous ledges, most of the contacts being gradational.

It should be pointed out that some of the highly laminated ledges have residue contents far less than those which are not laminated. For example ledges 802 and 803B of quarry T are highly laminated, as can be seen from Figure 3.4, but their residue contents are much lower than those for ledges 801 and 803A which are not laminated. The same is true of quarry K where the residue content of ledge 2, which is laminated, is less than the nonlaminated ledge 5.

The degree of lamination, therefore, is not a good indication of the total amount of argillaceous material present in the rock although it has generally been thought to be so in the past (82).

Table 5.2 Amount of Silt and Clay Size Residue

Sample No.	Quarry	Ledge No.	% Residue
T1	T	801*	25.8
T2	T	801*	26.5
T3	T	802	20.6
T4	T	802	8.3
T5	T	803A*	29.3
T7	T	803B	10.1
T8	T	803B	17.3
T10	T	Jeff.LS(7)	1.9
K1	K	5*	19.7
K3	K	5*	23.7
K5	K	5*	43.7
K7	K	5*	43.6
K9	K	5*	45.5
K11	K	4	8.5
K12	K	4	11.0
K13	K	4	10.1
K14	K	4	8.4
K15	K	3	4.9
K16	K	3	7.4
K17	K	3	8.0
K18	K	3	17.3
K18(b)	K	3	13.1
K19	K	2*	29.2
K20	L	6	37.7
L1	L	6	13.0
L2	L	6	11.6
L3	L	6*	22.0
L4	L	6	10.5
L5	L	6	10.3
L6	L	6	10.1
L7	L	6	8.6
L8	L	6	2.8

* Unsound on the basis of field performance.

5.3.1 Plasticity Characteristics

The Atterberg Limits were determined for the silt and clay fraction of the insoluble residue. For each quarry the liquid limit and plasticity index values were plotted on Cassagrande's plasticity chart as shown in Figures 5.4, 5.5, and 5.6. Figure 5.7 is a combined plot for the three quarries for comparison. As can be seen from these figures the residue from the Mississinewa Shale Member ranges from silt and clay of medium plasticity to silt of low plasticity, the former being characteristic of quarry T and the latter of quarry K. The residue from the Louisville limestone of quarry L is mostly clay of low plasticity.

5.3.2 Amount of Clay

Hydrometer analysis was performed to determine the amount of clay present in the silt and clay size fraction of the residue. The grain size distribution for each quarry is shown in Figures 5.8, 5.9, and 5.10. Material finer than 0.005 mm is considered to be clay. The results show that the amount of clay present is quite small in all three quarries. However, the relative difference in clay content between the three quarries is obvious, the residue from quarry T being most clayey and that from quarry K being least clayey with quarry L occupying the intermediate position.

The distribution curves also indicate maximum percentage of small size particles in quarry T and minimum in quarry K.

Chemical analyses of those ledges whose residue was subjected to hydrometer analysis are given in Table 5.3. The data were obtained from the Industrial Minerals Section of the Indiana Geological Survey. It is assumed that half of the alumina combines with silica to form clay

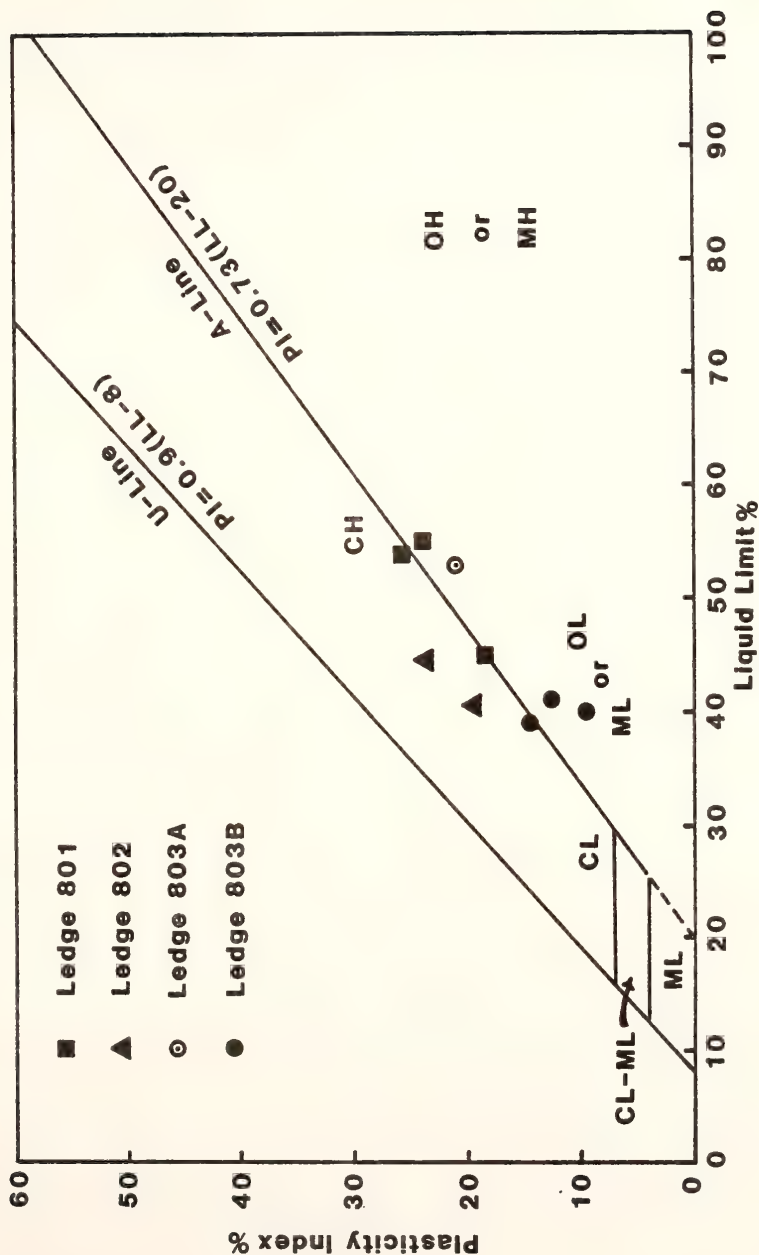


FIGURE 5.4: CASAGRANDE'S PLASTICITY CHART SHOWING TYPE OF INSOLUBLE RESIDUE (-200 SIEVE) FROM QUARRY T

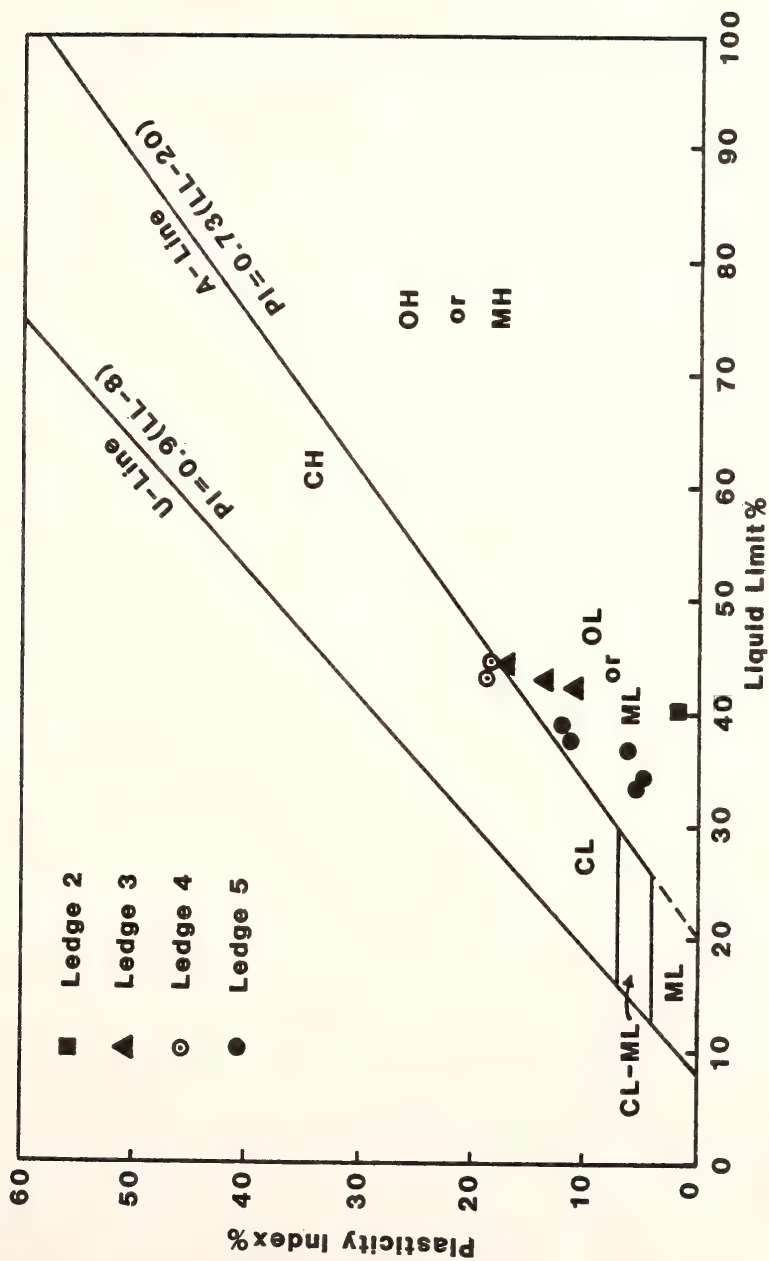


FIGURE 5.5: CASAGRANDE'S PLASTICITY CHART SHOWING TYPE OF INSOLUBLE RESIDUE (-200 SIEVE) FROM QUARRY K

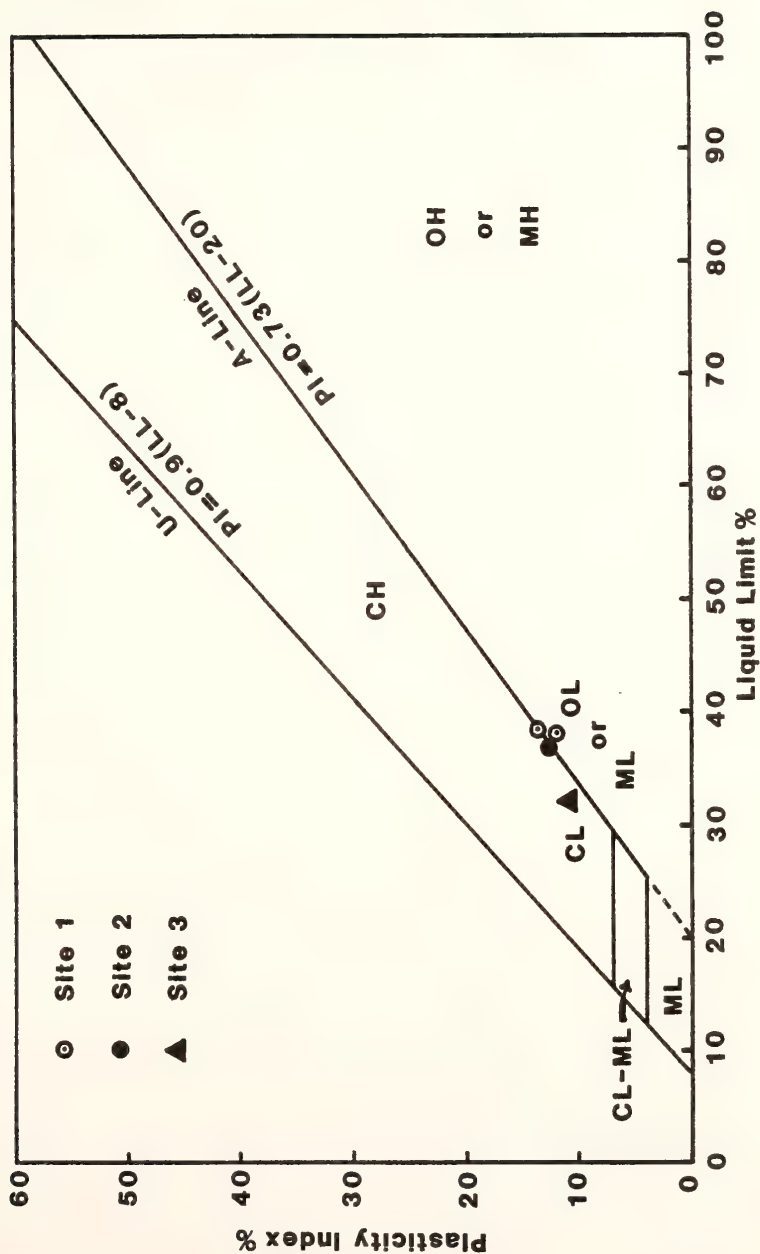


FIGURE 5.6: CASAGRANDE'S PLASTICITY CHART SHOWING TYPE OF INSOLUBLE RESIDUE (-200 SIEVE) FROM QUARRY L

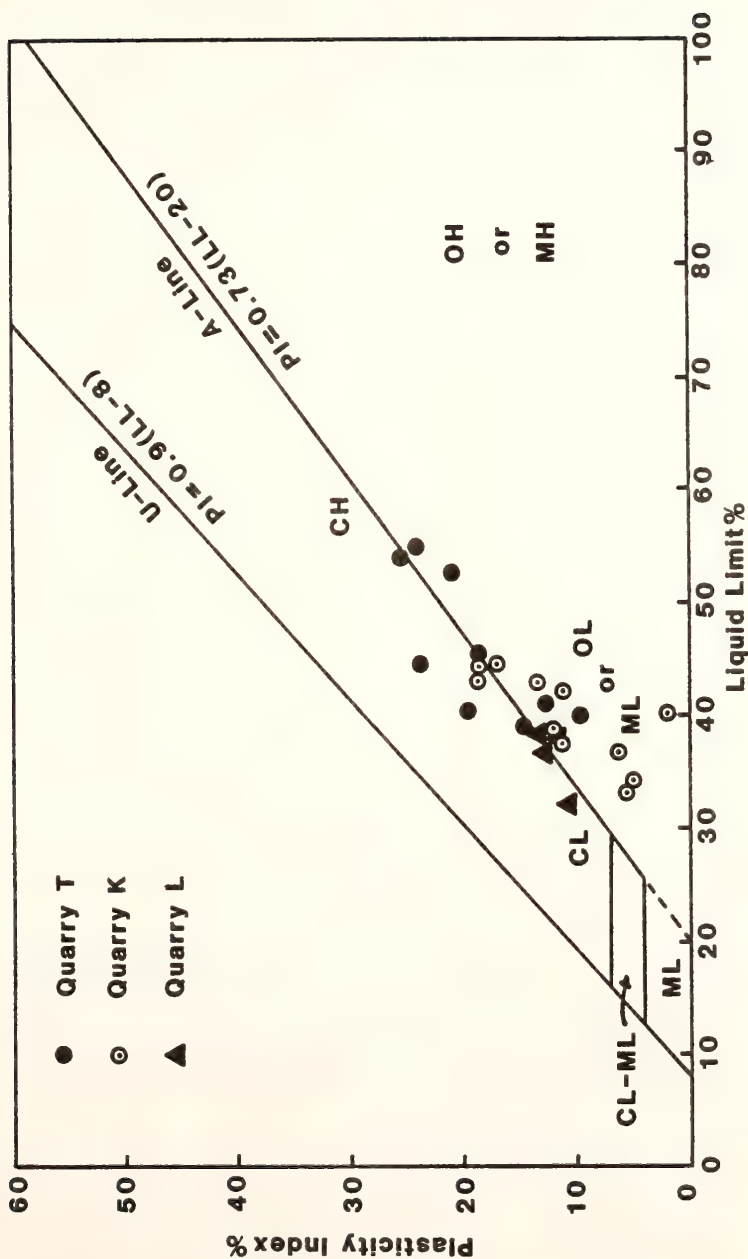


FIGURE 5.7: CASAGRANDE'S PLASTICITY CHART SHOWING TYPE OF INSOLUBLE RESIDUE (-200 SIEVE) FROM THE THREE QUARRIES

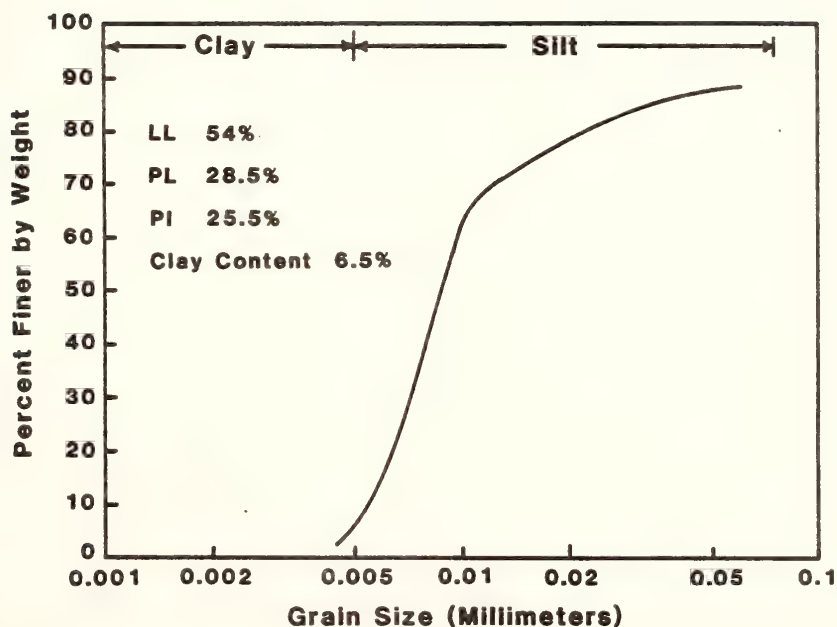
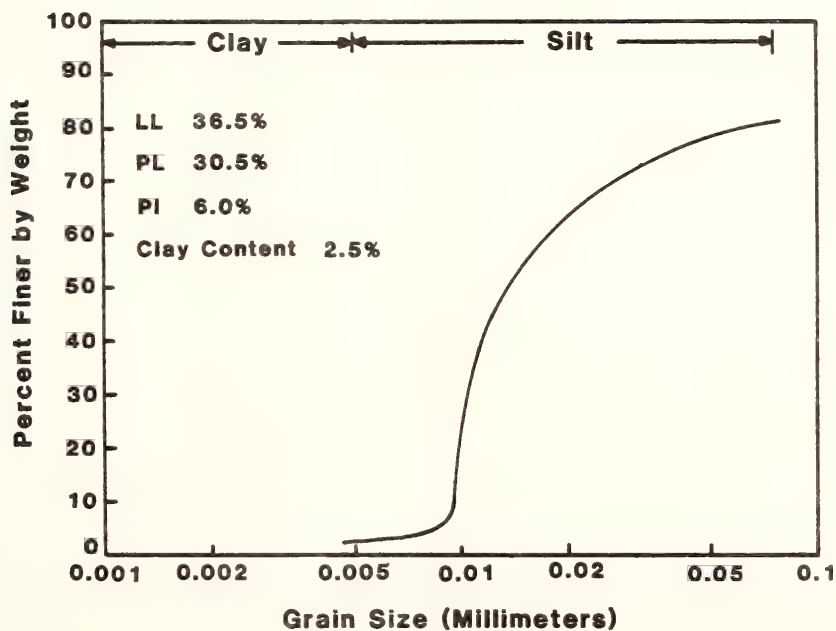


FIGURE 5.8: GRAIN SIZE DISTRIBUTION OF INSOLUBLE RESIDUE (PASSING 200 SIEVE), LEDGE 801, QUARRY T



**FIGURE 5.9: GRAIN SIZE DISTRIBUTION OF
INSOLUBLE RESIDUE (PASSING 200
SIEVE), LEDGE 5, QUARRY K**

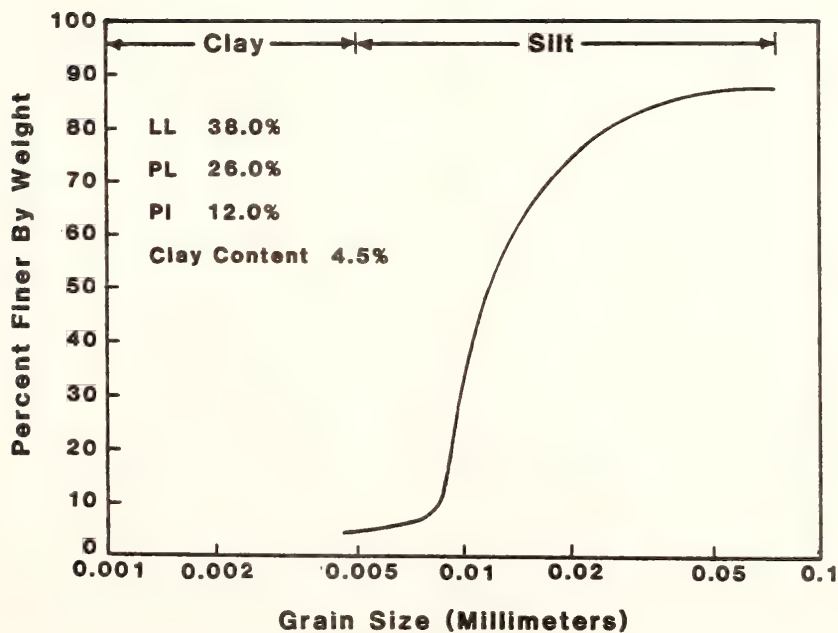


FIGURE 5.10: GRAIN SIZE DISTRIBUTION OF INSOLUBLE RESIDUE (PASSING 200 SIEVE), LEDGE 6 (1' FROM ROOF) , QUARRY L

Table 5.3 Chemical Analyses of Ledge Samples from the Three Quarries*
(Indiana Geological Survey)

Sample No.	Quarry	Ledge No.	Al ₂ O ₃ %	SiO ₂ %	Al ₂ O ₃ SiO ₂	Clay** %	Quartz(Silt) %	Clay/Silt
T1	T	801	3.93	16.50	0.23	4.70	13.75	0.34
T5	T	803A	3.60	17.20	0.21	4.32	14.68	0.29
K19	K	2	6.10	36.0	0.17	7.32	31.73	0.23
L3	L	6	2.70	11.9	0.22	3.24	10.01	0.32

* Chemical analysis of ledge 5 from quarry K was not available; however, ledge 5 and ledge 2 are quite similar.

** Al₂O₃:SiO₂ ratio in illite is 5:7. The percentage of clay is considered to be equal to the sum of Al₂O₃ and SiO₂ according to this ratio assuming that only half of Al₂O₃ combines with SiO₂.

minerals. Most of the remaining silica will then exist as silt size particles. On this basis, quarry T contains most clay and least silt, quarry K most silt and least clay with quarry L having intermediate position. This is in keeping with the results obtained by hydrometer analysis.

5.3.3 Type of Clay Minerals by X-Ray Diffraction

The silt and clay size fractions were also investigated for the type of clay minerals present using the X-ray diffraction method. Figures 5.11 to 5.14 show that the composition of the silt and clay fraction is the same for all ledges of the same quarry and also from one quarry to the other. Quartz appears as a conspicuous mineral in every case. Illite is the only clay mineral indicated by X-ray analysis of the powdered samples. Oriented specimens of clay were prepared and X-rayed to confirm the absence of other clay minerals. The corresponding diffractograms are shown in Figures 5.15, 5.16, and 5.17. The inclusion of only one peak at 10 angstroms confirms that illite is the only clay mineral present.

It was pointed out earlier that unsound ledges are characterized by a high insoluble residue content and its uniform distribution throughout the rock unit. The residue includes both silt and clay. It will be shown later that the amount and type of clay in the residue influences the degree of freeze-thaw damage and other related physical properties.

5.4 Absorption-Adsorption Characteristics

The results of absorption-adsorption test for the three quarries are shown in Table 5.4 and are plotted in Figures 5.18, 5.19, and 5.20.

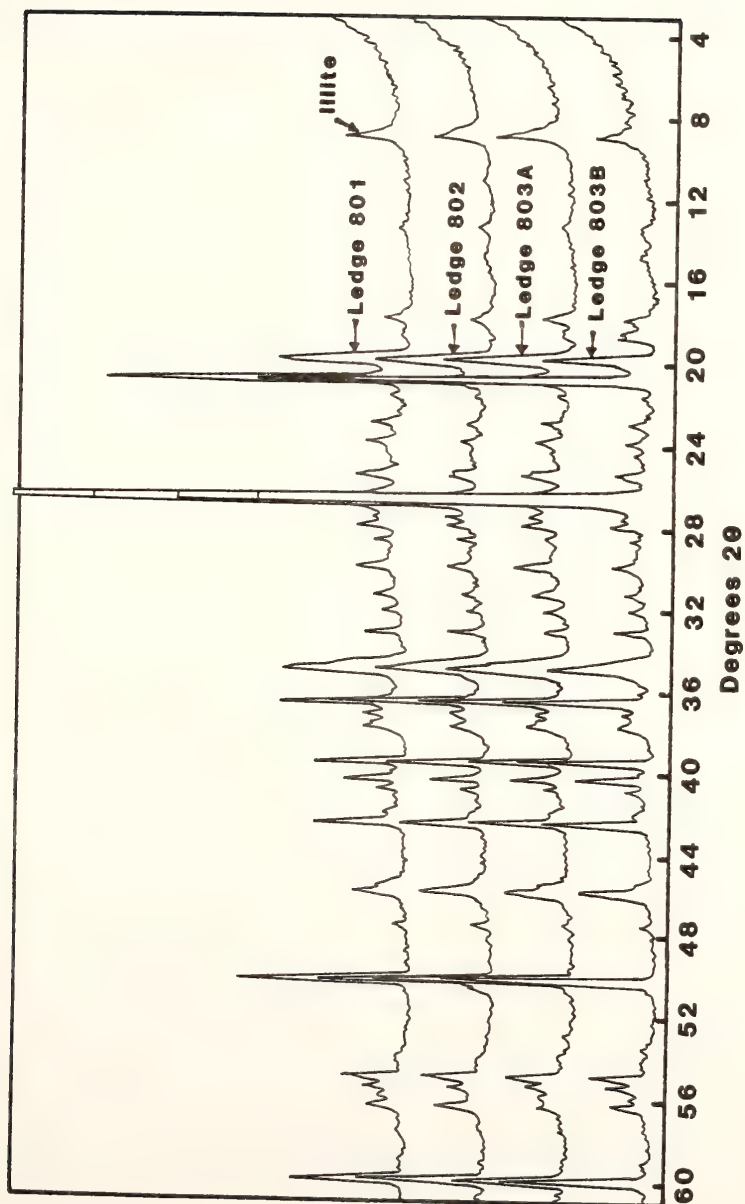


**FIGURE 5.11: X-RAY DIFFRACTOGRAMS OF INSOLUBLE RESIDUE FOR
DIFFERENT LEDGES OF QUARRY T**

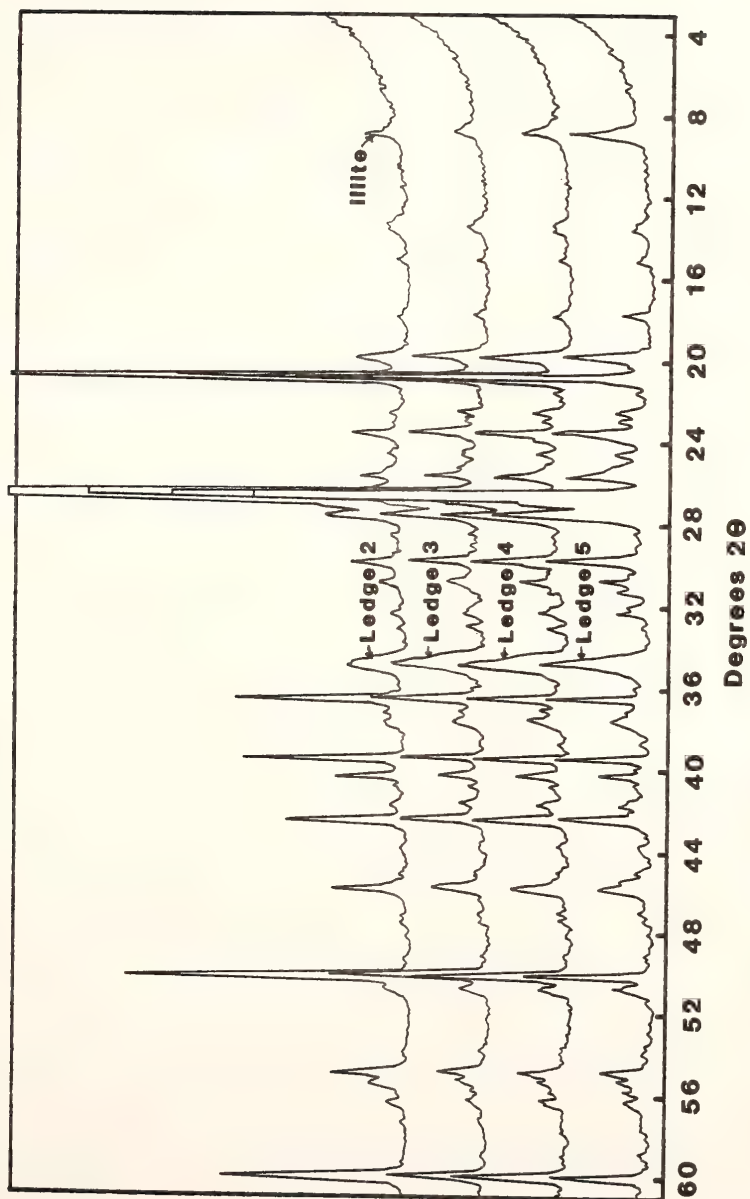
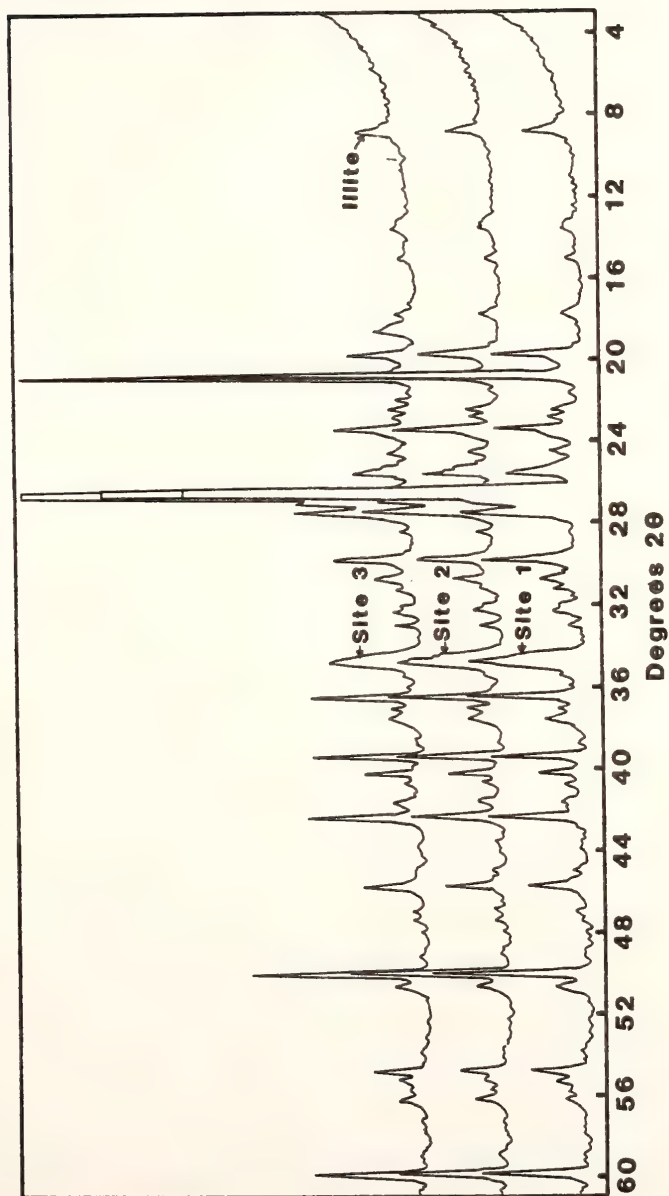


FIGURE 5.12: X-RAY DIFFRACTOGRAMS OF INSOLUBLE RESIDUE FOR
DIFFERENT LEDGES OF QUARRY K



**FIGURE 5.13: X-RAY DIFFRACTOGRAMS OF INSOLUBLE RESIDUE FOR
LEDGE 6 (DIFFERENT SITES) OF QUARRY L**

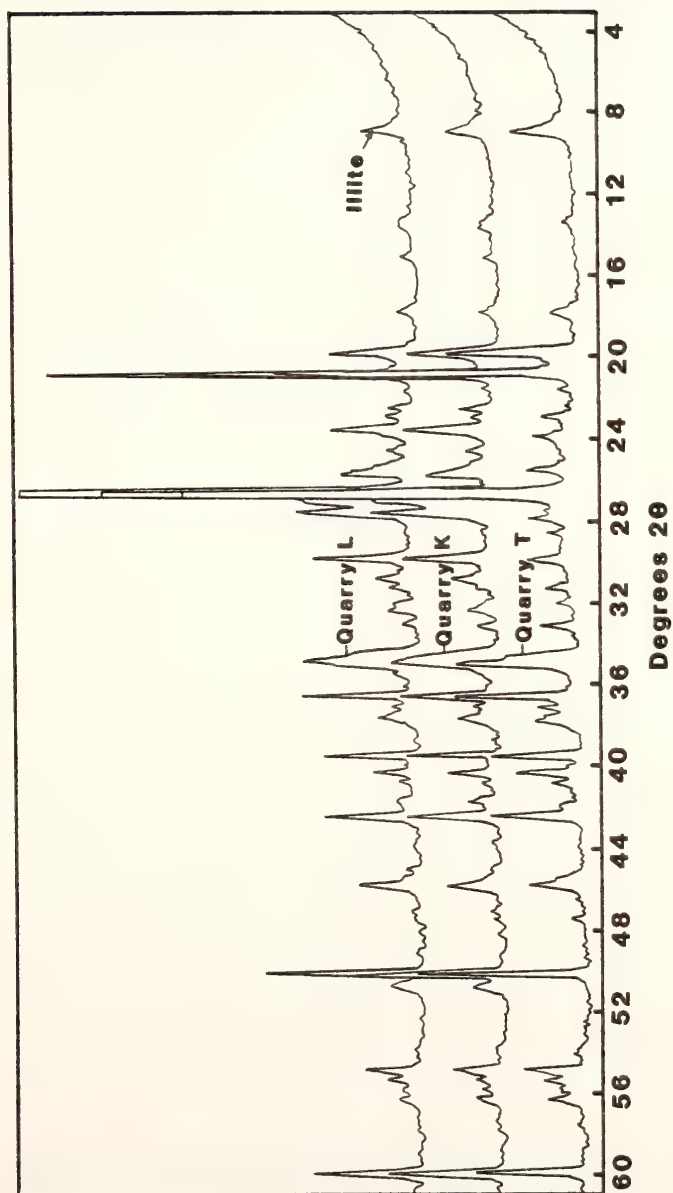


FIGURE 5.14: X-RAY DIFFRACTOGRAMS OF INSOLUBLE RESIDUE FOR QUARRIES T, K AND L

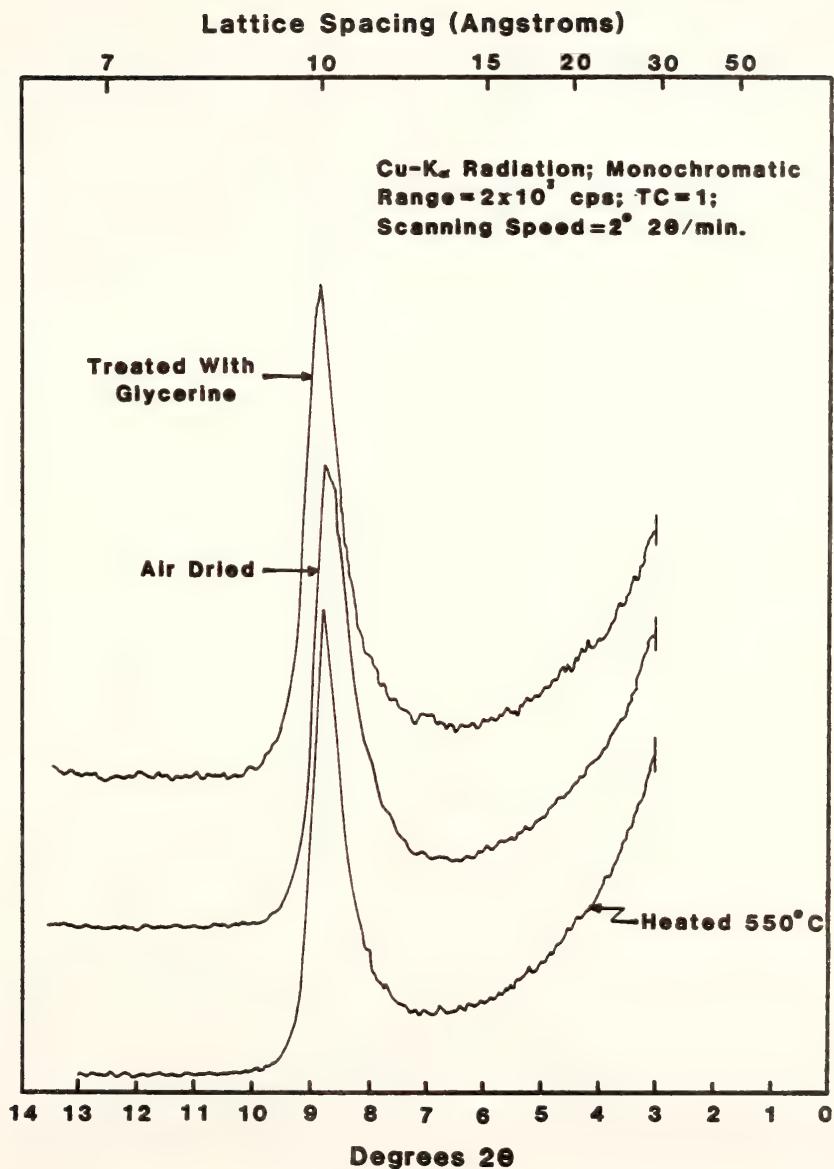


FIGURE 5.15: X-RAY DIFFRACTOGRAMS OF ORIENTED MOUNTS OF DIFFERENTLY TREATED CLAY FROM QUARRY T

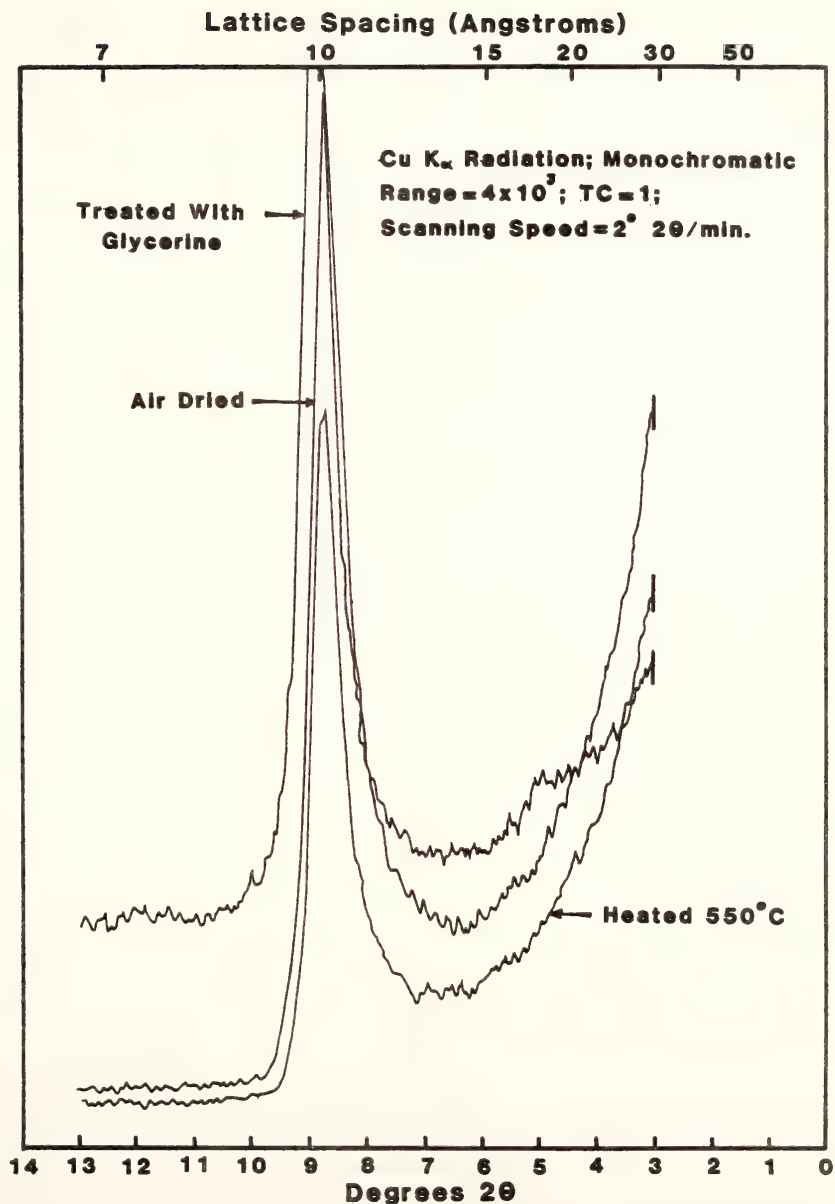


FIGURE 5.16: X-RAY DIFFRACTOGRAMS OF ORIENTED MOUNTS OF DIFFERENTLY TREATED CLAY FROM QUARRY K

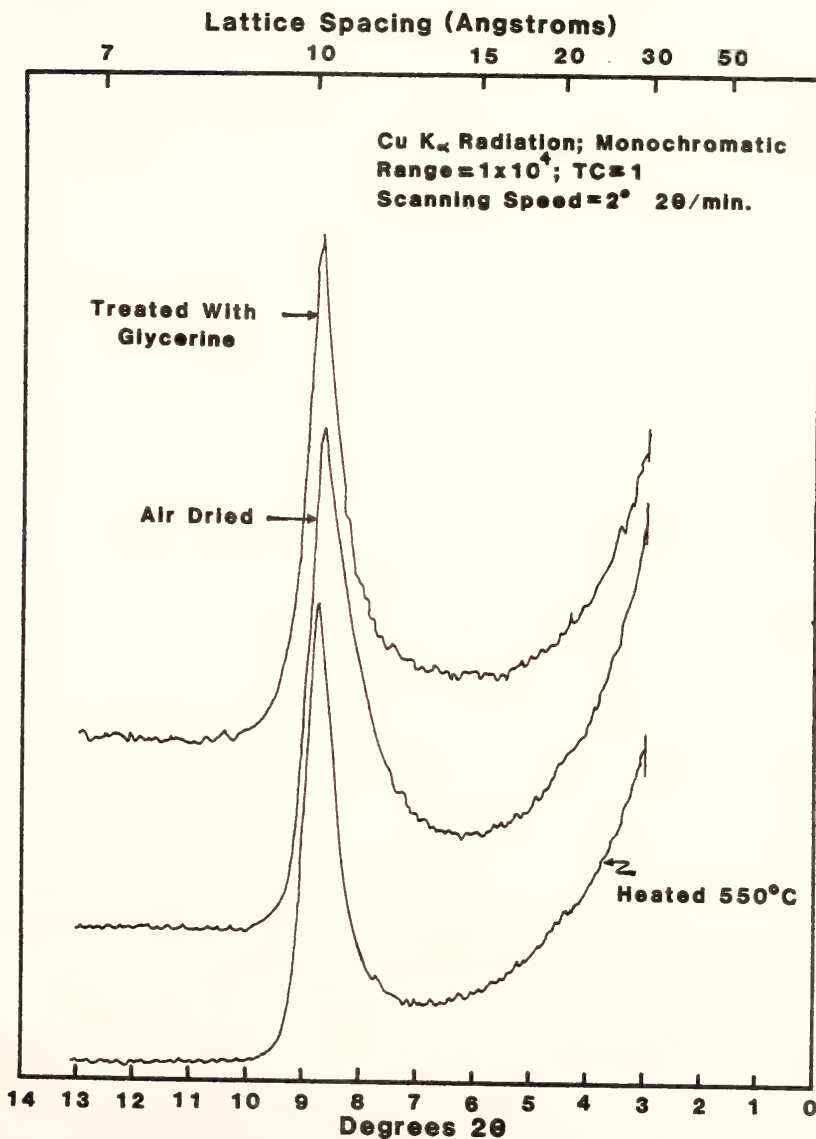


FIGURE 5.17: X-RAY DIFFRACTOGRAMS OF ORIENTED MOUNTS OF DIFFERENTLY TREATED CLAY FROM QUARRY L

Table 5.4 Results of Absorption-Adsorption Test

Sample No.	Quarry	Ledge No.	Absorption** (%)	Adsorption** (%)
T1	T	801*	6.21	3.00
T2	T	801*	6.24	3.58
T3	T	802	1.79	1.54
T4	T	802	0.99	0.76
T5	T	803A*	5.28	2.29
T7	T	803B	0.83	0.36
T10	T	Jeff. LS(7)	0.27	0.16
K1	K	5*	4.92	1.41
K3	K	5*	4.48	2.02
K5	K	5*	4.64	2.25
K7	K	5*	4.82	2.20
K9	K	5*	4.83	2.22
K11	K	4	1.98	0.22
K12	K	4	3.30	0.62
K13	K	4	3.20	0.72
K14	K	4	2.24	0.30
K15	K	3	1.77	0.18
K16	K	3	2.16	0.30
K17	K	3	1.24	0.33
K18	K	3	1.60	0.28
K19	K	a*	3.88	0.52
K20	K	2*	8.88	1.09
L1	L	6	1.15	0.35
L2	L	6	0.42	0.17
L3	L	6*	1.51	0.72
L4	L	6	2.86	0.57
L6	L	6	2.36	0.98
L7	L	6	0.72	0.35
L8	L	6	-	-

* Unsound on the basis of field performance.

**All values are an average of two tests.

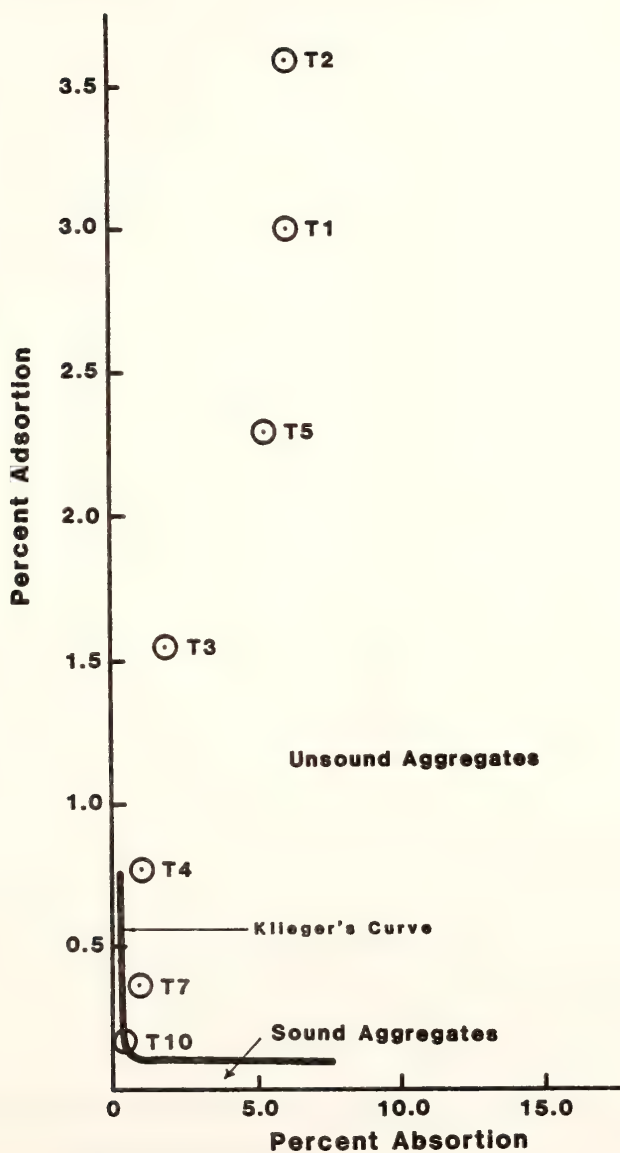


FIGURE 5.18: ADSORTION-ABSORPTION TEST RESULTS FOR QUARRY T

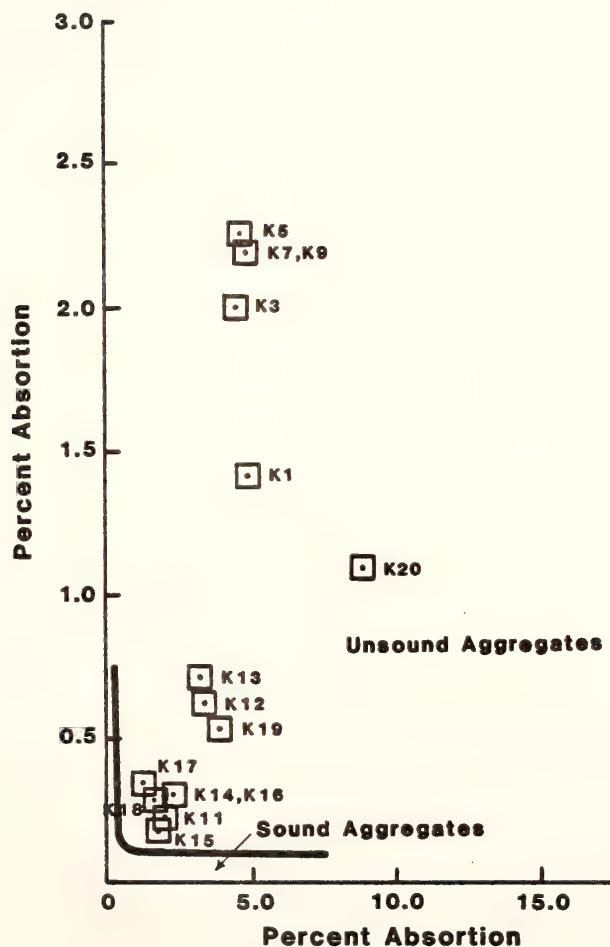


FIGURE 5.19: ADSORTION-ABSORPTION TEST RESULTS FOR QUARRY K

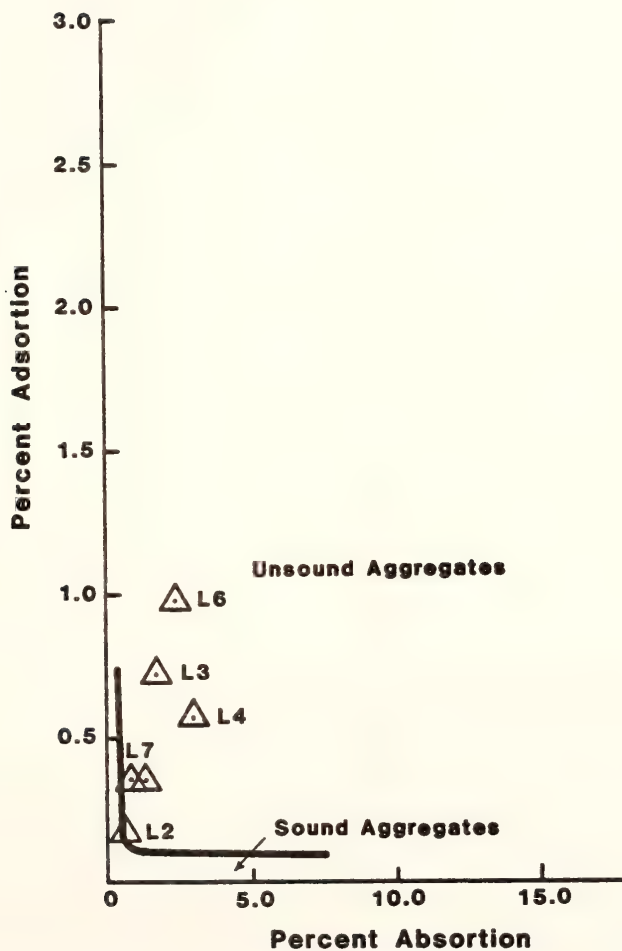


FIGURE 5.20: ADSORPTION-ABSORPTION TEST RESULTS FOR QUARRY L

Figure 5.21 is a combined plot presented for comparison. Only two or possibly three samples from all those taken from the three quarries pass the test. It is clear that the absorption-adsorption criterion as set out by Klieger et al. (91) is too stringent when the rocks involved are argillaceous and the failure mode is pitting and popouts. This is because argillaceous carbonates will generally have high adsorption due to their clay content and will break and popout under hydraulic pressure before that pressure is transmitted to the surrounding concrete to cause D-cracking. In other words those rocks which fail by pitting and popouts are not likely to pass D-cracking criteria. It will be shown later that other test results also support this conclusion.

Both absorption and adsorption are roughly proportional to the amount of argillaceous material present. A comparison between quarries T and K suggests that for the same residue content the rocks with clayey residue (quarry T) have higher absorption and adsorption than do the rocks with silty residue (quarry K), the effect on adsorption being more pronounced.

5.5 Pore Characteristics

5.5.1 Pore-Size Distribution

The size, shape, and distribution of pores in a rock comprise one of the most important properties in determining hydraulic pressure generated in aggregate and concrete during freezing (86).

The pore size distributions for individual ledge samples are given in Appendix D. The average distributions for different ledges in the three quarries are shown in Figures 5.22, 5.23, and 5.24. Those ledges which yield unsound aggregate are characterized by high and sharp

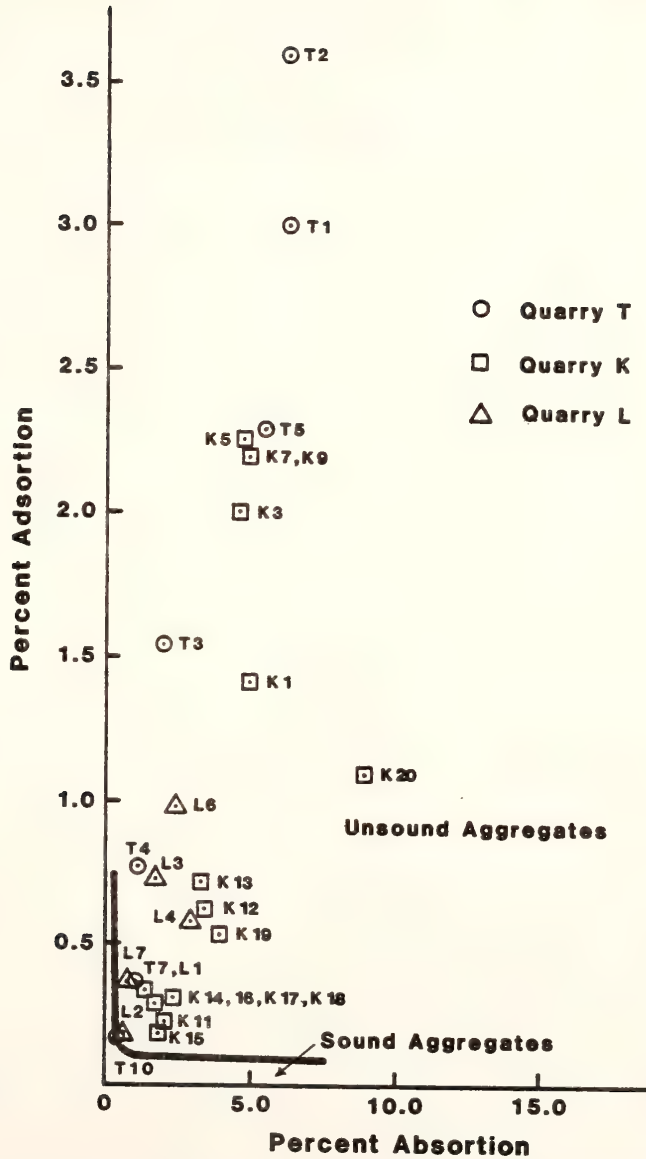


FIGURE 5.21: ABSORPTION-ADSORPTION TEST RESULTS FOR THE THREE QUARRIES

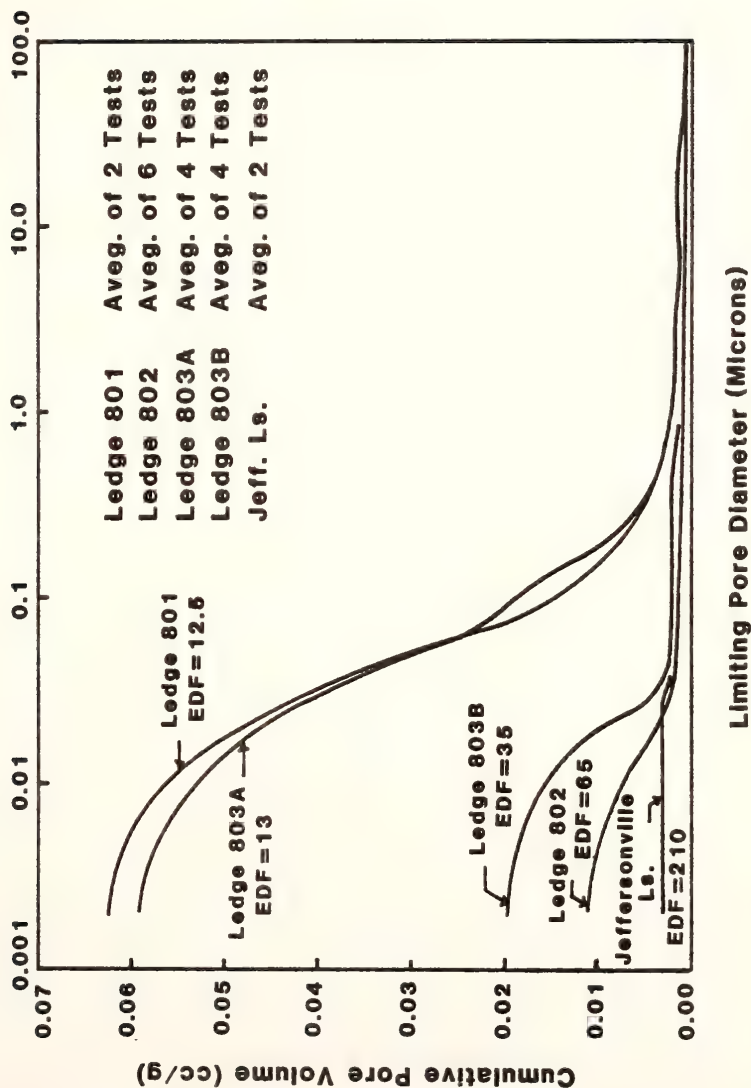


FIGURE 5.22: PORE-SIZE DISTRIBUTIONS FOR DIFFERENT LEDGES OF QUARRY T

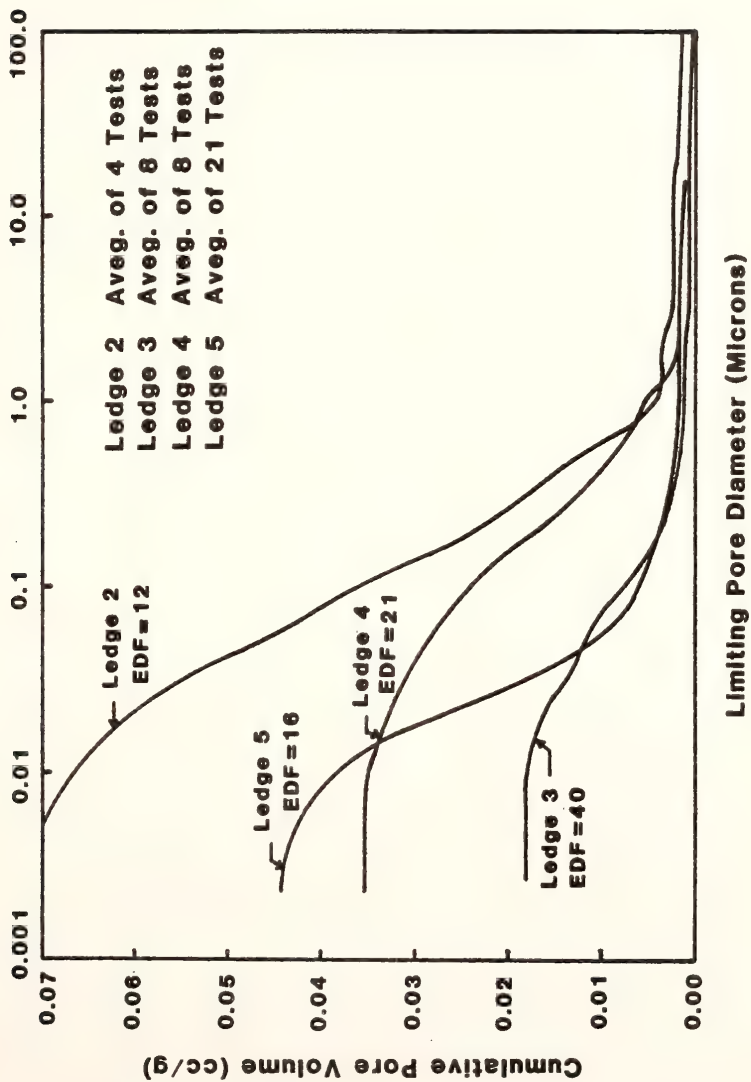


FIGURE 5.23: PORE-SIZE DISTRIBUTIONS FOR DIFFERENT LEDGES OF QUARRY K

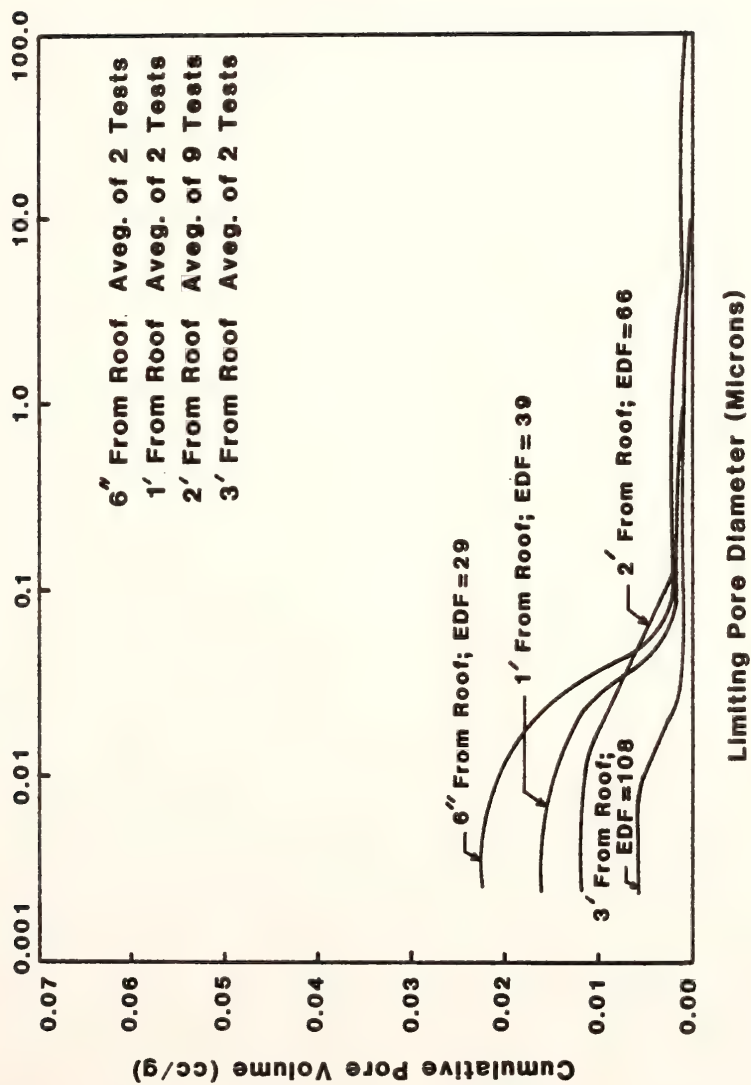


FIGURE 5.24: PORE SIZE DISTRIBUTIONS FOR DIFFERENT LEDGES OF QUARRY L

distribution curves indicating that more than 60% of their pores are smaller than 0.1 micron (10^{-4} mm) in diameter. Table 5.5 shows that most of these unsound ledges have EDF values less than 20. A comparison with the insoluble residue test data shows that for different ledges of the same quarry, the higher the residue content, the larger the volume of small sized pores. However, a comparison of quarry T with quarry K shows that, in addition to the total residue content, the type of residue also influences the pore size distribution. As was mentioned earlier, the residue passing the 200 sieve is more clayey in quarry T and more silty in quarry K. The total residue content is higher for quarry K (ledge 5) than for quarry T (ledges 801 and 803A). Yet, the volume of small sized pores is higher in quarry T than in quarry K. This comparison suggests that the more clayey the residue, the larger the volume of small sized pores.

From the above discussion it can be concluded that the worst aggregate from the freeze-thaw durability point of view is the one which contains a large amount (more than 20%) of insoluble residue of clay composition.

In Figure 5.25 and 5.26 the average pore size distributions for unsound aggregates from pavement cores are compared with those of the poor quality ledges from the respective quarries. This confirms that ledges 801 and 803A of quarry T and ledge 5 of quarry K yield the unsound aggregate. Ledge 2 of quarry K, although unsound, is not included in this comparison because aggregate pieces from it were not found in the cores investigated.

Table 5.5 Expected Durability Factors for Ledge Samples

Sample No.	Quarry	Ledge No.	EDF
T1	T	801*	12.5
T3	T	802	66.0
T4	T	802	63.5
T5	T	803A*	13.0
T7	T	803B	34.0
T10	T	Jeff LS (7)	210.0
K1	K	5*	18.0
K3	K	5*	17.0
K5	K	5*	16.0
K7	K	5*	15.5
K9	K	5*	15.5
K11	K	4	23.0
K12	K	4	23.0
K13	K	4	20.5
K14	K	4	19.0
K15	K	3	23.5
K16	K	3	31.5
K17	K	3	75.0
K18	K	3	45.0
K18(b)	K	3	18.0
K19	K	2*	14.0
K20	K	2*	10.5
L1	L	6	50.0
L2	L	6	36.0
L3	L	6*	32.0
L4	L	6	37.5
L5	L	6	45.0
L6	L	6	29.0
L7	L	6	52.0
L8	L	6	1296.0

* Unsound on the basis of field performance.

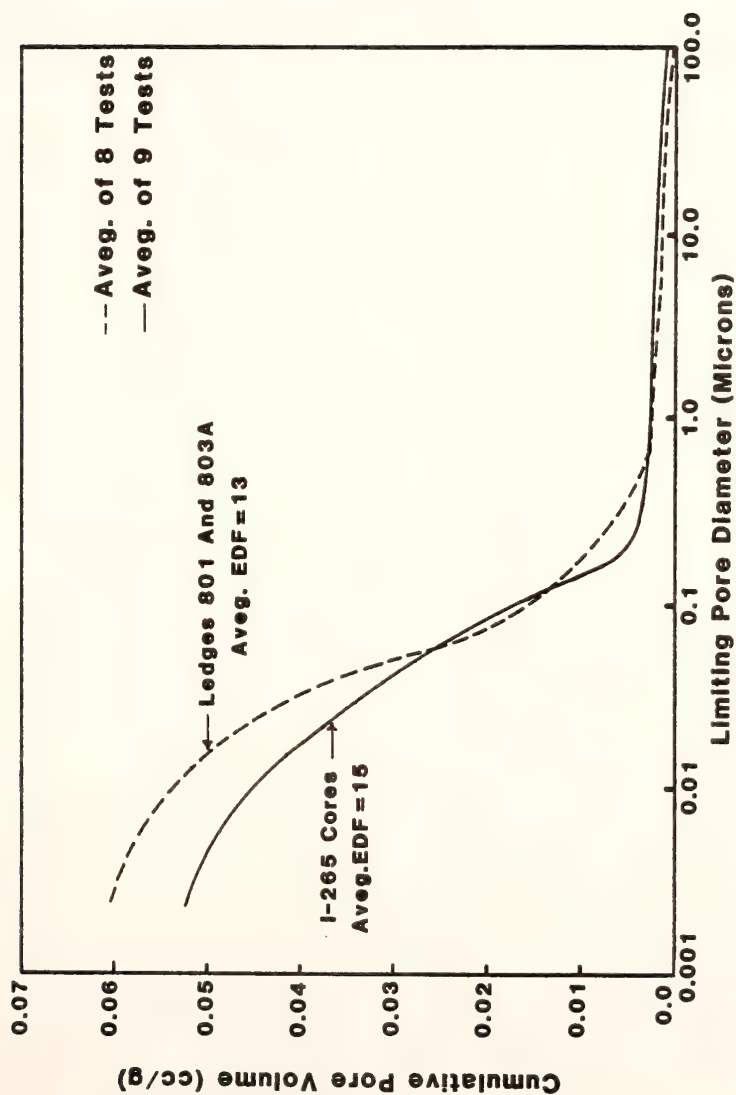


FIGURE 5.25: COMPARISON OF PORE-SIZE DISTRIBUTIONS FOR LEDGES 801 AND 803A OF QUARRY T AND UNSOUND AGGREGATE FROM I-265 CORES

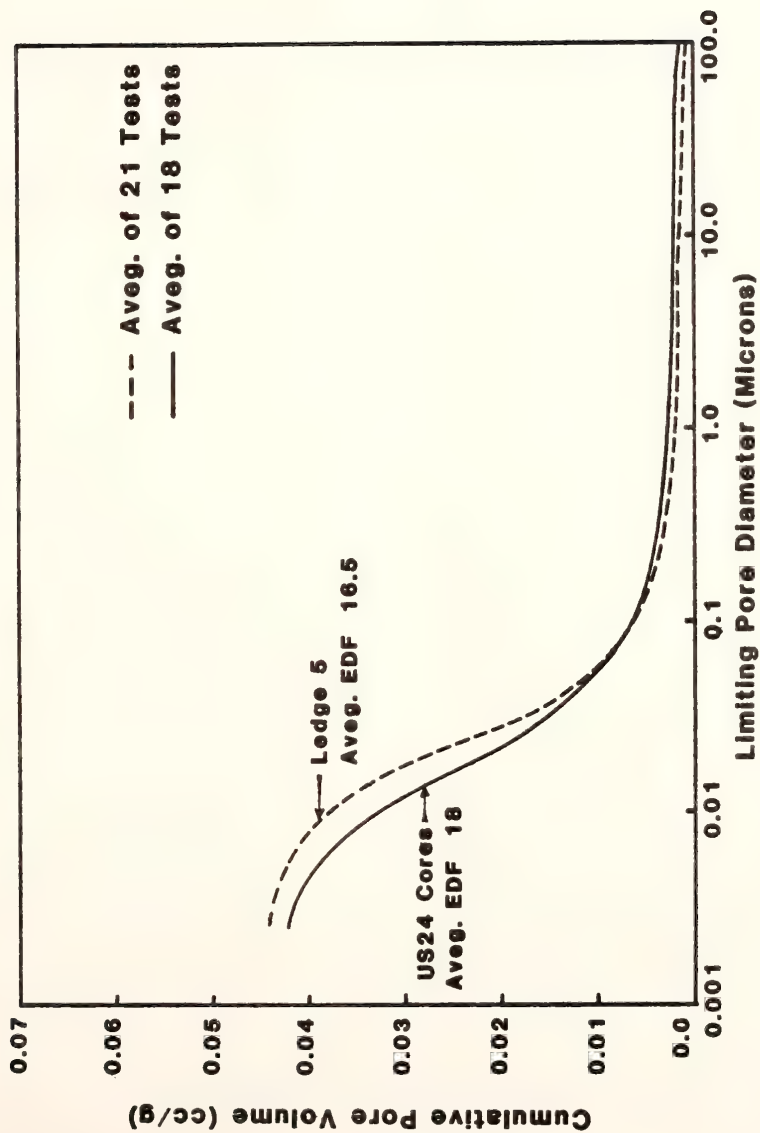


FIGURE 5.26: COMPARISON OF PORE-SIZE DISTRIBUTIONS FOR LEDGE 5 OF QUARRY K AND UNSOUND AGGREGATE FROM US-24 CORES

5.5.2 Iowa Pore Index Test

Another test used to study pore characteristics is the Iowa pore index test. The results of this test are shown in Table 5.6. The unsound aggregate samples are characterized by high values of secondary load which is also referred to as the "pore index". Based on the field performance, a secondary load value of 50 ml is chosen to distinguish between durable and nondurable aggregates. Samples K12, K13, K14, and K18(b) exhibit pore index values of more than 50 ml, yet no evidence of their poor performance was found in the field. This is because their insoluble residue content is less than 20%. These aggregates may be regarded as marginal. If the silt and clay content exceeds 20% and the pore index value is higher than 50 ml the aggregate should be considered unsound.

The state highway departments of Iowa and Illinois use a secondary load of 27 ml to separate sources of aggregate associated with D-cracking from those that have satisfactory service records (78). This value appears to be too low when the aggregate is argillaceous and the failure mode under investigation is pitting and popouts. A limit of 27 ml will reject all of the poor materials and many of the better quality aggregates discussed in this study. This means that an aggregate which passes D-cracking criterion of 27 ml will not result in pitting or popouts. However, there are aggregate uses in which D-cracking is not a consideration and hence general application of this criteria is not in order. More discussion on this subject is presented in section 5.8.

5.6 Sulphate Soundness and Freeze and Thaw Tests

Having established the physical properties of argillaceous carbonates, the next step was to study the influence of these properties on

Table 5.6 Results of Iowa Pore Index Test

Sample No.	Quarry	Ledge No.	Primary Load ** (ml)	Secondary Load** (ml)
T1	T	801*	84	141
T3	T	802	36	17
T4	T	802	26	19
T5	T	803A*	70	123
T7	T	803B	30	19
T10	T	Jeff. LS(7)	24	6
K1	K	5*	95	82
K3	K	5*	85	107
K5	K	5*	58	110
K7	K	5*	69	123
K9	K	5*	54	123
K11	K	4	183	37
K12	K	4	62	53
K13	K	4	82	65
K14	K	4	63	49
K15	K	3	64	32
K18	K	3	41	28
K18(b)	K	3	57	63
K19	K	2*	84	138
K20	K	2*	130	112
L1	L	6	33	29
L2	L	6	24	24
L3	L	6*	44	52
L4	L	6	22	22
L5	L	6	24	13
L6	L	6	28	25
L7	L	6	29	19
L8	L	6	27	9

* Unsound on the basis of field performance.

** All values are an average of at least two tests.

the results of commonly performed acceptance tests. Each sample was tested for sodium sulphate soundness, unconfined freeze and thaw in water and unconfined freeze and thaw in 5% salt solution.

The results of the soundness test are shown in Table 5.7. The aggregates which proved unsound in the field have losses ranging from 15-90% depending on the amount and type of argillaceous material and its manner of distribution. For equal amounts of insoluble residue content, those rocks in which the residue is silty (quarry K) tend to give rise to higher losses than those with more clayey residue (quarry T). Also, laminated rocks (T4, T7, K15-K18) break more than unlaminated ones for the same amount and type of residue.

The results of the unconfined freeze and thaw tests are shown in Table 5.8. In water the unsound aggregates have losses ranging from 7.86% to as much as 83.63%, again depending on the type, amount, and distribution of argillaceous material as well as on total pore volume. Generally speaking, the higher the percent insoluble residue and the more uniformly it is distributed, the higher the loss. Also, the higher the total pore volume, the higher the loss.

When 5% salt solution is used rather than water the losses for unsound aggregates range from 28.15% to 100%. The increase in loss due to salt solution is more pronounced in those rocks in which the argillaceous material is more clayey (T5, T7, and L series) than in which it is silty (K series).

5.7 Correlations

The results of the porosimeter test, the Iowa pore index test, the sulphate soundness test, and freeze-thaw tests were correlated with

Table 5.7 Results of Sodium Sulphate Soundness Test

Sample No.	Quarry	Ledge No.	S.S., 5 cycles
			% Loss
T1	T	801*	13.46
T3	T	802	-
T4	T	802	26.49
T5	T	803A*	32.14
T7	T	803B	29.82
T10	T	Jeff.LS(7)	2.68
K1	K	5*	14.65
K3	K	5*	34.52
K5	K	5*	73.13
K7	K	5*	90.51
K9	K	5*	91.77
K11	K	4	5.23
K12	K	4	8.70
K13	K	4	11.02
K14	K	4	12.23
K15	K	3	23.63
K16	K	3	24.18
K17	K	3	25.59
K18	K	3	24.11
K19	K	2*	28.81
K20	K	2*	93.27
L1	L	6	5.06
L2	L	6	11.02
L3	L	6*	9.70
L4	L	6	6.42
L5	L	6	7.10
L6	L	6	7.27
L7	L	6	5.64
L8	L	6	5.28

* Unsound on the basis of field performance.

Table 5.8 Results of Freeze and Thaw Tests

Sample	Quarry	Ledge No.	Freeze & Thaw (Total Immersion)		Freeze & Thaw (5% Salt Solution)	
			Cycles	% Loss	Cycles	% Loss
T1	T	801*	50	46.30	25	90.66
T3	T	802	50	14.07	25	37.40
T4	T	802	50	3.50	25	37.30
T5	T	803A*	50	61.01	25	93.46
T7	T	803B	50	3.68	25	47.37
T10	T	Jeff.LS(7)	50	1.40	25	1.39
K1	K	5*	50	9.03	25	28.15
K3	K	5*	50	20.56	25	54.00
K5	K	5*	50	40.48	25	99.67
K7	K	5*	50	62.85	25	99.40
K9	K	5*	50	59.72	25	100.00
K11	K	5	50	1.51	25	3.97
K12	K	4	50	3.64	25	15.42
K13	K	4	50	5.81	25	18.11
K14	K	4	50	4.93	25	2.74
K15	K	4	50	9.54	25	16.89
K13	K	3	50	20.06	25	36.92
K19	K	3	50	83.63	25	98.02
K20	K	2*	50	80.66	25	99.73
L1	K	2*	50	2.45	25	28.24
L2	L	6	50	3.53	25	43.23
L3	L	6	50	7.86	25	45.29
L4	L	6*	50	2.60	25	49.97
L5	L	6	50	1.56	25	36.25
L6	L	6	50	3.77	25	34.01
L7	L	6	50	2.97	25	13.75
L8	L	6	50	2.54	25	7.42

* Unsound on the basis of field performance.

the amount of insoluble residue. The results of porosimeter and pore index tests were also correlated to investigate the consistency with which the two tests measure the pore characteristics.

5.7.1 Percent Residue vs EDF

Figure 5.27 shows the relationship between insoluble residue content and expected durability factor. It can be seen that most of the aggregates which proved unsound in the field are characterized by residue contents higher than 20% and EDF values less than 20. Samples T3, K13, K14, and K18(b) are exceptions, however. T3 has more than 20% argillaceous material and is highly laminated. It has a high EDF value and is not associated with pitting and popouts. This is because the concentration of argillaceous material into laminations leaves the rock between the laminations sound and without many small pores. Such a rock, therefore, does not absorb enough water to generate detrimental hydraulic pressures on freezing. However, if the amount of argillaceous material exceeds 30% and if only a portion of it is concentrated in the form of laminations, as in K19 and K20, even the laminated rocks will be susceptible to freeze-thaw damage. K13, K14, and K18(b) have low EDF values, that is a large volume of small pores, but the amount of silt and clay is less than 13%. These aggregates did not fail in the field because their matrix is strong enough to resist hydraulic pressure. This is in keeping with Hadley's findings (113) that the uniform distribution of excessive amounts of silt and clay make the rock skeleton weak. L3 does not have a low EDF but does have a residue content of more than 20%. The residue is mostly uniformly distributed thus giving rise to a weak matrix which is

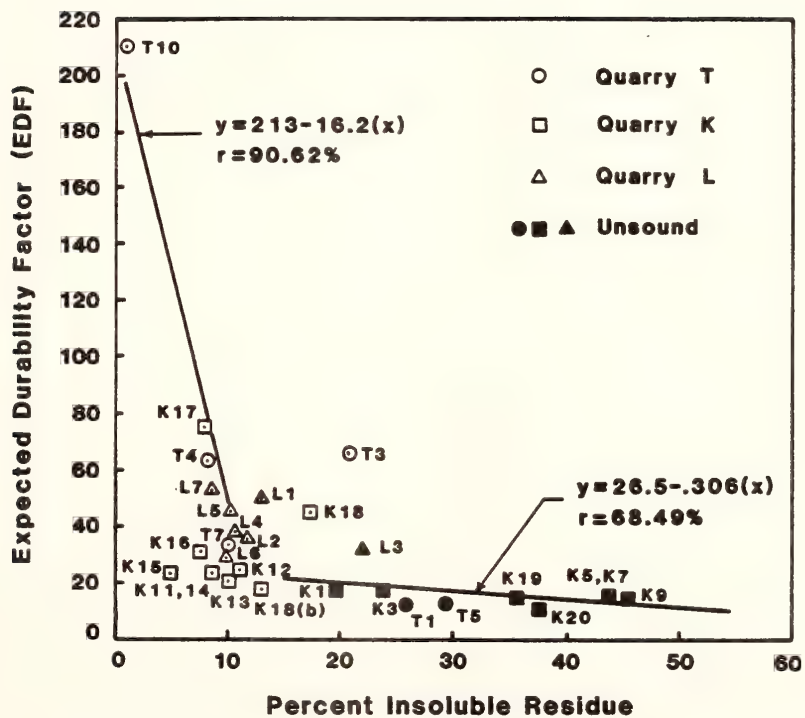


FIGURE 5.27: RELATIONSHIP BETWEEN INSOLUBLE RESIDUE CONTENT (PASSING 200 SIEVE) AND EXPECTED DURABILITY FACTOR

vulnerable to hydraulic pressure. K13, K14, and K18(b) can be regarded as marginal aggregates.

The above discussion shows a strong correlation between percent insoluble residue and field performance of argillaceous carbonates. Percent residue appears to be a better indicator of freeze-thaw durability than pore size characteristics when the carbonate aggregates are argillaceous and when the failure mode is aggregate disintegration and not D-cracking.

Kaneuji (41), in his work on D-cracking related to pore characteristics, proposed an EDF value of 50 to separate durable and nondurable aggregates. A durable aggregate for D-cracking will exceed the requirements to prevent pitting and popouts.

5.7.2 Percent Residue vs Pore Index

Figure 5.28 shows the relationship between residue content and pore index. The pore index is found to be generally proportional to the amount of insoluble residue, the correlation coefficient between the two being 85.87%. The scattering of the data points around the regression line is due to changes in the type and distribution of residue content.

5.7.3 Percent Residue vs Sulphate Soundness Loss

The relationship between residue content and sulphate soundness loss is shown in Figure 5.29. The data are quite scattered indicating a relatively weak correlation. However, a general increase of soundness loss with increasing residue content can still be seen. The scattering of data points is due to variations in the type and distribution of residue, the loss being higher for silty and laminated material. K20 (93.27% loss) is much more laminated than K19 and more silty than T5.

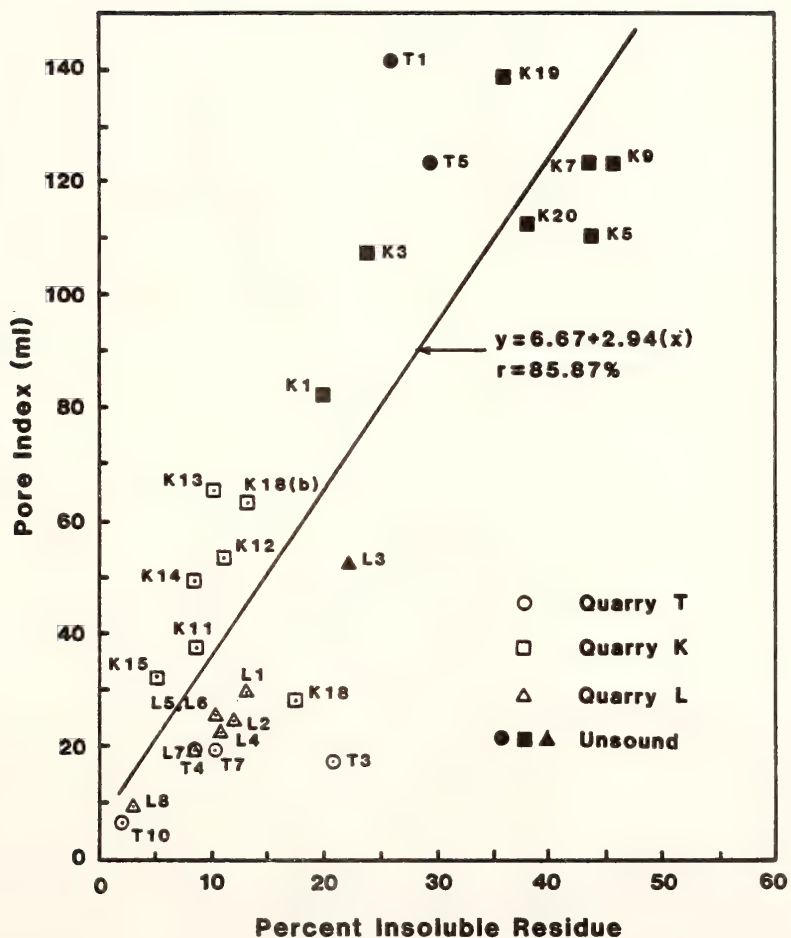


FIGURE 5.28: RELATIONSHIP BETWEEN INSOLUBLE RESIDUE CONTENT (PASSING 200 SIEVE) AND PORE INDEX

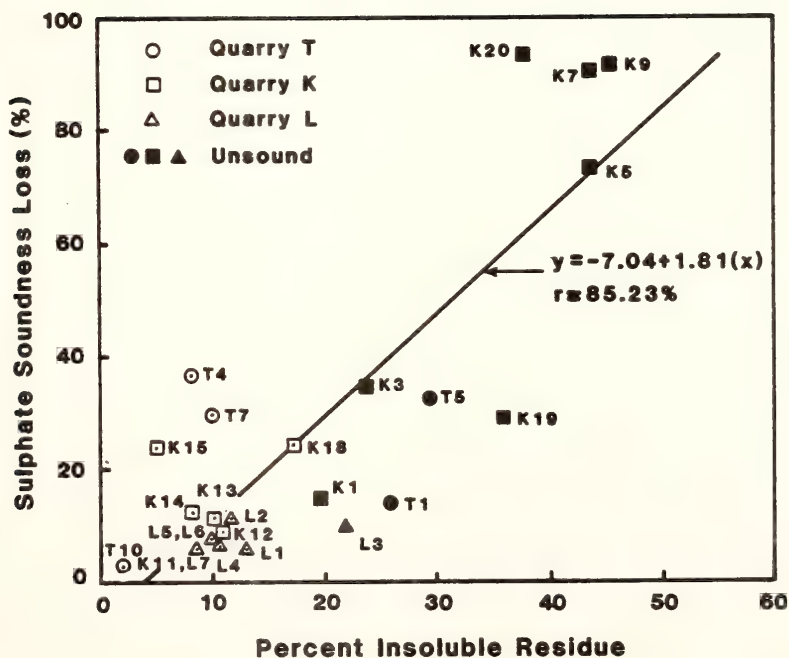


FIGURE 5.29: RELATIONSHIP BETWEEN INSOLUBLE RESIDUE CONTENT (PASSING 200 SIEVE) AND SODIUM SULPHATE SOUNDNESS LOSS

T4 and T7 are less argillaceous but exhibit higher losses because of their laminated nature.

5.7.4 Percent Residue vs Freeze-Thaw Loss

The correlation between percent residue and freeze-thaw loss of unconfined aggregate is shown in Figures 5.30 and 5.31. The freeze-thaw loss in plain water increases rapidly with an increase in residue content once the amount of residue exceeds 20%. Below 20% residue content the increase is gradual. K19 and K20 exhibit the highest freeze-thaw losses although their residue content is less than that of K5, K7, and K9. This is because the total volume of pores in K19 and K20 is higher than that of K5, K7, and K9. This shows the significance of pore volume in controlling freeze-thaw loss.

When 5% salt solution is used instead of water, the relationship between residue content and freeze-thaw loss becomes more linear as seen in Figure 5.31. The pronounced scattering of data points around 10% residue content is due to variations in the type and distribution of residue. For the same residue content, clayey and laminated rocks tend to have higher freeze-thaw losses in salt solution (T and L series are more clayey than K series).

5.7.5 EDF vs Pore Index

The mercury intrusion method is considered to be the most accurate for measuring pore-size distribution and predicting freeze-thaw durability (36-42). The method, however, requires expensive equipment and meticulous procedure. The Iowa pore index test, on the other hand, is inexpensive and easy to perform. In order to check the reliability of the pore index test, the pore index values were correlated with the

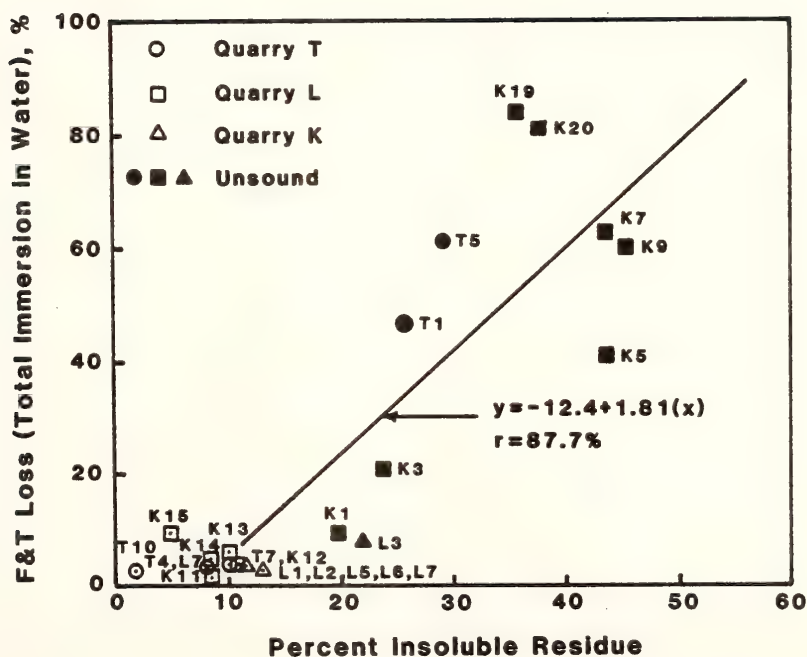


FIGURE 5.30: RELATIONSHIP BETWEEN INSOLUBLE RESIDUE CONTENT (PASSING 200 SIEVE) AND FREEZE-THAW LOSS IN WATER

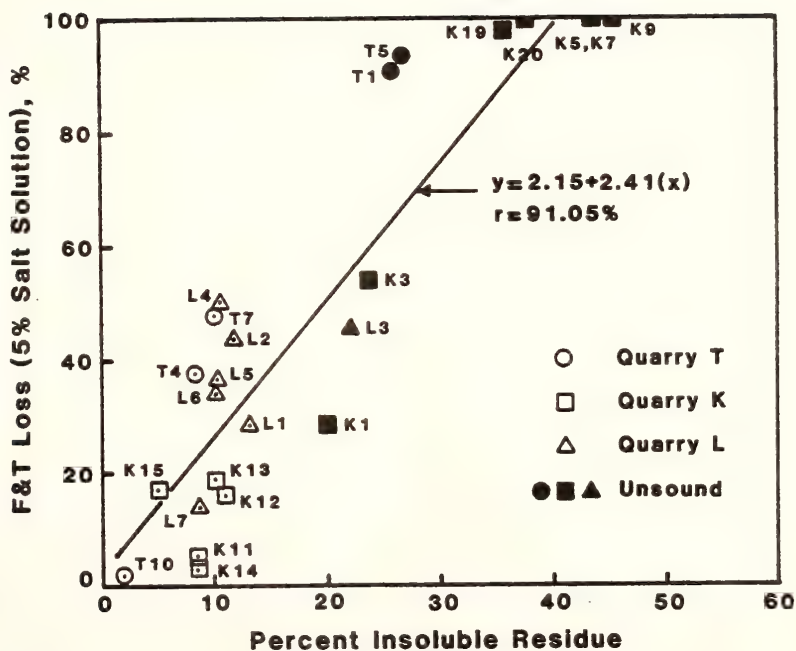


FIGURE 5.31: RELATIONSHIP BETWEEN INSOLUBLE RESIDUE CONTENT (PASSING 200 SIEVE) AND FREEZE-THAW LOSS IN 5% SALT SOLUTION

corresponding EDF values obtained by the mercury intrusion method as shown in Figure 5.32. For pore index values in excess of 30 ml or EDF values below 30, the results of the two tests show a strong correlation. The unsound aggregates also fall within these limits. Below pore index values of 30 ml, a small drop in the pore index results in a marked increase in EDF, i.e., a marked improvement in the aggregate quality. The scattering of data points between pore index values of 10 and 30 ml is due to variations in the amount, type, and distribution of argillaceous material.

The excellent correlation between the two tests suggests that the pore index test which is a quicker, simpler, and more economical procedure, may provide a replacement for the porosimeter test. A major advantage of the pore index test is the large volume of aggregate material tested (19.8 lbs) as compared with less than 5 grams of sample tested in the mercury intrusion method. This large volume averages out the local heterogeneities such as cherty nodules and lenses, argillaceous streaks, and pyritic concentrations. In this respect the pore index test provides a much more representative measure than does the mercury intrusion method. However, the pore size distribution is not provided by the pore index test.

5.7.6 EDF and Pore Index vs Freeze-Thaw Loss

In order to see how well the results of the two tests correlate with those of freeze-thaw tests, EDF and pore index values were plotted against freeze-thaw losses in water and in 5% salt solution respectively as shown in Figures 5.33 to 5.36. General linear trends are observed in all cases indicating a strong influence of pore characteristics on freeze-thaw loss and, hence, durability.

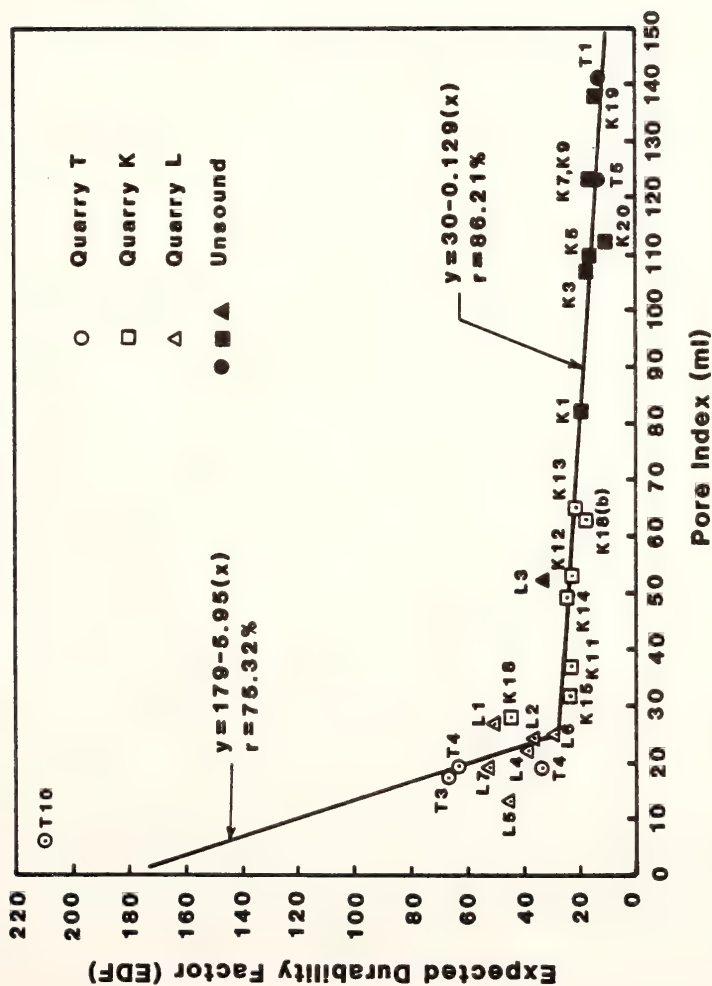


FIGURE 5.32: RELATIONSHIP BETWEEN PORE INDEX AND EXPECTED DURABILITY FACTOR

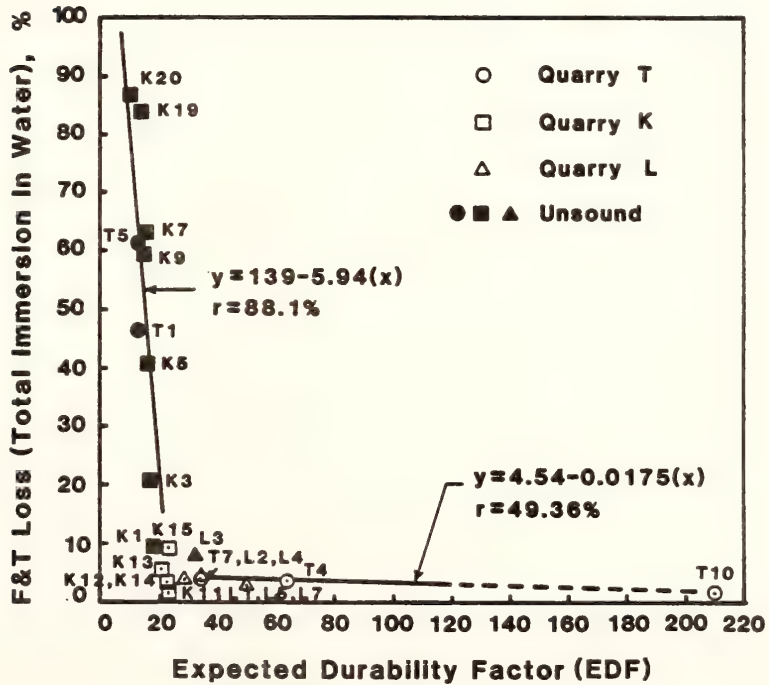


FIGURE 5.33: RELATIONSHIP BETWEEN EXPECTED DURABILITY FACTOR AND FREEZE-THAW LOSS IN WATER

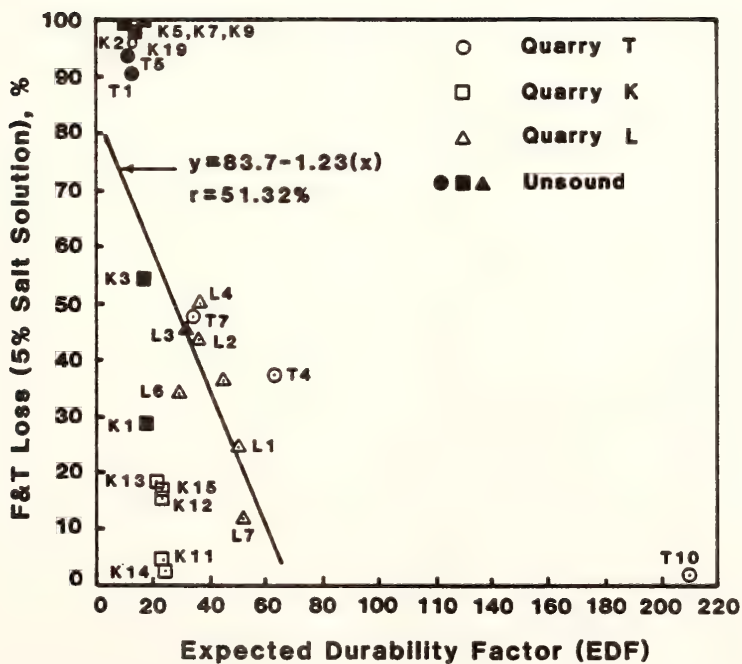


FIGURE 5.34: RELATIONSHIP BETWEEN EXPECTED DURABILITY FACTOR AND FREEZE-THAW LOSS IN 5% SALT SOLUTION

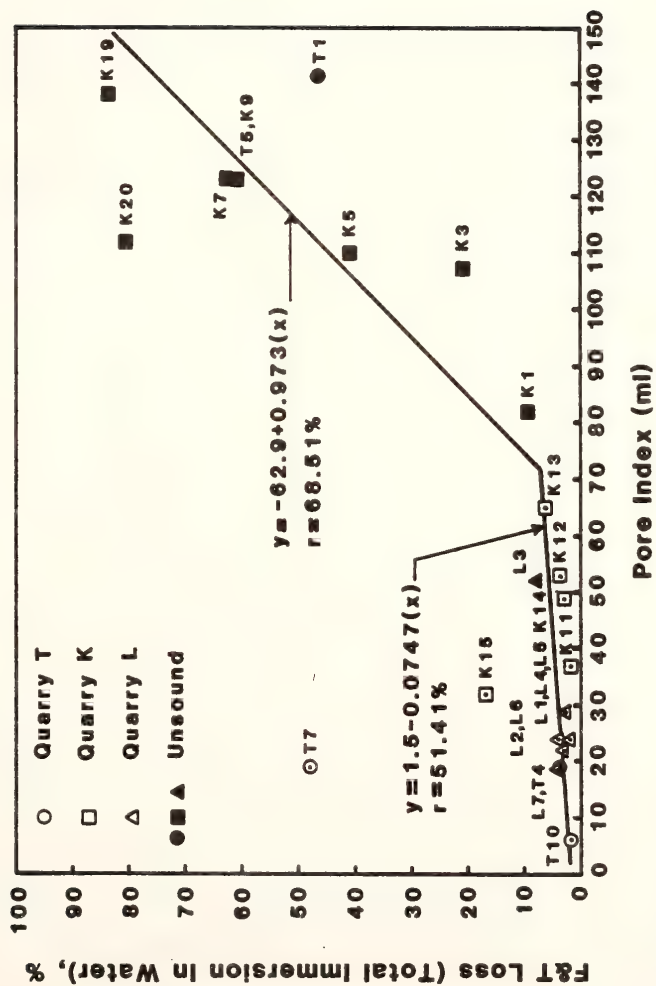


FIGURE 5.35: RELATIONSHIP BETWEEN PORE INDEX AND FREEZE-THAW LOSS IN WATER

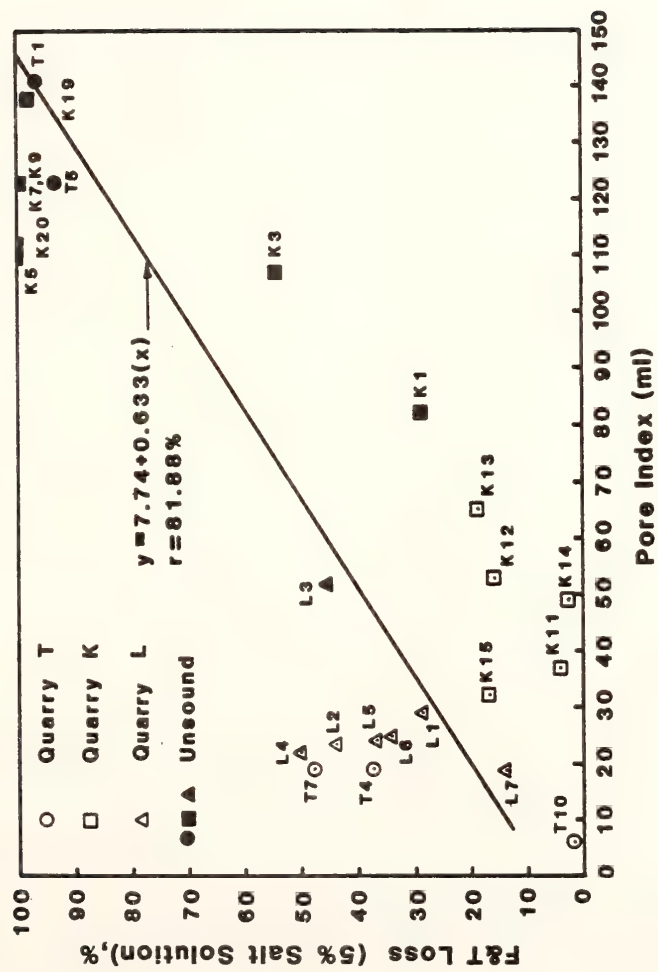


FIGURE 5.36: RELATIONSHIP BETWEEN PORE INDEX AND FREEZE-THAW LOSS IN 5% SALT SOLUTION

5.7.7 Texture vs Physical Properties

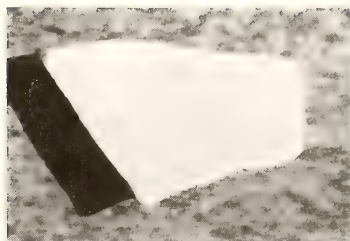
Figure 5.37 provides a summary of the relationship between aggregate texture and aggregate properties. Both samples are from quarry T and the insoluble residue in both cases is silty clay of medium plasticity. No evidence of failure of T3 was found in the field while T6 resulted in severe disintegration. This field performance is supported by the test results given at the bottom of the figure. The figure clearly shows that the importance of aggregate petrography in determining aggregate properties cannot be overemphasized. It reaffirms the earlier conclusion that only those argillaceous carbonates are unsound which contain excessive amounts of evenly distributed silt and clay and that the degree of lamination is no indication of the amount of argillaceous material or the extent of freeze-thaw damage. To reject laminated rocks without performing other tests is not a desirable practice.

5.8 D-cracking vs Pitting and Popouts

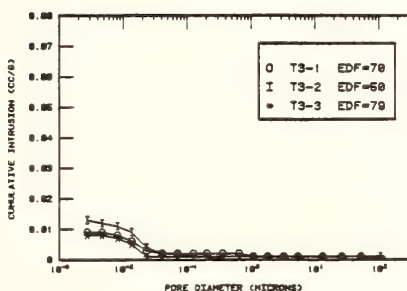
Lack of durability of aggregates in pavements is generally manifested as D-cracking or as aggregate disintegration in the form of pitting and popouts. The discussion in the previous pages shows that criteria established by others to prevent D-cracking are different and more severe than the criteria required to prevent the use of such argillaceous carbonates which may result in pitting and popouts over a relatively short period. It was shown that very few of the rocks under study pass the absorption-adsorption criterion to distinguish between sound and unsound aggregates. This is because the absorption-adsorption criterion is based on D-cracking as the failure mode.



Laminated (T3)

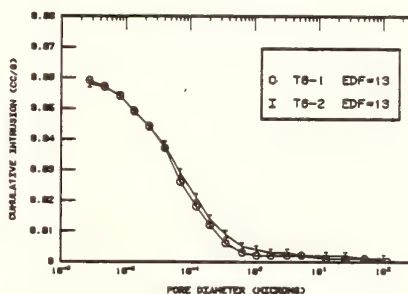


Non-laminated (T6)



Pore Size Distribution (T3)

Insoluble Residue	20.60%
Specific Gravity	2.47
Absorption	1.79%
Adsorption	1.54%
EDF	66.00
Pore Index	17.00
S.S. Loss	-
F&T Loss (Water)	14.07
F&T Loss (5% Salt)	37.40



Pore Size Distribution (T6)

Insoluble Residue	29.30%
Specific Gravity	2.35
Absorption	5.28%
Adsorption	2.29%
EDF	13.00
Pore Index	123.00
S.S. Loss	32.14
F&T Loss (Water)	61.01
F&T Loss (5% Salt)	93.46

In both rocks the clay is illite in composition and the insoluble residue is silty clay of medium plasticity.

FIGURE 5.37: RELATIONSHIP BETWEEN TEXTURE AND PHYSICAL PROPERTIES OF ARGILLACEOUS CARBONATES REGARDING FREEZE-THAW DURABILITY

Similarly if an EDF value of 50, as proposed by Kaneuji (41), is used, many argillaceous carbonates will be rejected which showed no evidence of failure by pitting and popouts in the field. In the present case all aggregates with EDF values above 20 were found to be durable except L3 (EDF=32). It has been found in Illinois and Iowa that all aggregates which have pore index values higher than 27 ml are associated with D-cracking. No aggregate with pore index values of less than 50 ml was found to cause pitting and popouts. Even aggregates with pore index values of more than 60 ml showed no disintegration provided the silt and clay content was less than 20%.

It is clear from the discussion above that separate criteria are needed to depict the two modes of failure. Application of D-cracking criteria will of course prevent both modes of failure. However, as D-cracking is only associated with concrete pavements, use of D-cracking criteria will exclude many aggregates which can be safely used in bituminous pavements. Also, when such highly argillaceous aggregates, as discussed in this study, are involved, D-cracking is not expected to control the immediate mode of failure. Pitting and popouts are likely to occur well before D-cracking in concrete pavements if the aggregates are prone to this first problem. Also, D-cracking can sometimes be controlled by good drainage and hence perhaps lower quality aggregates can be used in certain situations. However, since the aggregates which resulted in pitting and popouts do not pass the D-cracking criteria, the potential for D-cracking of portland cement concrete pavements over a longer period of time exists.

CHAPTER 6

MECHANISMS OF FREEZE-THAW DETERIORATION

The deterioration of concrete exposed to freezing and thawing is caused by the expansion of freezing water in the void system of cement paste or concrete aggregates. Only those mechanisms which explain aggregate deterioration are discussed here.

6.1 Critical Saturation

The importance of the degree of saturation and its relation to aggregate deterioration has been emphasized by Powers (86), Verbeck and Landgren (22), Dolch (31-35), and many others (25-28). Aggregates dilate and break or cause disruption of the surrounding paste by the generation of high hydraulic pressures during freezing. The magnitude of the hydraulic pressure developed in aggregates depends on their degree of saturation (proportion of total void space filled with water), permeability, and the size of the aggregate particle (114). One cubic centimeter of water occupies 1.09 cubic centimeter of space after freezing and those voids in aggregate which are more than 91.7% full of water will be subjected to destructive hydraulic pressures when freezing water turns to ice, unless the excess water can be expelled from the voids during freezing. When the degree of saturation is more than 91.7%, the aggregate is said to be critically saturated. Hydraulic pressures as high as 2900 psi at -4°F may develop if the

pore water cannot escape during freezing (114). If the hydraulic pressure exceeds the tensile strength of the rock, the aggregate will break or popout. This theory of critical saturation is accepted without question.

Since the expanding water from the aggregate is expelled into the surrounding paste, its porosity, permeability, and air content are also involved in the problem of aggregate durability (22). The time required for an aggregate in concrete to become critically saturated is of great practical significance and depends upon its pore characteristics and the thickness and the permeability of the mortar cover (22).

6.2 Influence of Pore Characteristics

Many investigators (22, 31-42, 86, 115) consider pore characteristics of an aggregate to be the most important property in determining its durability in freezing and thawing. Lewis and Dolch (113) point out that the behavior of aggregate particles when exposed to freezing and thawing depends primarily upon the pore structure, permeability, and degree of saturation of the aggregate particle. Since the permeability is controlled by the size and continuity of pores, these two porosity characteristics are considered to be the most important. The total porosity is of secondary importance. The harmful pore size is large enough to permit water readily to enter much of the pore space but not large enough to permit easy drainage. Verbeck and Landgren (22) claim that for aggregates with similar pore size distributions, the one with high porosity should require more time to attain any particular degree of saturation than the one of low porosity.

Therefore, the aggregates of some intermediate porosity may show the worst performance. Kaneuji (41) quantified the relationship between pore size distribution and freeze-thaw durability of coarse aggregate in concrete in terms of "expected durability factor".

6.3 Failure Mechanisms

Verbeck and Landgren (22) have analyzed the mechanisms of freeze-thaw failure of the aggregates in concrete. They proposed three different types of aggregate response to freezing.

6.3.1 Elastic Accommodation

Part of the excess volume of water created by the freezing of a critically saturated aggregate can be accommodated by the elastic expansion of the aggregate. This is true of aggregates with low porosity in which expansion is generally within the limits of tensile strength. The following equation gives the tensile stress which is developed in an aggregate on freezing (22).

$$P = \frac{0.09 W_f E}{3(1-2\mu)}$$

where P = internal ice pressure, psi.

W_f = volumetric fraction of freezable water in aggregate
cc/cc = porosity of a saturated aggregate.

E = modulus of elasticity of aggregate, psi, and

μ = Poisson's ratio of aggregate.

The tensile strength of the aggregate must be equal to or greater than the tensile stress given by the above equation in order to elastically accommodate the expansion without failure.

Even if the aggregate particle can expand elastically to accommodate the increased volume of ice, the surrounding concrete paste may

not be able to withstand such an expansion. Thus the aggregate can cause concrete deterioration even if it is itself not fractured.

6.3.2 Critical Size of the Aggregate

According to Powers' hypothesis of hydraulic pressure (86, 116) the magnitude of hydraulic pressure developed in the saturated aggregate during freezing depends on the rate of freezing and the porosity, permeability, and the size of the aggregate particle. The critical distance is the maximum distance the water can travel through the porous material without generating hydraulic pressure higher than the material's tensile strength. If it is smaller than the size of the aggregate, the aggregate will fail internally. The maximum permissible size or the "critical size" of the aggregate can be estimated as follows (22):

$$L_{\max} = \frac{27.7 K T}{0.09 d W_f/dt}$$

where: L_{\max} = maximum permissible size - "critical size", in.

K = permeability coefficient of aggregate, cm/sec.

T = tensile strength of aggregate, psi, and

$d W_f/dt$ = rate of freezing of water.

Verbeck and Landgren (22) found that critical size can vary from 0.5 inch for rocks with fine pores and low permeability such as chert and shale to above 30 inches for some highly permeable dolomites.

According to the critical size hypothesis, cherts, shales, and some carbonates with fine pores are susceptible to fracturing and popouts when frozen in a saturated condition and when their size exceeds the critical distance.

6.3.3 Expulsion of Water from Aggregates into Paste

An aggregate with high porosity will have an absorption greater than that which can be accommodated elastically (about 0.1%). If such an aggregate particle is frozen in concrete in a critically saturated condition, the excess water due to freezing must be expelled into the surrounding paste. If the size of the aggregate is smaller than its critical size and if the paste is air entrained, neither the aggregate nor the paste will fail. If the paste is not air entrained it will fail. Trouble from this mechanism will occur mostly around the periphery of the aggregate particle and there must be sufficient entrained air bubbles in the paste not only to accommodate its own excess of water during freezing but also the water expelled from the aggregate particle.

According to this mechanism, highly porous rocks with large pores and high permeabilities have no danger of deterioration from freezing and thawing. Rocks with medium fine pores will cause more trouble by expulsion of the excess water into the surrounding paste and may cause popouts and expansion cracks (114). Rocks of very fine pores such as claystones, siltstones, cherts, and shales do not saturate rapidly but they do become highly saturated. These rocks are very susceptible to popouts because excessive hydraulic pressures are built up within the rock particle causing it to expand and fracture the concrete to the surface (114).

6.3.4 Dunn and Hudec's Hypothesis of Sorbed Water

In 1966 Dunn and Hudec (87) advanced a new hypothesis to explain the deterioration of argillaceous carbonate rocks. They claimed that

frost sensitivity of these rocks is not the result of hydraulic pressure during freezing as suggested by Powers and Verbeck. The disruptive force is believed instead to result from expansion of sorbed, ordered water on clay surfaces. To explain the expansion and contraction on wetting and drawing of some argillaceous carbonate rocks, it was postulated that the pore space around each clay particle is such that when water is sorbed by the clay, force is exerted against the pore walls. The clays in expansive rocks are rejected from the growing dolomite crystals during their growth, and form more or less connected network, thereby becoming "wetable" or available to water.

Cold differential-thermal-analysis equipment was used to show that water did not freeze in unsound argillaceous carbonate rocks even at temperatures as low as -40°C . Calculations of theoretical freezing points for sorbed water, based on adsorption isotherms, also demonstrated that the least sound rocks had the most nonfreezable water. This hypothesis is in radical conflict with most concepts of frost deterioration.

6.4 Role of De-icing Salts

The effects of de-icing salts on concrete durability have been studied by several investigators (117-121). De-icing salts exert an adverse effect on concrete, probably by increasing the severity of the freezing and thawing effects.

The salts normally used are NaCl and CaCl_2 , and their repeated application with intervening periods of freezing or drying results in surface scaling of concrete as well as aggregate disintegration.

The salts enhance freeze-thaw deterioration through the build up of osmotic pressures (118). When solutions of different concentrations of soluble materials are separated by a semi-permeable barrier, the solvent particles move through the barrier toward the solution of greater concentration and a differential head is set up between the two solutions. The salt concentrations increase as the water begins to freeze. This osmotic action causes movement of water toward the top layer of the slab where freezing takes place. Experimental work by Verbeck and Kleiger (118) shows that the greatest damage occurs when concrete is exposed to 2 to 4% concentrations of salt solution. This is due to the optimum combination of freezable water and osmotic pressure. If the concentration increases above 4%, there is a decrease in deterioration. The higher concentration of salt may lower the freezing temperature of salt solution and create an anti-freeze effect (114).

Since the greatest deterioration occurs at relatively low salt concentrations, Verbeck and Klieger (116) believe the attack to be primarily physical and not chemical in nature. Work by Mather (119, 120) supports this argument.

If the de-icing salts are applied within a few weeks of the placing of concrete, the damage would be more severe (4). Also, the most severe damage is found to occur when concrete is subjected to alternate freezing and thawing with the de-icer solution remaining on top of the specimen rather than being replaced with fresh water prior to each refreezing (118). De-icing salts not only give rise to osmotic pressures, but also provide an additional source of surface moisture in freezing water by melting ice and snow (114). Walburger

(121) has shown that as snow and ice are melted by deicing salts, the temperature in the saturated zone immediately below the surface can drop markedly because of the large heat of fusion of ice. This temperature drop will result in additional freezing.

6.5 Application of Failure Mechanisms to Aggregates Studied

In order to investigate the mechanisms responsible for deterioration of argillaceous carbonates in Indiana pavements, it is necessary to keep the following facts in mind:

1. The failure mode in all cases was aggregate disintegration in the form of pitting and popouts.
2. Only the aggregate was damaged; no damage was observed in the surrounding mortar. However, in the case of bituminous pavements a "drying" of the bituminous matrix around aggregate particles was observed.
3. The damage was purely of physical nature. No chemical reaction was observed between the aggregate and the paste or within the aggregate.

Argillaceous carbonate rocks with a high percentage and uniform distribution of silt and clay are characterized by high porosity, low permeability, and small pore sizes. Because of these characteristics they tend to become highly saturated and absorb large amounts of water. On freezing this water generates high hydraulic pressures. The large amount and uniform distribution of argillaceous material also results in low tensile strength and low Young's modulus. Therefore, the hydraulic pressure developed in argillaceous carbonate aggregates is too high to be accommodated elastically.

The expulsion of water from aggregate to portland cement paste does not seem to be a controlling mechanism either because of the following reasons:

1. No damage at the aggregate-paste interface was observed.
2. More than 60% pores in the unsound aggregates are finer than 0.1 micron (1000\AA). The capillary pores in the surrounding paste can be as large as 0.5 microns (5000\AA). Therefore, in case of such fine aggregates, the water in the paste freezes before that in the aggregate. The expanding water from the paste will fill most of the entrained air bubbles leaving very little space for the expanding water from aggregate particle. Also the frozen paste will tend to block the movement of any water that tends to come out of the aggregate particle.
3. Argillaceous carbonate aggregates used in Indiana pavements are so weak that they easily break under high hydraulic pressure before the expanding water can be forced out of the aggregate into the surrounding paste.

Aggregate response by critical size seems to be the most probable mechanism of failure of the aggregates investigated in this study. Because of the low permeability and the low tensile strength of the unsound aggregates their critical distance is expected to be quite small. Assuming a tensile strength of 700 psi (122), a freezing rate of 1.06×10^{-3} cm/sec (22), a permeability coefficient of 2×10^{-9} cm/sec (123), and using the equation given in section 6.3.2, a critical distance of 0.41 inch is obtained. Indeed many aggregate pieces which showed disintegration in the field were smaller than $\frac{1}{2}$ inch

(Figure 3.15). The critical distance being so small, the hydraulic pressure being so high, and the tensile strength being low, the aggregate disintegration by pitting and popouts is obviously the most likely mode of failure.

The large amount of uniformly distributed argillaceous material is considered to influence the aggregate disintegration in two ways:

- 1) By acting as an osmotic membrane. Interstitial silt and clay act as an osmotic membrane giving rise to osmotic pressures when de-icing salt solutions permeate into the aggregate pores.
- 2) By weakening the rock structure. Presence of large amounts of silt and clay structurally weaken the rock (113). Thin section study shows that in those rocks which have low argillaceous content, the dolomite rhombs are largely interpenetrating and form a rigid structural framework. With the increase in silt and clay content, the structural framework is disrupted, and many of the dolomite rhombs no longer interpenetrate their neighbors. As the silt and clay content exceeds 20%, the rock structure becomes quite weak with dolomite rhombohedra scattered loosely in a matrix of silt, clay, and some calcite (Figure A-5). The tensile strength of such a rock will be very low.

Vacuum absorption tests conducted in a mixture of equal amounts of kerosene and SAE 10 oil showed a small increase in the absorption of unsound aggregates from quarries T and K after freezing and thawing of these aggregates. The tests were performed in connection with another study (124). The increase in absorption was too small to be

used as a criterion for judging unsound aggregates. However, it appears that freezing and thawing changes the pore structure of unsound aggregates so that they tend to absorb more volatiles. This probably explains the "drying" of the bituminous pavement around disintegrating aggregates.

The cross-overs on US 24 were very severely damaged as the aggregate particles were completely disintegrated and removed as seen in Figure 3.16-3.18. This is because:

1. The cross-overs were opened to traffic soon after the pavement was constructed while the rest of the pavement was allowed to cure for many weeks. The weaker the concrete, the more severe the freeze-thaw damage.
2. The cross-overs were exposed to excessive amounts of de-icing salts within a few weeks of the placing of the concrete because of a very severe winter. This favored more severe damage (4). Also, the rest of the road being closed, the cross-overs were subjected to greater traffic flow which resulted in higher salt concentrations.
3. Salt solutions, once absorbed, probably remained inside aggregate particles during repeated cycles of freezing and thawing due to their low permeability. This created the most severe condition according to findings by Verbeck and Klieger (118).

Dunn and Hudec's hypothesis of sorbed water does not appear to be applicable to the argillaceous carbonates from Indiana. This is because:

1. No evidence of deterioration of these rocks on wetting and drying was found which is contrary to the case for rocks tested by Dunn and Hudec. Results of 10 cycles of wetting and drying on 6 of the ledge samples are supplied in Appendix G. Each cycle consisted of 24 hours of saturation followed by 24 hours of drying. For the unsound aggregate samples the loss in weight ranges from 0.00% to 0.22%. Sample T3, which is laminated but proved sound in freeze-thaw, is the only sample which shows a significant loss of 2.26%.
2. The clay content of the rocks is not high enough to sorb so much water as is required to create disruptive forces. Dunn and Hudec in their published reports (87, 88) do not indicate the total amount of clay present in the rocks tested by them. However, they describe their rocks as highly clayey, the clay being illite, kaolinite, and chlorite in composition. In Indiana carbonates illite is the only clay mineral present.

During the past 30 years two major approaches to the study of frost resistance in rocks have emerged. Proponents of the first approach are mostly engineers and they include such people as Powers, Verbeck, and Dolch. They consider pore characteristics as the most important property in determining frost resistance. The other approach was proposed by geologists such as Lemish, B and K. Mather, and Mielenz and it considers mineralogy and petrography to be as critical regarding pore characteristics. The present study shows that the two approaches are complimentary. Pore characteristics are certainly important but it is the mineralogy and petrography which

determine the pore characteristics and other physical properties of rocks related to their durability in concrete. It has been shown that porosity, pore size, permeability, and tensile strength are related to the amount and distribution of argillaceous material. These properties in turn control the magnitude of hydraulic pressure and the kind of aggregate response to freezing and thawing. Frost susceptible carbonate aggregates are characterized by high porosity, abundance of fine pores, and low permeability which are a consequence of a high percentage and a uniform distribution of argillaceous material.

The fact that some rocks in which the argillaceous material was either less than 20% or was not evenly distributed did not fail inspite of their large volume of fine pores clearly points out the importance of mineralogy and texture.

CHAPTER 7

SUMMARY, CONCLUSIONS, AND RECOMMENDATIONS

7.1 Summary

The important findings of this research can be summarized as follows:

1. Unsound argillaceous carbonate aggregates are characterized by a bulk specific gravity of less than 2.5, an absorption of more than 4%, and a degree of saturation greater than 90%.
2. Durability of argillaceous carbonates depends on the amount, type, and manner of distribution of argillaceous material which includes both silt and clay. Rocks in which the amount of silt and clay size residue exceeds 20% and is uniformly distributed throughout should be considered unsound. Laminated rocks are not necessarily unsound even if their residue content exceeds 20%. However, if the insoluble residue is greater than 30%, and if a large portion of it is uniformly distributed, even the laminated rocks are likely to be unsound.
3. For the same amount of insoluble residue content, the volume of small pores is higher when the residue is clayey than when it is silty. Therefore, the worst aggregates from a durability point of view are those which contain more than 20% argillaceous material of clay composition which is evenly distributed throughout the rock.

4. Illite is the only clay mineral present in the aggregates investigated.
5. Pore-size distribution curves of unsound argillaceous carbonates are conspicuously high and sharp with more than 60% pores being smaller than 0.1 micron in diameter. EDF values of less than 20 and pore index values of more than 50 are characteristic of these rocks.
6. The pass-fail criteria established by others to prevent D-cracking are more stringent than those required to prevent pitting and popouts of argillaceous carbonates. Use of D-cracking criteria to prevent both modes of failure will exclude many aggregates which can be safely used in bituminous pavements.
7. The insoluble residue test shows the best correlation with the field performance of argillaceous carbonates.
8. The sodium sulphate soundness test is not a good indicator of durability because of a relatively poor correlation between residue content and soundness loss. However, when the soundness loss exceeds 10% the aggregate should be looked upon with suspicion.
9. The Iowa pore index test is a simple, reliable, and economical test for isolating unsound argillaceous carbonates.
10. Unconfined freeze-thaw tests in water may allow the use of some unsound argillaceous carbonates and may fail some sound ones. However, if the test is used a value of 9% loss is recommended. Unconfined freeze-thaw tests in 5% salt solution appear to be somewhat more reliable in preventing the use of unsound aggregates as they simulate field conditions better. A loss of 30% appears to correlate best with the field performance. Argillaceous

carbonates in which freeze and thaw loss in 5% salt solution exceeds 30% and silt and clay content exceeds 20% should be rejected.

7.2 Conclusions

Based on the findings listed above, the following conclusions can be drawn regarding the objectives set out for this research.

1. The insoluble residue test is the most reliable procedure for predicting the durability characteristics of argillaceous carbonate rocks. Petrographic examination is very helpful for preliminary examination but does not indicate the total amount of argillaceous material.
2. Insoluble residue content and pore size distribution show the best correlation with the field performance of argillaceous carbonates.
3. A combined use of insoluble residue test and the Iowa pore index test can serve as a simple and reliable procedure to detect the frost susceptible argillaceous carbonate aggregates.

7.3 Recommendations

The insoluble residue content and pore characteristics being the two most reliable indicators of freeze-thaw durability of argillaceous carbonates, the following test procedure is recommended.

1. The insoluble residue test should be performed on all argillaceous carbonates.
2. The Iowa pore index test should be performed on those samples which contain more than 20% silt and clay.
3. If the amount of silt and clay residue exceeds 20% and if the pore index value is higher than 50 ml, the aggregate should be rejected.

4. Pitting and popouts can be prevented in argillaceous aggregates if the previous criteria are applied. The D-cracking criteria are more stringent and they should only be applied for those situations in which D-cracking will be a concern or in which D-cracking is possible.

BIBLIOGRAPHY

BIBLIOGRAPHY

1. Lewis, D.W., "Research on Concrete Aggregates", Engineering Bulletin, Purdue University, Series No. 71, 1950, p. 70.
2. McLaughlin, J.F., Woods, K.B., Mielenz, R.C., and Rockwood, N.C., "Distribution Production and Engineering Characteristics of Aggregates", Section 16, Highway Engineering Handbook, McGraw Hill, 1960.
3. Hveem, F.N. and Smith, T.W., "A Durability Test for Aggregates", Highway Research Record No.62, 1964, p. 119.
4. Neville, A.M., "Properties of Concrete", Third Edition, Pitman, 1981.
5. Dolar-Mantuani, L., "Soundness and Deleterious Substances", Chapter 47, ASTM STP 169B, American Society for Testing and Materials, 1980, p. 744.
6. Larson, T.D., Doettcher, A., Cady, P., Franzen, M., and Reed, J., "Identification of Concrete Aggregates Exhibiting Frost Susceptibility", National Cooperative Highway Research Program, Report No. 15, Highway Research Board, 1965, 66 pages.
7. Larson, T.D., Cady, P., Franzen, M., and Reed, J., "A Critical Review of Literature Treating Methods of Identifying Aggregates Subject to Destructive Volume Changes When Frozen in Concrete and a Proposed Program of Research", National Cooperative Highway Research Program, Special Report No. 80, Highway Research Board, 1964, 81 pages.
8. Dolar-Mantuani, L., "Petrographic Examination of Natural Concrete Aggregates", Record No. 120, Highway Research Board, 1966, p. 7.
9. Lemish, J., Rush, F.E., and Hiltrop, C.L., "Relationship of Physical Properties of Some Iowa Carbonate Aggregates as Related to Durability of Concrete", Bulletin No. 196, Highway Research Board, 1958, p. 29.
10. Bisque, R.E. and Lemish, J., "Chemical Characteristics of Some Carbonate Aggregate as Related to Durability of Concrete", Bulletin No. 196, 1958, p. 29.

11. Indiana Department of Highways, Materials and Test Division, "Proposed Modification of Freeze-Thaw Soundness Tests of Coarse Aggregates", Personal Communication, 1980.
12. Mather, K. and Mather B., "Method of Petrographic Examination of Aggregates for Concrete", Proceedings, American Society for Testing and Materials, vol. 50, 1950, p. 1288.
13. Mielenz, R.C., "Petrographic Examination", ASTM STP 169B, American Society for Testing and Materials, 1980, p. 539.
14. Lounsbury, R.W. and West, T.R., "Petrography of Some Indiana Aggregates in Relation to Their Engineering Properties", Proceedings, 16th Annual Highway Geology Symposium, 1965, p. 24.
15. West, T.R. and Johnson, R.B., "Analysis of Textural and Physical Factors Contributing to Abrasion Resistance of Some Indiana Carbonate Aggregates", Proceedings, Indiana Academy of Science, vol. 75, 1966, p. 153.
16. West, T.R., "Textural Analysis and Engineering Testing of Degrading Base Coarse Aggregates", Proceedings, 7th Annual Engineering Geology and Soils Engineering Symposium, 1969, p. 247.
17. West, T.R., Johnson, R.B., and Smith, N.M., "Tests for Evaluation of Degradation of Base Coarse Aggregates", National Cooperative Highway Research Program, Report No. 93, Highway Research Board, 1970, 92 pages.
18. West, T.R. and Okagbue, C.O., "Grain Size Analysis and Petrographic Examination of a Gravel Deposit Relative to Engineering Quality", North Central Section, Geological Society of America, Abstracts of Programs, 1980, p. 280.
19. Shakoor, A. and West, T.R., "Petrographic Examination of Aggregates Used in Bituminous Overlays for Indiana Pavements as Related to Their Polishing Characteristics", Proceedings, 30th Annual Highway Geology Symposium, 1980, p. 185.
20. Roper, H., Cox, J.E., and Erlin, B., "Petrographic Studies on Concrete Containing Shrinking Aggregate", Journal of Research, Portland Cement Association Research and Development Laboratories, vol. 6, No. 3, 1964, p. 2.
21. Erlin, B., "Methods Used in Petrographic Studies of Concrete", Analytical Techniques for Hydraulic Cements and Concrete, ASTM STP 395, American Society for Testing and Materials, 1965, p. 3.
22. Verbeck, G. and Landgren, R., "Influence of Physical Characteristics of Aggregates on Frost-Resistance of Concrete", Proceedings, American Society for Testing and Materials, vol. 60, 1960, p. 1063.

23. Brewer, J.E., "Corps of Engineers Procedure in the Development of a New Limestone or Dolomite Source", The Ohio Journal of Science, vol. 62, No. 2, 1966, p. 188.
24. Gilson, J.L., "The Carbonate Rocks", Chapter 8, Industrial Minerals and Rocks, American Institute of Mining, Metallurgical and Petroleum Engineers, New York, 1960.
25. Sweet, H.S., "Research on Concrete Durability as Affected by Coarse Aggregates", Proceeding, American Society for Testing and Materials, vol. 48, 1948, p. 988.
26. Woods, K.B., Sweet, H.S., and Shelburne, T.E., "Pavement Blowups Correlated with Source of Coarse Aggregate", Proceedings, Highway Research Board, vol. 25, 1945, p. 147.
27. Lewis, D.W. and Woods, K.B., "Research as Related to the Development of Aggregate Specifications", Proceedings, 35th Annual Road School, Purdue University, 1949.
28. Cantrill, C. and Campbell, L., "Selection of Aggregates for Concrete Pavement Based on Service Records", Proceedings, American Society for Testing and Materials, vol. 34, 1939, p. 937.
29. Wray, F.N. and Lichtefeld, H.J., "The Influence of Test Methods on Moisture Absorption and Resistance of Coarse Aggregate to Freezing and Thawing", Proceedings, American Society for Testing and Materials, vol. 40, 1940, p. 1007.
30. Rhoades, R. and Mielenz, R.C., "Petrography of Concrete Aggregates", Proceedings, American Concrete Institute Journal, No. 6, vol. 42, 1946, p. 581.
31. Lewis, D.W., Dolch, W.L., and Woods, K.B., "Porosity Determinations and the Significance of Pore Characteristics of Aggregates", Proceedings, American Society for Testing and Materials, vol. 53, 1953, p. 449.
32. Dolch, W.L., "Permeability and Absorptivity of Indiana Limestone Coarse Aggregates", Ph.D Thesis, Purdue University, 1956.
33. Dolch, W.L., "Studies of Limestone Aggregate by Fluid-Flow Methods", Proceedings, American Society for Testing and Materials, vol. 59, 1959, p. 1204.
34. Dolch, W.L., "Porosity", ASTM STP 169A, American Society for Testing and Materials, 1966, p. 443.
35. Dolch, W.L., "Porosity", Chapter 37, ASTM STP 169B, American Society for Testing and Materials, 1980, p. 646.
36. Hiltrop, C.W. and Lemish, J., "Relationship of Pore Size Distribution and Other Rock Properties to Serviceability of Some Carbonate Aggregates", Bulletin 239, Highway Research Board, 1960, p. 1.

37. Roy, C.J., Thomas, L.A., Weissmann, R.C., and Schneider, R.C., "Geological Factors Related to Quality of Limestone Aggregates", Proceedings, Highway Research Board, vol. 34, 1955, p. 400.
38. Walker, R.D. and Hsieh, T., "Relationship Between Aggregate Pore Characteristics and Durability of Concrete Exposed to Freezing and Thawing", Highway Research Record 226, 1968, p. 41.
39. Lange, H. and Modry, S., "Determination of the Frost Resistance of Limestone Aggregates in the Light of Porosity Investigations", RILEM International Symposium on Durability of Concrete, Prague, 1970, p. B-129.
40. Koh, Y. and Kamada, E., "The Influence of Pore Structure of Concrete Made with Absorptive Aggregates on the Frost Durability of Concrete", Proceedings, RILEM/IUPAC Conference on Pore Structure and Properties of Materials, Prague, vol. 2, 1973, p. F-45.
41. Kaneuji, M., "Correlation Between the Pore Size Distribution and Freeze-Thaw Durability of Coarse Aggregate in Concrete", Ph.D Thesis, Purdue University, 1978.
42. Lindgren, M.N., "The Prediction of Freeze-Thaw Durability of Coarse Aggregate in Concrete by Mercury Intrusion Porosimeter", M.S. Thesis, Purdue University, 1980.
43. Bloem, D.L., "Soundness and Deleterious Substances", ASTM STP 169A, American Society for Testing and Materials, 1966, p. 497.
44. Woolf, D.O., "Relation Between Sodium Sulphate Soundness Tests and Absorption of Sedimentary Rock", Public Road, 1927, p. 225.
45. Woolf, D.O., "Improvement in the Uniformity of Accelerated Soundness Test of Coarse Aggregate", Bulletin 187, American Society for Testing and Materials, 1953, p. 42.
46. Garrity, L.V. and Kriege, H.F., "Studies of Accelerated Soundness Tests", Proceedings, Highway Research Board, vol. 15, 1935, p. 237.
47. Paul, I., "Magnesium Sulphate Accelerated Soundness Test on Concrete Aggregates", Proceedings, Highway Research Board, vol. 12, 1932, p. 319.
48. Vollick, C.A. and Skillman, E.I., "Correlation of Sodium Sulphate Soundness of Coarse Aggregate with Durability and Compressive Strength of Air-Entrained Concrete", Proceedings, American Society for Testing and Materials, vol. 52, 1952, p. 1159.
49. Walker, S. and Proudley, C.E., "Studies of Sodium and Magnesium Sulphate Soundness Tests", Proceedings, American Society for Testing and Materials, vol. 36, Part I, 1936, p. 327.

50. Wuerpel, C.E., "Modified Procedure for Testing Aggregate Soundness by Use of Magnesium Sulphate", Proceedings, American Society for Testing and Materials, vol. 39, 1939, p. 882.
51. Dolar-Mantuani, L., "Petrography Aids Study of Concrete Aggregates", Ontario Hydro Research News, vol. 5, 1953, p. 22.
52. Dolar-Mantuani, L., "Concrete Aggregate Examination by Prolonged Copper Nitrate Staining Method", Ontario Hydro Research News, vol. 14, 1962, p. 2.
53. Dolar-Mantuani, L., "Harmful Constituents in Natural Concrete Aggregates in Ontario", Proceedings, 24th International Geological Congress, Montreal, Section 13, 1972, p. 227.
54. Rhoades, R. and Mielenz, R.C., "Petrographic and Mineralogic Characteristics of Aggregates", Symposium on Mineral Aggregates, ASTM STP 83, American Society for Testing and Materials, 1948, p. 20.
55. Mielenz, R.C., "Petrography Applied to Portland Cement Concrete", Reviews in Engineering Geology, Geological Society of America, 1962, p. 1.
56. Mielenz, R.C., "Petrographic Examination of Concrete Aggregates", Bulletin, Geological Society of America, vol. 57, 1946, p. 309.
57. Mather, K., "Crushed Limestone Aggregates for Concrete", Transactions, Mining Engineering, American Institute of Mining Engineering, 1953, p. 1022.
58. Mather, K., "Applications of Light Microscopy in Concrete Research", Symposium on Light Microscopy, ASTM STP 132, American Society for Testing and Materials, 1953, p. 51.
59. Blaine, R.L., Hunt, C.M., and Tomes, L.A., "Use of Internal Surface Area Measurements on Freezing and Thawing of Materials", Proceedings, Highway Research Board, vol. 32, 1953, p. 298.
60. Fears, F.K., "Correlation Between Concrete Durability and Air-Void Characteristics", Air Voids in Concrete and Characteristics of Aggregates, Bulletin 196, Highway Research Board, 1958, p. 17.
61. Fears, F.K., "Determination of Pore Size of Four Indiana Limestones", M.S. Thesis, Purdue University, 1950.
62. Walker, R.D., "Identification of Aggregate Causing Poor Concrete Performance When Frozen", National Cooperative Highway Research Program, Report No. 12, Highway Research Board, 1965, 47 pages.
63. Larson, T.D. and Cady, P.D., "Identification of Frost Susceptible Particles in Concrete Aggregates", National Cooperative Highway Research Program, Report No. 66, Highway Research Board, 1969, 62 pages.

64. Walker, R.D., Pennee, H.J., Hazlett, W.H., and Ong, W.J., "One Cycle Slow Freeze Test for Evaluating Aggregate Performance in Frozen Concrete", National Cooperative Highway Research Program, Report No. 65, Highway Research Board, 1969.
65. Burggraf, R., Ward, E.M., and Orland, P.H., "Report on Cooperative Freezing-and-Thawing Tests of Concrete", National Cooperative Highway Research Program, Special Report No. 47, Highway Research Board, 1959.
66. Tremper, B. and Spellman, D.L., "Test for Freeze-Thaw Durability of Concrete Aggregates", Bulletin 305, Highway Research Board, 1961, p. 28.
67. Brink, R.H., "Rapid Freezing and Thawing Test for Aggregates", Bulletin 201, Highway Research Board, 1958, p. 15.
68. Scholer, C.H. and Stoddard, A.E., "Proposed Method of Testing Concrete and Concrete Aggregates by Freezing and Thawing", Proceedings, American Society for Testing and Materials, vol. 32, Part I, 1932, p. 364.
69. ACI Committee 201, "Durability of Concrete in Service, Chapter 1, Freezing and Thawing", Journal No. 12, American Concrete Institute, 1962, p. 1774.
70. Committee on Durability of Concrete", Progress Report", Proceedings, Highway Research Board, vol. 24, 1944, p. 174.
71. Flack, L.H., "Freezing and Thawing Resistance of Concrete as Affected by the Method of Test", Proceedings, American Society for Testing and Materials, vol. 57, 1957, p. 1077.
72. Jackson, F.H., "The Resistance of Concrete to Frost Action", Public Roads, No. 2, vol. 13, 1932, p. 32.
73. Klieger, P., "Notes on the Effect of Maximum Size of Aggregates on Tests for Frost Resistance", The International Sub-Committee on Concrete for Large Dams, Paper presented to 5th International Congress on Large Dams, Question No. 19, Paper No. 9, R 70, 1955, p. 335.
74. Legg, F.E., Jr., "Freeze-Thaw Durability of Michigan Concrete Aggregates", Freeze-Thaw Durability of Aggregate in Concrete, Bulletin 143, Highway Research Board, 1956, p. 1.
75. Blackburn, J.B., "Freeze and Thaw Durability of Air-Entrained Concrete Using Indiana Aggregates", Proceedings, 28th Annual Meeting of the Highway Research Board, Dec. 1948, p. 171.
76. Whitney, M.O., "Considerations Involved in the Making of Freezing and Thawing Tests of Concrete", A Symposium, Proceedings, American Society for Testing and Materials, vol. 46, 1946, p. 1198.

77. Powers, T.C., "Basic Considerations Pertaining to Freezing and Thawing Tests", Proceedings, American Society for Testing and Materials, vol. 55, 1955, p. 1132.
78. Myers, J.D. and Dubberke, W., "Iowa Pore Index Test", Interim Report, Iowa Department of Transportation, Highway Division, 1980.
79. Lamar, J.E., "Acid Etching in the Study of Limestones and Dolomites", Illinois Geological Survey, Circular No. 156, 1950, 47 p.
80. Friedman, G.M., "Identification by Staining Methods of Minerals in Carbonate Rocks", Subsurface Geology, Edited by LeRoy, L.W., LeRoy, D.O., and Raes, J.W., Colorado School of Mines, Fourth Edition, 1977, p. 96.
81. Ives, William, Jr., "Evaluation of Acid Etching of Limestone", Bulletin No. 114, Part 1, State Geological Survey of Kansas, 1955, p. 48.
82. Willman, H.B., "Resistance of Chicago Area Dolomites to Freezing and Thawing", Bulletin 168, Illinois Geological Survey, 1944, p. 250.
83. Powers, T.C., "A Working Hypothesis for Further Studies of Frost Resistance of Concrete", Proceedings, American Concrete Institute Journal, vol. 41, 1945, p. 245.
84. Powers, T.C. and Brownyard, T.L., "Studies of the Physical Properties of Hardened Portland Cement Paste", Proceedings, American Concrete Institute Journal, Part 8, vol. 43, 1947, p. 933.
85. Powers, T.C., "The Air Requirement of Frost Resistant Concrete", Proceedings, Highway Research Board, vol. 29, 1949, p. 184.
86. Powers, T.C. and Helmuth, R.A., "Theory of Volume Changes in Hardened Portland Cement Paste During Freezing", Proceedings, Highway Research Board, vol. 32, 1953, p. 285.
87. Dunn, J.R. and Hudec, P.P., "Water, Clay, and Rock Soundness", The Ohio Journal of Science, vol. 62, No. 2, 1966, p. 153.
88. Dunn, J.R. and Hudec, P.P., "Frost and Sorption Effects in Argillaceous Rocks", Highway Research Record No. 393, Highway Research Board, 1972, p. 65.
89. Stark, D., "Characteristics and Utilization of Coarse Aggregates Associated with D-Cracking", Living with Marginal Aggregates, ASTM STP 597, American Society for Testing and Materials, 1976, p. 45.
90. Stark, D. and Klieger, P., "Effect of Maximum Size of Coarse Aggregates on D-Cracking in Concrete Pavements", Record No. 441, Highway Research Board, 1973, p. 33.

91. Klieger, P., Monfore, G., Stark, D., and Teske, W., "D-Cracking of Concrete Pavements in Ohio", Portland Cement Association, Report No. OHIO-DOT-11-74, 1974.
92. McInnis, C. and Lau, E.C., "Maximum Aggregate Size Effect on Frost Resistance of Concrete", Proceedings, American Concrete Institute Journal, vol. 68, 1971, p. 144.
93. Fulton, F.S., "Concrete Technology", A South Africa Handbook, The Portland Cement Institute, Johannesburg, South Africa, 1961.
94. Carr, D.D., French, R.R., and Ault, C.H., "Crushed Stone Aggregate Resources of Indiana", Bulletin 42-H, Indiana State Geological Survey, 1971, p. 33.
95. Patton, J.B., "Petrology of Laminated Limestones in Indiana", Roads and Streets, vol. 97, No. 8, 1954, p. 85.
96. Pinsak, A.P. and Shaver, R.H., "The Silurian Formations of Northern Indiana", Bulletin 32, Indiana State Geological Survey, 1964, 87 pages.
97. Shaver, R.H. and others, "Stratigraphy of Silurian Rocks of Northern Indiana", Field Conference Guide Book No. 10, Indiana State Geological Survey, 1961, 62 pages.
98. French, R.R., "Crushed Stone Resources of Devonian and Silurian Rocks of Indiana", Bulletin 37, Indiana State Geological Survey, 1967, 45 pages.
99. Cummings, E.R. and Shrock, R.R., "The Geology of Silurian Rocks of Northern Indiana", Publication No. 75, Indiana Department of Conservation, 1928, 226 pages.
100. Cummings, E.R., "Reefs or Bioherms?", Geological Society of America Bulletin, vol. 43, 1932, p. 331.
101. Wayne, W.J., "Urban Geology of Madison County, Indiana", Special Report No. 10, Indiana State Geological Survey, 1975, 24 pages.
102. Furbush, M.A. and Styers, K.E., "The Relationship of Skid Resistance to Petrography of Aggregates", Final Report, Bureau of Materials, Testing and Research, Pennsylvania Department of Transportation, 1972, 34 pages.
103. Mitchell, W.A., "Oriented Aggregate Specimens of Clay for X-ray Analysis made by Pressure", Clay Minerals Bulletin No. 2, 1953, p. 76.
104. Brown, G., "A Semi-Micro Method for the Preparation of Soil Clays for X-ray Diffraction Studies", Journal Soil Sciences, vol. 4, 1953, p. 229.

105. Kinter, E.B. and Diamond, S., "A New Method for Preparation and Treatment of Oriented Aggregate Specimens of Soil Clays for X-ray Diffraction Analysis", Soil Sciences, vol. 81, No. 2, 1956, p. 111.
106. Thiesen, A.A. and Harward, M.E., "A Paste Method for Preparation of Slides for Clay Mineral Identification by X-ray Diffraction", Proceedings, American Society, Soil Science, vol. 26, 1962, p. 91.
107. Washburn, E.W., "Note on a Method of Determining the Distribution of Pore Size in a Porous Material", Proceedings, National Academy of Sciences, vol. 7, 1921, p. 115.
108. Winslow, D.W. and Diamond, S., "A Mercury Porosimetry Study of the Evolution of Porosity in Portland Cement", Journal of Materials, American Society for Testing and Materials, vol. 5, No. 3, 1970, p. 564.
109. Mather, K., "Relation of Absorption and Sulphate Test Results of Concrete Sands", Bulletin 144, American Society for Testing and Materials, 1947, p. 26.
110. Lang, F.C. and Hughes, C.A., "Accelerated Freezing and Thawing as a Quality Test for Concrete Aggregates", Proceedings, American Society for Testing and Materials, vol. 31, Part II, 1935, p. 364.
111. Wuerpel, C.E., "Factors Affecting the Testing of Concrete Aggregate Durability", Proceedings, American Society for Testing and Materials, vol. 38, Part I, 1938, p. 327.
112. Judd, W.R. and Shakoor, A., "Density", Chapter 3, Physical Properties of Rocks and Minerals, McGraw Hill/Cindas Data Series on Material Properties, vol. II-2, 1981, p. 29.
113. Hadley, D.W., "Alkali Reactivity of Dolomitic Carbonate Rocks", Highway Research Record No. 45, 1964, p. 1.
114. Cordon, W.A., "Freezing and Thawing of Concrete-Mechanisms and Control", American Concrete Institute Monograph No. 3, 1966, 99 pages.
115. Lewis, D.W. and Dolch, W.L., "Porosity and Absorption", Significance of Tests and Properties of Concrete and Concrete Aggregates, ASTM STP 169, American Society for Testing and Materials, 1956, p. 303.
116. Powers, T.C., "Resistance to Weathering-Freezing and Thawing", ASTM STP 169, American Society for Testing and Materials, 1956, p. 182.

117. Gonnerman, H.F., Timms, A.G., and Taylor, A.G., "Effects of Calcium and Sodium Chlorides on Concrete When Used for Ice Removal", Journal American Concrete Institute, vol. 33, Nov.-Dec. 1936, p. 107.
118. Verbeck, G.J. and Klieger, P., "Studies of 'Salt' Scaling of Concrete", Bulletin 150, Highway Research Board, 1957, p. 1.
119. Mather, B., "Concrete Need Not Deteriorate", Concrete International, vol. 1, No. 9, Sept. 1979, p. 32.
120. Mather, B., A discussion of the paper "Mechanisms of the CaCl_2 attack on Portland Cement Concrete", by Chatterji, B., Cement and Concrete Research, vol. 9, No. 1, Jan. 1979, p. 135.
121. Walburger, R., "Scaling of Concrete Surfaces", M.S. Thesis, Bulletin Engineering Experiment Station, Utah State University, 1966.
122. Singh, M.M., "Strength of Rock", Chapter 5, Physical Properties of Rocks and Minerals, McGraw Hill/Cindas Data Series on Material Properties, vol. II-2, 1981, p. 83.
123. Wolff, R.G., "Porosity, Permeability, Distribution Coefficients, and Dispersivity", Chapter 4, Physical Properties of Rocks and Minerals, McGraw Hill/Cindas Data Series on Material Properties, vol. II-2, 1981, p. 45.
124. Fein, M.R., (Graduate Student), Summer Research Project, Purdue University, 1981, personal communication.

APPENDICES

APPENDIX A
PETROGRAPHIC ANALYSIS

APPENDIX A

PETROGRAPHIC ANALYSIS

This appendix includes the petrographic description of the ledge samples. Polished slabs and thin sections were studied under binocular and polarizing microscopes, respectively.

The term "argillaceous material" is used to include both silt and clay.

It is to be noted that the percentage of quartz shown under "mineral composition" includes only those quartz grains which were larger than 0.01 mm. Quartz grains smaller than this size were included in the silt fraction. If all quartz grains smaller than 0.075 mm were considered as silt, the percentage of silt would increase and that of quartz would decrease by small amounts as compared with their percentages given in the descriptions included in this Appendix.

Sample No. T1

Ledge 801

Quarry T

Megascopic Description

Light grey, very fine-grained, massive. Small, irregular pockets and veins of relatively coarser calcite and quartz are present. The polished surface appears sugary under binocular microscope.

Microscopic DescriptionTexture

Microcrystalline; euhedral rhombs of dolomite form the basic mosaic with calcite and quartz being interstitial. Grain size varies from 0.01 mm to 0.05 mm for the main body of the rock and from 0.1 mm to 0.3 mm for coarser calcite of veins and pockets.

Mineral Composition

The rock consists of dolomite, calcite, silt and clay, and quartz. Pyrite is present as an accessory mineral.

Dolomite 65.0%: Occurs as euhedral to subhedral, poorly interlocked grains.

Many dolomite grains are zoned due to the presence of clay cutons.

Calcite 10.0%: Occurs as very small, anhedral, interstitial grains and as veins and pockets of coarser calcite.

Quartz 8.0%: Occurs as anhedral, interstitial grains of detrital origin.

The grain size varies from 0.01 mm to 0.05 mm.

Silt and clay 15.0%: Occurs in three forms:

1. As finely divided, dust-like, material evenly distributed throughout the rock.
2. As occasional concentrations around grain boundaries.
3. As small, thin, flakes with relatively high relief and birefringence.

The optical properties of clay flakes suggest that it is illite in composition.

Pyrite 2.0%: Occurs as euhedral to anhedral grains distributed randomly.

Rock Type: Argillaceous Dolomite

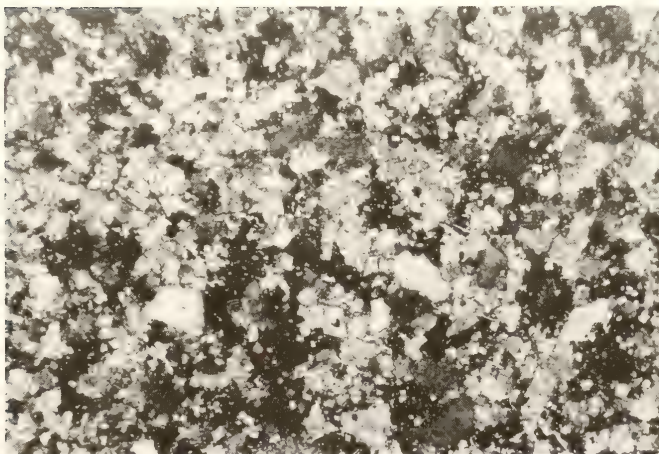


Figure A-1: Photomicrograph of Sample T1 (magnification: 250x)

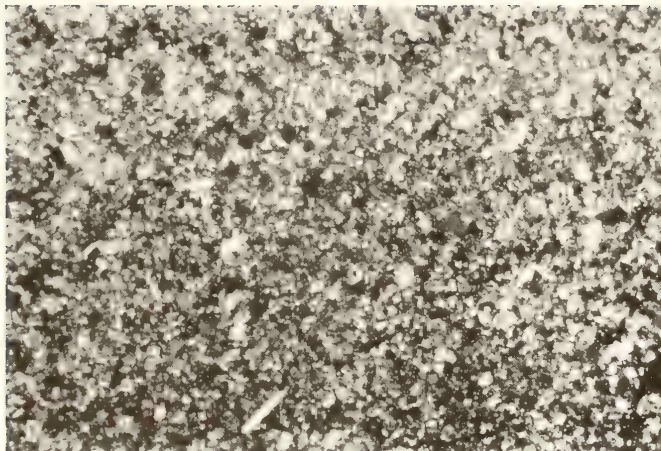


Figure A-2: Photomicrograph of Sample T2 (magnification: 125x)

Sample No. T2

Ledge 801

Quarry T

Megascopic Description

Light grey, very fine-grained, massive. Polished surface appears sandy and porous. Small cavities filled with pyrite are common.

Microscopic Description

Texture

Microcrystalline. Euhedral to subhedral dolomite surrounds the interstitial calcite and quartz. Grain size varies from 0.01 mm to 0.05 mm. Small pores (0.15 mm to 0.1 mm) are present throughout.

Mineral Composition

The rock consists of dolomite, calcite, silt and clay, and quartz. Pyrite is a conspicuous accessory.

Dolomite 60.0%: Occurs as euhedral to subhedral, rhombic grains which surround relatively large quartz grains and associated calcite. Many grains are zoned due to the presence of clay cutons.

Calcite 15.0%: Occurs as microcrystalline, interstitial material intimately associated with silt and clay.

Quartz 8.0%: Occurs as interstitial, anhedral grains of detrital origin ranging in size from 0.05 mm to 0.1 mm.

Silt and Clay 15.0%: Occur in three forms:

1. As finely divided material uniformly distributed throughout the rock.
2. As concentrations around grain boundaries.
3. As thin, long flakes of clay (illite) aligned parallel to each other.

Pyrite 2.0%: Occurs as:

1. Square, rectangular, and triangular cross sections randomly distributed throughout the rock.
2. Cavity fillings.
3. Thin streaks.

Alteration of pyrite to limonite is common.

Rock Type: Argillaceous Dolomite

Sample No. T3

Ledge 802

Quarry T

Megascopic Description

Grey brown, medium to coarse-grained, argillaceous. Streaks and bands of highly argillaceous material alternate with more calcareous portions in a parallel fashion giving rise to a foliated structure. Irregular and curved fractures parallel to the argillaceous laminations are common. Minerals like clay, pyrite and quartz are concentrated along these fractures. The rock breaks easily.

Microscopic DescriptionTexture

Medium grained; terrigenous and organic fragments of coarser calcite are embedded in a fine-grained granular matrix of calcite, dolomite, and argillaceous material. The calcareous fragments are highly variable in size and shape. Elongated calcite fragments are aligned parallel to argillaceous laminations. Alteration of calcite to dolomite and inclusions of cryptocrystalline quartz (chalcedony) are common occurrences.

Mineral Composition

The rock consists of calcite, dolomite, and silt and clay as the major constituents. Quartz, chalcedony, and pyrite form the main accessory minerals.

Calcite 50.0%: It occurs in two modes:

1. Large clastic fragments which are mostly organic (recrystallized fossils) in origin and range in size from 0.5 mm to 2.0 mm (35.0%). Many of these grains have irregular boundaries due to their replacement by dolomite. Some grains are fibrous, some contain chalcedonic inclusions, and still some others show perfect rhombohedral cleavage.
2. As microcrystalline, interstitial material in the ground mass intimately associated with clay (15.0%).

Dolomite 20.0%: Occurs as euhedral, rhombic, grains and is confined to the groundmass. The grain size varies from 0.01 mm to 0.05 mm.

Silt and Clay 20.0%: occur as:

1. Finely divided material uniformly distributed throughout the rock mass.
2. Small, elongated, grains.
3. Laminations (iron stained). The clay is illite in composition.

Quartz 8.0%: It occurs as anhedral grains in the groundmass ranging in size from 0.02 mm to 0.05 mm. It is especially concentrated along fractures.

Pyrite 1.5%: Occurs as individual grains, as irregular growths along grain boundaries, and is especially concentrated along fractures. The grain size is quite variable.

Chalcedony 0.5%: It occurs as cryptocrystalline material along fractures and as a replacement product of calcareous fossils.

Rock Type: Argillaceous Dolomitic Limestone

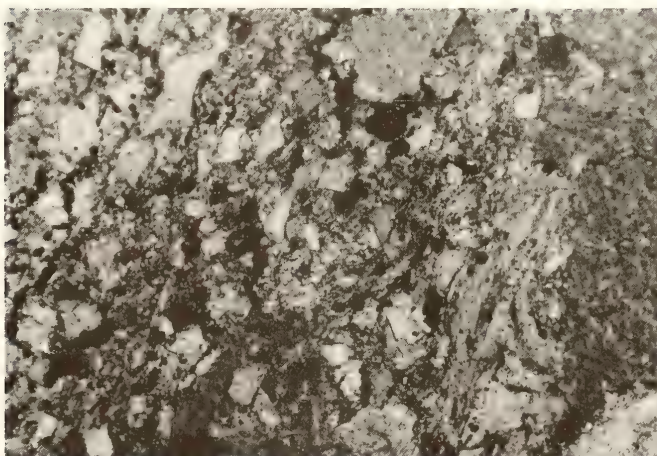


Figure A-3: Photomicrograph of Sample T3 (magnification: 250x)

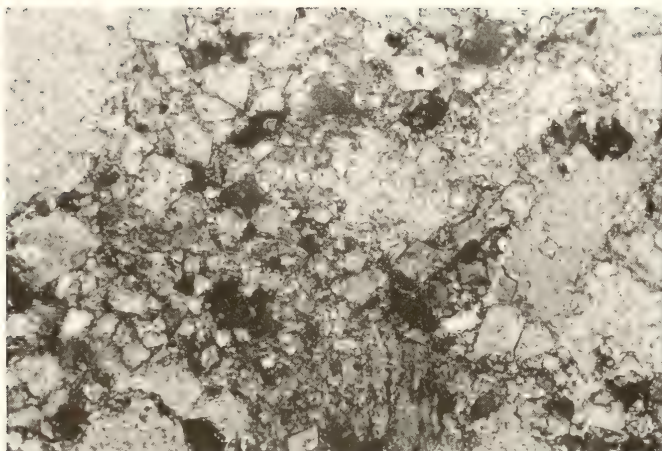


Figure A-4: Photomicrograph of Sample T4 (magnification: 250x)

Sample No. T4

Ledge 802

Quarry T

Megascopic Description

Light grey, medium-grained, and massive. Large calcite fragments are cemented together by a fine grained, crystalline, matrix.

Texture

Clastic fragments of calcite are embedded in a fine-grained matrix of crystalline dolomite, calcite, and argillaceous material. The clastic fragments are both terrigenous and organic in origin, subangular to subrounded, and range in size from 0.5 mm to 1.5 mm. In the matrix, dolomite occurs as euhedral grains while calcite and clay are fine-grained and interstitial.

Mineral Composition

The rock is composed mainly of calcite, dolomite, and argillaceous material. Quartz and pyrite constitute the main accessories.

Calcite 65.0%: It occurs in two modes:

1. Large clastic grains of terrigenous and organic origin (45.0%). Many grains are fibrous. Alteration to euhedral dolomite is common and so are inclusions of cryptocrystalline quartz and fine clay.
2. As fine-grained to cryptocrystalline material in the matrix, interstitial between dolomite grains (20%).

Dolomite 25.0%: It occurs only in the matrix as euhedral grains. The grains vary in size from less than 0.01 mm to 0.05 mm. At places, the rhombic grains are well interlocked.

Silt and Clay 6.0%: occur as:

1. Fine, evenly distributed material throughout the rock.
2. Small, elongated flakes of illite.

Quartz 3.0%: It constitutes an important accessory mineral, is detrital in origin and anhedral in shape. It is confined only to the matrix. Grains are 0.05 mm in size or less.

Pyrite 1.0%: occurs as:

1. Anhedral to subhedral grains.
2. Irregular growths along grain boundaries in the matrix.

Rock Type: Argillaceous Dolomitic Limestone

Sample No. T5

Ledge 803A

Quarry T

Megascopic Description

Light grey, fine-grained, massive. Under binocular microscope, the surface appears rough and sugary. The sugary texture gives rise to numerous small cavities on cut surfaces. A few cavities are filled with recrystallized dolomite. Concentration of pyrite in thin irregular veins is common. Pyrite shows alteration to limonite.

Microscopic DescriptionTexture

Fine-grained. Euhedral, equidimensional rhombs of dolomite form a continuous mosaic disturbed only by occasional cavity fillings and irregular streaks of pyrite. The general size of dolomite grains ranges from 0.02 mm to 0.05 mm while the recrystallized dolomite in cavities can be as large as 0.2 mm.

Mineral Composition

The rock consists predominantly of dolomite with smaller amounts of interstitial calcite, quartz, and argillaceous material. Pyrite is the only identifiable accessory mineral.

Dolomite 70%: It occurs as euhedral, equidimensional grains which are poorly interlocked and uniformly distributed throughout the rock to give it a sugary texture. Many grains show zoning due to variation in the iron content.

Calcite 5.0%: It occurs as fine grained interstitial material.

Silt and Clay 22.0%: These occur in two forms:

1. Mostly as finely divided material evenly distributed throughout the rock mass.
2. As occasional thin flakes of clay (0.05 mm long) which show high relief, fairly high birefringence, and parallel extinction.

The optical properties suggest that the clay is illite in composition.

Quartz 2.5%: It is detrital, anhedral, and uniformly distributed.

Pyrite 0.5%: Occurs generally as irregular veins which pinch and swell. Individual, subhedral grains are also present.

Rock Type: Argillaceous Dolomite

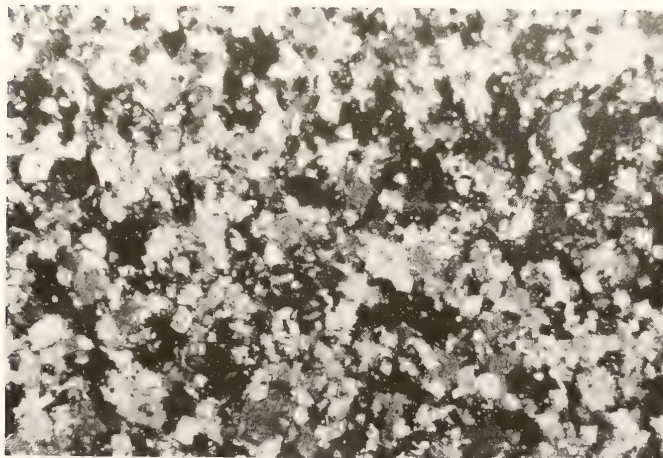


Figure A-5: Photomicrograph of Sample T5 (magnification: 250x)

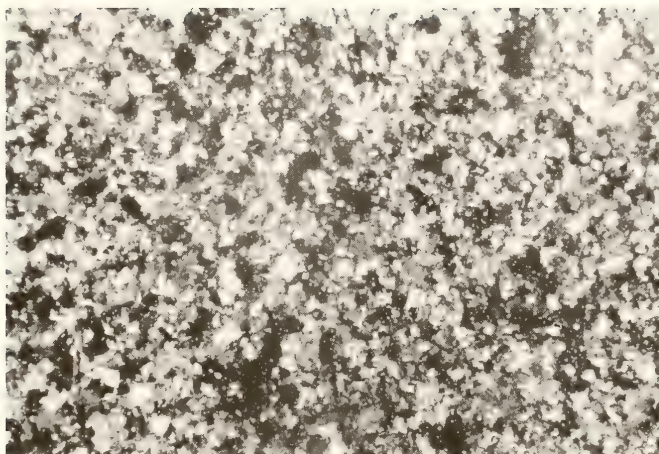


Figure A-6: Photomicrograph of Sample T6 (magnification: 125x)

Sample No. T6

Ledge 803A

Quarry T

Megascopic Description

Light grey, fine grained, massive. The polished surface appears sugary and pitted with micro-cavities. Patches of recrystallized, coarse grained, calcite and dolomite are present. Thin, irregular streaks of pyrite are a characteristic feature.

Microscopic Description

Texture

Fine grained. Euhedral, rhombic grains of dolomite form a weak matrix with calcite, quartz and argillaceous material being interstitial. Coarse-grained calcite and dolomite fill a few cavities. Pyrite forms irregular growths and streaks. The average grain size varies from 0.02 mm to 0.05 mm.

Mineral Composition

The rock consists chiefly of dolomite, finely divided silt and clay, calcite, and minor amount of quartz. Pyrite is the only accessory mineral.

Dolomite 65.0%: Occurs as euhedral to subhedral, equidimensional, rhombic grains with inclusions of very finely divided clay. Coarse grained dolomite also occurs as cavity fillings.

Calcite 12.0%: Occurs as interstitial material between dolomite grains as well as cavity fillings.

Silt and Clay 20.0%: Occur in two forms:

1. As very finely divided material distributed evenly throughout the rock and giving a dirty appearance to calcite and dolomite.
2. As occasional, elongated flakes with relatively high relief and high birefringence.

The clay is illite in composition

Quartz 2.5%: Occurs as anhedral grains and is detrital in origin.

Pyrite 0.5%: Occurs as individual grains as well as a replacement product forming irregular growths.

Rock Type: Argillaceous Dolomite

Sample No. T7

Ledge 803B

Quarry T

Megascopic Description

Light grey to brownish grey, medium-grained, biofragmental, argillaceous. Larger calcareous fragments of recrystallized fossils are surrounded by a fine-grained granular matrix. Laminations of more argillaceous rock alternate with less argillaceous ones.

Microscopic DescriptionTexture

Partly clastic with calcareous biofragments of medium to coarse size (0.5 mm - 1.0 mm) embedded in a fine-grained granular matrix of dolomite, calcite, and argillaceous material. Although most of the calcareous fragments are of organic origin, some terrigenous grains are also present. The fragments are highly variable in shape but circular cross-sections are the most common. In the matrix the dolomite occurs as euhedral to subhedral grains while calcite is anhedral and interstitial.

Mineral Composition

The rock is composed mainly of calcite, dolomite, and argillaceous material with pyrite and quartz as the accessory minerals.

Calcite 60%: Occurs in two forms:

1. As coarse-grained clastic fragments which are mostly recrystallized fossils and range in size from 0.5 mm to 2.0 mm (35%). Replacement to dolomite is a common feature. Some grains are fibrous while many others show wavy extinction, cleavage, or twinning.
2. As fine grained interstitial material in the groundmass (25%), where it is microcrystalline and intimately associated with clay.

Dolomite 28%: It is confined only to the groundmass. The grain size varies from 0.01 mm to 0.1 mm.

Silt and Clay 10%: Occur as:

1. Finely divided material evenly distributed through out the rock.
2. Small, elongated flakes of illite.
3. Streaks and laminations.

Quartz 1.5%: Occurs as anhedral, interstitial grains (0.02 mm - 0.05 mm) in the groundmass.

Pyrite 0.5%: Occurs as small, individual grains and as irregular streaks.

Chalcedony: Occurs as spherulitic replacements of calcareous fragments. Only a few grains are present.

Rock Type: Argillaceous Dolomitic Limestone

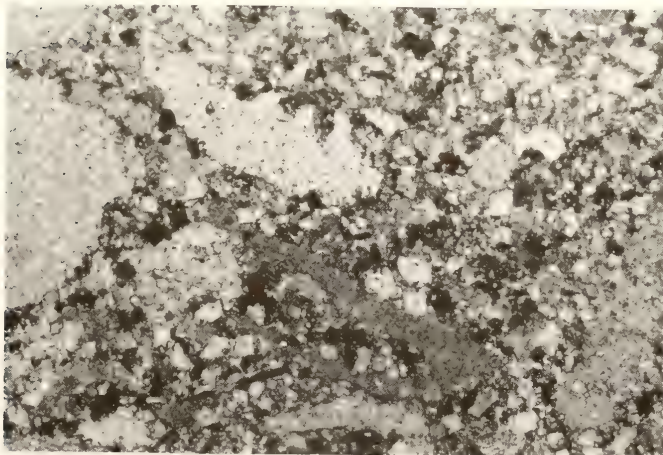


Figure A-7: Photomicrograph of Sample T7 (magnification: 62.5x)

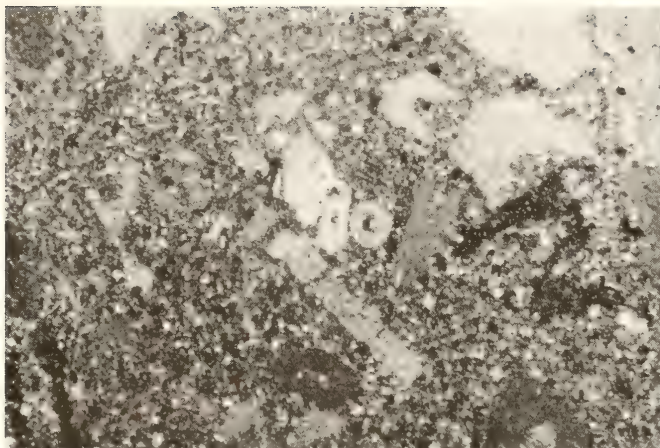


Figure A-8: Photomicrograph of Sample T8 (magnification: 62.5x)

Sample No. T8

Ledge 803B

Quarry T

Megascopic Description

Light grey, fine to medium-grained, biofragmental, massive, coarse grained, clastic fragments are surrounded by a fine-grained matrix which appears granular under binocular microscope. A few microfractures are present.

Microscopic Description

Texture

Clastic with calcareous biofragments embedded in a fine-grained granular matrix of calcite, dolomite, and clay. These fragments are highly variable in size and shape with the general range of size being 0.2 mm to 2.0 mm. Calcite shows various stages of alteration to dolomite with the replacement first starting in the middle of the grain.

Mineral Composition

The rock consists of calcite, dolomite, and argillaceous material as the major constituents and quartz, pyrite, and chalcodony as the accessory minerals.

Calcite 55.0%: It occurs in two forms:

1. As coarse-grained clastic fragments which are recrystallized fossil remains (30%). A wide variety of shapes and a range of sizes are present. Replacement by dolomite is very common. Some calcite is fibrous in nature.
2. As cryptocrystalline interstitial material in the matrix where it is intimately associated with argillaceous materials (25%).

Dolomite 30.0%: Occurs as euhedral to subhedral grains (0.01 mm - 0.05 mm) which are confined to the matrix only.

Silt and Clay 13.0%: Silt and clay occur as:

1. Finely divided, interstitial material intimately associated with the calcite of the matrix and present as impurities in the calcareous fragments.
2. As small flakes of clay the optical properties of which suggest the clay to be illite in composition.

Quartz 1.5%: Occurs as small (0.01 mm - 0.05 mm), anhedral, grains of detrital origin through out the rock.

Pyrite 0.5%: Occurs as subhedral to anhedral grains which show alteration to limonite.

Chalcodony: Occurs as a replacement product of calcite. Only a few grains are present.

Rock Type: Argillaceous Dolomitic Limestone

Sample No. T9

Ledge 803B

Quarry T

Megascopic Description

Light grey, medium to coarse-grained, biofragmental, and cherty. Streaks and lenses of siliceous material, thin irregular streaks of argillaceous material, and irregular fractures are common features.

Microscopic DescriptionTexture

Clastic with medium size (0.25 mm - 2.0 mm) calcareous and siliceous fragments embedded in a fine-grained matrix of calcite, dolomite, and silt and clay. The calcite fragments are organic in origin and frequently show replacement by euhedral dolomite, chalcedony, and microcrystalline quartz. Fractures are commonly filled with calcite or microcrystalline to cryptocrystalline silica.

Mineral Composition

The rock consists of calcite, dolomite, silt and clay, and microcrystalline to cryptocrystalline silica as the essential minerals. Quartz and pyrite form the accessories.

Calcite 65.0%: It occurs in two forms:

1. As biofragments of coarse grained calcite which are highly variable in size and shape (35%). These fragments show extensive alteration to dolomite and siliceous material. At places, the calcite has been completely silicified giving rise to pockets, lenses, and streaks of siliceous material.
2. As fine-grained, interstitial material intimately associated with silt and clay and frequently replaced by silica (30%).

Dolomite 15.0%: Occurs only in the groundmass as euhedral, rhombic grains (0.02 mm - 0.07 mm).

Silt and clay 15.0%: These are present as:

1. Very fine-grained, interstitial material.
2. Irregular, contorted streaks.
3. Impurities within large calcite fragments.

Chalcedony 4.5%: Occurs as a replacement product of calcite and as cavity and fracture fillings. At places it is typically spherulitic in form.

Pyrite 0.5%: Occurs as individual grains and irregular growths throughout the rock mass.

Rock Type: Argillaceous Dolomitic Limestone

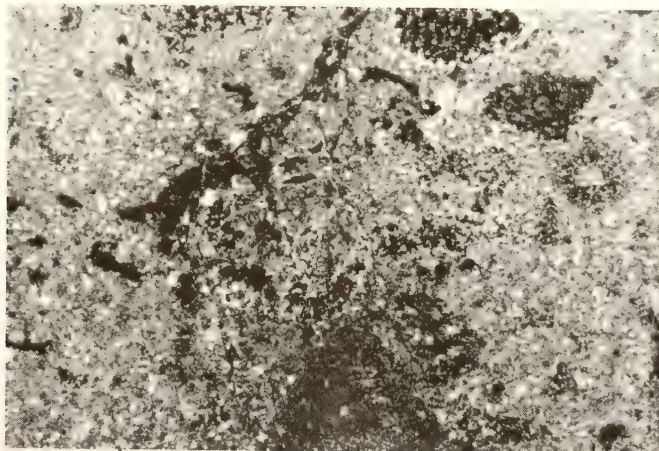


Figure A-9: Photomicrograph of Sample T9 (magnification: 62.5x)

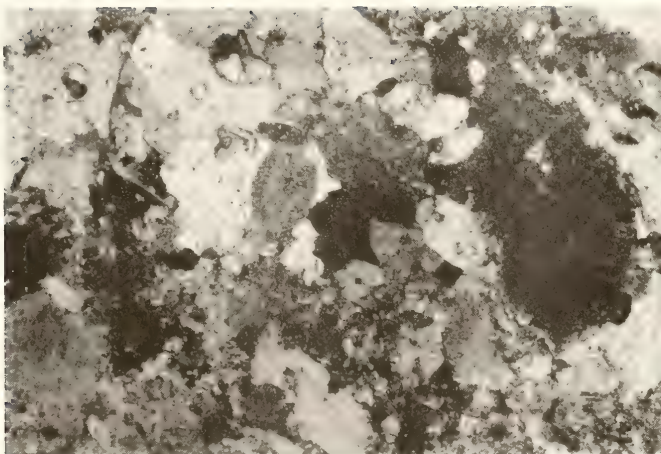


Figure A-10: Photomicrograph of Sample T10 (magnification: 62.5x)

Sample No. T10

Ledge 7

Quarry T

Megascopic Description

Greyish brown, medium to coarse grained, hard, and massive. Under binocular microscope the polished surface appears dense, compact, and crystalline.

Microscopic Description

Texture

Medium to coarse grained, crystalline calcite is cemented together by a fine grained matrix of calcite and dolomite. Calcite crystals are well interlocked giving rise to a dense and compact rock. Some grains have sutured outlines. The calcite grains range in size from 0.2mm to 4.0 mm. Dolomite forms euhedral grains which are generally 0.3 mm or less in size.

Mineral Composition

The rock consists of calcite and dolomite as the major constituents. Clay, chalcedony, carbonaceous material, and pyrite occur as accessories.

Calcite 85.0%: Occurs as well interlocked grains which are highly variable in size (0.2mm-4.0mm). Both crystalline and fibrous varieties are present. Many crystalline grains show perfect rhombohedral cleavage. Replacement of calcite by dolomite is common.

Dolomite 10.0%: Occurs as euhedral to subhedral grains ranging in size from 0.3 mm to 0.5 mm.

Clay 2.0%: Occurs as finely distributed material throughout the rock.

Chalcedony 1.5%: Occurs as a conspicuous accessory in the form of irregular growths. However, spherulitic growths can also be seen.

Carbonaceous Matter 1.5%: Occurs as finely disseminated material inside larger calcite grains.

Pyrite 0.0%: Only a few small, discrete grains are present. Limonite staining is also a common feature.

Rock Type: Limestone

Sample No. K1

Ledge 5

Quarry T

Megascopic Description

Light grey, fine-grained, argillaceous; streaks of light brown color indicate concentrations of argillaceous material. Small, elongated, cavities (0.2 mm - 0.8 mm) are present. The polished surface appears granular.

Microscopic DescriptionTexture

Very fine-grained, granular. Detrital, anhedral grains of quartz (0.03 mm - 0.01 mm) and euhedral rhombs of dolomite (0.03 mm - 0.1 mm) are cemented together by an even finer-grained matrix of calcite and clay. Silt and clay also occur as streaks and flakes. A weak alignment of elongated quartz grains and clay flakes can be seen.

Mineral Composition

The rock consists of calcite, dolomite, quartz, and argillaceous material. Pyrite is an important accessory.

Dolomite 50.0%: It occurs as small, euhedral to subhedral, rhombs which are more or less uniformly distributed and appear quite dirty because of argillaceous impurities. Some grains are zoned due to variation in iron content.

Calcite 20.0%: It occurs mostly as microcrystalline to cryptocrystalline material intimately associated with silt and clay. Some larger grains with cleavage are also present.

Silt and Clay 12.0%: Occur in three forms:

1. As finely divided material intimately associated with calcite and dolomite.
2. As thin, elongated, isolated flakes with a high relief, a relatively high birefringence, and a weak alignment.
3. As thin, irregular, contorted streaks.

The optical properties suggest the clay to be illite in composition.

Quartz 7.5%: Occurs as small (0.03 mm - 0.1 mm), clear, anhedral grains of detrital origin.

Pyrite 0.5%: Occurs as isolated, anhedral to subhedral, grains (0.01 mm - 0.2 mm) and as irregular growths and streaks.

Rock Type: Argillaceous Calcareous Dolomite

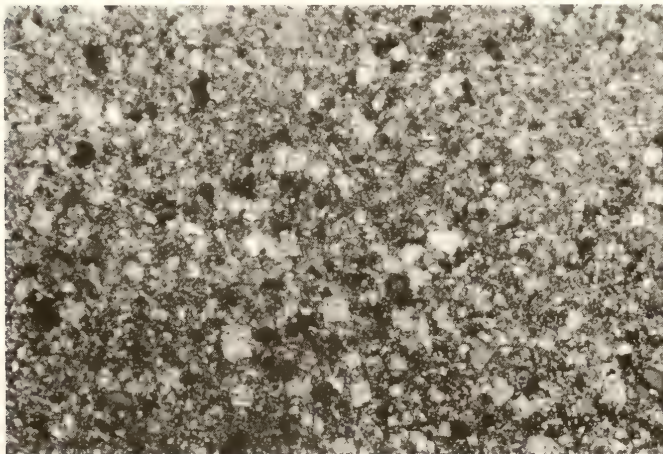


Figure A-11: Photomicrograph of Sample K1 (magnification: 125x)

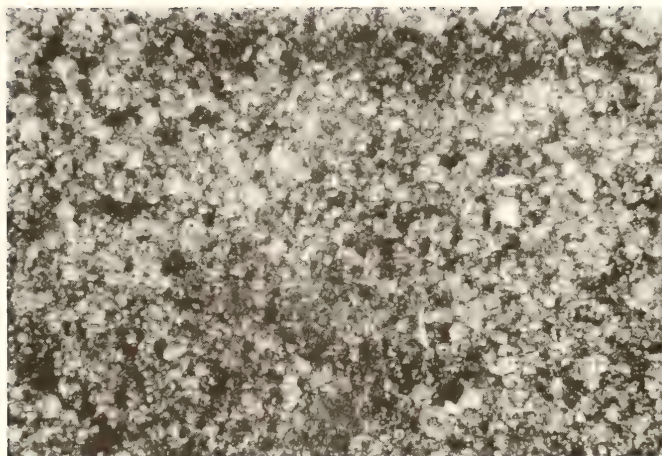


Figure A-12: Photomicrograph of Sample K2 (magnification: 125x)

Sample No. K2

Ledge 5

Quarry K

Megascopic Description

Light grey, fine-grained, banded, argillaceous. Bands, lenses, and streaks of more argillaceous material alternate with less argillaceous zones in an irregular fashion. Pockets of coarsely crystalline, secondary calcite measuring up to 1 cm are common and so are small cavities (0.2 mm - 0.5 mm) which result from dolomitization of calcite. The polished surface appears granular.

Microscopic Description

Texture

Fine-grained, granular; euhedral, equidimensional grains of dolomite and anhedral quartz are cemented together by a mixture of very fine grained calcite and argillaceous material. Both quartz and dolomite range in size from 0.02 mm to 0.1 mm with 0.05 mm being the average. The largest grains are always those of detrital quartz.

Mineral Composition

The rock is composed of dolomite, calcite, silt and clay, and quartz as the major constituents with pyrite as the only accessory mineral.

Dolomite 50.0%: Occurs as euhedral to subhedral rhombic crystals which are heavily contaminated by the presence of argillaceous matter and show zoned structure in many cases.

Calcite 20.0%: Occurs as microcrystalline to cryptocrystalline, interstitial, material intimately associated with silt and clay.

Silt and Clay 15.0%: Occur in three forms:

1. As finely distributed material throughout the rock mass. This is the most common mode of occurrence.
2. As individual, tabular flakes showing a weak parallelism.
3. As irregular streaks of dirty brown color.

Quartz 4.5%: Occurs as small, anhedral, detrital grains evenly distributed throughout the rock.

Pyrite 0.5%: Occurs as anhedral to subhedral, isolated grains.

Rock Type: Argillaceous Calcareous Dolomite

Sample No. K3

Ledge 5

Quarry K

Megascopic Description

Light grey, fine-grained, argillaceous. Numerous small cavities are present. These are irregular in shape and range in size from 0.2 mm to 2.0 mm. The polished surface appears granular.

Microscopic DescriptionTexture

Fine grained. Euhedral to subhedral grains of dolomite and anhedral grains of quartz are surrounded by a fine-grained matrix of calcite, dolomite, and argillaceous material. Quartz forms the largest grains (0.15 mm) but it is highly variable in size, the range being 0.02 mm to 0.15 mm. Dolomite rhombs are fairly well interlocked and range in size from 0.02 mm to 0.07 mm. On the whole, relatively coarse-grained zones are present in a fine-grained matrix of similar composition in an irregular fashion.

Mineral Composition

The rock is composed of dolomite, calcite, quartz, and argillaceous material with pyrite as the accessory mineral. A few grains of orthoclase are also present.

Dolomite 60.0%: Occurs as euhedral to subhedral, rhombic grains. The grains contain inclusions of silt and clay and some grains are zoned.

Calcite 15.0%: Occurs as cryptocrystalline, interstitial material closely associated with argillaceous material.

Silt and Clay 20.0%: Occurs as:

1. Finely distributed material throughout the rock. This is the chief mode of occurrence.
2. Thin, needle-like flakes which show relatively high relief and high birefringence.
3. Very thin, dirty brown, contorted streaks.

The clay is illite in composition.

Quartz 4.5%: Occurs as small, anhedral grains throughout the rock mass.

Pyrite 0.5%: Occurs as individual grains of anhedral to subhedral outline.

Rock Type: Argillaceous Calcareous Dolomite

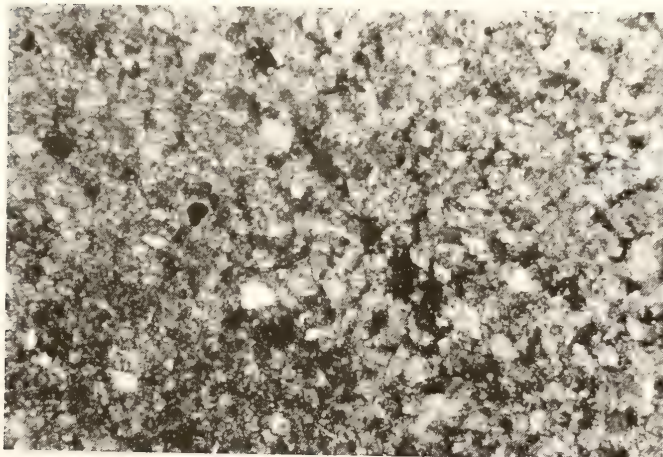


Figure A-13: Photomicrograph of Sample K3 (magnification: 125x)

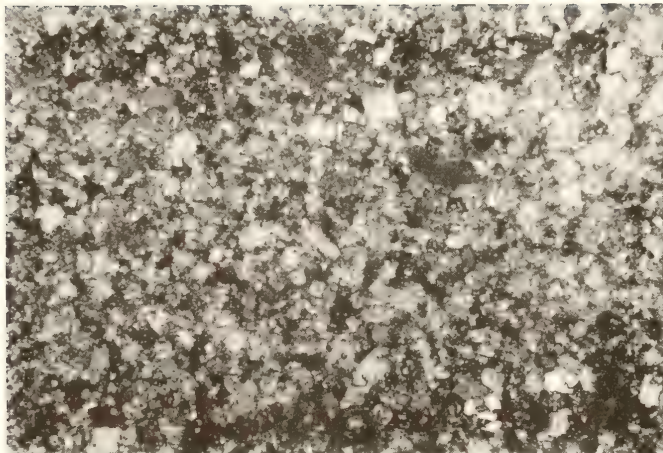


Figure A-14: Photomicrograph of Sample K4 (magnification: 125x)

Sample No. K4

Ledge 5

Quarry K

Megascopic Description

Light grey, fine-grained, argillaceous. Small cavities (max. size 1 mm) of variable size, shape, and depth are common. Polished surface appears sugary when examined under binocular microscope.

Microscopic Description

Texture

Fine grained. Dolomite occurs as rhombohedral, fairly well interlocked, grains with anhedral quartz, cryptocrystalline calcite, and finely divided silt and clay forming the interstitial material. Quartz forms the largest grains but generally both quartz and dolomite range in size from 0.02 mm to 0.2 mm with 0.05 mm being the average.

Mineral Composition

The rock is composed of dolomite, calcite, silt and clay, and quartz as the essential constituents and pyrite as an accessory mineral. A few grains of orthoclase are present.

Dolomite 60.0%: Occurs as euhedral to subhedral grains which contain finely divided silt and clay as impurities. Perfect zoning is seen in some grains.

Calcite 15.0%: Occurs as cryptocrystalline, interstitial material intimately associated with silt and clay.

Silt and Clay 18.0%: Occur as:

1. Finely divided, interstitial material closely associated with calcite which has not yet dolomitized. This is the dominant mode of occurrence.
2. Thin, long, tabular flakes.
3. A few thin, dirty brown, contorted streaks.

Quartz 6.3%: Occurs as anhedral, detrital grains scattered throughout the rock mass.

Pyrite 0.5%: Occurs as anhedral to subhedral grains many of which can be seen replacing dolomite.

Rock Type: Argillaceous Calcareous Dolomite

Megascopic Description

Light grey to light tan brown, fine-grained, highly argillaceous. Relatively dark colored argillaceous areas curve around light colored carbonate areas. Under the binocular microscope, the polished surface appears sugary and granular. Microcavities which are a characteristic feature of the upper part of the ledge are generally absent and when present are very small (0.1 mm or less).

Microscopic DescriptionTexture

Fine-grained. Euhedral to subhedral grains of dolomite and anhedral grains of quartz are surrounded by a matrix of very fine-grained dolomite, calcite, and argillaceous material. Both dolomite and quartz are very variable in size but the general range is from 0.02 mm to 0.07 mm with 0.04 mm being the average. Needle-like flakes of clay are abundant but show no preferred orientation. Pyrite generally occurs as irregular growths and as streaks.

Mineral Composition

The rock is composed of calcite, dolomite, silt and clay, and quartz as the chief minerals with silt and clay being strikingly dominant. Pyrite is the important accessory mineral.

Dolomite 45.0%: Occurs as euhedral to subhedral grains. Most of the grains show the presence of argillaceous impurities and many are zoned. Relatively good interlocking of the rhombic grains characteristic of the upper parts of the ledge is destroyed due to the abundance of argillaceous material.

Calcite 10.0%: Occurs as cryptocrystalline interstitial material. The calcite and argillaceous material are so intimately associated with each other that the two cannot be clearly separated under the microscope.

Silt and Clay 37.0%: Occur in three forms:

1. As extremely fine-grained, interstitial material and as impurity in dolomite. This is the dominant mode of occurrence.
2. As numerous, long (0.15 mm), needle like flakes showing high relief and high birefringence.
3. As curved, roughly parallel streaks of dirty brown color.

Quartz 7.0%: Occurs as anhedral, angular to subangular grains uniformly distributed throughout the rock.

Pyrite 1.0%: Occurs as

1. Individual grains.
2. Irregular growths around dolomite grains.
3. Streaks (0.25 mm thick).

Rock Type: Argillaceous Dolomite

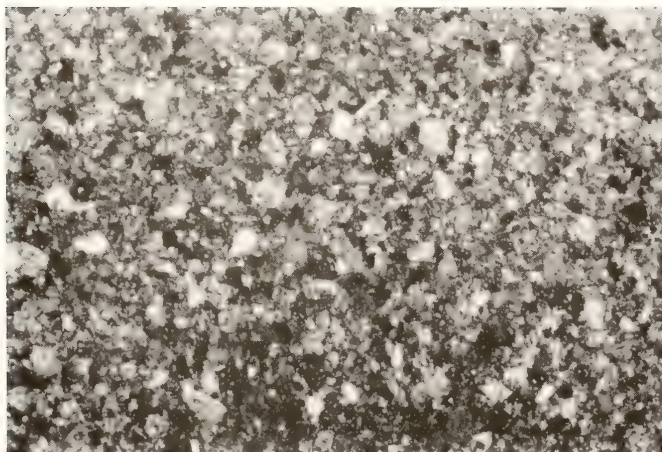


Figure A-15: Photomicrograph of Sample K5 (magnification: 125x)

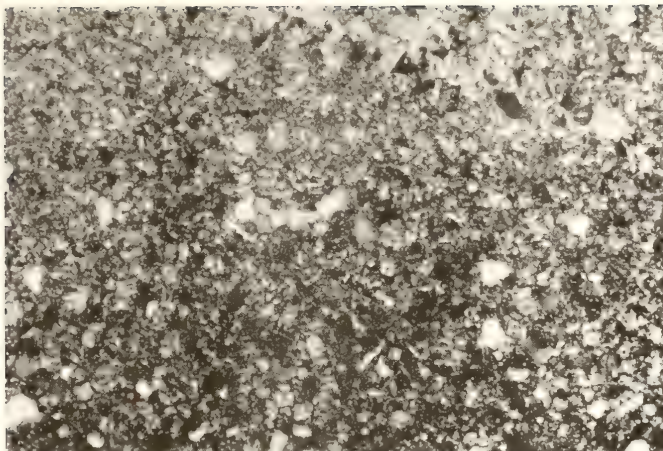


Figure A-16: Photomicrograph of Sample K6 (magnification: 125x)

Sample No. K6

Ledge 5

Quarry K

Megascopic Description

Light grey, fine-grained, argillaceous. Irregular streaks and patches of argillaceous material and localized concentrations of pyrite are characteristic features. Polished surface, when examined under binocular microscope, appears granular.

Microscopic Description

Texture

Fine-grained. Euhedral, rhombic crystals of dolomite and anhedral, angular to subangular, grains of quartz are surrounded by a fine-grained matrix of dolomite, calcite, and silt and clay. The grain size is variable. Localized areas of coarser grain size alternate with finer-grained areas in an irregular manner. The size of larger grains varies from 0.02 mm to 0.15 mm. Pyrite occurs as irregular growths.

Mineral Composition

The rock consists of dolomite, calcite, silt and clay, and quartz. Pyrite is present as an accessory mineral.

Dolomite 50.0%: Occurs as euhedral to subhedral, rhombic crystals most of which are highly contaminated with argillaceous impurities and show zoned structure due to variation in iron and clay contents.

Calcite 5.0%: Occurs as cryptocrystalline, interstitial material intimately associated with silt and clay and difficult to differentiate from them.

Silt and Clay 35.0%: Occur in three forms:

1. As very finely divided material evenly distributed throughout the rock. This is the chief mode of occurrence.
2. As thin, elongated (0.2 mm), needle like flakes without any preferred orientation. These are quite common.

The optical properties show the clay to be of illite composition.

Quartz 9.0%: Occurs as anhedral, angular to subangular, grains distributed throughout the rock.

Pyrite 1.0%: Occurs as:

1. Individual, anhedral to subhedral grains.
2. Irregular growths around dolomite grains.
3. Irregular, discontinuous, pinching and swelling streaks.

Rock Type: Argillaceous Dolomite

Megascopic Description

Light grey to light brown, fine-grained, highly argillaceous. Argillaceous material is seen to surround small, oval-shaped areas of carbonate material. Argillaceous material is also concentrated in the form of lenses and more or less rounded bodies. Very thin, black streaks of pyrite are present.

Microscopic DescriptionTexture

Very fine-grained with about 50% material being clastic in nature (silt, clay, and quartz). Euhedral and subhedral grains of dolomite and anhedral grains of quartz are embedded in a very fine-grained, highly argillaceous matrix of dolomite, silt and clay, and some calcite. The larger dolomite and quartz grains range in size from 0.02 mm to 0.05 mm. Elongated, tabular grains of hydromuscovite (illite) are quite common.

Mineral Composition

The major constituents of the rock are silt and clay, dolomite, quartz, and calcite. Pyrite is the only accessory mineral present.

- Dolomite 45.0%: Occurs as euhedral to subhedral rhombic grains which contain large proportions of silt and clay as impurities. Dolomite occurs in two modes:
1. Relatively large grains (0.02 mm - 0.05 mm).
 2. In the matrix with calcite and argillaceous material.

Many grain boundaries are masked by silt and clay.

Calcite 5.0%: Occurs as microcrystalline, interstitial material intimately associated with silt and clay.

Silt and Clay 35.0%: Occur in three forms:

1. As finely divided material evenly distributed throughout the rock.
2. As elongated, tabular flakes randomly oriented and distributed.
3. As thin, irregular, dirty brown streaks.

Quartz 14.5%: Occurs as anhedral, angular to subangular grains more or less evenly distributed.

Pyrite 0.5%: Occurs as:

1. Individual, anhedral grains.
2. Irregular growths.
3. Thin streaks.

Some grains show alteration to limonite.

Rock Type: Silty Dolomite or Dolomitic Siltstone

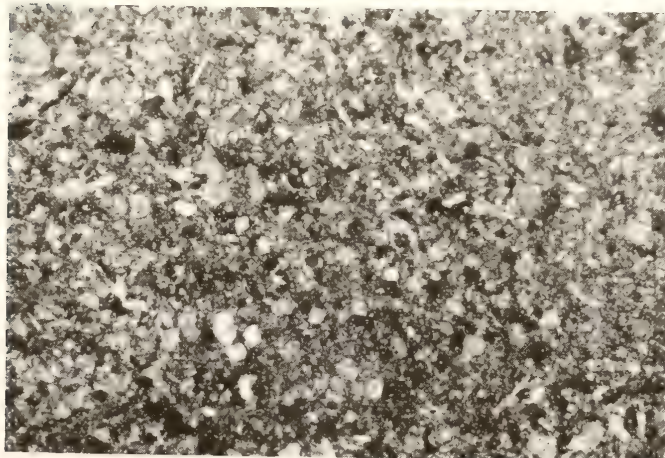


Figure A-17: Photomicrograph of Sample K7 (magnification: 125x)

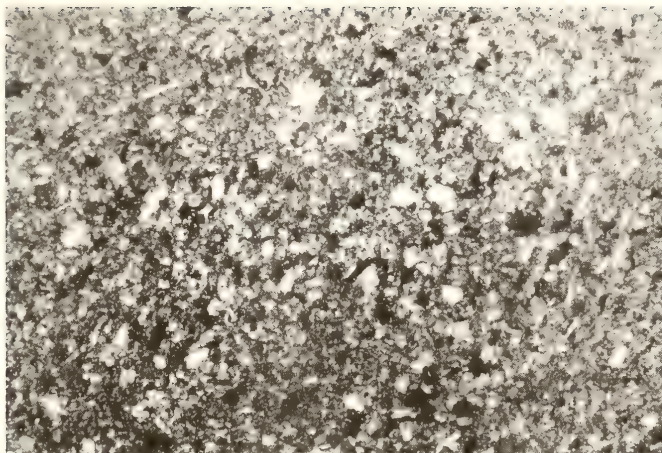


Figure A-18: Photomicrograph of Sample K8 (magnification: 125x)

Sample No. K8

Ledge 5

Quarry K

Megascopic Description

Light gray to light brown, fine-grained, highly argillaceous, massive. Wavy streaks of argillaceous material are very abundant. Areas of carbonate material (light grey) alternate with areas of more argillaceous material (light brown) in an irregular fashion. Pyrite growths as large as 1 mm can be seen. The polished surface appears sugary.

Microscopic Description

Texture

Very fine-grained, partly clastic. Euhedral to anhedral grains of dolomite and anhedral grains of quartz are surrounded by a fine-grained matrix of calcite, dolomite, quartz, silt and clay. Both dolomite and quartz are bi-modal. The larger grains range in size from 0.02 mm to 0.06 mm. Elongated, tabular flakes of hydromuscovite (illite) are very common but show no preferred orientation. Pyrite forms individual grains and irregular growths.

Mineral Composition

The rock consists of dolomite, silt and clay, quartz, and calcite with pyrite as an accessory mineral.

Dolomite 45.0%: Occurs as euhedral to subhedral grains which contain abundant silt and clay as impurities. Argillaceous material also masks the grain boundaries. Many grains are also zoned due to variation of clay and iron content.

Calcite 5.0%: Occurs as microcrystalline, interstitial, material.

Silt and Clay 35.0%: Occur as:

1. Very fine grained, interstitial, material evenly distributed throughout the rock. This is the chief mode of occurrence.
2. Elongated, tabular, flakes showing relatively high relief and high birefringence.
3. Irregular streaks of dirty brown color.

Quartz 14.5%: Occurs as anhedral, angular to subangular, evenly distributed grains.

Pyrite 0.5%: Occurs as:

1. Isolated grains.
2. Irregular, circular growths (upto 1 mm).
3. Thin, long streaks.

Rock Type: Silty Dolomite or Dolomitic Siltstone

Sample No. K9

Ledge 5

Quarry K

Megascopic Description

Light grey to light brown, fine-grained, highly argillaceous. Irregular streaks of argillaceous material are common. Lens-shaped bodies (1.5 mm long, 1 mm wide) of carbonate material are surrounded by relatively darker, more argillaceous material. No cavities or fractures are seen. The polished surface appears sugary and granular under the binocular microscope.

Microscopic DescriptionTexture

Very fine-grained, partly clastic. Euhedral to subhedral grains of dolomite and anhedral grains of quartz varying in size from 0.02 mm to 0.06 mm are surrounded by a fine-grained matrix of dolomite, silt and clay, quartz, and some calcite. Elongated, tabular grains of hydromuscovite (illite) are common and are sometimes aligned parallel to the boundaries of dolomite grains.

Mineral Composition

The rock consists of dolomite, silt and clay, quartz, and some calcite with pyrite as an accessory.

Dolomite 45.0%: Occurs as euhedral to subhedral rhombic grains heavily contaminated with argillaceous material which masks the boundaries of many grains. Many grains are zoned.

Calcite 5.0%: Occurs as microcrystalline, interstitial, material intimately associated with silt and clay.

Silt and Clay 35.0%: Occur in three forms:

1. As very fine-grained, evenly distributed material. This is the major mode of occurrence.
2. As elongated, tabular flakes which are generally randomly oriented except in some cases when they are aligned parallel to the boundaries of dolomite grains.
3. As local concentrations and streaks.

Quartz 15.0%: Occurs as anhedral, angular to subangular grains.

Pyrite: Only a few grains are present. It occurs as irregular growths and as isolated grains.

Rock Type: Silty Dolomite or Dolomitic Siltstone

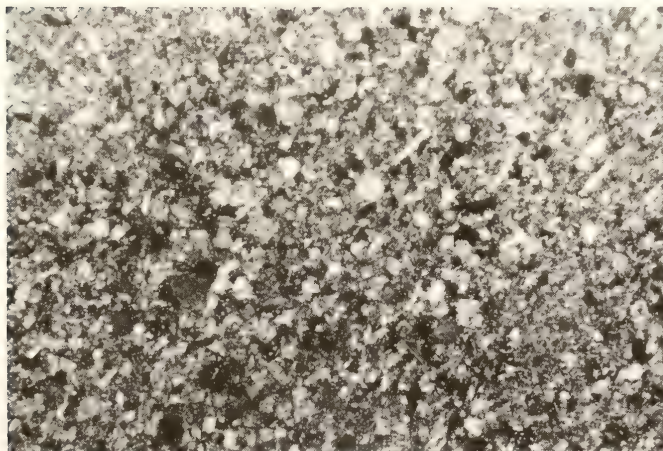


Figure A-19: Photomicrograph of Sample K9 (magnification: 125x)

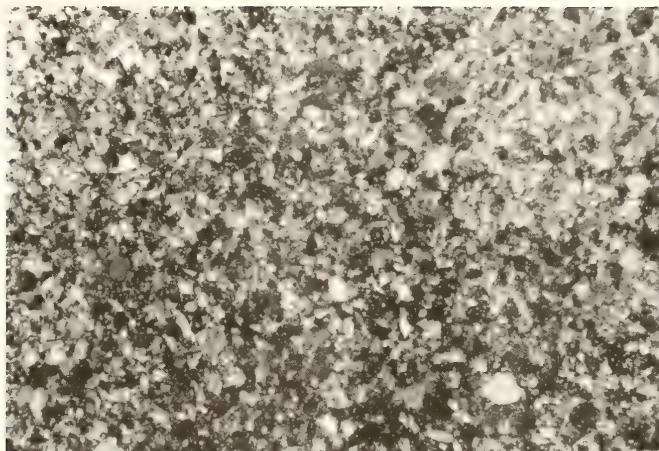


Figure A-20: Photomicrograph of Sample K10 (magnification: 125x)

Sample No. K10

Ledge 5

Quarry K

Megascopic Description

Light grey to light brown, fine-grained, highly argillaceous. Wavy streaks of argillaceous material are roughly parallel to each other and enclose between them lens-shaped, lighter colored, areas which consist mostly of carbonates and quartz. Argillaceous material is also concentrated in the form of discrete bodies. The polished section appears granular under binocular microscope. Streaks and localized growths of pyrite can also be seen.

Microscopic Description

Texture

Very fine-grained, partly clastic. Euhedral to subhedral grains of quartz are surrounded by a fine-grained matrix of dolomite, silt and clay, quartz, and some calcite. The larger grains of both dolomite and quartz range in size from 0.02 mm to 0.07 mm while the grain size in the matrix is generally less than 0.01 mm. In the proximity of clay streaks, dolomite and quartz are much more finely crystalline. Elongated flakes of clay are randomly oriented but at some places they are aligned parallel to the boundaries of dolomite rhombs. Pyrite forms discrete grains as well as tends to grow around other minerals.

Mineral Composition

The rock is essentially composed of dolomite, silt and clay, quartz, and small amounts of calcite. Pyrite is the only accessory mineral present.

Dolomite 45.0%: Occurs as euhedral rhombic crystals, highly variable in size, and rich in argillaceous impurities. Many dolomite grains are zoned due to the presence of clay cutons and many have masked boundaries due to the abundance of argillaceous material.

Calcite 5.0%: Occurs as microcrystalline, interstitial material intimately associated with silt and clay.

Silt and Clay 33.0%: Occur in three forms:

1. As very finely divided material, evenly distributed throughout the rock mass. This is the dominant mode of occurrence.
2. As elongated, tabular flakes which are illite in composition.
3. As irregular streaks of fine dusty nature.

Quartz 16.5%: Occurs as angular to subangular grains of detrital origin.

Pyrite 0.5%: Occurs as:

1. Discrete, anhedral to subhedral grains.
2. Irregular growths along the boundaries of dolomite, quartz, and illite.

Rock Type: Silty Dolomite or Dolomitic Siltstone

Sample No. K11

Ledge 4

Quarry K

Megascopic Description

Light grey, medium-grained, biofragmental, clastic. Large calcareous fragments of organic (fossil) origin are cemented together by a fine-grained matrix. An examination of the polished surface under binocular microscope shows the presence of microfractures and some very small cavities (0.5 mm).

Microscopic DescriptionTexture

Medium-grained, partly clastic. Large (0.25 mm - 2.0 mm) calcareous fragments of crystalline calcite, representing complete and broken fossils, are surrounded by a tight mosaic of euhedral rhombs of crystalline dolomite. The interstitial spaces between dolomite crystals are filled with crystalline calcite, quartz, and argillaceous material. The large calcite fragments are being replaced by dolomite everywhere resulting in irregular grain boundaries. Pyrite occurs mostly as discrete grains.

Mineral Composition

The rock is mainly composed of calcite and dolomite with some quartz and silt and clay. Pyrite and chalcedony are present as accessory minerals.

Dolomite 60.0%: Occurs as a mosaic of well interlocked, euhedral grains.

The grains are highly variable in size and range from less than 0.01 mm to 0.15 mm.

Calcite 25.0%: Occurs mostly as recrystallized fossil fragments. It is being replaced by dolomite everywhere and by chalcedony at a few places. Some microcrystalline calcite is also present as an interstitial material intimately associated with clay.

Silt and Clay 12.0%: Occur mostly as:

1. Finely divided material evenly distributed throughout the rock.
2. Tabular grains with relatively high relief and a high birefringence. These show that the clay is illite in composition.
3. A few irregular streaks of dirty brown color.

Quartz 1.5%: Occurs as small, angular to subangular, grains.

Chalcedony 1.0%: Occurs as a replacement product of calcite in the form of small patches.

Pyrite 0.5%: Occurs mostly as isolated, anhedral to subhedral, grains.

Rock Type: Argillaceous Calcareous Dolomite

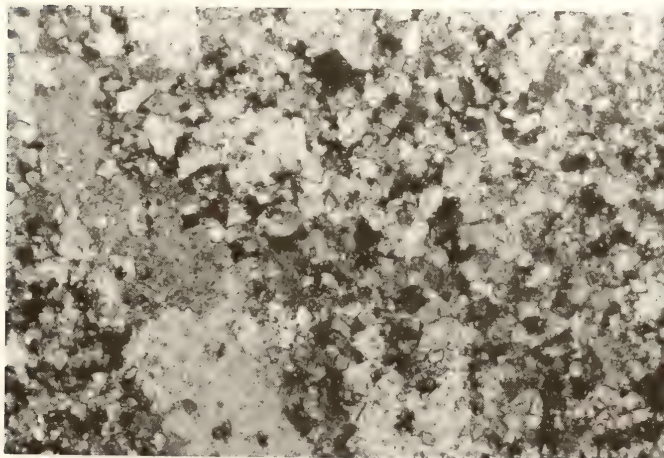


Figure A-21: Photomicrograph of Sample K11 (magnification: 125x)

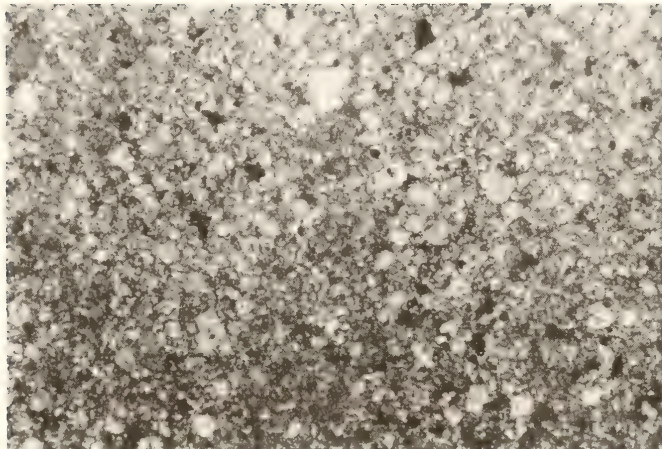


Figure A-22: Photomicrograph of Sample K12 (magnification: 125x)

Sample No. K12

Ledge 4

Quarry K

Megascopic Description

Light tan grey, fine to medium-grained, semi-clastic, argillaceous. Large calcite fragments are surrounded by a fine-grained matrix. Under binocular microscope, the polished surface appears granular. Irregular microcracks, filled with secondary crystalline calcite, are common.

Microscopic Description

Texture

Fine to medium-grained, crystalline. Biofragments of crystalline calcite, ranging in size from 0.25 mm to 1.5 mm, are surrounded by a fine-grained matrix composed largely of dolomite, calcite, and argillaceous material. The dolomite of the matrix is fine-grained (0.05 mm and less), euhedral, and well interlocked. In almost all cases, replacement of calcite by dolomite begins at the center of the fragment. Pyrite occurs as subhedral grains throughout the rock.

Mineral Composition

The rock consists of calcite, dolomite, and argillaceous material with pyrite as the accessory mineral.

Dolomite 65.0%: Occurs as euhedral to subhedral grains highly contaminated with argillaceous material. Many grains show zoned structure due to the presence of clay cutons.

Calcite 20.0%: Occurs in three forms:

1. As medium size biofragments of crystalline calcite.
2. As veins and linings of crystalline calcite along microfractures.
3. As interstitial, microcrystalline variety intimately associated with silt and clay.

Silt and Clay 13.0%: Occurs as:

1. Finely divided material evenly distributed throughout the rock mass.
2. Occasional flakes which are small and tabular. The optical properties of these flakes suggest that the clay is illite in composition.

Quartz 0.5%: Occurs as a few anhedral grains of very small size (0.02 mm).

Pyrite 1.5%: Occurs as small (0.05 mm and less), euhedral to anhedral, grains scattered throughout.

Rock Type: Argillaceous Calcareous Dolomite

Sample No. K13

Ledge 4

Quarry K

Megascopic Description

Light grey, medium to fine-grained, biofragmental, argillaceous. Calcareous fragments of medium size (0.2 mm - 1.0 mm) are embedded in a very fine-grained matrix. The polished surface appears granular when examined under binocular microscope. The matrix is seen to consist of crystalline dolomite.

Microscopic DescriptionTexture

Medium to fine-grained. Biofragments of crystalline calcite are embedded in a mosaic of very finely crystalline dolomite with interstitial silt and clay and some calcite. Dolomite crystals in the matrix range in size from 0.07 mm to less than 0.01 mm with the average being 0.03 mm. They are euhedral to subhedral in shape and are well interlocked. Replacement of coarse calcite by dolomite is very common and begins at the center of the calcite fragments.

Mineral Composition

The rock consists of calcite, dolomite, and argillaceous material with pyrite and chalcidony as the accessory minerals.

Dolomite 70.0%: Occurs as euhedral to subhedral, well interlocked grains.

These are heavily contaminated with clay and many are zoned due to the presence of clay cutons.

Calcite 20.0%: Occurs in two forms:

1. As biofragments of crystalline calcite.
2. As microcrystalline material intimately associated with silt and clay.

Silt and Clay 10.0%: Occur in two forms:

1. Finely divided material evenly distributed throughout the rock.
2. A few elongated, tabular grains of illite with relatively high relief and high birefringence.

The clay is illite in composition.

Quartz 0.5%: Occurs as small (0.03 mm and less), anhedral grains.

Chalcidony 0.5%: Occurs as a replacement product of calcite in microcrystalline form.

Pyrite: Only a few discrete, small (0.03 mm and less) grains are present.

Rock Type: Argillaceous Calcareous Dolomite

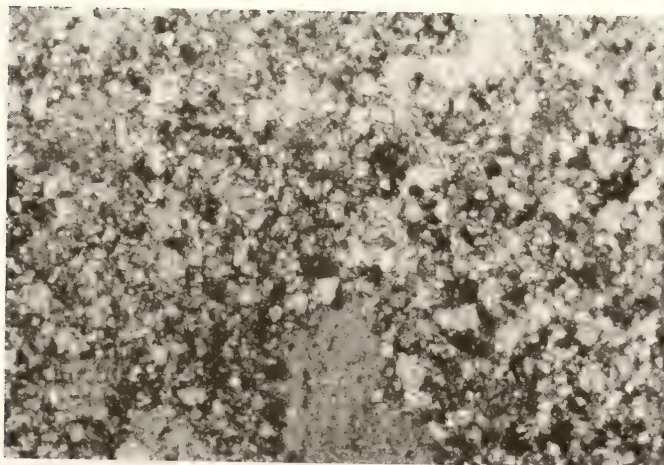


Figure A-23: Photomicrograph of Sample K13 (magnification: 125x)

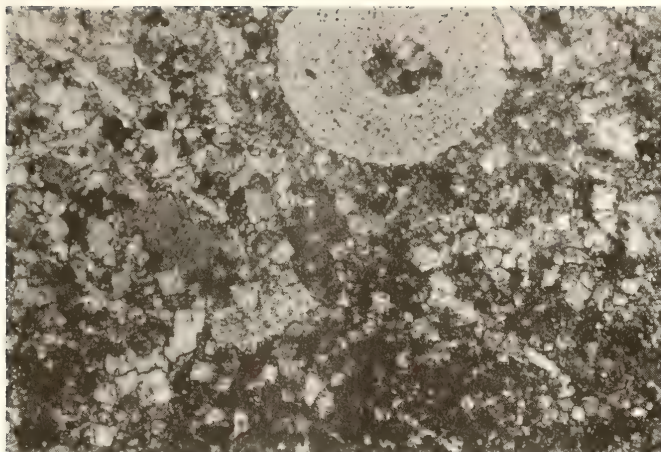


Figure A-24: Photomicrograph of Sample K14 (magnification: 125x)

Sample No. K14

Ledge 5

Quarry K

Megascopic Description

Tan gray, fine to medium grained, biofragmental, argillaceous. Larger fragments of crystalline calcite are surrounded by a fine-grained matrix. The fragments are very variable in size and shape. The size ranges from 0.2 mm to 1.5 mm and the shape includes circular, crescent-like, rectangular, and argillaceous portions alternate with less argillaceous zones. Argillaceous material is also concentrated in the form of bands and streaks. Under binocular microscope, the polished surface appears granular. Presence of pyrite crystals as large as 1 mm is very conspicuous.

Microscopic Description

Texture

Medium to fine grained, semi-clastic. Crystalline calcareous fragments are abundantly distributed in a fine-grained matrix. The matrix consists of a fairly well interlocked mosaic of euhedral, crystalline, dolomite with interstitial calcite and silt and clay. Dolomite grains vary in size from 0.07 mm to less than 0.01 mm. Replacement of calcite by dolomite and chalcidony and the localized growth of coarse-grained pyrite are characteristic features.

Mineral Composition

The rock consists of calcite, dolomite, and argillaceous material with pyrite and chalcidony as the accessory minerals. Traces of quartz are also present.

Dolomite 60.0%: Occurs as finely crystalline material constituting the major portion of the matrix. The grains contain argillaceous material as impurities and some are zoned.

Calcite 27.0%: Occurs in two forms:

1. Biofragments of crystalline calcite.
2. Interstitial material of microcrystalline nature intimately associated with silt and clay.

Silt and Clay 10.0%: Occurs in the following forms:

1. As very finely divided, dust like, material evenly distributed throughout the rock. This is the most common mode of occurrence.
2. As a few elongated, tabular flakes.
3. As irregular, dirty brown streaks.

Chalcidony 2.0%: Occurs as a replacement product of calcite. Spherulitic growths are common.

Pyrite 1.0%: Occurs as:

1. Small (less than 0.04 mm), individual grains.
2. Localized growths of larger grains (up to 1.0 mm).
3. Thin streaks of very small grains.

Rock Type: Argillaceous Calcareous Dolomite

Megascopic Description

Light grey to tan brown, partly clastic, heterogeneous, argillaceous. More argillaceous parts of the rock alternate with less argillaceous ones in a very irregular manner. Coarse-grained calcareous fragments of highly variable shape and size are surrounded by a fine-grained matrix. Microfractures, filled with secondary calcite, are common. Microcavities of irregular shape are also present. The polished surface appears granular when examined under binocular microscope.

Microscopic DescriptionTexture

Fine to medium-grained, heterogeneous, partly clastic. Biofragments of medium size (0.3 mm - 1.5 mm) and consisting of crystalline calcite are surrounded by chert and a fine-grained matrix of carbonate and argillaceous material. Chert covers large areas of (a few sq cm); it is generally microcrystalline but large spherulitic growths are not uncommon. Dolomite of the matrix occurs as anhedral to subhedral grains varying in size from 0.05 mm to less than 0.01 mm.

Mineral Composition

The rock consists essentially of calcite, dolomite, chert, and argillaceous material with pyrite as an accessory mineral. Traces of quartz are also present.

Dolomite 20.0%: Occurs as euhedral to subhedral grains constituting a major portion of the fine-grained matrix. Dolomite grains are heavily contaminated with argillaceous material and many contain clay cutons (zoning).

Calcite 12.0%: Occurs in three forms:

1. As biofragments of coarsely crystalline calcite showing perfect cleavage in many cases.
2. As microcrystalline, interstitial material in the matrix where it is intimately associated with silt and clay.
3. As a secondary, crystalline, mineral lining microfractures.

Chert 60.0%: Occurs as a replacement of calcite fragments and forms irregular but large growths. It is mostly microcrystalline. Spherulitic growths are common. It contains inclusions of unaltered carbonate and of argillaceous material.

Silt and Clay 7.5%: Occurs in three forms:

1. As very finely divided, dust-like material evenly distributed throughout the rock mass. This is the major mode of occurrence.
2. As very thin, elongated flakes.
3. As irregular streaks and localized concentrations.

Pyrite 0.5%: Occurs as small grains (0.02 mm).

Rock Type: Highly Cherty Dolomite

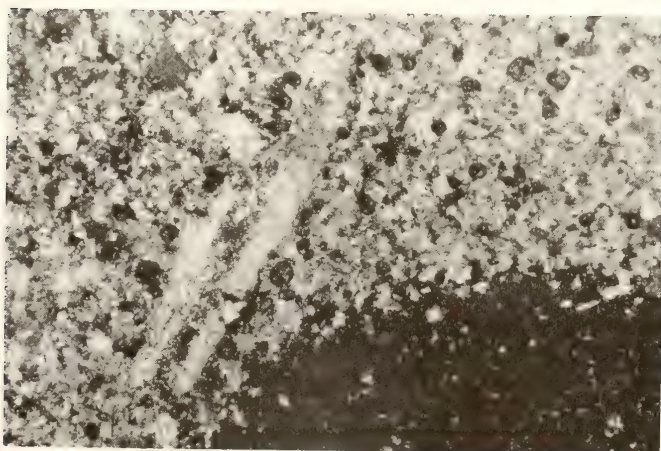


Figure A-25: Photomicrograph of Sample K15 (magnification: 125x)

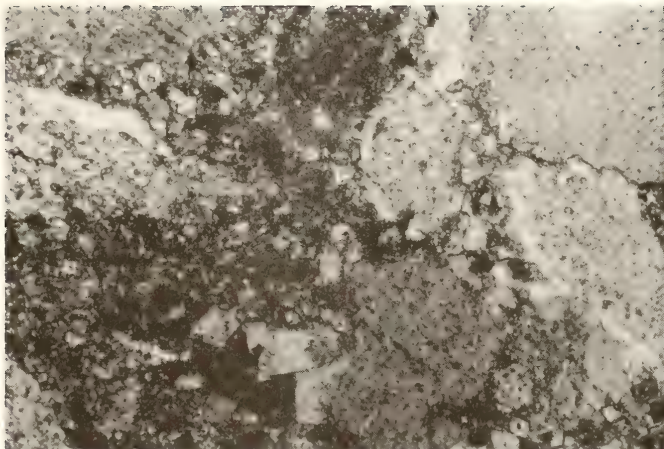


Figure A-26: Photomicrograph of Sample K16 (magnification: 125x)

Sample No. K16

Ledge 3

Quarry K

Megascopic Description

Light tan brown, fine to coarse-grained, biofragmental, partly clastic, argillaceous. Calcareous fossil fragments, highly variable in size and shape, are cemented together by a fine grained matrix. Long hair-line cracks are also present. Small cavities, filled with calcite, are present. Polished surface appears granular.

Microscopic Description

Texture

Large size (0.2 mm - 4.0 mm) biofragments of crystalline calcite are surrounded by a matrix of fine grained (0.07 mm and less) dolomite, microcrystalline calcite, and finely divided silt and clay. Streaks of finely divided silt and clay cut across both the matrix and larger fragments. Replacement of calcite by dolomite and chalcledony is a common feature.

Mineral Composition

The rock consists of calcite, dolomite, and argillaceous material; pyrite and chalcledony are the chief accessory minerals.

Calcite 60.0%: Occurs in two forms:

1. As coarsely crystalline biofragments. This is the chief mode of occurrence.
2. As microcrystalline material in the matrix intimately associated with silt and clay.

Dolomite 25.0%: Occurs in the ground mass as euhedral to subhedral grains.

Most of the grains enclose silt and clay as an impurity. Some grains are zoned. At places the boundaries of dolomite grains cannot be seen clearly due to the abundance of clay.

Silt and Clay 12.0%: Occur in three forms:

1. As finely divided material evenly distributed throughout the rock.
2. As concentrations along cleavage traces in fossil fragments.
3. As thin, dirty brown streaks.

The clay is illite in composition.

Chert (Chalcledony) 2.5%: Occurs as a replacement product of calcite in microcrystalline form. Spherulitic growths are also common.

Quartz: Occurs as a trace only, forming small (0.02 mm), scattered, grains.

Pyrite 0.5%: Occurs as small (0.05 mm and less), anhedral to subhedral grains distributed randomly.

Rock Type: Argillaceous Biofragmental Limestone

Sample No. K17

Ledge 3

Quarry K

Megascopic Description

Light tan brown, fine to medium-grained, biofragmental, argillaceous. Areas rich in coarse grained fossil fragments alternate with those areas which are finer grained and contain fewer fossil fragments. Irregular microfractures and streaks of argillaceous material are present.

Microscopic DescriptionTexture

Large (0.2 mm to 2.0 mm) fossil fragments are distributed irregularly in a fine-grained matrix of dolomite, calcite, and argillaceous material. The dolomite is euhedral, finely crystalline (0.01 mm - 0.07 mm), and frequently dirty due to silt and clay impurities. Calcite is microcrystalline while silt and clay are evenly distributed like dust. On the whole, the rock has a heterogeneous texture.

Mineral Composition

Calcite 55.0%: Occurs in two forms:

1. As medium-sized calcareous fragments of organic origin. Where recrystallized, it is clear and shows perfect rhombohedral cleavage.
2. In the ground mass as small crystalline fragments as well as microcrystalline material intimately associated with clay.

Extensive replacement of calcite by dolomite and chalcidony can be seen.

Dolomite 33.0%: Occurs as euhedral to subhedral grains in the matrix varying in size from 0.07 mm to less than 0.01 mm. Many grain boundaries are obscured behind dust-like argillaceous material.

Silt and Clay 8.0%: Occur in three forms:

1. As finely divided material uniformly disseminated throughout the rock (most common).
2. Inside fossil fragments along cleavage traces.
3. As thin, irregular, dirty brown streaks which cut across the matrix and the biofragments.

Chert (Chalcidony) 3.5%: Occurs as a replacement product of calcite. Replacement occurs in a peculiar agate-like pattern.

Pyrite 0.5%: Occurs as:

1. Small (0.02 mm - 0.05 mm), anhedral to subhedral, randomly scattered grains.
2. Large (more than 1 mm), irregular, growths.

Rock Type: Argillaceous Biofragmental Limestone

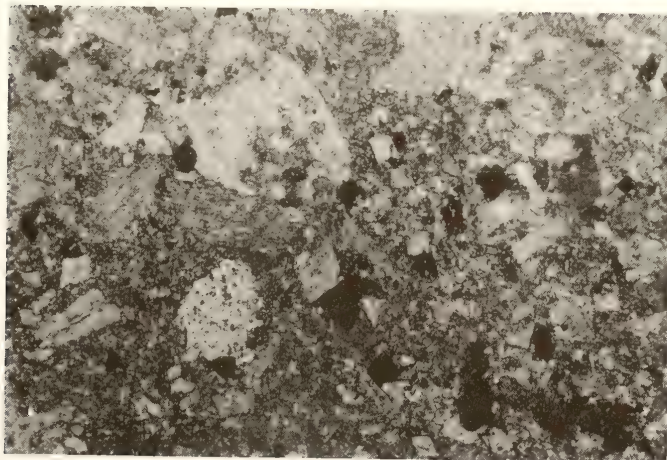


Figure A-27: Photomicrograph of Sample K17 (magnification: 125x)

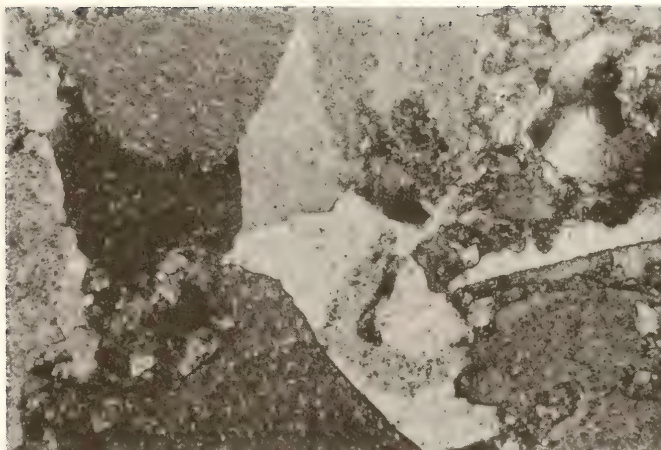


Figure A-28: Photomicrograph of Sample K18 (magnification: 125x)

Sample No. K18

Ledge 3

Quarry K

Megascopeic Description

Light tan brown, fine to medium-grained, biofragmental, argillaceous. Large calcareous fragments are surrounded by a dirty white matrix. The biofragments are highly variable in shape (circular, prismatic, crescent shaped, u-shaped, needle-like, etc.). Irregular cracks are present.

Microscopic Description

Texture

Fine to medium-grained, biofragmental. Biofragments ranging in size from 0.2 mm to 2.0 mm are cemented together by a fine-grained matrix that consists of euhedral, finely crystalline (0.07 mm and less) dolomite, very small fragments of crystalline calcite, microcrystalline calcite, and argillaceous material. Replacement of calcite by dolomite and chalcidony is very common. Some of the calcareous fragments are fibrous.

Mineral Composition

The rock is composed of calcite, dolomite and argillaceous material with chalcidony and pyrite being accessory minerals.

Calcite 60.0%: Occurs in two forms:

1. As large biofragments of crystalline calcite. The calcite contains lots of silt and clay within the crystal structure. However, where the calcite has recrystallized it is almost free of argillaceous impurities.
2. As finely crystalline to microcrystalline material in the matrix. It is intimately associated with silt and clay and difficult to differentiate from them.

Dolomite 22.0%: Occurs as small (less than 0.07 mm), euhedral to subhedral, rhombic grains with argillaceous impurities. Some grains contain clay cutons (zoned).

Silt and Clay 15.0%: Occurs in the following forms:

1. As finely divided, dirty brown material evenly distributed throughout the rock.
2. As fine material within the crystal structure concentrated along cleavage traces and outside along grain boundaries.
3. As thin, irregular, dirty brown streaks.

Chalcidony 2.5%: Occurs as a replacement product of calcite in microcrystalline form.

Pyrite 0.5%: Occurs as small (0.05 mm and less), discrete grains of anhedral to subhedral shape scattered throughout.

Rock Type: Argillaceous Dolomitic Limestone

Megascopic Description

Light tan brown, fine to medium-grained, biofragmental, argillaceous. Medium-sized calcareous fragments are embedded in a fine-grained matrix. Streaks of argillaceous material roughly parallel to each other are clearly seen. Alignment of elongated calcite fragments parallel to the silt and clay streaks is another characteristic feature.

Under the binocular microscope, many of the calcite fragments appear to be distorted and stretched out parallel to the clay streaks like a gneissic structure.

Microscopic DescriptionTexture

Fine to medium-grained, granular. Biofragments of crystalline calcite, ranging in size from 0.02 mm to 1.0 mm, are surrounded by a granular matrix which forms the bulk of the rock. The matrix consists of euhedral to subhedral grains of dolomite (0.08 mm to less than 0.01 mm), microcrystalline calcite, quartz, and finely distributed silt and clay. Alteration of coarse calcite to fine dolomite and chalcidony is common.

Mineral Composition

The rock consists of calcite, dolomite argillaceous material, and quartz. Pyrite and chalcidony are the accessories.

Dolomite 45.0%: Occurs in the matrix as euhedral, rhombic grains. Many grains are zoned due to the presence of clay cutons.

Calcite 20.0%: Occurs in two forms:

1. As biofragments of crystalline calcite heavily contaminated with silt and clay.
2. As microcrystalline material in the matrix.

Silt and Clay 29.0%: Occur in the following forms:

1. As finely divided, evenly distributed material.
2. As impurities within the crystal structure, especially along cleavage traces.
3. As thin, elongated flakes.
4. As thin, irregular streaks.

Quartz 3.0%: Occurs as small (0.02 mm - 0.05 mm), discrete, angular to subangular grains scattered throughout.

Chalcidony 1.0%: Occurs as a replacement product of calcite in small spherulitic bodies.

Pyrite 2.0%: Occurs as:

1. Small (0.01 mm - 0.1 mm), discrete, anhedral to subhedral grains.
2. Small, irregular growths.
3. Thin, irregular streaks.

Rock Type: Argillaceous Calcareous Dolomite

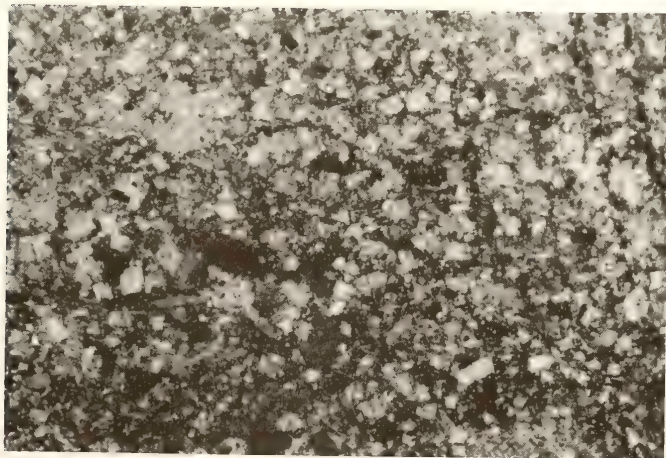


Figure A-29: Photomicrograph of Sample K19 (magnification: 125x)

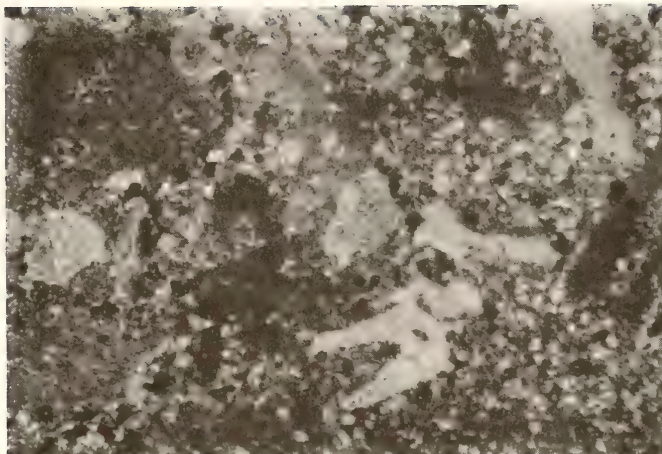


Figure A-30: Photomicrograph of Sample L1 (magnification: 62.5x)

Sample No. L1

Ledge 6

Quarry L

Megascopic Description

Light gray to light tan brown, fine to medium-grained, biofragmental, argillaceous. Calcareous fragments ranging in size from 0.2 mm to 1.5 mm are surrounded by a fine-grained matrix. The rock is heterogeneous in the sense that portions of matrix with only a few fragments alternate with large areas full of biofragments in an irregular fashion. Thin streaks of pyrite and argillaceous material are present. When examined under binocular microscope, the matrix appears granular.

Microscopic Description

Texture

Fine to medium-grained, biofragmental. Calcareous fragments are highly variable in shape. Dolomite of the matrix is euhedral with rhombic crystals varying in size from 0.07 mm to 0.01 mm and less. Calcite of the matrix is microcrystalline. Argillaceous material is mostly uniformly distributed.

Mineral Composition

The rock consists of calcite, dolomite, and silt and clay. Quartz, chalcedony, and pyrite are present as accessory minerals.

Calcite 50.0%: Occurs in two forms:

1. As biofragments consisting of crystalline calcite. Some fragments consist of fibrous calcite.
2. As microcrystalline material in the matrix intimately associated with argillaceous material.

Dolomite 37.0%: Occurs as euhedral to subhedral, rhombic grains which form a major portion of the matrix. Average grain size is 0.04 mm. Inclusions of silt and clay are common.

Silt and Clay 10.0%: Occur in three forms:

1. As finely divided material evenly distributed throughout the rock. This is the most common mode of occurrence.
2. As inclusions in biofragments concentrated along cleavage traces.
3. As a few irregular streaks.

Quartz 1.0%: Occurs as small (0.04 mm), angular to subangular grains scattered randomly.

Chalcedony 1.5%: Occurs as a replacement product of calcite.

Pyrite 0.5%: Occurs as:

1. Small, euhedral to subhedral, discrete grains.
2. Very fine streaks.

Rock Type: Argillaceous Dolomitic Limestone

Sample No. L2

Ledge 6

Quarry L

Megascopic Description

Light tan brown, fine to medium-grained, biofragmental, argillaceous, hard. Fossil fragments of various sizes and shapes are surrounded by a fine-grained matrix. Concentration of pyrite in the form of streaks is present. Irregular microfractures are common along some of which the rock tends to break easily. Under the binocular microscope, the matrix appears finely granular.

Microscopic DescriptionTexture

Fine to medium-grained, biofragmental. Calcareous fragments of small to medium size (0.2 mm - 1.0 mm) are embedded in a very fine-grained matrix of dolomite, calcite and argillaceous material. Dolomite is euhedral, finely crystalline (0.01 mm - 0.07 mm), and contains inclusions of silt and clay. Calcite of the ground mass is microcrystalline and intimately associated with silt and clay.

Mineral Composition

The rock consists of calcite, dolomite, silt and clay, and quartz. Chalcedony and pyrite are accessory minerals.

Calcite 50.0%: Occurs in two forms:

1. As biofragments of crystalline and fibrous calcite. Replacement of crystalline calcite by fine-grained dolomite and chalcedony is common and so are the silt and clay impurities.
2. As microcrystalline, interstitial material.

Dolomite 35.0%: Occurs as fine (avg. size: 0.04 mm), euhedral, rhombic grains.

Silt and Clay 13.0%: Occur in two forms:

1. As finely divided material, evenly distributed throughout the rock. This is the major mode of occurrence.
2. As dust-like material concentrated along cleavage traces within calcite and dolomite grains.

The optical properties suggest that the clay is illite in composition.

Quartz 0.5%: Occurs as small (0.02 mm - 0.05 mm), discrete, angular to subangular grains.

Chert (Chalcedony) 1.0%: Occurs as a replacement product of calcite in microcrystalline form.

Pyrite 0.5%: Occurs as small (avg. size: 0.04 mm), discrete grains distributed randomly.

Rock Type: Argillaceous Dolomitic Limestone

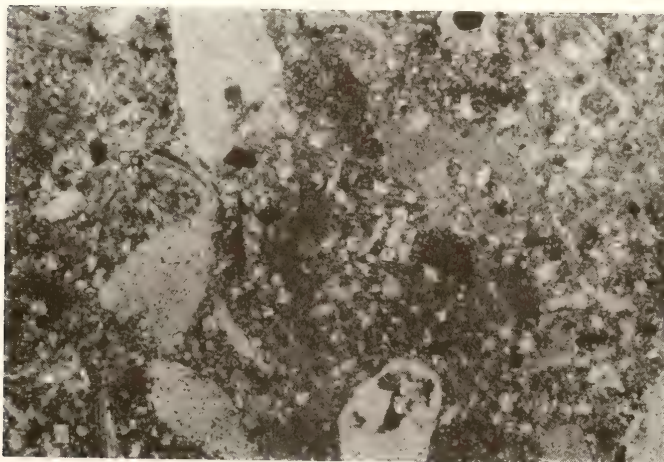


Figure A-31: Photomicrograph of Sample L2 (magnification: 62.5x)

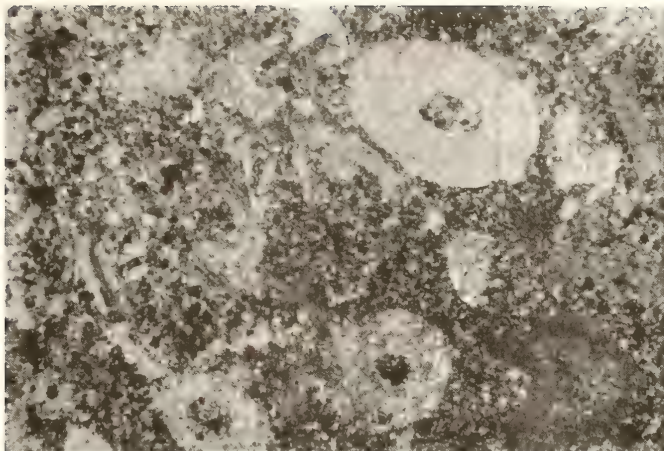


Figure A-32: Photomicrograph of Sample L3 (magnification: 62.5x)

Sample No. L3

Ledge 6

Quarry L

Megascopic Description

Light tan grey, fine to medium-grained, biofragmental, argillaceous, compact and hard. Larger calcareous fragments of different shapes are cemented together by a fine grained matrix. An examination of the polished surface with binocular microscope shows the matrix to be finely crystalline.

Microscopic Description

Texture

Fine to medium-grained. Biofragments consisting of crystalline calcite and ranging in size from 0.2 mm to 2.0 mm are embedded in a fine grained matrix of euhedral crystalline dolomite (0.06 mm and less), microcrystalline calcite, and argillaceous material. Replacement of calcite by fine grained dolomite and chalcedony is a common feature. Some fragments consist of fibrous calcite.

Mineral Composition

The rock consists of calcite, dolomite, and argillaceous material with quartz, chalcedony, and pyrite as the accessories.

Calcite 45.0%: Occurs in two forms:

1. As biofragments of crystalline and fibrous calcite with abundant inclusions of silt and clay.
2. As microcrystalline calcite in the matrix intimately associated with silt and clay.

Dolomite 33.0%: Occurs in the matrix as very finely crystalline, euhedral grains (0.06 mm to less than 0.01 mm). Inclusions of silt and clay are abundant.

Silt and Clay 20.0%: Occur mostly as:

1. Finely divided, evenly distributed, material throughout the rock.
2. Inclusions in calcite and dolomite grains, especially concentrated along cleavage traces and fibers.

The clay is illite in composition.

Quartz 0.5%: Occurs as small (avg. size: 0.04 mm), anhedral, angular grains.

Chalcedony 1.0%: Occurs as a replacement product of calcite in the form of small, discrete bodies or within larger calcite crystals.

Pyrite 0.5%: Occurs as very small (0.02 mm), euhedral to subhedral, discrete grains.

Rock Type: Argillaceous Dolomitic Limestone

Sample No. L4

Ledge 6

Quarry L

Megascopic Description

Light tan brown, fine to medium-grained, biofragmental, argillaceous, hard and massive. Calcareous fragments from previous fossils up to 2.0 mm in size are randomly distributed in a fine grained matrix. Irregular streaks of argillaceous material are present. Sealed-up, hair-line cracks are also present. Polished surface appears finely granular under binocular microscope.

Microscopic DescriptionTexture

Fine to medium-grained, biofragmental. Fragments of crystalline calcite ranging in size from 0.2 mm to 2.0 mm are surrounded by a fine grained matrix of dolomite, calcite, and argillaceous material. Dolomite is euhedral, finely crystalline (0.01 mm - 0.1 mm), and well interlocked. Calcite of the matrix is microcrystalline and intimately associated with clay. Silt and clay are generally evenly distributed. Pyrite forms discrete grains. Alteration of calcite into dolomite and chalcidony is common.

Mineral Composition

The rock consists of calcite, dolomite, and argillaceous material with quartz, chalcidony, and pyrite as the accessory minerals.

Calcite 55.0%: Occurs in two forms:

1. As biofragments of crystalline calcite. Some fragments are fibrous, however.
2. As very small fragments and as microcrystalline material in the matrix.

Dolomite 34.0%: Occurs in the matrix as euhedral to subhedral grains ranging in size from 0.01 mm to 0.1 mm and fairly well interlocked. Dust-like inclusions of silt and clay are abundant.

Silt and Clay 8.0%: Occur as:

1. Finely divided material evenly distributed throughout the rock mass (as interstitial material in the matrix and as inclusions in calcite and dolomite grains).
2. Thin, irregular, contorted streaks.

Quartz 0.5%: Occurs as small, discrete grains smaller than 0.05 mm.

Chalcidony 1.5%: Occurs as a replacement product of calcite.

Pyrite 1.0%: Occurs as small (0.03 mm), discrete, euhedral to subhedral grains that are randomly distributed.

Rock Type: Argillaceous Dolomitic Limestone

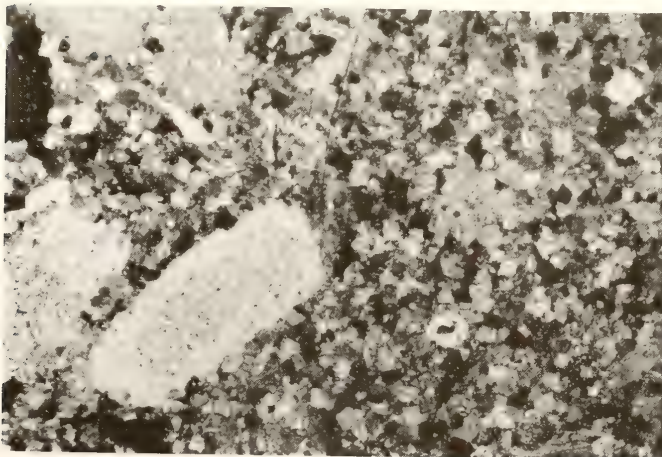


Figure A-33: Photomicrograph of Sample L4 (magnification: 62.5x)

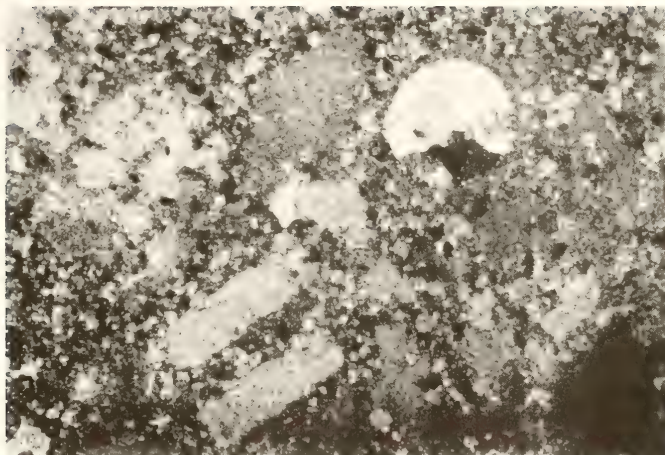


Figure A-34: Photomicrograph of Sample L5 (magnification: 62.5x)

Sample No. L5

Ledge 6

Quarry L

Megascopic Description

Light tan brown, biofragmental, argillaceous, compact and hard. Fossil fragments of various shapes and sizes are embedded in a fine grained matrix. Under the binocular microscope, the matrix appears partly granular.

Microscopic Description

Texture

Fine to medium-grained, biofragmental. Calcareous fragments ranging in size from 0.2 mm to 2.0 mm are surrounded by a fine grained matrix of euhedral, crystalline dolomite, microcrystalline calcite, and finely divided silt and clay. The calcite, silt, and clay are intimately associated and are difficult to differentiate from each other. Replacement of calcite by dolomite generally starts at the center of the grain and is a common feature.

Mineral Composition

The rock consists of calcite, dolomite, and argillaceous material with quartz, chalcedony, and pyrite as the accessory minerals.

Calcite 55.0%: Occurs in two forms:

1. As large sized (0.2 mm - 2.0 mm) fossil fragments of various shapes consisting mostly of crystalline calcite and occasionally of fibrous calcite.
2. As very small fragments and microcrystalline material in the matrix. It is interstitial to dolomite.

Dolomite 33.0%: Occurs as euhedral, fine-grained (.01 mm - 0.1 mm), rhombic crystals which make up the major portion of the matrix. Many grains are zoned due to the presence of clay cutons.

Silt and Clay 10.0%: Occurs in two forms:

1. As finely divided material, evenly distributed throughout the rock.
2. As fine, dust-like inclusions in calcite and dolomite grains, especially concentrated along the cleavage traces.

Relatively high relief and high order interference colors suggest that the clay is illite.

Quartz: Occurs as a few small (less than 0.05 mm), angular to subangular grains.

Chalcedony 1.5%: Occurs as a replacement product of calcite in the form of spherulitic or irregular bodies.

Pyrite 0.5%: Occurs mostly as euhedral to subhedral grains of very small size (less than 0.03 mm) which are distributed randomly. Also forms a few irregular growths.

Rock Type: Argillaceous Dolomitic Limestone

Megascopic Description

Light tan brown, fine to medium-grained, biofragmental, argillaceous, compact and hard. Fossil fragments of various shapes and sizes are surrounded by a fine grained matrix. A few thin wavy streaks of argillaceous material are present. Under the binocular microscope, the matrix appears partly granular.

Microscopic DescriptionTexture

Fine to medium-grained, biofragmental. Larger fragments (0.2 mm - 1.5 mm) of crystalline calcite and organic origin are cemented together by a fine grained matrix of euhedral dolomite crystals (0.01 mm - 0.07 mm), microcrystalline calcite, and finely distributed silt and clay. Thin, curved streaks of dirty brown color are common. Replacement of calcite by dolomite is responsible for the irregular boundaries of these fragments. Calcite in the matrix is intimately associated with silt and clay.

Mineral Composition

The rock consists of calcite, dolomite, and silt and clay. Quartz, chalcedony, and pyrite are the accessories.

Calcite 55.0%: Occurs in two forms:

1. As biofragments of crystalline and fibrous calcite. Dust like inclusion of silt and clay are common.
2. As microcrystalline material in the matrix.

Alteration of calcite to dolomite and chalcedony is common.

Dolomite 33.0%: Occurs as very finely crystalline, euhedral, rhombic grains with silt and clay impurities. Many grains are zoned.

Silt and Clay 7.0%: Occur as:

1. Finely divided material evenly distributed throughout the rock.
2. Dust-like inclusions in calcite and dolomite.
3. Dirty brown, thin, wavy streaks.
4. A few thin, elongated flakes.

Optical properties suggest that the clay is illite.

Quartz 3.5%: Occurs as small (less than 0.05 mm), angular to subangular grains which are randomly distributed.

Chert (Chalcedony) 1.0%: Occurs as spherulitic and irregular bodies and replaces calcite everywhere.

Pyrite 0.5%: Occurs as very small (less than 0.03 mm), euhedral to subhedral grains.

Rock Type: Argillaceous Dolomitic Limestone

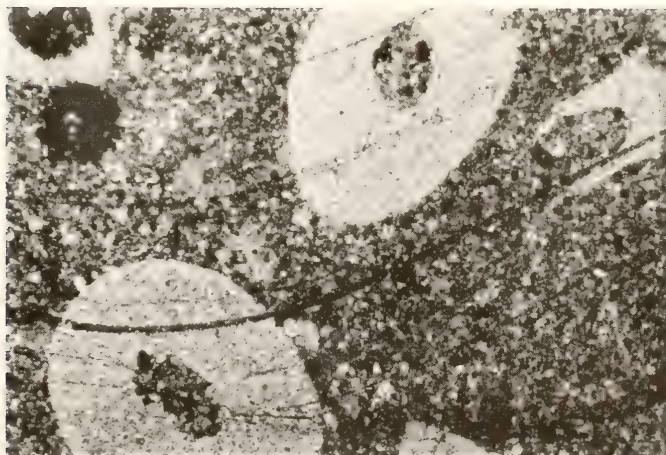


Figure A-35: Photomicrograph of Sample L6 (magnification: 62.5x)

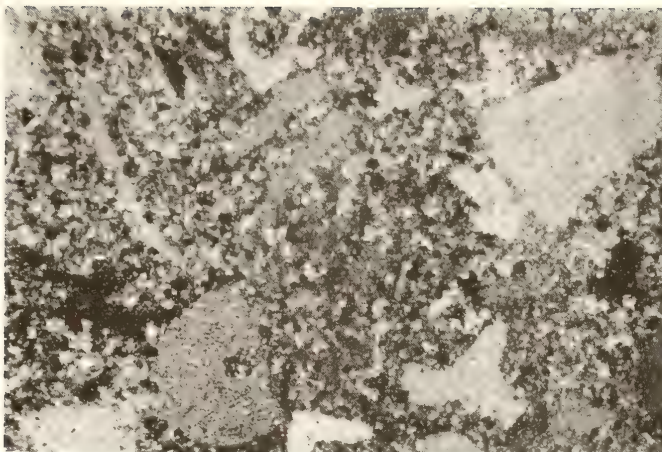


Figure A-36: Photomicrograph of Sample L7 (magnification: 62.5x)

Sample No. L7

Ledge 6

Quarry L

Megascopic Description

Light tan brown, fine to medium-grained, biofragmental, argillaceous, compact and hard. Large biofragments of various shapes are randomly distributed in a fine-grained matrix. Light brown, more argillaceous areas alternate with light grey, carbonate areas in an irregular fashion. Irregular streaks of argillaceous material are present. Under binocular microscope, the matrix appears partly granular.

Microscope Description

Texture

Fine to medium-grained, bioclastic. Biofragments of crystalline and fibrous calcite ranging in size from 0.2 mm to 2.0 mm are surrounded by a fine grained matrix composed of crystalline dolomite, very small calcite fragments, microcrystalline calcite, and finely divided silt and clay. Dolomite forms euhedral, rhombic grains (0.01 mm - 0.07 mm). Inclusions of fine silt and clay are abundant. Calcite fragments are being replaced by dolomite and chalcedony.

Mineral Composition

The rock consists of calcite, dolomite, and silt and clay with quartz, chert, and pyrite as the accessory minerals.

Calcite 50.0%: Occurs in two forms:

1. As large biofragments consisting mostly of crystalline calcite and occasionally of fibrous calcite.
2. As microcrystalline material in the matrix intimately associated with silt and clay.

Dolomite 38.0%: Occurs as finely crystalline, euhedral, rhombic grains fairly well interlocked at places. Most of the grains contain inclusions of fine silt and clay.

Silt and Clay 8.0%: Occurs as:

1. Finely divided material evenly distributed throughout the rock. This is the major mode of occurrence.
2. Dust-like inclusions in calcite and dolomite.
3. A few thin, elongated, flakes with high relief and high birefringence.
4. Thin, irregular, and contorted streaks of dirty brown color.

The optical properties suggest the clay to be illite in composition.

Quartz 2.5%: Occurs as small (0.03 mm - 0.06 mm), angular to subangular grains uniformly distributed throughout.

Chalcedony 1.0%: Occurs as a replacement product of calcite and forms spherulitic as well as irregular bodies.

Pyrite 0.5%: Occurs as very small (less than 0.04 mm), euhedral to subhedral grains irregularly scattered.

Rock Type: Argillaceous Dolomitic Limestone

Sample No. L8

Ledge 6

Quarry L

Megascopic Description

Light tan brown, fine to medium-grained, fossiliferous, hard and compact. Concentration of fine grained, granular pyrite gives rise to irregular areas of dark grey color. Veins and pockets of coarse, crystalline, calcite are common.

Microscopic DescriptionTexture

Fine to medium grained, fossiliferous. Fossil fragments of crystalline and fibrous calcite, ranging in size from 0.2 mm to 1.0 mm, are embedded in a matrix of microcrystalline calcite, euhedral dolomite, and some argillaceous material. Replacement of coarse grained calcite by pyrite is a common feature.

Mineral Composition

The rock consists primarily of calcite with some dolomite. Pyrite is the chief accessory mineral.

Calcite 90.0%: Occurs in two forms:

1. As coarse-grained, crystalline calcite of fossil fragments, veins, and pockets. Fibrous variety is not uncommon.
2. As microcrystalline material constituting the bulk of the matrix.

Dolomite 7.0%: Occurs as fine, euhedral, rhombic grains more or less evenly distributed throughout the matrix. Some grains contain clay cutons.

Silt and Clay 1.0%: Occurs as finely divided, dust-like material throughout the rock.

Pyrite 2.0%: Occurs as:

1. Discrete, anhedral grains and as irregular growths.
2. Fine grained, granular material which replaces and borders fossil fragments.

Chalcedony: Occurs as a replacement product of calcite in the form of small, irregular growths. Only traces of it are present.

Rock Type: Limestone

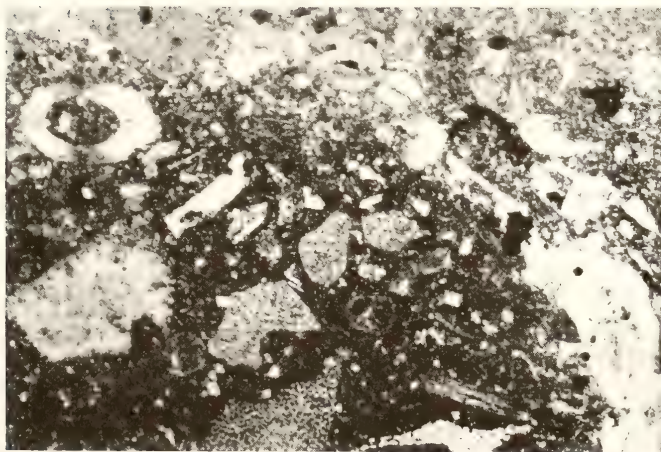


Figure A-37: Photomicrograph of Sample L8 (magnification: 62.5x)

APPENDIX B

ACID ETCHING OF LEDGE SAMPLES

APPENDIX B

ACID ETCHING OF LEDGE SAMPLES

Results of the acid etching of some ledge samples are presented. In case of laminated samples, the shaly laminations clearly stand above the etched surface. Non-laminated etched samples exhibit either smooth or pitted surfaces even when they contain greater amounts of argillaceous material. The etching test appears to be a useful technique for enhancing the laminated nature of argillaceous carbonates but does not provide information about the total amount of argillaceous material present.

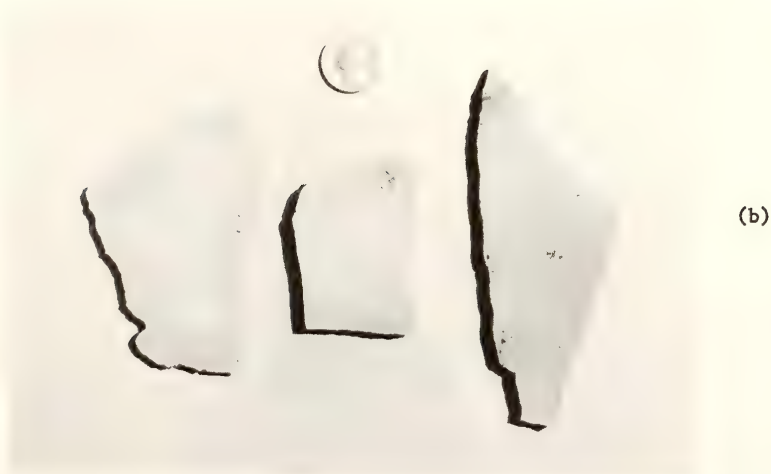
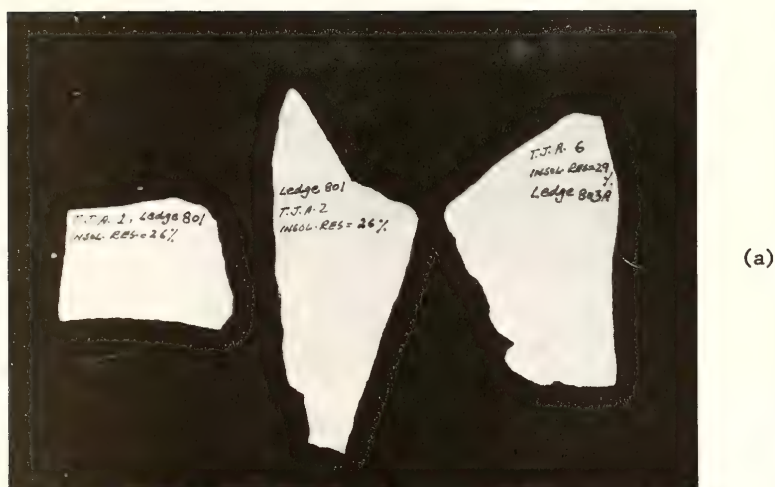


Figure B-1: Results of Acid Etching of Samples from Quarry T;
(a) Unetched, (b) Etched.

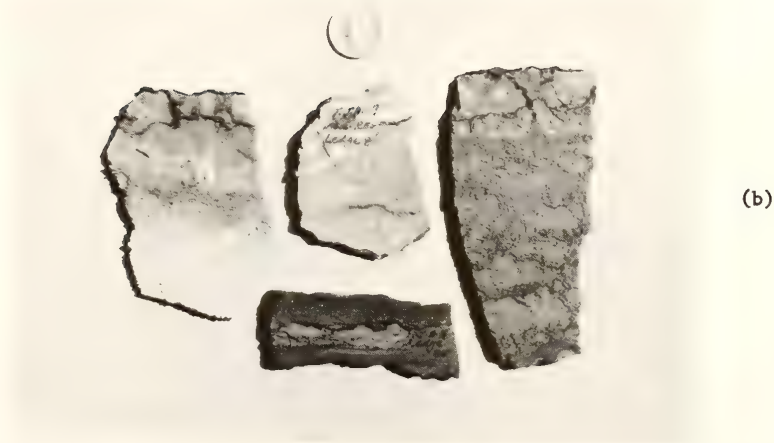
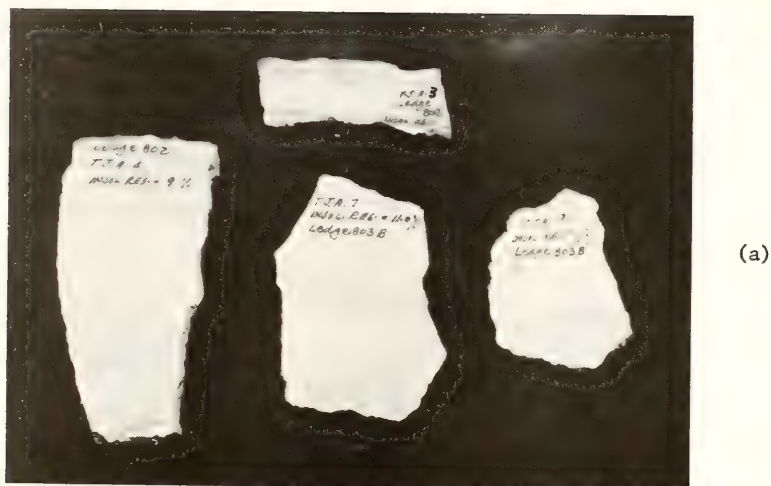
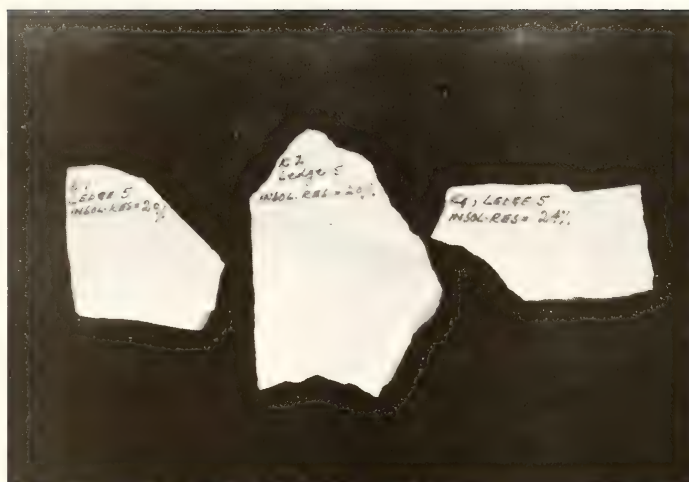
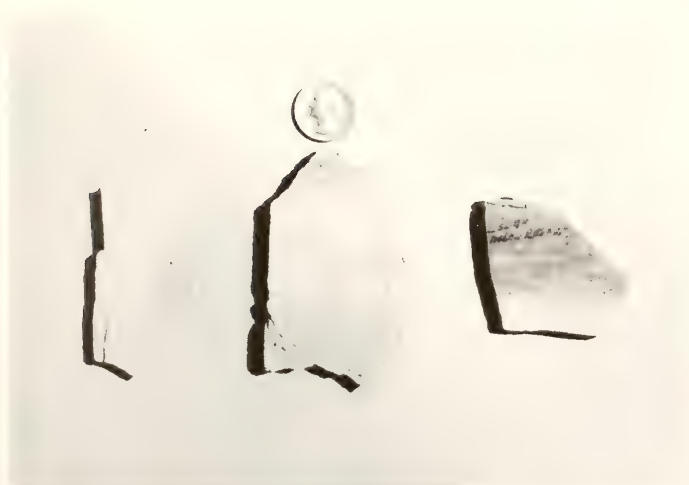


Figure B-2: Results of Acid Etching of Samples from Quarry T;
(a) Unetched, (b) Etched.



(a)



(b)

Figure B-3: Results of Acid Etching of Samples from Quarry K;
(a) Unetched, (b) Etched.

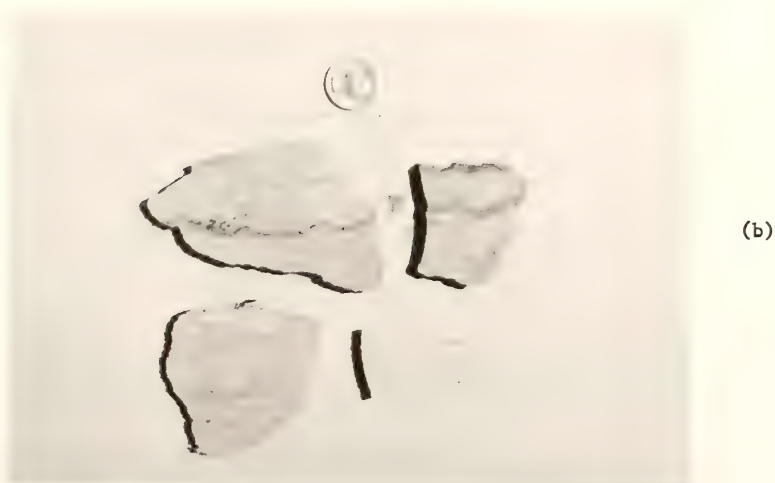
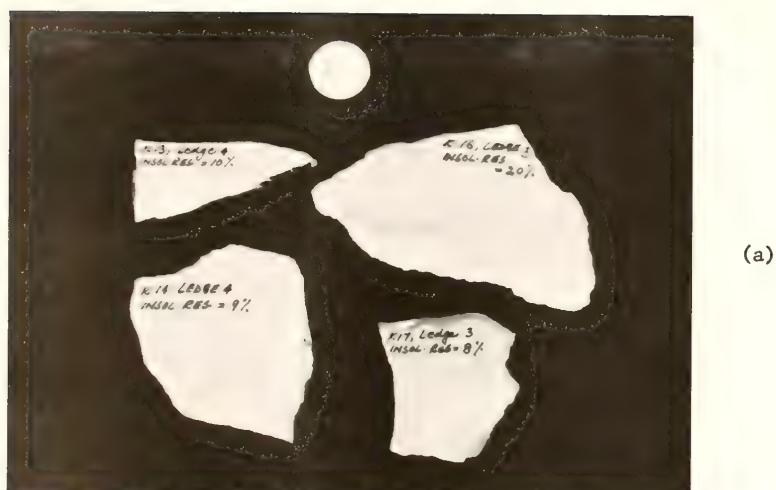


Figure B-4: Results of Acid Etching of Samples from Quarry K;
(a) Unetched, (b) Etched.

APPENDIX C

INSOLUBLE RESIDUE AND ATTERBERG LIMITS

APPENDIX C

INSOLUBLE RESIDUE AND ATTERBERG LIMITS

This Appendix contains the results of insoluble residue test and the liquid limit and plastic limit values of the silt and clay fraction of insoluble residue. The minerals present in the residue, as seen under the binocular microscope, are listed in the order of decreasing proportion.

The mesh size for different sieves used in the residue test is given below:

<u>Sieve No.</u>	<u>Mesh Size (Millimeters)</u>
4	4.75
8	2.40
16	1.20
30	0.60
50	0.30
100	0.15
200	0.075

Sample No. T1 Ledge 801 Quarry T

<u>Sieve No.</u>	<u>Cumulative % of Total Wt. Retained</u>
4	0.00
8	0.02
16	0.06
30	0.09
50	0.13
100	0.19
200	0.37

Silt and clay content (-200 fraction) 25.83%

LL = 54.0% PL = 28.6% PI = 25.4%

Insoluble minerals: quartz, pyrite

Sample No. T2 Ledge 801, Site 2 Quarry T

<u>Sieve No.</u>	<u>Cumulative % of Total Wt. Retained</u>
4	0.00
8	0.01
16	0.03
30	0.05
50	0.06
100	0.11
200	0.25

Silt and clay content (-200 fraction) 26.50%

LL = 55.0% PL = 31.0% PI = 24.0%

Insoluble minerals: quartz, pyrite

Sample No. T3 Ledge 802 (Shaly layer) Quarry T

<u>Sieve No.</u>	<u>Cumulative % of Total Wt. Retained</u>
4	0.00
8	0.05
16	0.13
30	0.20
50	0.30
100	0.34
200	0.44

Silt and clay content (-200 fraction) 20.6%

LL = 44.5% PL = 20.9% PI = 23.6%

Insoluble minerals: quartz, pyrite, chert

Sample No. T4

Ledge 802

Quarry T

<u>Sieve No.</u>	<u>Cumulative % of Total Wt. Retained</u>
4	0.00
8	0.09
16	0.13
30	0.17
50	0.27
100	0.32
200	0.43

Silt and clay content (-200 fraction) 8.30%

LL = 40.3% PL = 20.8% PI = 19.5%

Insoluble minerals: quartz, pyrite, chert

Sample No. T5

Ledge 803A

Quarry T

<u>Sieve No.</u>	<u>Cumulative % of Total Wt. Retained</u>
4 4	0.00
8	0.01
16	0.03
30	0.05
50	0.06
100	0.07
200	0.11

Silt and clay content (-200 fraction) 29.30%

LL = 52.6% PL = 31.7% PI = 20.9%

Insoluble minerals: quartz, pyrite, chert

Sample No. T7

Ledge 803B

Quarry T

<u>Sieve No.</u>	<u>Cumulative % of Total Wt. Retained</u>
4	0.02
8	0.16
16	0.28
30	0.41
50	0.56
100	0.68
200	0.76

Silt and clay content (-200 fraction) 10.10%

LL = 39.0% PL = 24.5% PI = 14.5%

Insoluble minerals: quartz, chert, pyrite

Sample No. T8 Ledge 803B, Shaly Layers Quarry T

<u>Sieve No.</u>	<u>Cumulative % of Total Wt. Retained</u>
4	1.31
8	2.35
16	2.77
30	3.00
50	3.22
100	3.36
200	3.44

Silt and clay content (-200 fraction) 17.30%

LL = 39.9% PL = 30.4% PI = 9.5%

Insoluble minerals: chert, quartz, pyrite, some pieces of sandstone

Sample No. T10 Ledge 7 (Jeff. L.S.) Quarry T

<u>Sieve No.</u>	<u>Cumulative % of Total Wt. Retained</u>
4	0.26
8	0.82
16	1.23
30	1.61
50	2.00
100	2.39
200	2.57

Silt and clay content (-200 fraction) 1.87%

Insoluble minerals: chert (porous), quartz, carbonaceous shale

Note: Insufficient sample to determine LL and PL.

Sample K1 Ledge 5 Quarry K

<u>Sieve No.</u>	<u>Cumulative % of Total Wt. Retained</u>
4	0.06
8	0.10
16	0.13
30	0.15
50	0.16
100	0.18
200	0.31

Silt and clay content (-200 fraction) 19.74%

LL = 37.5% PL = 26.1% PI = 11.4%

Insoluble minerals: quartz, pyrite, soft lumps of fine sand and silt.

Sample K3

Ledge 5

Quarry K

<u>Sieve No.</u>	<u>Cumulative % of Total Wt. Retained</u>
4	0.03
8	0.11
16	0.17
30	0.24
50	0.28
100	0.33
200	0.43

Silt and clay content (-200 fraction) 23.7%

LL = 38.7% PL = 26.7% PI = 12.0%

Insoluble minerals: quartz, pyrite, soft lumps of fine sand and silt

Sample No. K5

Ledge 5

Quarry K

<u>Sieve No.</u>	<u>Cumulative % of Total Wt. Retained*</u>
4	1.00
8	1.64
16	2.87
30	3.21
50	3.34
100	3.60
200	4.25

Silt and clay content (-200 fraction) 43.70%

LL = 34.3% PL = 29.4% PI = 4.9%

Insoluble minerals: soft lumps of fine sand and silt; quartz, pyrite.

Sample No. K7

Ledge 5

Quarry K

<u>Sieve No.</u>	<u>Cumulative % of Total Wt. Retained*</u>
4	1.46
8	4.00
16	4.90
30	5.35
50	5.57
100	5.81
200	6.30

Silt and clay content (-200 fraction) 43.60%

LL = 36.8% PL = 30.5% PI = 6.3%

Insoluble minerals: soft lumps of fine sand and silt; quartz, pyrite

* Mostly lumps of fine sand and silt

Sample No. K9

Ledge 5

Quarry K

<u>Sieve No.</u>	<u>Cumulative % of Total Wt. Retained*</u>
4	1.56
8	3.00
16	4.58
30	4.77
50	5.37
100	6.10
200	6.48

Silt and clay content (-200 fraction) 45.5%

LL = 33.6% PL = 28.1% PI = 5.5%

Insoluble minerals: soft lumps of fine sand and silt; quartz, pyrite

Sample No. K11

Ledge 4

Quarry K

<u>Sieve No.</u>	<u>Cumulative % of Total Wt. Retained</u>
4	0.00
8	0.06
16	0.09
30	0.12
50	0.16
100	0.25
200	0.67

Silt and clay content (-200 fraction) 8.50%

Insoluble minerals: quartz, pyrite

Sample No. K12

Ledge 4

Quarry K

<u>Sieve No.</u>	<u>Cumulative % of Total Wt. Retained</u>
4	0.00
8	0.00
16	0.00
30	0.01
50	0.02
100	0.03
200	0.09

Silt and clay content (-200 fraction) 11.0%

Insoluble Minerals: quartz, pyrite

* Mostly lumps of silt and fine sand

Sample No. K13

Ledge 4

Quarry T

<u>Sieve No.</u>	<u>Cumulative % of Total Wt. Retained</u>
4	0.00
8	0.01
16	0.03
30	0.04
50	0.06
100	0.08
200	0.10

Silt and clay content (-200 fraction) 10.10%

LL = 44.5% PL = 26.2% PI = 18.3%

Insoluble minerals: chert, quartz, pyrite

Sample No. K14

Ledge 4

Quarry K

<u>Sieve No.</u>	<u>Cumulative % of Total Wt. Retained</u>
4	0.00
8	0.16
16	0.27
30	0.39
50	0.55
100	0.69
200	0.81

Silt and clay content (-200 fraction) 8.40%

LL = 43.0% PL = 24.4% PI = 18.6%

Insoluble minerals: chert, quartz, pyrite

Sample No. K15

Ledge 3

Quarry K

<u>Sieve No.</u>	<u>Cumulative % of Total Wt. Retained*</u>
4	5.24
8	7.20
16	8.00
30	8.68
50	9.28
100	9.68
200	10.02

Silt and clay content (-200 fraction) 4.9%

Insoluble minerals: chert, quartz, pyrite

Sample No. K16

Ledge 3

Quarry K

<u>Sieve No.</u>	<u>Cumulative % of Total Wt. Retained*</u>
4	5.20
8	8.47
16	9.73
30	10.70
50	11.40
100	11.93
200	12.30

Silt and clay content (-200 fraction) 7.40%

LL = 42.2% PL = 31.2% PI = 11.0%

Insoluble minerals: chert, quartz, pyrite, soft siliceous aggregates

Sample No. K17

Ledge 3

Quarry K

<u>Sieve No.</u>	<u>Cumulative % of Total Wt. Retained</u>
4	0.03
8	0.13
16	0.20
30	0.26
50	0.35
100	0.45
200	0.53

Silt and clay content (-200 fraction) 8.50%

LL = 44.5% PL = 27.4% PI = 17.1%

Insoluble minerals: chert, pyrite, quartz, soft siliceous aggregations

Sample No. K18

Ledge 3

Quarry K

<u>Sieve No.</u>	<u>Cumulative % of Total Wt. Retained</u>
4	0.37
8	0.80
16	0.99
30	1.20
50	1.29
100	1.47
200	1.62

Silt and clay content (-200 fraction) 17.30%

LL = 43.0% PL = 30.6% PI = 13.4%

Insoluble minerals: chert, quartz, pyrite, soft siliceous aggregations

* Mostly chert material

Sample No. K18(b)

Ledge 3

Quarry K

<u>Sieve No.</u>	<u>Cumulative % of Total Wt. Retained*</u>
4	0.00
8	3.30
16	5.30
30	6.40
50	7.00
100	7.40
200	7.80

Silt and clay content (-200 fraction) 13.1%

Insoluble minerals: chert, quartz, pyrite

Sample K19

Ledge 2

Quarry K

<u>Sieve No.</u>	<u>Cumulative % of Total Wt. Retained</u>
4	0.81
8	1.76
16	2.77
30	3.57
50	4.43
100	5.16
200	6.53

Silt and clay content (-200 fraction) 29.20%

LL = 40.2% PL = 38.5% PI = 1.8%

Insoluble minerals: soft lumps of fine sand and silt

Sample No. K20

Ledge 2

Quarry K

<u>Sieve No.</u>	<u>Cumulative % of Total Wt. Retained</u>
4	2.06
8	4.38
16	4.98
30	5.12
50	5.54
100	5.82
200	6.26

Silt and clay content (-200 fraction) 37.7%

LL = 38.9% PL = 36.8% PI = 2.1%

Insoluble minerals: soft lumps of fine sand and silt

* Mostly chert material

Sample No. L1 Ledge 6, Site 1, 3' from top Quarry L

<u>Sieve No.</u>	<u>Cumulative % of Total Wt. Retained</u>
4	0.00
8	0.02
16	0.03
30	0.03
50	0.04
100	0.05
200	0.06

Silt and clay content (-200 fraction) 13.0%

Insoluble minerals: pyrite, quartz

Sample No. L2 Ledge 6, Site 1, 2' from top Quarry L

<u>Sieve No.</u>	<u>Cumulative % of Total Wt. Retained</u>
4	0.00
8	0.00
16	0.00
30	0.02
50	0.05
100	0.07
200	0.09

Silt and clay content (-200 fraction) 11.56%

LL = 38.3% PL = 25.3% PI = 13.0%

Insoluble minerals: pyrite, quartz, some soft aggregations of fine sand and silt

Sample No. L3 Ledge 6, Site 1, 1' from top Quarry L

<u>Sieve No.</u>	<u>Cumulative % of Total Wt. Retained</u>
4	0.00
8	0.00
16	0.00
30	0.00
50	0.00
100	0.00
200	0.01

Silt and clay content (-200 fraction) 22.00%

LL = 38.1% PL = 26.1% PI = 12.0%

Insoluble minerals: pyrite, quartz, some soft aggregations of fine sand and silt

Sample No. L4 Ledge 6, Site 2, 2' from top Quarry L

<u>Sieve No.</u>	<u>Cumulative % of Total Wt. Retained</u>
4	0.00
8	0.00
16	0.00
30	0.01
50	0.03
100	0.04
200	0.05

Silt and clay content (-200 fraction) 10.52%

LL = 37.0% PL = 24.6% PI = 12.4%

Insoluble minerals: pyrite, quartz

Sample No. L5 Ledge 6, Site 2, 2' from top Quarry L
(cherty)

<u>Sieve No.</u>	<u>Cumulative % of Total Wt. Retained</u>
4	0.00
8	0.01
16	0.02
30	0.03
50	0.04
100	0.05
200	0.08

Silt and clay content (-200 fraction) 10.3%

Insoluble minerals: pyrite, quartz

Sample No. L6 Ledge 6, Site 3, near top Quarry L

<u>Sieve No.</u>	<u>Cumulative % of Total Wt. Retained</u>
4	0.01
8	0.02
16	0.08
30	0.16
50	0.23
100	0.26
200	0.32

Silt and clay content (-200 fraction) 10.13%

LL = 32.3% PL = 21.5% PI = 10.7%

Insoluble minerals: pyrite, quartz, pyritiferous shale

Sample No. L7

Ledge 6, Site 3, 2' from top

Quarry L

<u>Sieve No.</u>	<u>Cumulative % of Total Wt. Retained</u>
4	0.00
8	0.00
16	0.03
30	0.12
50	0.18
100	0.20
200	0.27

Silt and clay content (-200 fraction) 8.64%

Insoluble minerals: pyrite, quartz, pyritiferous shale

Sample No. L8

Ledge 6, Site 3, 8' from top

Quarry L

<u>Sieve No.</u>	<u>Cumulative % of Total Wt. Retained</u>
4	0.00
8	0.00
16	0.00
30	0.01
50	0.02
100	0.03
200	0.04

Silt and clay content (-200 fraction) 2.82%

Insoluble minerals: pyrite, quartz

APPENDIX D

PORE-SIZE DISTRIBUTIONS

APPENDIX D

PORE-SIZE DISTRIBUTIONS

The pore-size distributions for different ledge samples, as measured by mercury intrusion porosimeter, are presented in this appendix. Some of the ledge samples collected in the beginning of this research were not sufficient for all the tests. Additional samples were collected at a later stage from locations as close to those as shown in Table 4.1. Samples L1', L2', L3', and K18-b, included in this appendix, were collected during this second stage of sampling.

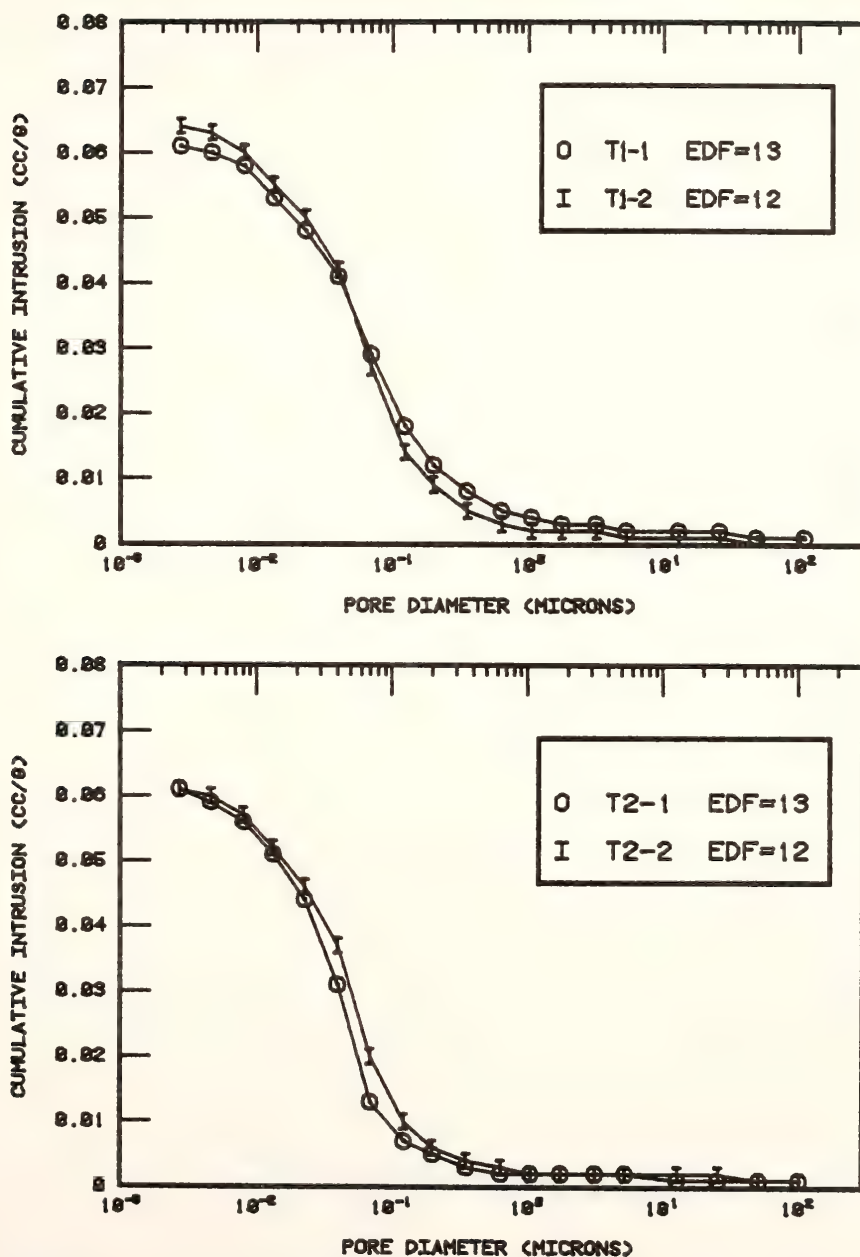


Figure D-1: Pore-size distributions for samples T1(top) and T2(bottom).

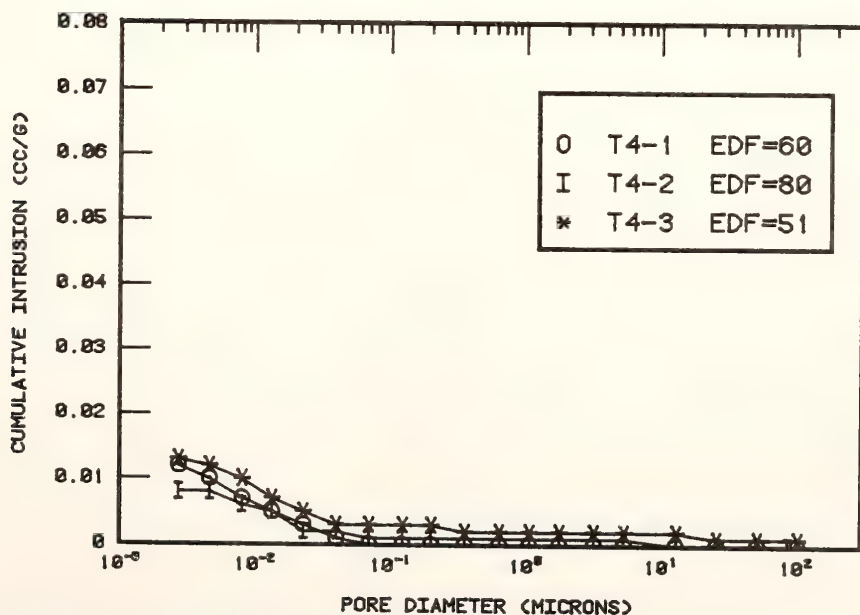
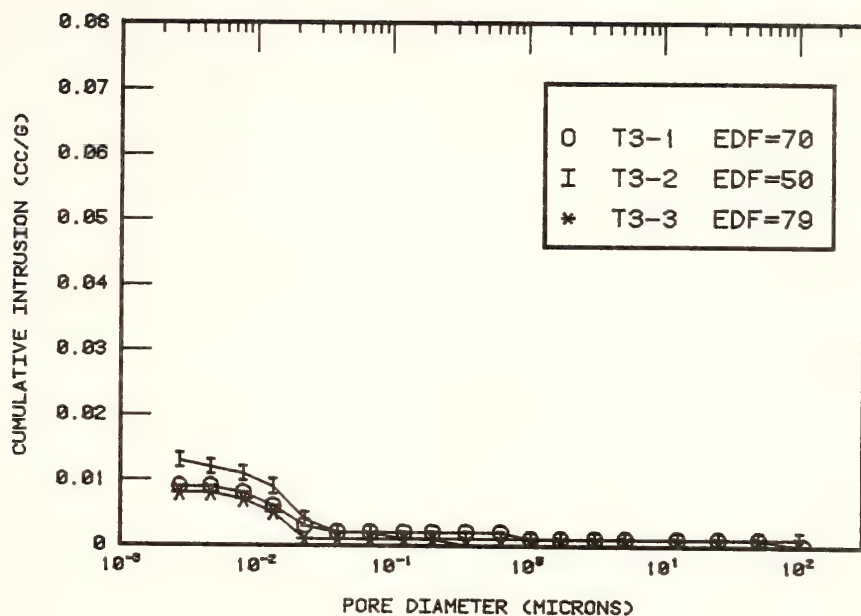


Figure D-2: Pore-size distributions for samples T3(top) and T4(bottom).

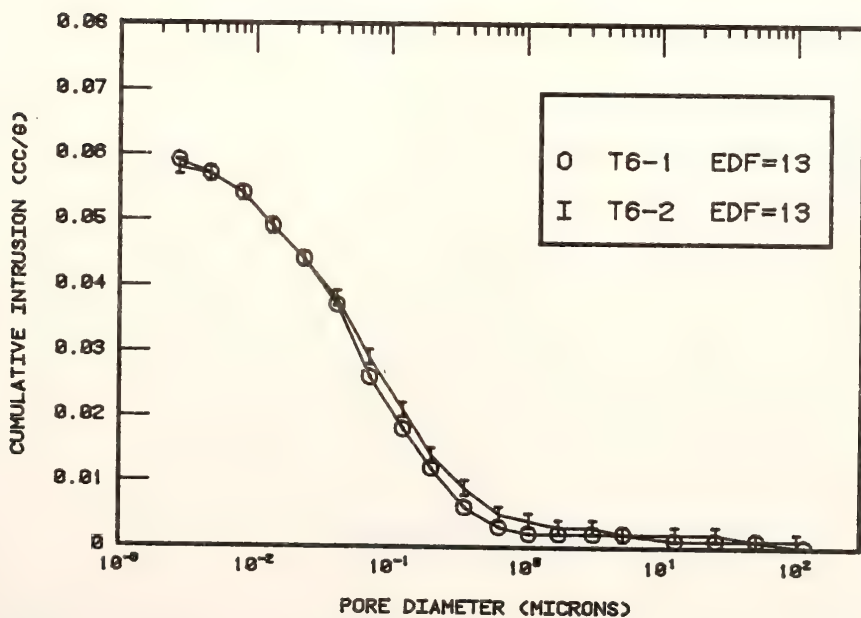
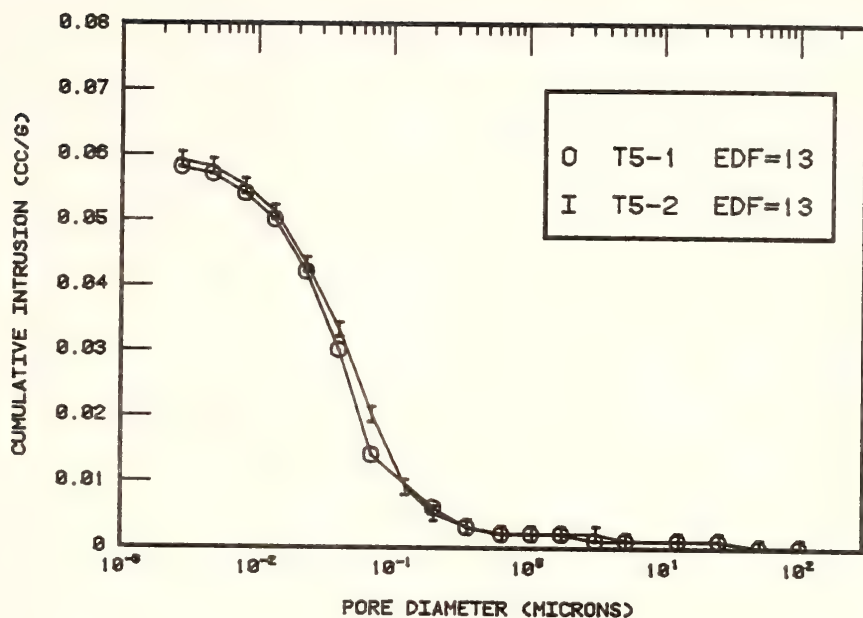


Figure D-3: Pore-size distributions for samples T5(top) and T6(bottom).

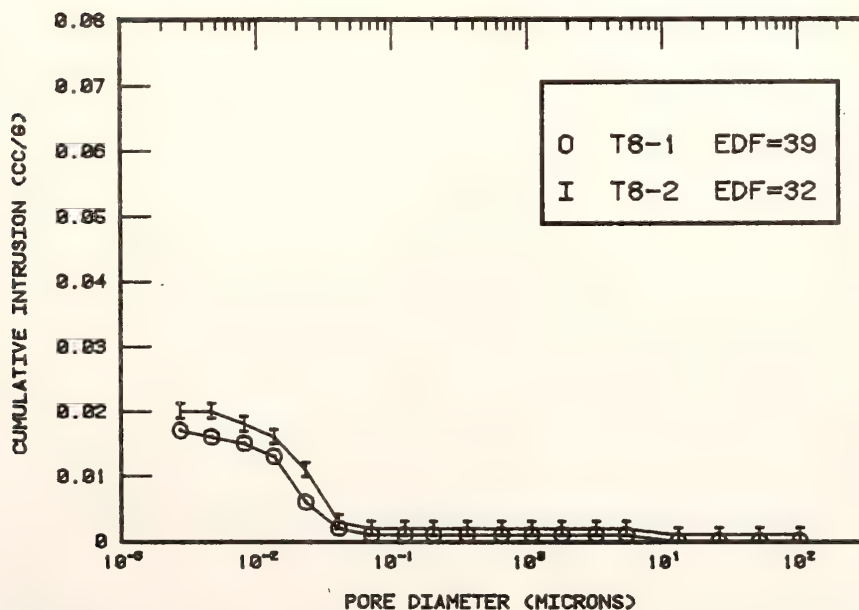
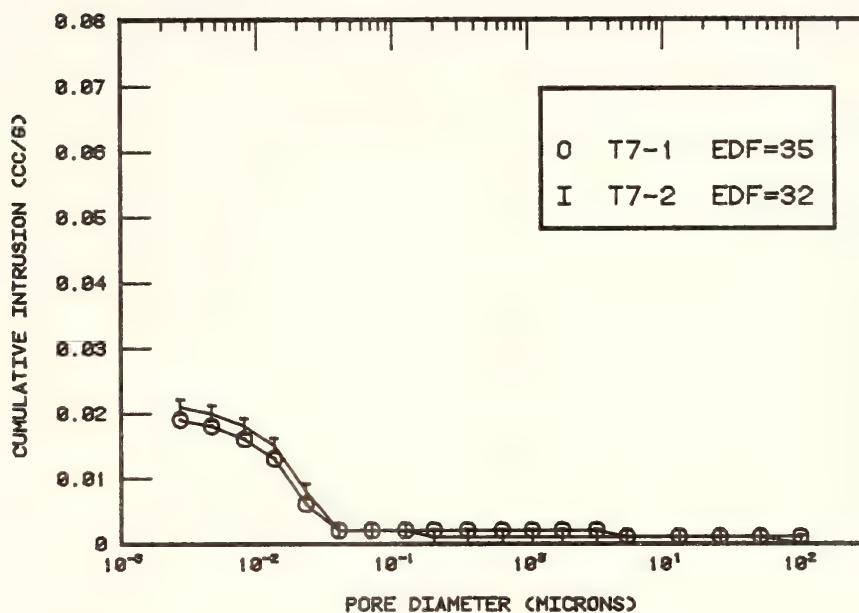


Figure D-4: Pore-size distributions for samples T7(top) and T8(bottom).

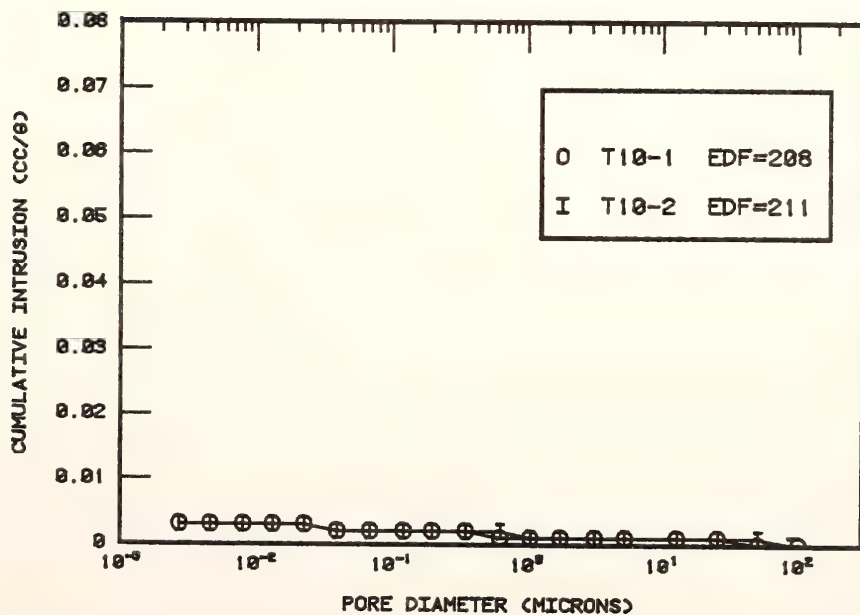
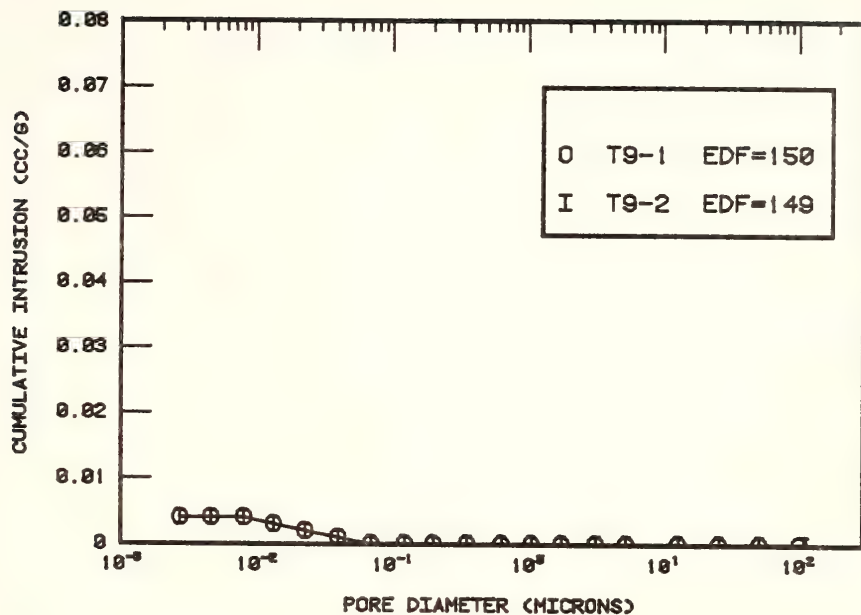


Figure D-5: Pore-size distributions for samples T9(top) and T10(bottom).

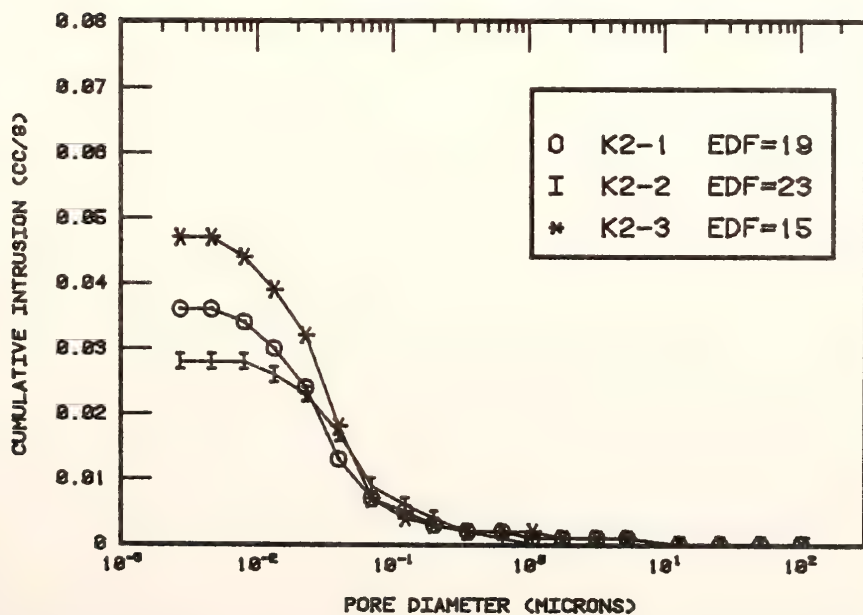
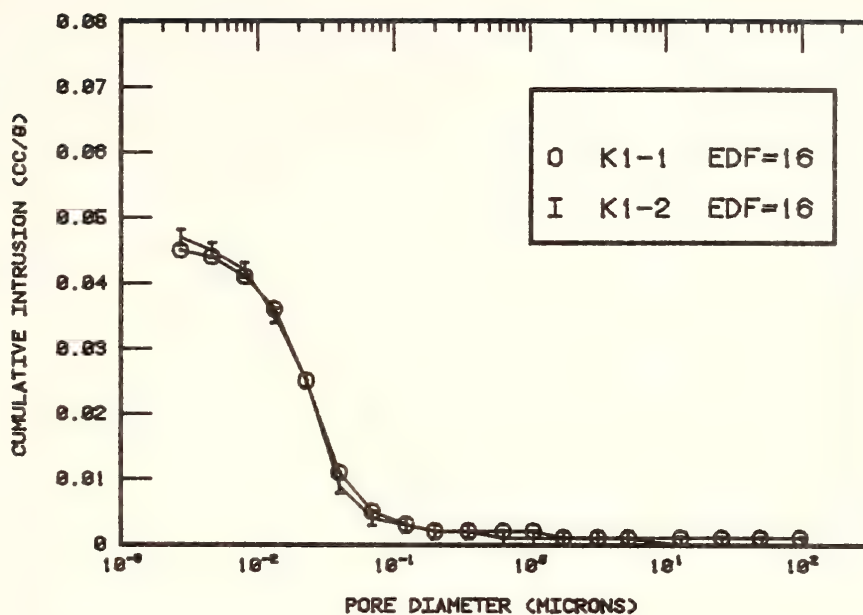


Figure D-6: Pore-size distributions for samples K1(top) and K2(bottom).

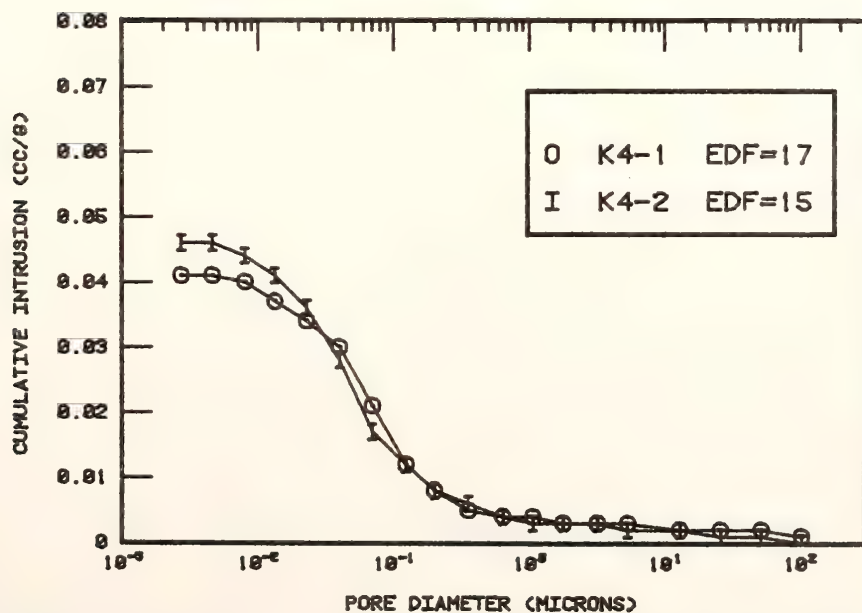
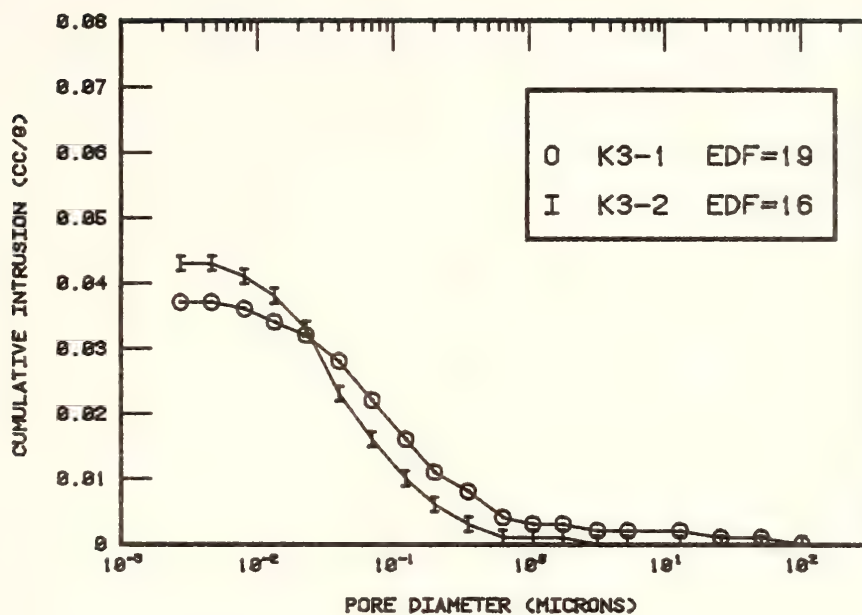


Figure D-7: Pore-size distributions for samples K3(top) and K4(bottom).

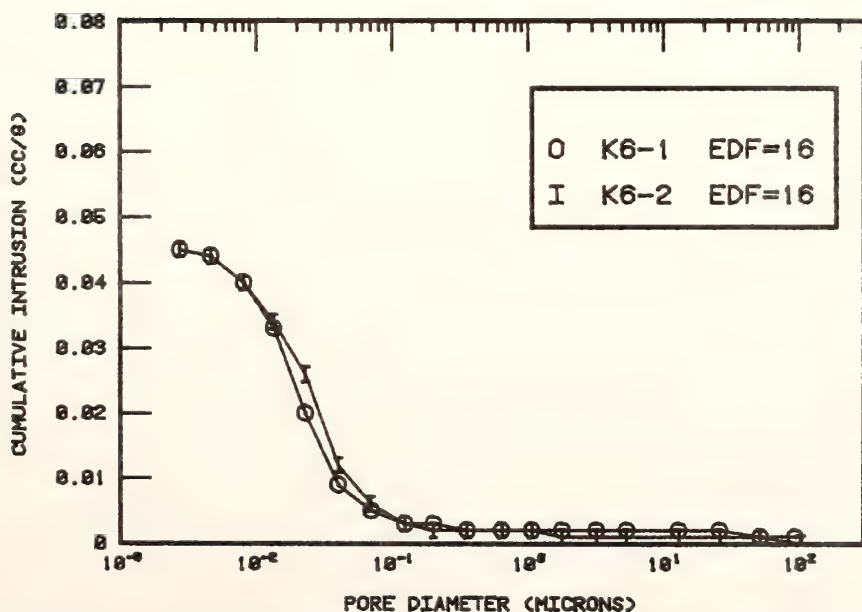
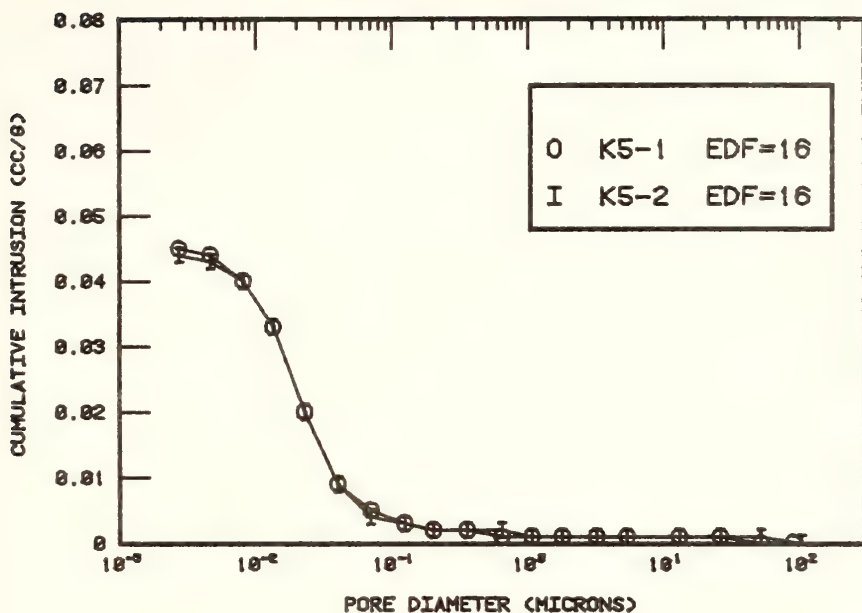


Figure D-8: Pore-size distributions for samples K5(top) and K6(bottom).

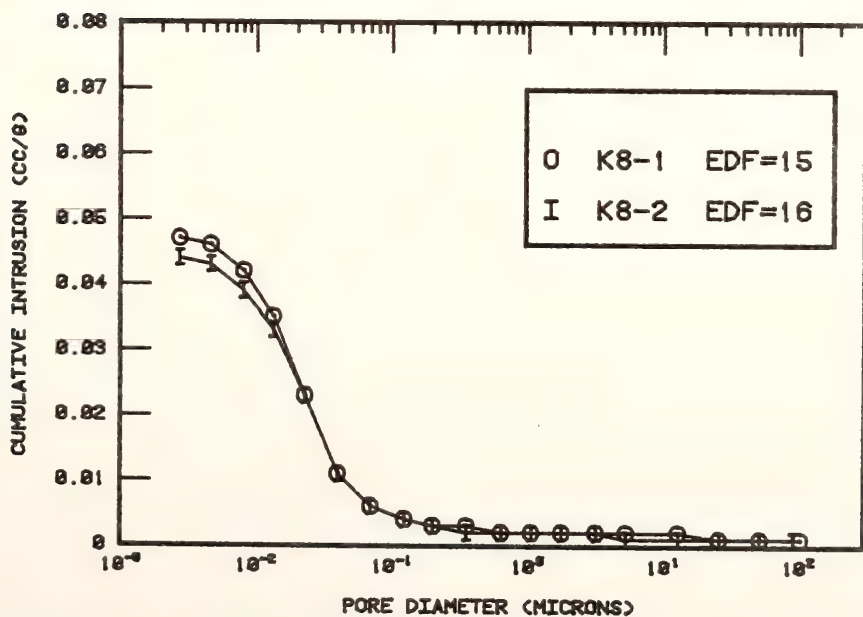
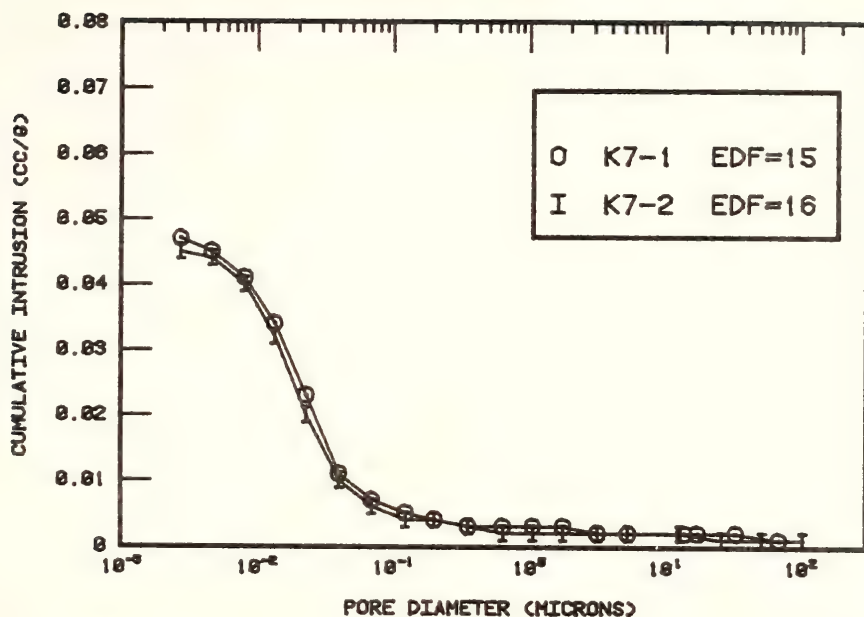


Figure D-9: Pore-size distributions for samples K7(top) and K8(bottom).

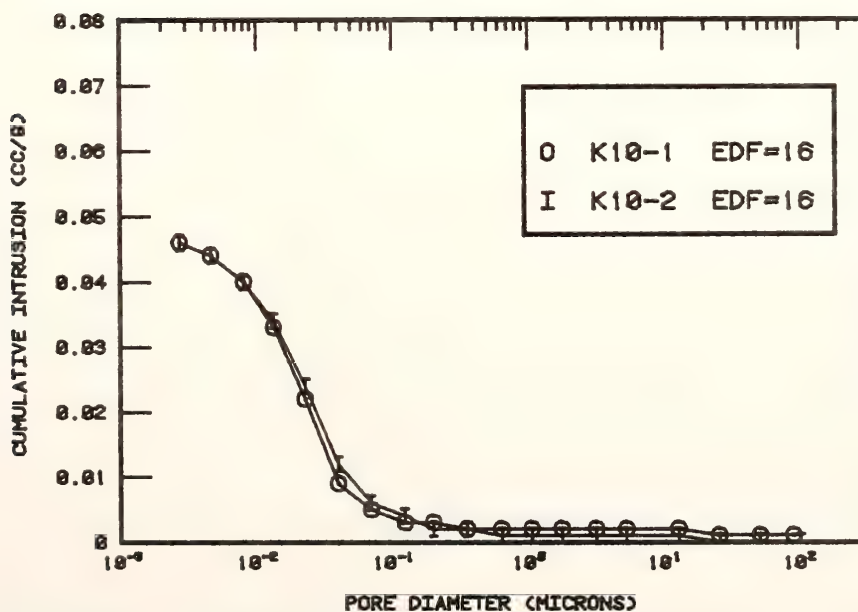
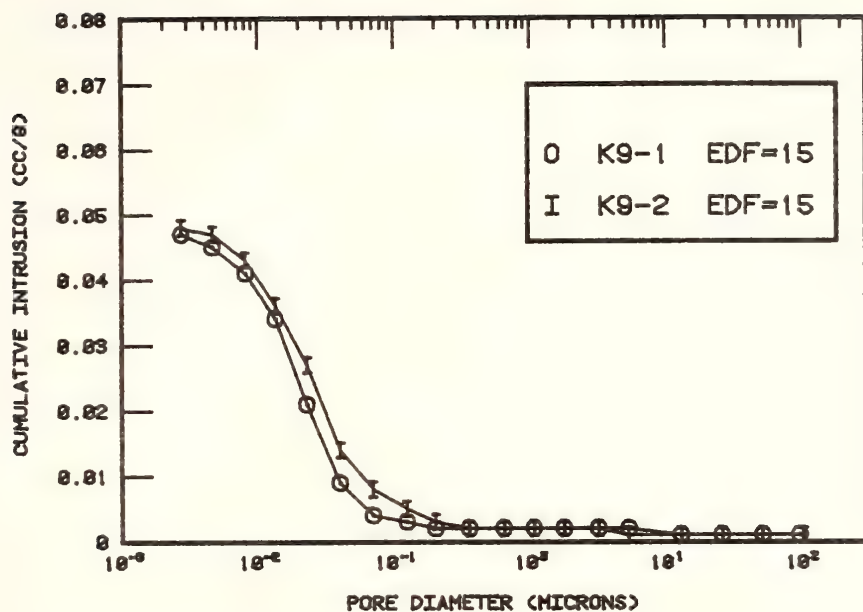


Figure D-10: Pore-size distributions for samples K9(top) and K10(bottom).

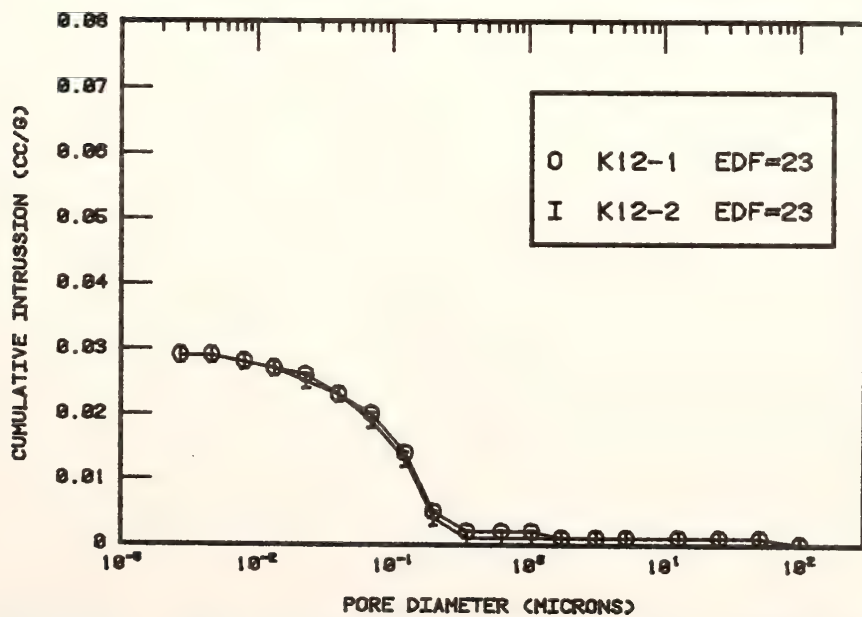
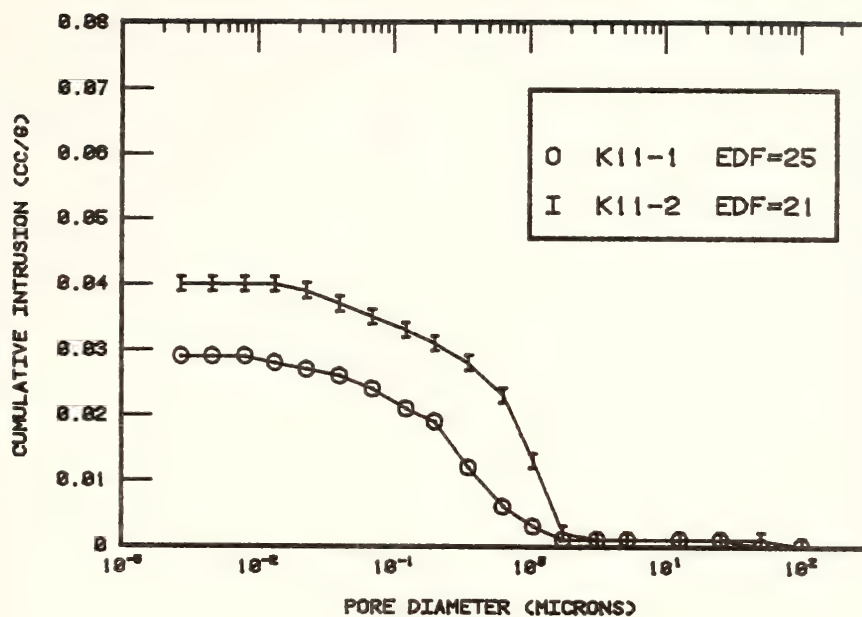


Figure D-11: Pore-size distributions for samples K11(top) and K12(bottom).

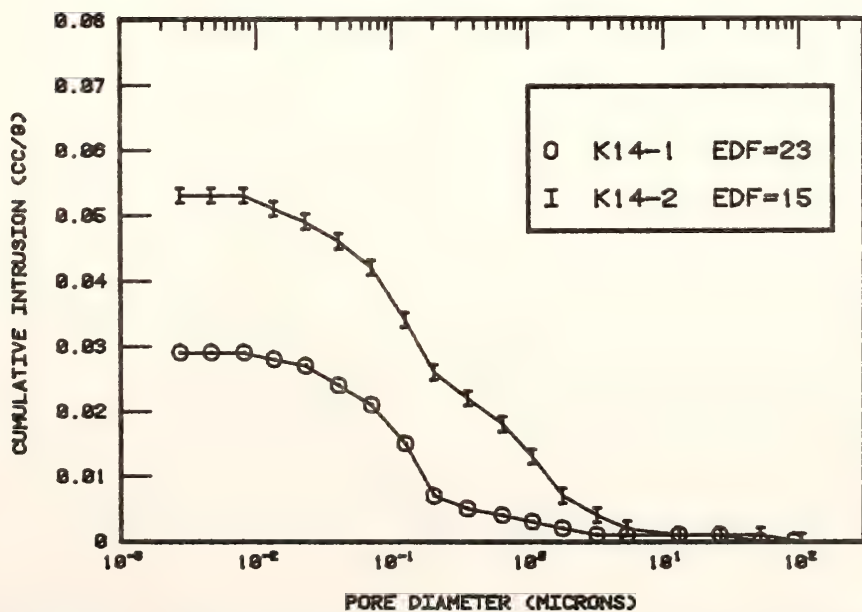
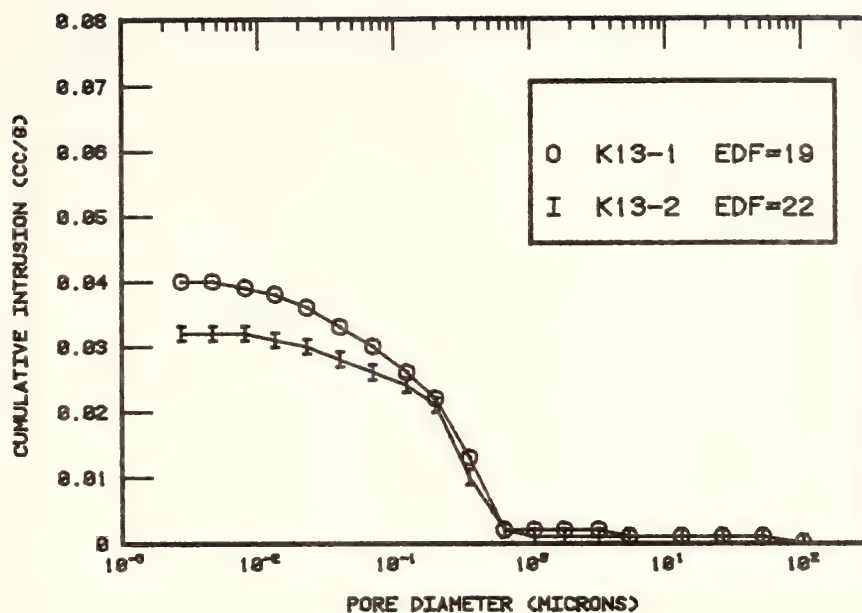


Figure D-12: Pore-size distributions for samples K13(top) and K14(bottom).

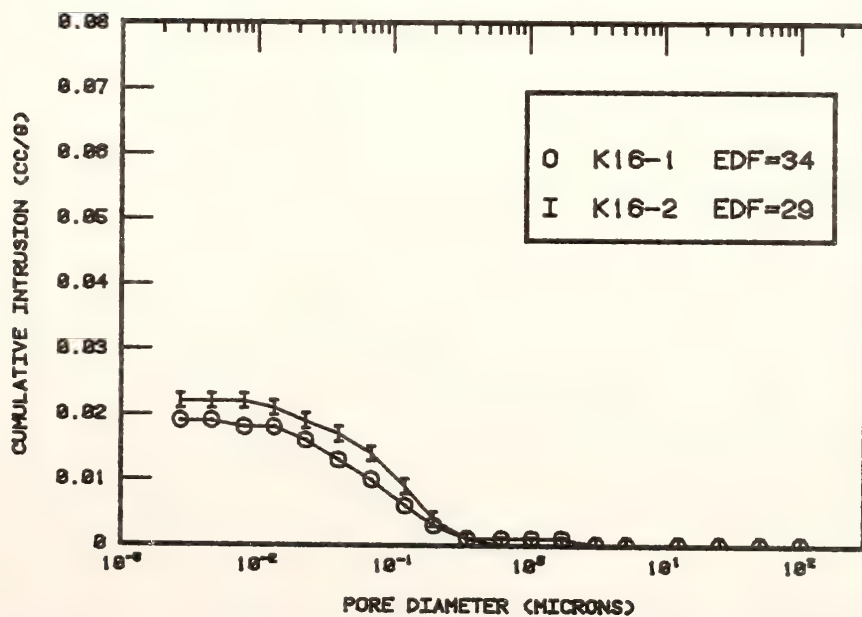
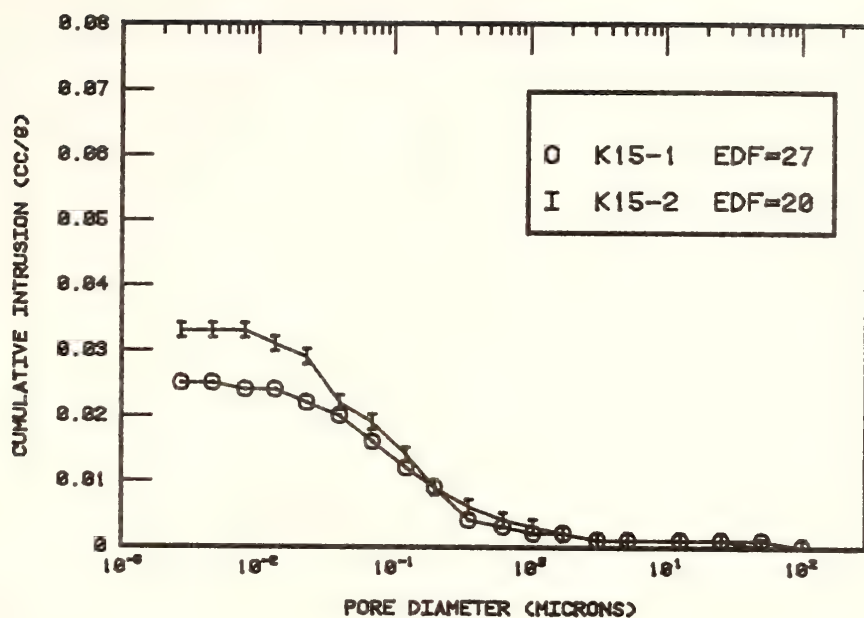


Figure D-13: Pore-size distributions of samples K15(top) and K16(bottom).

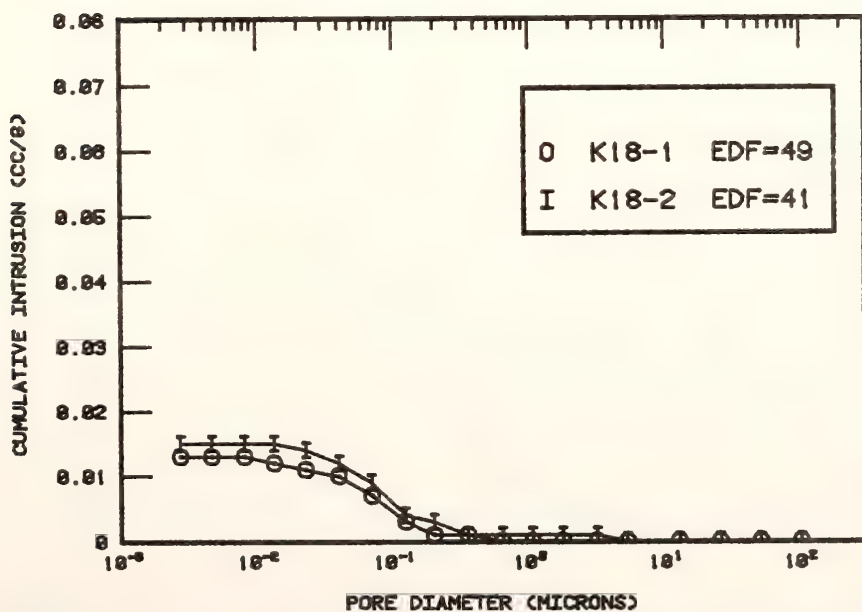
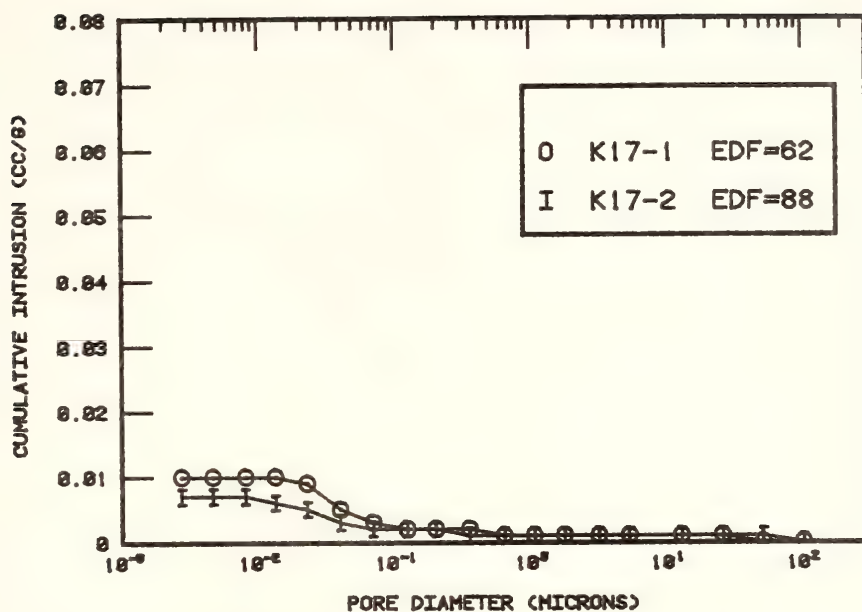


Figure D-14: Pore-size distributions for samples K17(top) and K18(bottom).

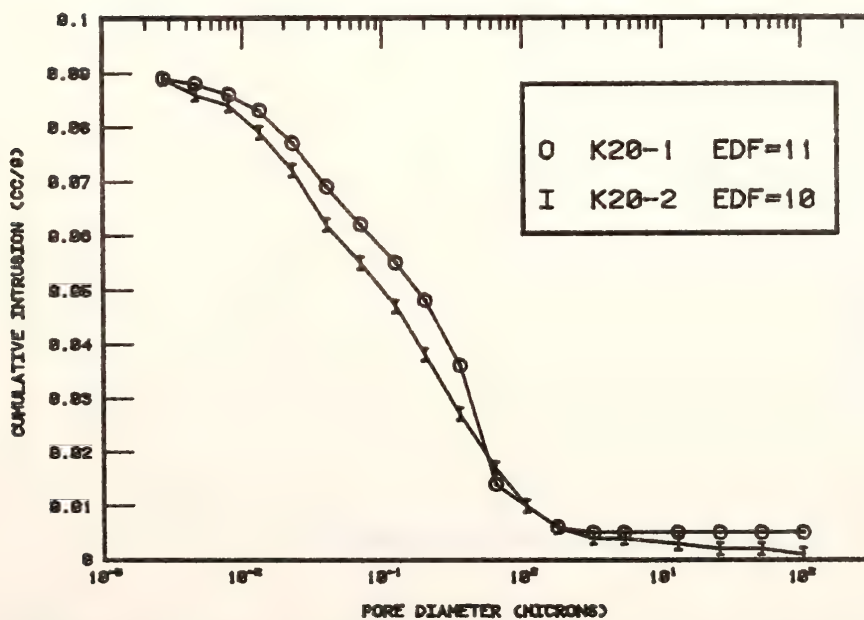
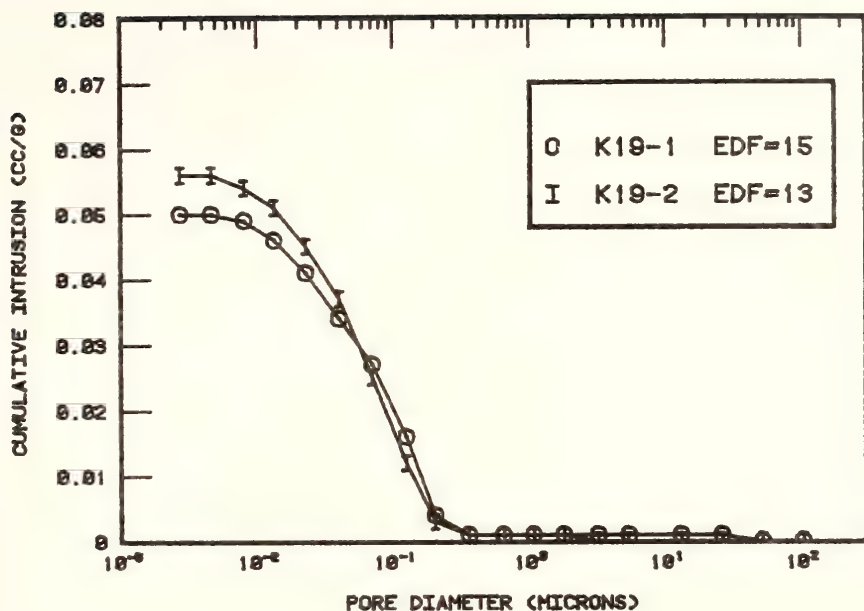


Figure D-15: Pore-size distributions for samples K19(top) and K20(bottom).

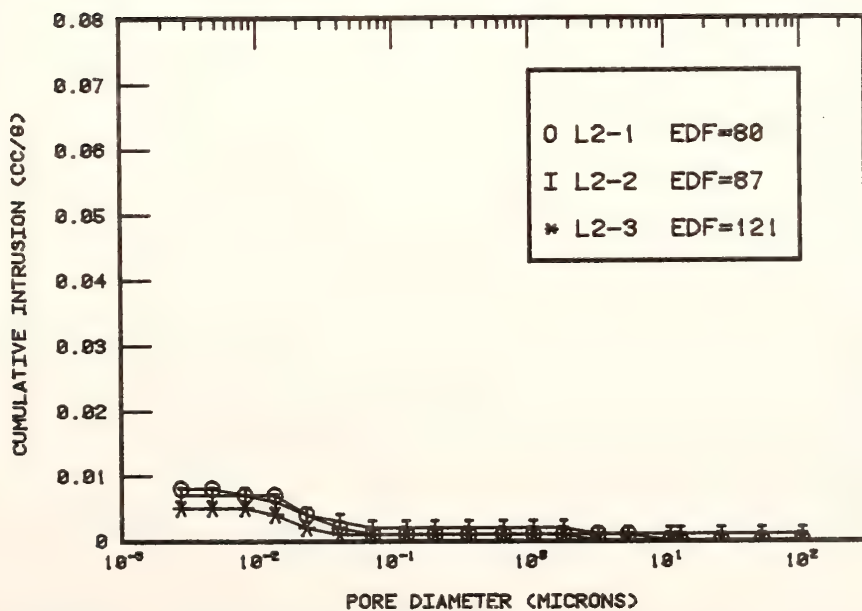
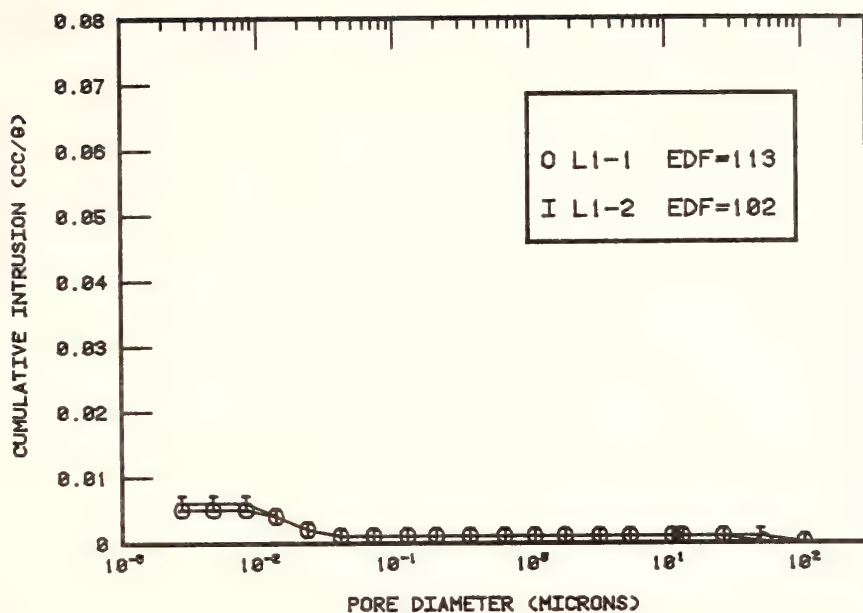


Figure D-16: Pore-size distributions for samples L1(top) and L2(bottom).

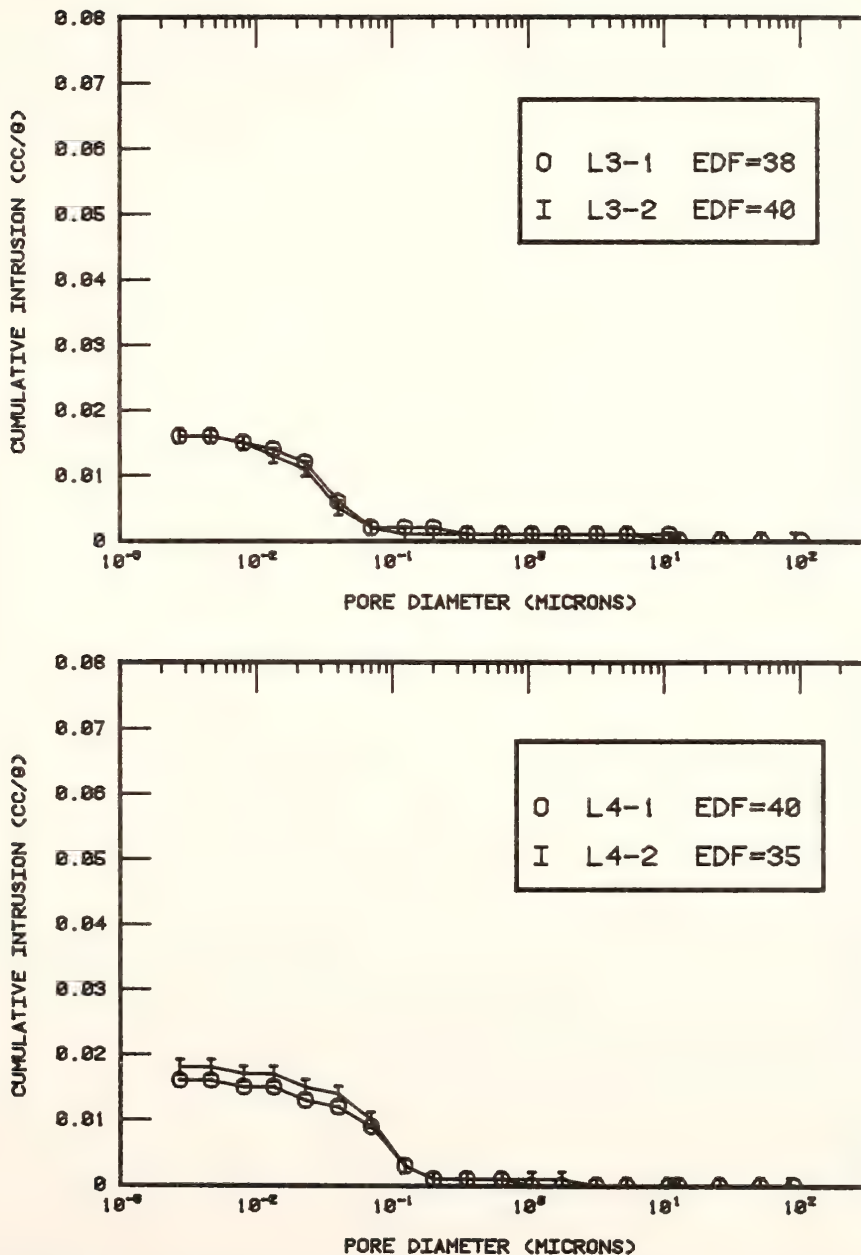


Figure D-17: Pore-size distributions for samples L3(top) and L4(bottom).

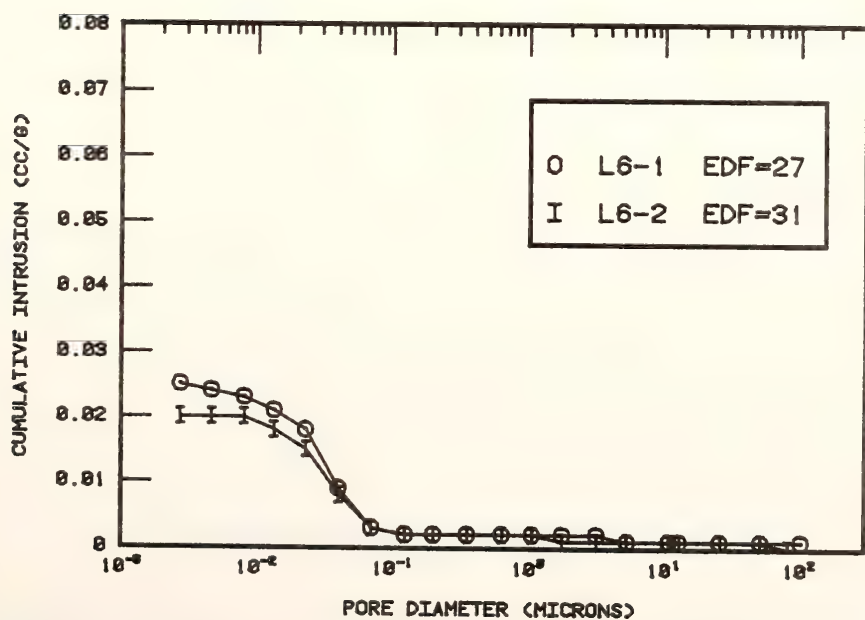
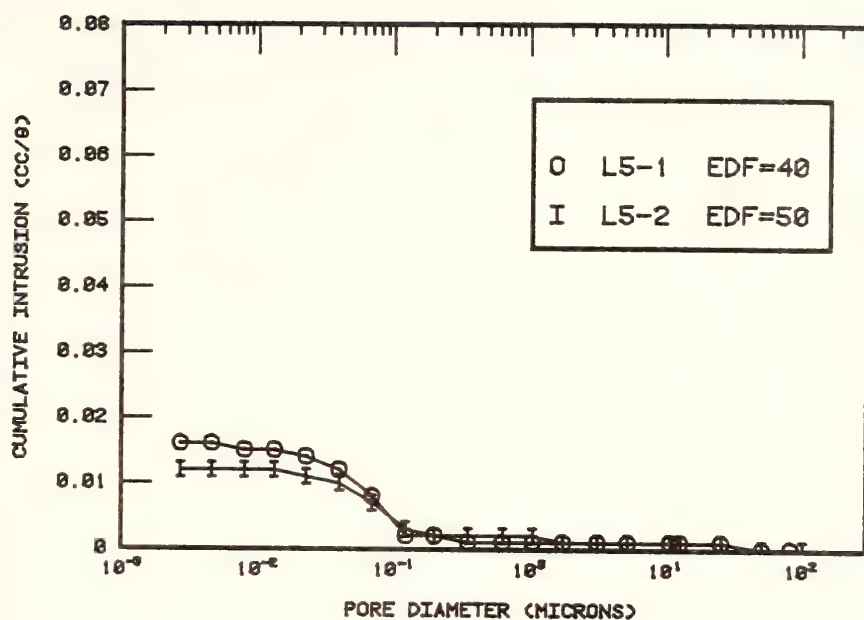


Figure D-18: Pore-size distributions for samples L5(top) and L6(bottom).

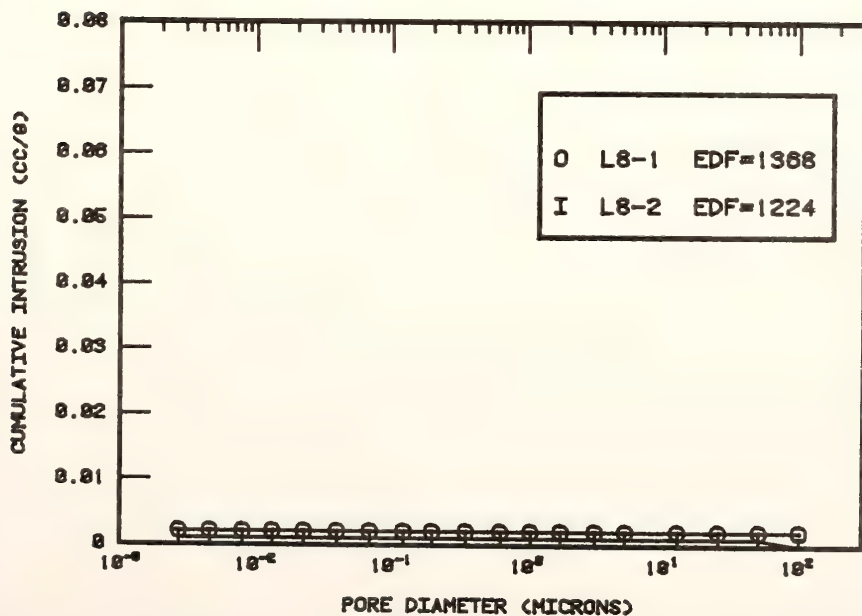
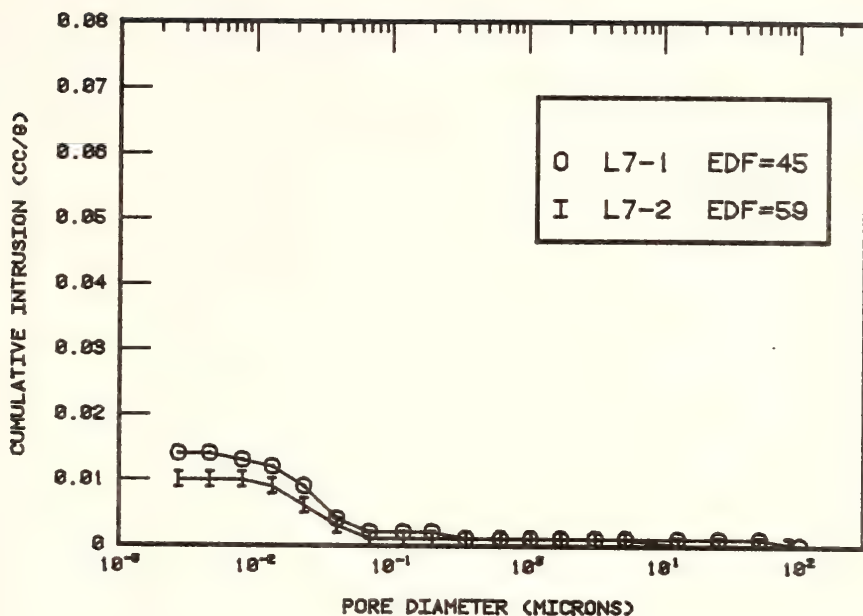


Figure D-19: Pore-size distributions for samples L7(top) and L8(bottom).

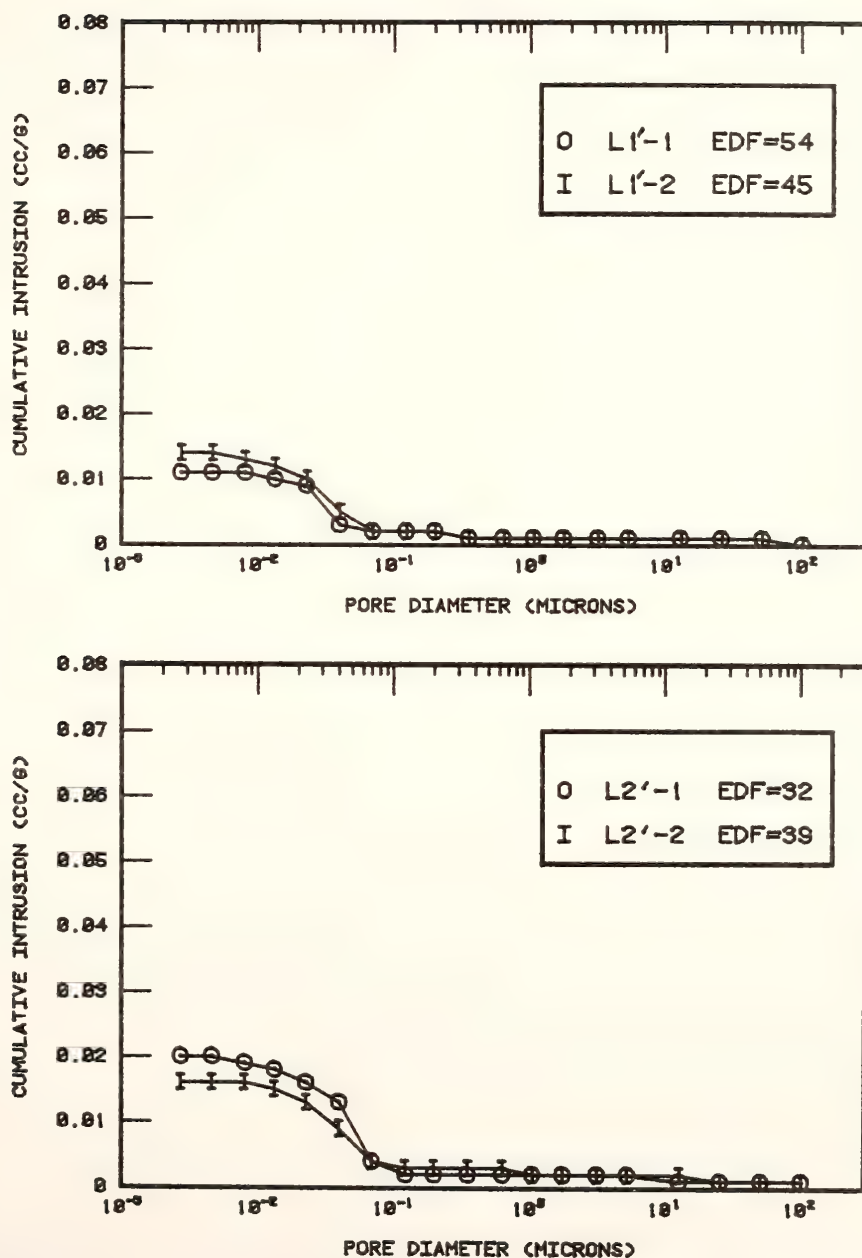


Figure D-20: Pore-size distributions for samples L1'(top) and L2'(bottom).

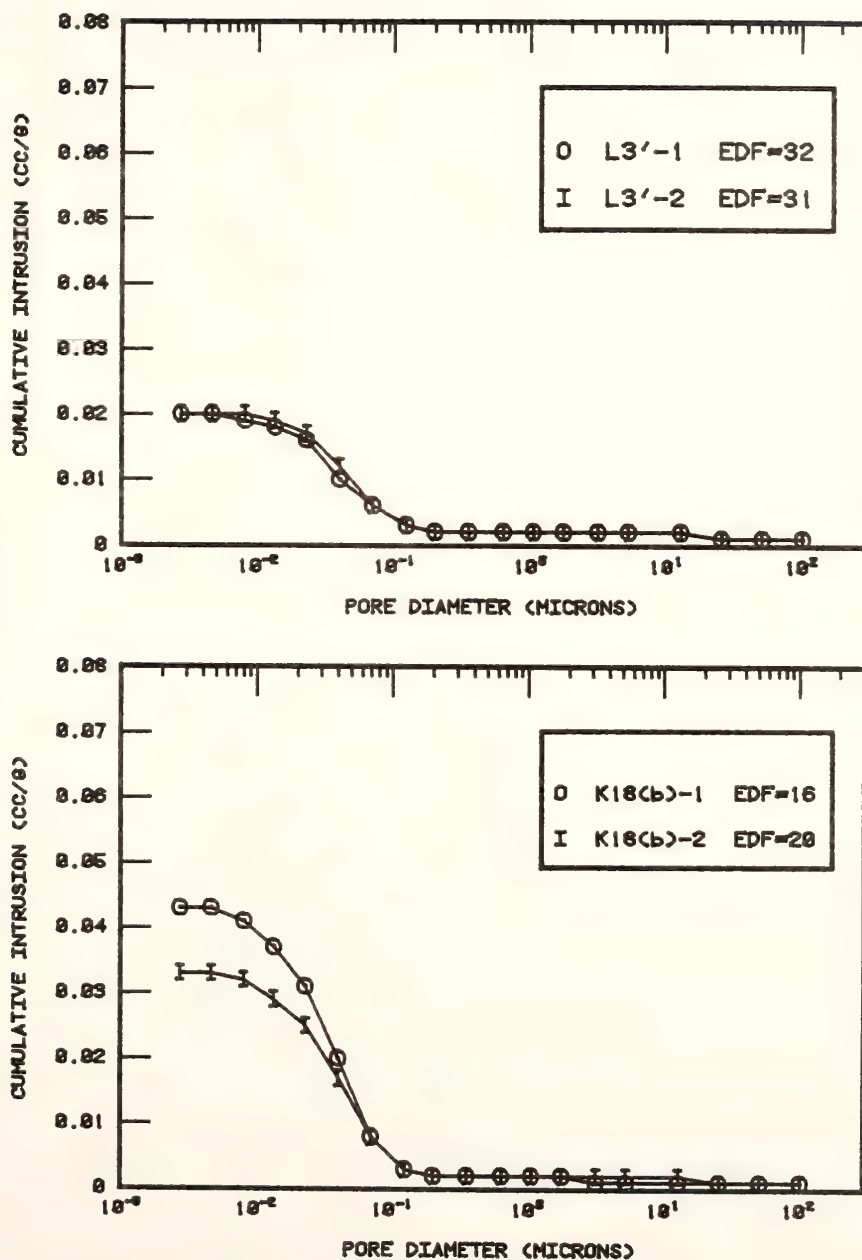


Figure D-21: Pore-size distributions for samples L3'(top) and K18-b(bottom).

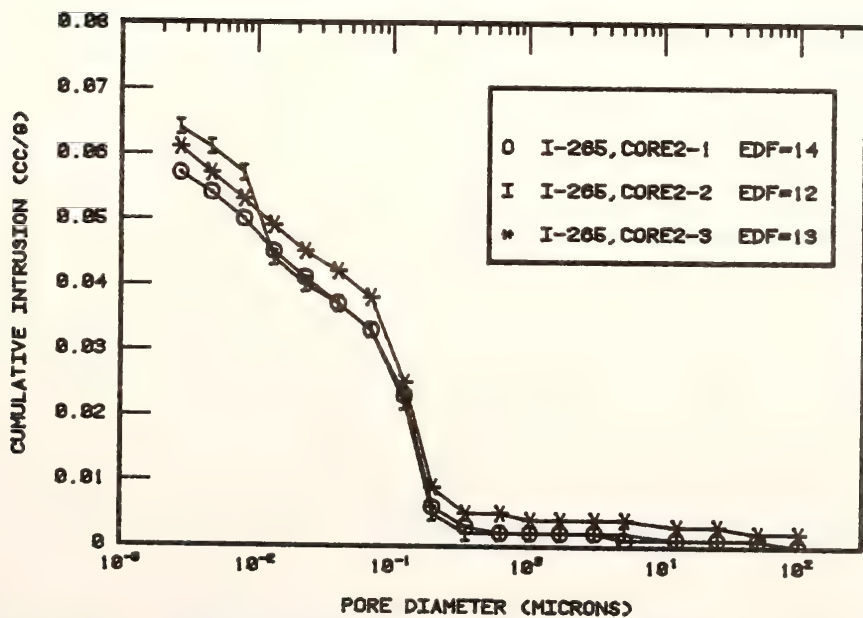
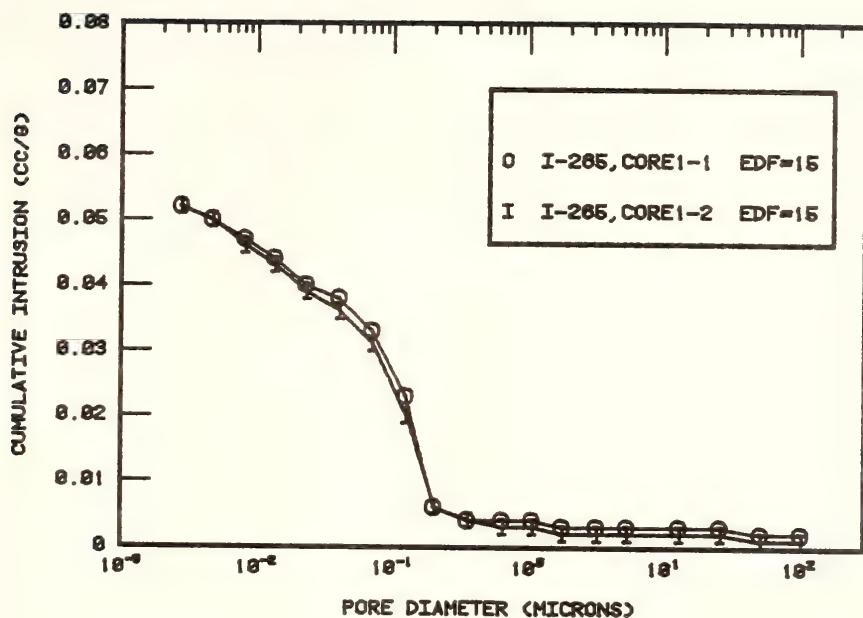


Figure D-22: Pore-size distributions for damaged aggregate from Cores 1 (top) and 2 (bottom) taken from I-265.

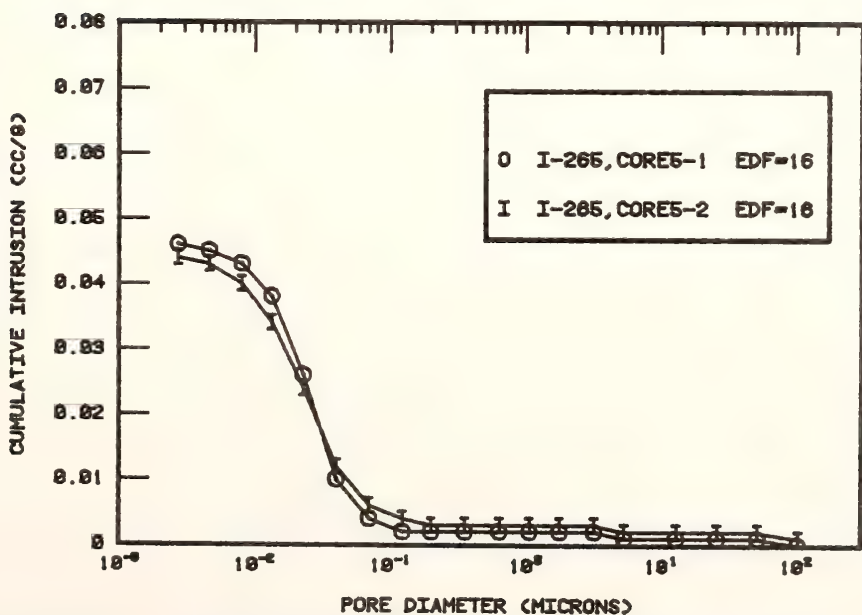
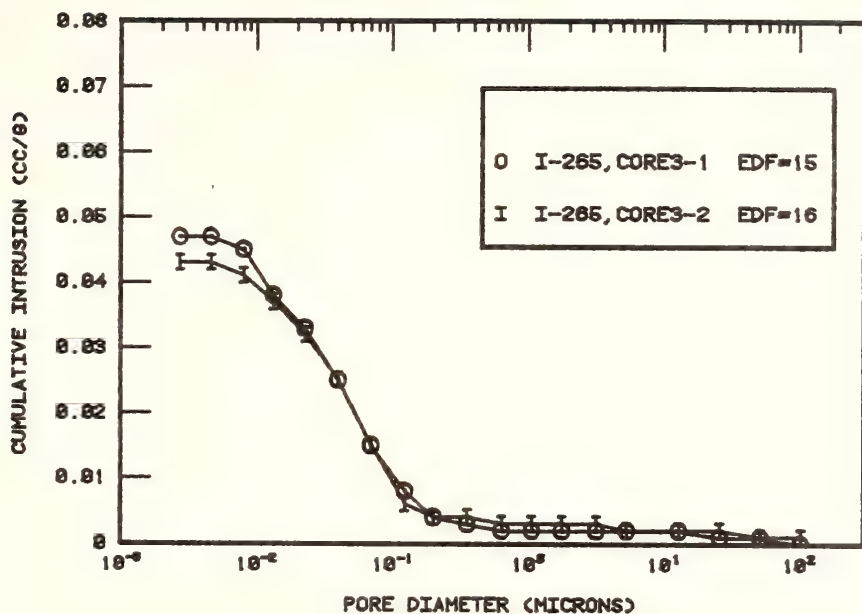


Figure D-23: Pore-size distributions for damaged aggregate from Cores 3 (top) and 5(bottom) taken from I-265.

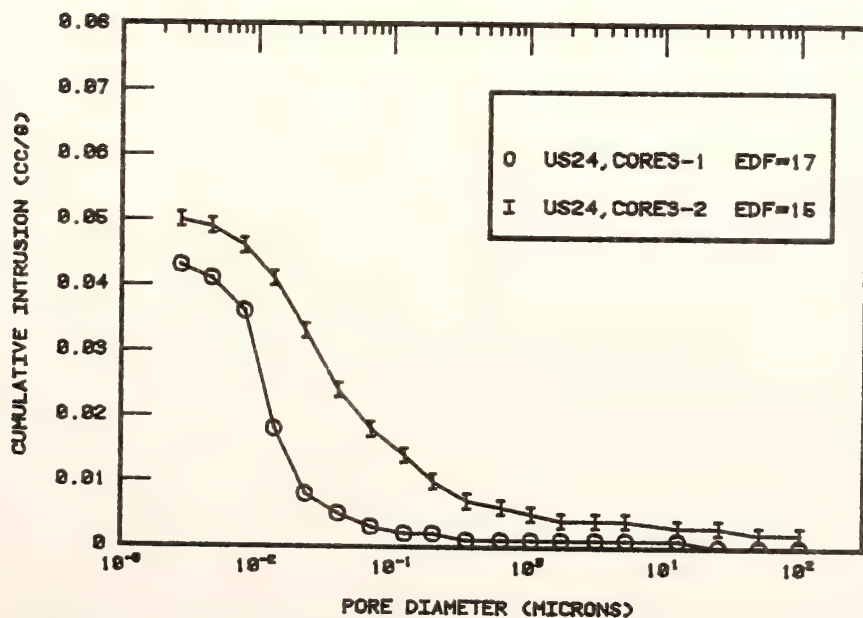
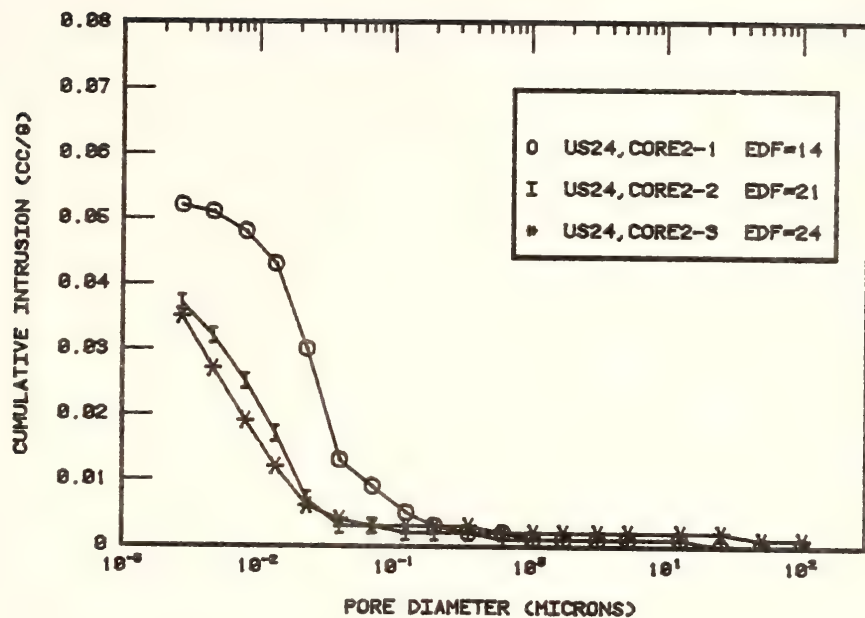


Figure D-24: Pore-size distributions for damaged aggregate from Cores 2 (top) and 3(bottom) taken from US-24.

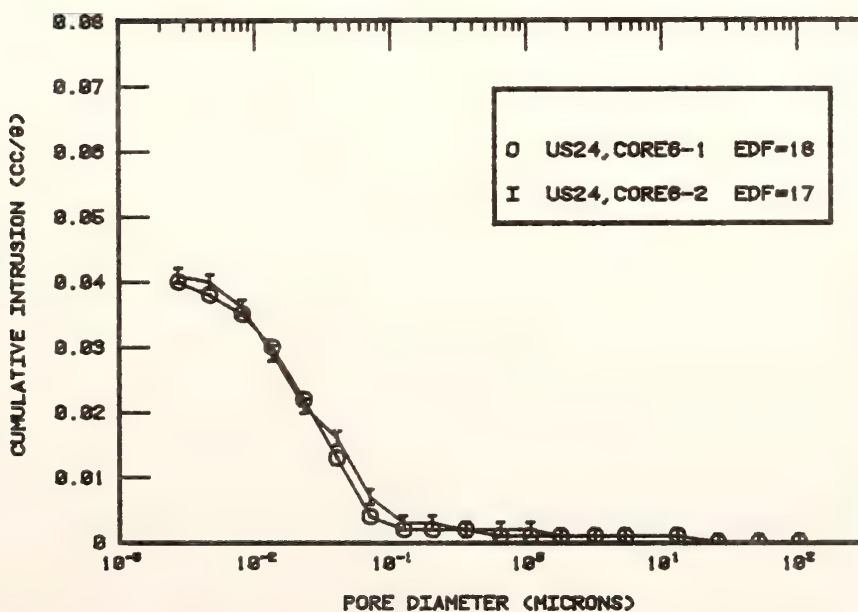
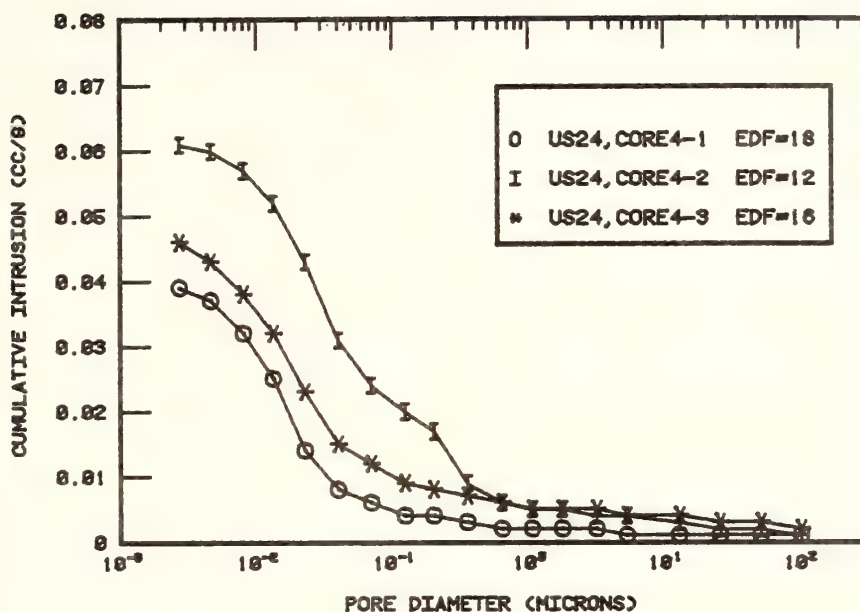


Figure D-25: Pore-size distributions for damaged aggregate from Cores 4 (top) and 6 (bottom) taken from US-24.

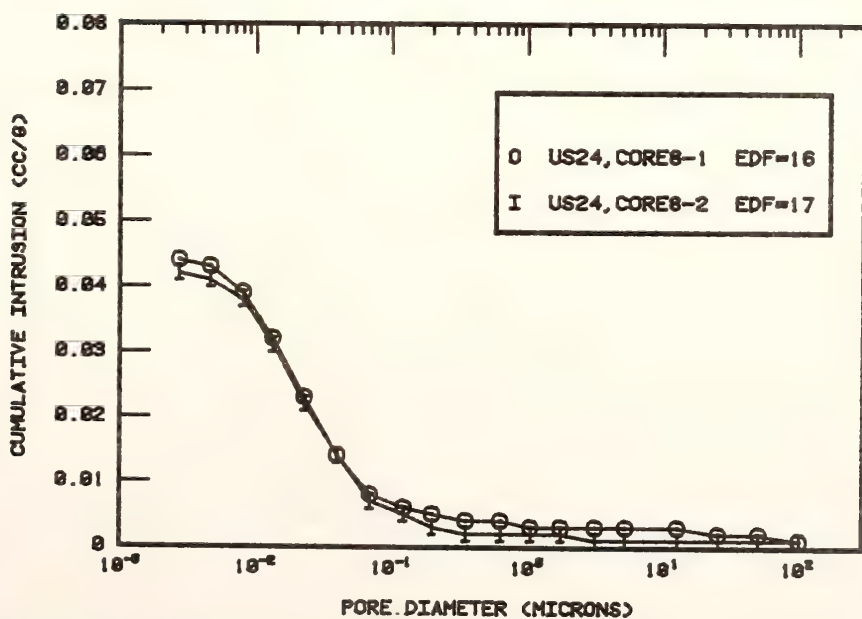
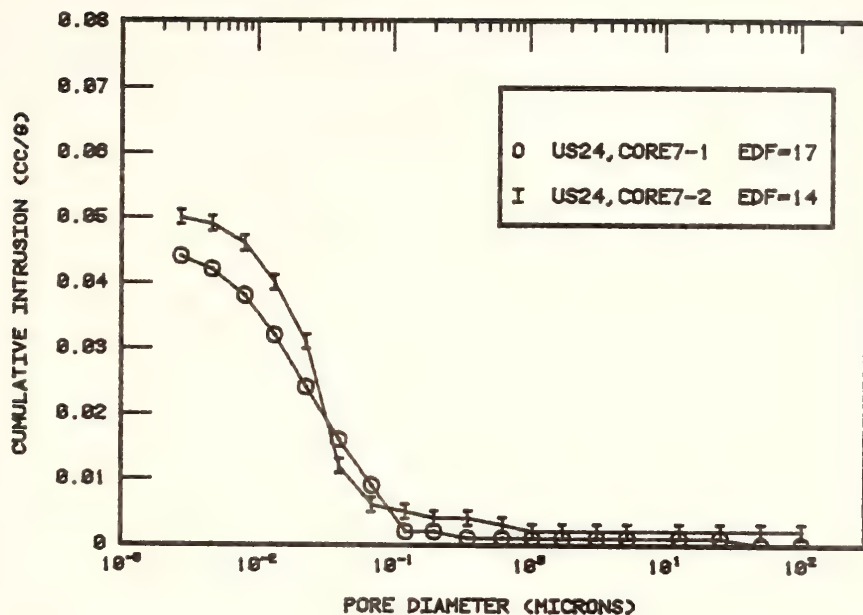


Figure D-26: Pore-size distributions for damaged aggregate from Cores 7 (top) and 8(bottom) taken from US-24.

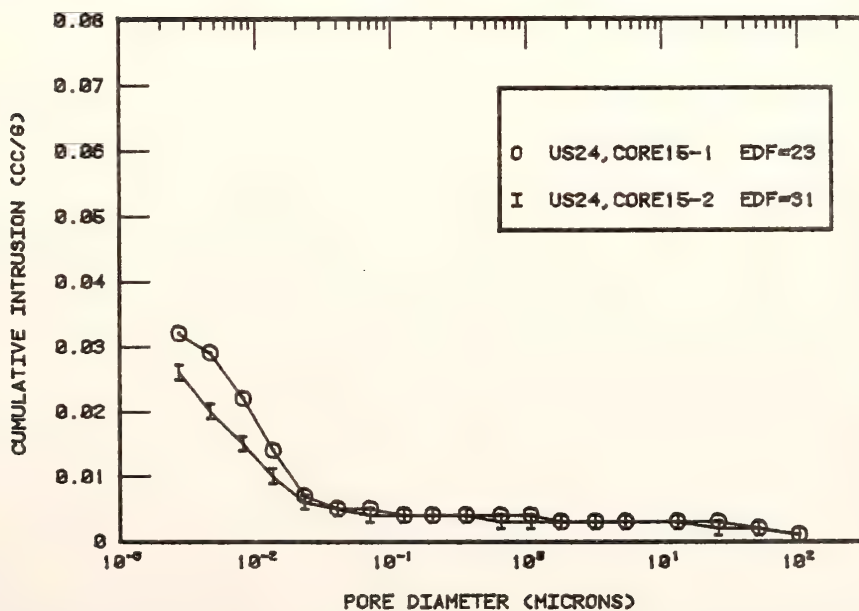
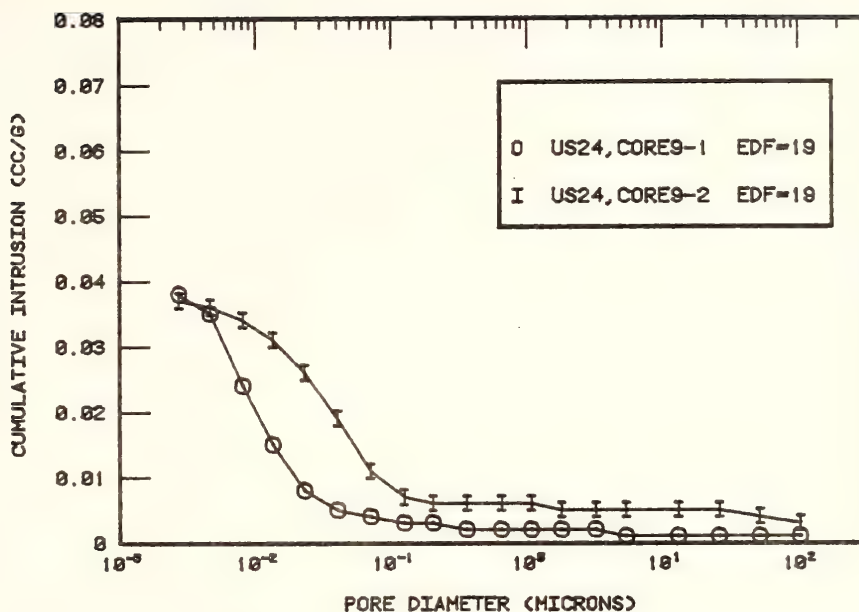


Figure D-27: Pore-size distributions for damaged aggregate from Cores 9 (top) and 15(bottom) taken from US-24.

APPENDIX E
RESULTS OF SODIUM SULPHATE SOUNDNESS
AND FREEZE-THAW TESTS

Table E-1. Itemized Listing of Soundness Losses on Individual Portions of the Test Samples and Calculated Weighted Loss

Sample No.	Test Portion Sieve Size	Gradation of Sample (%)	S.S. Soundness Loss		F&T Loss in Water		F&T Loss in 5% Salt	
			Actual (%)	Weighted (%)	Actual (%)	Weighted (%)	Actual (%)	Weighted (%)
T1	-1 1/2 +3/4	28	9.60	2.69	31.46	8.81	83.08	23.26
	- 3/4 +3/8	52	16.73	8.70	66.57	34.62	94.47	49.13
	- 3/8 + #4	20	10.33	2.07	14.33	2.87	91.33	18.27
	TOTALS			13.46		46.30		90.66
T3	-1 1/2 +3/4	28			6.24	1.75	7.32	2.05
	- 3/4 +3/8	52	Insufficient		11.04	6.21	53.06	27.59
	- 3/8 + #4	20	Sample		30.56	6.11	38.82	7.76
	TOTALS					14.07		37.40
T4	-1 1/2 +3/4	28	27.11	7.59	1.00	0.28	31.30	8.76
	- 3/4 +3/8	52	29.80	15.50	4.27	2.22	43.98	22.87
	- 3/8 + #4	20	17.00	3.40	5.00	1.00	28.33	5.67
	TOTALS			26.49		3.50		37.30
T5	-1 1/2 +3/4	28	22.96	6.43	51.26	14.53	80.13	22.43
	- 3/4 +3/8	52	36.49	18.98	84.10	43.73	99.80	51.90
	- 3/8 + #4	20	33.67	6.73	14.67	2.97	95.67	19.13
	TOTALS			32.14		61.01		93.46
T7	-1 1/2 +3/4	28	21.30	5.96	1.79	0.50	31.37	8.78
	- 3/4 +3/8	52	37.56	19.53	3.67	1.91	54.59	28.39
	- 3/8 + #4	20	21.67	4.33	6.33	1.27	51.00	10.20
	TOTALS			29.82		3.68		47.37
T10	-1 1/2 +3/4	28	1.73	0.48	0.53	0.15	0.39	0.11
	- 3/4 +3/8	52	3.08	1.60	1.50	0.78	1.68	0.88
	- 3/8 + #4	20	3.00	0.60	2.33	0.47	2.00	0.40
	TOTALS			2.68		1.40		1.39

Table E-1 continued

Sample No.	Test Portion Sieve Size	Gradation of Sample (%)	S.S. Soundness Loss Actual (%)	S.S. Soundness Loss Weighted (%)	F&T Loss in Water Actual (%)	F&T Loss in Water Weighted (%)	F&T Loss in 5% Salt Actual (%)	F&T Loss in 5% Salt Weighted (%)
K1	-1 1/2 +3/4	28	12.41	3.47	4.71	1.32	24.13	6.76
	- 3/4 +3/8	52	16.12	8.38	13.67	7.11	35.89	18.66
	- 3/8 + #4	20	14.00	2.80	3.00	0.60	13.67	2.73
	TOTALS			14.65		9.03		28.15
K3	-1 1/2 +3/4	28	25.57	7.16	27.62	7.73	46.28	12.96
	- 3/4 +3/8	52	40.94	21.29	22.61	11.76	61.62	32.04
	- 3/8 + #4	20	30.33	6.07	5.33	1.07	45.00	9.00
	TOTALS			34.52		20.56		54.00
K5	-1 1/2 +3/4	28	52.82	14.79	47.37	13.26	100.00	28.00
	- 3/4 +3/8	52	88.21	45.87	48.63	25.29	100.00	52.00
	- 3/8 + #4	20	62.33	12.47	9.67	1.93	98.33	19.67
	TOTALS			73.13		40.48		99.67
K7	-1 1/2 +3/4	28	87.24	24.43	59.12	16.55	100.00	28.00
	- 3/4 +3/8	52	99.10	51.53	83.52	43.43	100.00	52.00
	- 3/8 + #4	20	73.00	14.60	14.33	2.87	97.00	19.40
	TOTALS			90.56		62.85		99.40
K9	-1 1/2 +3/4	28	87.18	24.41	72.39	20.27	100.00	28.00
	- 3/4 +3/8	52	98.90	51.43	64.58	33.58	100.00	52.00
	- 3/8 + #4	20	79.67	15.93	29.33	5.87	100.00	20.00
	TOTALS			91.77		59.72		100.00
K11	-1 1/2 +3/4	28	3.75	1.05	1.86	0.52	0.79	0.22
	- 3/4 +3/8	52	6.12	3.18	1.39	0.72	5.28	2.75
	- 3/8 + #4	20	5.00	1.00	1.33	0.27	5.00	1.00
	TOTALS			5.23		1.51		3.97

Table E-1 continued

Sample No.	Test Portion Sieve Size	Gradation of Sample (%)	S.S. Soundness Loss		F&T Loss in Water		F&T Loss in 5% Salt	
			Actual (%)	Weighted (%)	Actual (%)	Weighted (%)	Actual (%)	Weighted (%)
K12	-1 1/2 +3/4	28	6.55	1.83	2.53	0.71	8.11	2.27
	- 3/4 +3/8	52	11.11	5.80	3.19	1.66	18.23	9.48
	- 3/8 + #4	20	5.33	1.07	6.33	1.27	18.33	3.67
	TOTALS			8.70		3.64		15.42
K13	-1 1/2 +3/4	28	10.69	2.99	7.45	2.09	11.45	3.21
	- 3/4 +3/8	52	11.85	6.16	5.75	2.99	20.71	10.77
	- 3/8 + #4	20	9.33	1.87	3.67	0.73	20.67	4.13
	TOTALS			11.02		5.81		18.11
K14	-1 1/2 +3/4	28	9.58	2.68	3.96	1.11	1.12	0.31
	- 3/4 +3/8	52	15.15	7.88	3.89	2.02	3.00	1.56
	- 3/8 + #4	20	8.33	1.67	9.00	1.80	4.33	0.87
	TOTALS			12.23		4.93		2.74
K15	-1 1/2 +3/4	28	23.22	6.50	9.02	2.53	13.66	3.82
	- 3/4 +3/8	52	27.43	14.26	10.01	5.21	21.41	11.14
	- 3/8 + #4	20	14.33	2.87	9.00	1.80	9.67	1.93
	TOTALS			23.63		9.54		16.89
K16	-1 1/2 +3/4	28	32.26	9.03	Insufficient Sample			
	- 3/4 +3/8	52	24.90	12.95				
	- 3/8 + #4	20	11.00	2.20				
	TOTALS			24.18				
K17	-1 1/2 +3/4	28	37.54	10.51	Insufficient Sample			
	- 3/4 +3/8	52	24.25	12.61				
	- 3/8 + #4	20	12.33	2.47				
	TOTALS			25.59				

Table E-1 continued

Sample No.	Test Portion Sieve Size	Gradation of Sample (%)	S.S. Soundness Loss			F&T Loss in Water			F&T Loss in 5% Salt		
			Actual (%)	Weighted (%)	Actual (%)	Actual (%)	Weighted (%)	Actual (%)	Actual (%)	Weighted (%)	Weighted (%)
K18	-1 1/2 +3/4	28	19.26	5.39	31.20	8.74		34.59		9.68	
	- 3/4 +3/8	52	29.46	15.32	17.01	8.85		42.77		22.24	
	- 3/8 + #4	20	17.00	3.40	12.33	2.47		25.00		5.00	
	TOTALS			24.11		20.06				36.92	
K19	-1 1/2 +3/4	28	25.55	7.15	97.81	27.39		100.00		28.00	
	- 3/4 +3/8	52	27.29	14.19	95.08	49.44		99.90		51.95	
	- 3/8 + #4	20	37.33	7.47	34.00	6.80		90.33		18.07	
	TOTALS			28.81		83.63				98.02	
K20	-1 1/2 +3/4	28	92.73	25.97	92.52	25.91		100.00		28.00	
	- 3/4 +3/8	52	93.79	48.77	90.03	46.82		100.00		52.00	
	- 3/8 + #4	20	92.67	18.53	39.67	7.93		98.67		19.73	
	TOTALS			93.27		80.66				99.73	
L1	-1 1/2 + 3/4	28	5.85	1.64	1.90	0.53		17.47		4.89	
	- 3/4 +3/8	52	5.81	3.02	2.79	1.45		38.49		20.02	
	- 3/8 + #4	20	2.00	0.40	2.33	0.47		16.67		3.33	
	TOTALS			5.06		2.45				28.24	
L2	-1 1/2 +3/4	28	15.23	4.26	3.01	0.84		40.91		11.45	
	- 3/4 +3/8	52	11.59	6.03	4.27	2.22		27.79		14.45	
	- 3/8 + #4	20	3.67	0.73	2.33	0.47		86.67		17.33	
	TOTALS			11.02		3.53				43.23	
L3	-1 1/2 +3/4	28	8.41	2.35	3.84	1.08		30.19		8.45	
	- 3/4 +3/8	52	12.22	6.35	8.17	4.25		58.92		30.64	
	- 3/8 + #4	20	5.00	1.00	12.67	2.53		31.00		6.20	
	TOTALS			9.70		7.86				45.29	

Table E-1 continued

Sample No.	Test Portion Sieve Size	Gradation of Sample (%)	S.S. Soundness Loss		F&T Loss in Water		F&T Loss in 5% Salt	
			Actual (%)	Weighted (%)	Actual (%)	Weighted (%)	Actual (%)	Weighted (%)
L4	-1 1/2 +3/4	28	7.28	2.04	2.80	0.78	38.14	10.68
	- 3/4 +3/8	52	6.75	3.51	2.09	1.09	48.39	25.16
	- 3/8 + #4	20	4.33	0.87	3.67	0.73	70.67	14.13
	TOTALS			6.42		2.60		49.97
L5	-1 1/2 +3/4	28	5.19	1.45	0.93	0.26	17.38	4.87
	- 3/4 +3/8	52	10.10	5.25	1.48	0.77	48.28	25.11
	- 3/8 + #4	20	2.00	0.40	2.67	0.53	31.33	6.27
	TOTALS			7.10		1.56		36.25
L6	-1 1/2 +3/4	28	4.81	1.35	2.45	0.68	20.43	5.72
	- 3/4 +3/8	52	9.21	4.79	4.66	2.42	42.86	22.29
	- 3/8 + #4	20	5.67	1.13	3.33	0.67	30.00	6.00
	TOTALS			7.27		3.77		34.01
L7	-1 1/2 +3/4	28	4.34	1.21	0.93	0.26	7.13	2.00
	- 3/4 +3/8	52	7.75	4.03	3.67	1.91	16.70	8.68
	- 3/8 + #4	20	2.00	0.40	4.00	0.80	15.33	3.07
	TOTALS			5.64		2.97		13.75
L8A*	-1 1/2 +3/4	28	4.19	1.17	1.44	0.40	5.54	1.55
	- 3/4 +3/8	52	7.40	3.85	2.47	1.28	8.64	4.49
	- 3/8 + #4	20	2.00	0.40	3.33	0.67	4.00	0.80
	TOTALS			5.42		2.35		6.84
L8B*	-1 1/2 +3/4	28	5.02	1.40	0.98	0.27	5.21	1.46
	- 3/4 +3/8	52	6.04	3.14	3.18	1.66	8.48	4.41
	- 3/8 + #4	20	3.00	0.60	4.00	0.80	10.67	2.13
	TOTALS			5.14		2.73		8.00

* L8A and L8B are from the same elevation but two different locations horizontally. Average values for % loss are used in Tables 5.7 and 5.8 for sample No. L8.

APPENDIX F
DEGREE OF SATURATION

APPENDIX F

DEGREE OF SATURATION

This appendix includes the calculations to determine degree of saturation in two different ways using the data from other tests.

1. In the first table, data from specific gravity and absorption test are used to determine degree of saturation. Based on the mineral composition of each rock type, a weighted average value of the specific gravity of solids (G_s) was assumed.
2. In the second table, degree of saturation is calculated using data from mercury porosimeter test and absorption-adsorption test. Many samples show degree of saturation values higher than 100%. This is because the volume of pores measured by mercury intrusion method does not include the volume of pores larger than 500 microns, but the absorption values include the water present in these larger pores.

Those samples which show a degree of saturation higher than 100% should be considered fully saturated.

Table F-1: Determination of Degree of Saturation from Specific Gravity and Absorption Data

Sample No.	Rock Type	Assumed Sp. Gravity of Solids G_s	Oven-Dry Weight (g) W_d	48-Hour Saturation Height (g) W_m	Submerged Height (g) W_b	Volume of Sample (cc) $V_m = (W_m - W_d) / \gamma_w$	Volume of Solids (cc) $V_s = \frac{W_d}{G_s \times \gamma_w}$	Volume of Void (cc) $V_v = V_m - V_s$	Volume of Water (cc) $V_w = (W_m - W_d) / \gamma_w$	Degree of Saturation (%) $S_r = \frac{V_w}{V_v} \times 100$
T1*	Argillaceous Dolomite	2.72	119.00	125.10	74.70	50.4	43.75	6.65	6.10	91.73
T2*	"	2.72	109.00	114.70	68.00	46.7	40.07	6.63	5.70	86.00
T3	Argillaceous Dolomitic Limestone	2.70	47.00	47.65	28.65	19.00	17.53	1.47	0.65	44.21
T4	Dolomitic Limestone	2.74	325.10	326.80	203.60	123.20	118.65	4.55	1.7	37.36
T5*	Argillaceous Dolomite	2.72	186.70	194.00	117.70	76.30	67.90	8.40	9.3	110.71**
T6*	"	2.72	41.30	43.50	25.95	17.55	15.18	2.37	2.20	92.83
T7	Argillaceous Dolomitic Limestone	2.74	191.55	192.50	120.20	72.30	69.91	2.39	0.95	39.75
T8	"	2.76	336.5	343.3	214.20	129.1	121.92	7.18	6.80	94.71
T9	Cherty Dolomitic Limestone	2.72	121.85	123.00	76.00	47.00	44.80	2.20	1.15	52.27
T10	Limestone	2.72	179.20	179.7	113.00	66.70	65.88	0.82	0.50	60.97
K1*	Argillaceous Calcareous Dolomite	2.77	205.00	214.50	130.90	83.60	74.00	9.60	9.50	98.96
K3*	"	2.77	255.90	268.50	163.40	105.10	92.38	12.72	12.60	99.06
K5*	Silty Dolomite or Dolomitic Siltstone	2.72	99.80	104.40	62.80	41.60	36.69	4.91	4.60	93.69
K7*	"	2.72	139.60	146.60	88.00	58.60	51.32	7.28	7.00	96.15
K9*	"	2.72	121.70	127.60	76.60	51.0	44.74	6.26	5.90	94.25

Table F-1 continued

K11	Argillaceous Calcareous Dolomite	2.75	125.90	129.30	79.20	50.10	45.78	4.32	3.40	78.70
K12	"	2.77	89.60	91.85	57.00	34.85	32.35	2.50	2.25	90.00
K13	"	2.77	50.80	52.00	32.45	19.55	18.34	1.21	1.20	99.17
K14	"	2.77	116.00	118.4	73.90	44.50	41.88	2.62	2.40	91.60
K15	Cherty Dolomite	2.73	185.50	190.60	116.70	73.90	67.95	5.95	5.10	85.71
K16	Limestone	2.72	106.80	108.70	67.30	41.40	39.26	2.14	1.90	88.75
K17	"	2.72	116.00	118.00	73.20	44.80	42.64	2.16	2.00	92.59
K18	Argillaceous Dolomitic Limestone	2.75	46.40	47.20	29.50	17.70	16.87	0.83	0.80	96.38
K19*	Argillaceous Dolomite	2.77	143.30	151.20	91.50	59.70	51.73	7.97	7.90	99.12
K20*	"	2.77	98.70	105.60	62.90	42.70	35.63	7.07	6.90	97.59
L1	Argillaceous Dolomitic Limestone	2.72	70.20	70.70	43.80	26.90	25.81	1.09	0.50	45.87
L2	"	2.72	233.3	234.70	147.00	87.70	85.77	1.93	1.40	72.54
L3*	Argillaceous Limestone	2.72	136.80	140.50	86.40	54.10	50.29	3.81	3.70	97.11
L4	"	2.72	60.20	61.20	37.50	23.70	22.13	1.57	1.00	63.69
L5	"	2.74	224.50	228.50	142.30	86.20	81.83	4.27	4.0	93.68
L6	"	2.74	233.90	238.70	148.10	90.60	85.36	5.24	4.80	91.60
L7	Cherty Limestone	2.72	270.20	271.90	170.30	104.60	99.34	2.26	1.70	75.22
L8	Limestone	2.74	61.10	61.50	38.70	22.80	22.30	0.50	0.40	80.00

* Unsound on the basis of field performance

** Can be assumed as 100%. The data for this specimen may be erroneous

Table F-2: Determination of Degree of Saturation from Vacuum Absorption Values and Mercury Porosimeter Data

Sample No.	Total Pore Volume** cc/g	24 Hour*** Vacuum Absorption cc/g	Degree of**** Saturation %
T1*	0.0625	0.0621	99.36
T2*	0.0610	0.0623	102.13
T3	0.0100	0.0117	117.00
T4	0.0110	0.0099	90.00
T5*	0.0585	0.0528	90.25
T7	0.0200	0.0082	41.00
T10	0.0030	0.0027	90.00
K1*	0.0460	0.0492	106.95
K3*	0.0400	0.0431	107.75
K5*	0.0445	0.0463	104.04
K7*	0.0460	0.0474	103.04
K9*	0.0475	0.0469	98.74
K11	0.0345	0.0195	56.52
K12	0.0290	0.0323	111.38
K13	0.0360	0.0333	92.50
K14	0.0410	0.0228	55.61
K15	0.0290	0.0183	63.10
K16	0.0205	0.0219	106.82
K17	0.0085	0.0093	109.00
K18	0.0140	0.155	110.70
K19*	0.0530	0.0550	103.77
K20*	0.0890	0.0848	95.28
L2	0.0066	0.0042	63.63
L3*	0.0160	0.151	94.37
L4	0.0170	0.0286	168.23
L6	0.0225	0.0236	104.88
L7	0.0120	0.0072	60.00

* Unsound on the basis of field performance.

** Obtained from mercury porosimeter test.

*** Obtained from absorption-adsorption test.

**** Values higher than 100% result because porosimeter measures the volume of micro-pores only whereas absorption represents volume of water in both macro and micro-pores.

APPENDIX G
DETERIORATION OF LEDGE SAMPLES
ON WETTING AND DRYING

APPENDIX G
DETERIORATION OF LEDGE SAMPLES
ON WETTING AND DRYING

This appendix presents the results of 10 cycles of wetting and drying on ledge samples. Each cycle consisted of 24 hours of saturation followed by 24 hours of oven drying. Percent loss in weight after 10 such cycles is taken to represent the extent of deterioration on wetting and drying.

Except for T3, all samples resulted in pitting and popouts in the field but their deterioration is insignificant on wetting and drying. T3 shows maximum deterioration on wetting and drying but no evidence of its poor performance was found in the field.

Figure G-1 compares the original samples with their state after 10 cycles of wetting and drying.

Table G-1: Loss in weight of ledge samples on wetting and drying

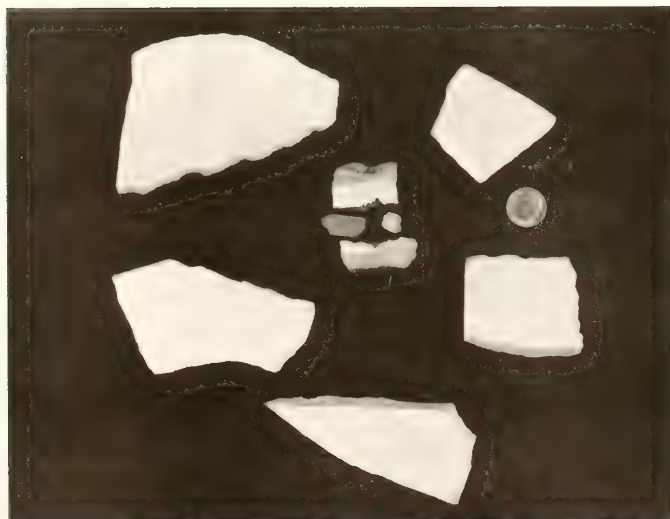
Sample* No.	Original Weight(g)	Weight After Each Cycle of Wetting and Drying (g)										% Loss after 10 Cycles
		(1)	(2)	(3)	(4)	(5)	(6)	(7)	(8)	(9)	(10)	
T1	22.80	22.80	22.80	22.80	22.75	22.75	22.75	22.75	22.75	22.75	22.75	0.22
T3**	19.90	19.90	19.90	19.75	19.60	19.50	19.50	19.50	19.50	19.50	19.45	2.26
T5	98.20	98.20	98.20	98.20	98.20	98.15	98.15	98.15	98.15	98.15	98.15	0.05
K8	50.60	50.60	50.60	50.60	50.60	50.60	50.60	50.60	50.60	50.60	50.60	0.00
K19	54.20	54.20	54.20	54.20	54.20	54.15	54.15	54.15	54.15	34.15	34.15	0.09
L3	57.80	57.80	57.80	57.80	57.80	57.75	57.75	57.75	57.75	57.75	57.75	0.09

* Except for T3, all samples represent unsound aggregates on the basis of field performance.

** T3 is highly laminated. Its deterioration on wetting and drying in a confined state in concrete could be much less than in an unconfined state.



(a)



(b)

Figure G-1: Wetting and drying of ledge samples: (a) original samples; (b) after 10 cycles of wetting and drying.

VITA

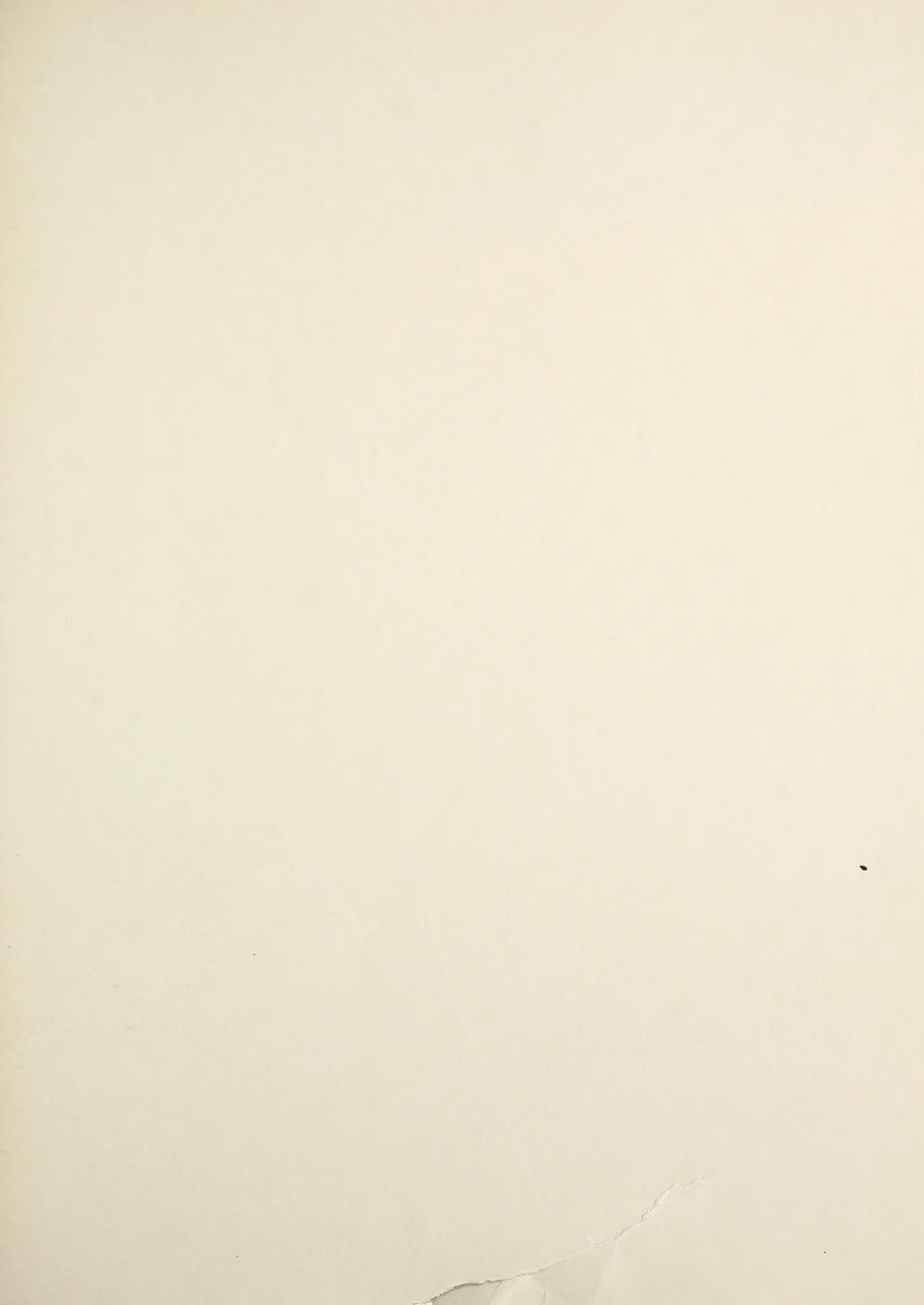
VITA

Abdul Shakoor was born on June 30, 1942, in Sheikhpura, Pakistan. He received his primary and secondary education in Lahore, Pakistan.

He earned his Bachelor of Science and Master of Science degrees in Geology from Punjab University, Lahore, Pakistan, in 1963 and 1964 respectively. He was awarded a Master of Science degree in engineering geology from Leeds University, England, in 1968. He enrolled in Purdue University in June 1977 from where he obtained his Master of Science degree in engineering geology in December 1978.

He served Punjab University as an assistant professor in engineering geology from 1965 to 1977. During his education at Purdue University he worked as a teaching and a research assistant.

He is married to Roohi Mukhtar and they have two children, daughter Najia, and son Qasim.



COVER DESIGN BY ALDO GIORGINI